REPORT NO. DOT-TSC-OST-73-29, III

CONCEPT FOR A SATELLITE-BASED ADVANCED AIR TRAFFIC MANAGEMENT SYSTEM

Volume III. Subsystem Functional Description

R. G. Loeliger
F. S. Nakamota
R. A. Gronlund
H. T. Freedman
J. W. Petway
R. J. Meisch
C. A. Wolfe

FEBRUARY 1974

FINAL REPORT

DOCUMENT IS AVAILABLE TO THE PUBLIC THROUGH THE NATIONAL TECHNICAL INFORMATION SERVICE, SPRINGFIELD, VIRGINIA 22151.

Prepared for

DEPARTMENT OF TRANSPORTATION

OFFICE OF THE SECRETARY

Office of Systems Engineering

Washington DC 20590

NOTICE

The contents of this report reflect the views of Rockwell International/Autonetics Division. The contents do not necessarily reflect the official views or policy of the Department of Transportation. This report does not constitute a standard, specification, or regulation.

NOTICE

This document is distributed under the sponsorship of the Department of Transportation in the interest of information exchange. The United States Government assumes no responsibility for contents or use, thereof.

Technical Report Documentation Page

1. Report No.	2. Government Accession No.	3. Recipient's Catalog No.
DOT-TSC-OST-73-29, III		

4. Title and Subtitle	5. Report Date
CONCEPT FOR A SATELLITE-BASED ADVANCED AIR TRAFFIC MANAGEMENT SYSTEM Volume III, Subsystem Functional Description	February 1974
	6. Performing Organization Code
7. Author(s) *R.G.Loeliger,F.S.Nakamoto,R.A.Gronlund, H.T.Freedman,J.W.Petway,R.J.Meisch,C.A.Wolfe	8. Performing Organization Report No. DOT-TSC-OST-73-29, III
9. Performing Organization Name and Address Autonetics 3370 Miraloma Avenue Anaheim CA 92803	10. Work Unit No. (TRAIS) S404/R-4509
	11. Contract or Grant No. DOT-TSC-508
12. Sponsoring Agency Name and Address Department of Transportation Office of the Secretary Office of Systems Engineering Washington DC 20590	13. Type of Report and Period Covered Final Report October 1972 through October 1973
	14. Sponsoring Agency Code

15. Supplementary Notes

*Under contract to: Department of Transportation, Transportation Systems Center, Kendall Square, Cambridge, MA 02142

16. Abstract

This volume presents a detailed description of the subsystems that comprise the Satellite-Based Advanced Air Traffic Management System. Described in detail are the surveillance, navigation, communications, data processing, and airport subsystems. The electronics required to implement each subsystem is also presented. The subsystem descriptions include a detailed description of the subsystem mechanization, the rationale for its selection, and the expected performance of each subsystem. The electronics are presented in block diagram form. Particular emphasis is placed on the integrated avionic hardware associated with each subsystem mechanization.

Included in the mechanization description of each subsystem are the basic analyses, algorithms, and equations that were used to implement the subsystem. The details of the analyses and assumptions underlying the data presented in this volume can be found in Volume IX of this report.

17. Key Words	18 Distribution Statement
Subsystem Mechanization, Surveillance, Navigation, Communications, Data Processing, Airport Surveillance and Navigation	DOCUMENT IS AVAILABLE TO THE PUBLIC THROUGH THE NATIONAL TECHNICAL INFORMATION SERVICE, SPRINGFIELD, VIRGINIA 22151.

19. Security Classif. (of this report)	20. Security Classif. (of this page)	21. No. of Pages	22. Price
UNCLASSIFIED	UNCLASSIFIED	218	

Form DOT F 1700.7 (8-72)

☆ U. S. GOVERNMENT PRINTING OFFICE : 1973 725-504/328

CONTENTS

CONTENTS (continued)

ILLUSTRATIONS

ILLUSTRATIONS (continued)

ILLUSTRATIONS (continued)

TABLES

GLOSSARY

AATMS	Advanced Air Traffic Management System
ACC	Airport Control Center
ADF	Automatic Direction Finder
ADIZ	Air Defense Identification Zone
AGL	Above Ground Level
AMF	Analog Matched Filter
AOPA	Aircraft Owners and Pilots Association
ARINC	Aeronautical Radio, Inc.
ARTCC	Air Route Traffic Control Center
ARTS	Automated Radar Terminal System
ATC	Air Traffic Control
ATCAC	Air Traffic Control Advisory Committee
ATCRBS	Air Traffic Control Radar Beacon System
ATCS	Air Traffic Control System
ATM	Air Traffic Management
CA	California
CARD	Civil Aviation Research and Development
CAS	Collision Avoidance System
CCC	Continental Control Center
CNI	Communication Navigation Identification
CNMAC	Critical Near Midair Collisions
COMM	Communications
CONUS	Continental United States
CP	Central Processor
CST	Central Standard Time
CW	Continuous Wave

GLOSSARY (continued)

DABS	Discrete Address Beacon System
DOD	Department of Defense
DOT	Department of Transportation
DME	Distance Measuring Equipment
DNSDP	Defense Navigation Satellite Development Program
DNSS	Defense Navigation Satellite System
ERP	Effective Radiated Power
ESRO	European Satellite Reserach Organization
EST	Eastern Standard Time
ETA	Estimated Time of Arrival
FAA	Federal Aviation Administration
F&E	Facilities and Equipment
FL	Florida
FM	Frequency Modulation
FSS	Flight Service Station
GA	General Aviation
GAATMS	Ground-Based Advanced Air Traffic Management System
GDOP	Geometric Dilution of Precision
GFE	Government Furnished Equipment
IAC	Instantaneous Airborne Count
ICAO	International Civil Aviation Organization
ID	Identification
IFR	Instrument Flight Rules
ILS	Instrument Landing System
IMC	Instrument Meteorological Conditions

GLOSSARY (continued)

I/O	Input/Output
IOP	Input Output Processor
IPC	Intermittent Positive Control
IPS	Instructions Per Second
IR	Infrared
JFK	Kennedy International Airport
LA	Los Angeles
LAT	Latitude
LAX	Los Angeles International Airport
LORAN	Long Range Navigation
LOS	Line-of-sight
LRR	Long Range Radar
MIPS	Million Instructions Per Second
MLS	Microwave Landing System
MODEM	Modulator-Demodulator
MSL	Mean Sea Level
MTBF	Mean Time Between Failures
NAFEC	National Aviation Facilities Experimental Center
NAD	North American Datum
NAS	National Airspace System
NASA	National Aeronautics and Space Administration
NAV	Navigation
NDB	Non-Directional Radio Beacon
NEF	Noise Exposure Factor
NFCC	National Flow Control Center

GLOSSARY (continued)

NMAC	Near Midair Collisions
NOTAM	Notice to Airmen
NOZ	Normal Operating Zone
NWS	National Weather Service
O&M	Operations and Maintenance
PCA	Positively Controlled Airspace
PIREPS	Pilot Reports
PN	Pseudo-Noise
PPM	Pulse Position Modulation
PWI	Pilot Warning Indicator
RAM	Random Access Memory
RCAG	Remote Control Air-to-Ground Facility (Present System)
RCAGT	Remote Communication Air-Ground Terminal
RCC	Regional Control Center
R&D	Research and Development
RDT&E	Research, Development, Test, and Evaluation
RF	Radio Frequency
RNAV	Area Navigation
ROM	Read-Only Memory
SAATMS	Satellite-Based Advanced Air Traffic Management System
SAMUS	State Space Analysis of Multisensor System
SID	Standard Instrument Departure
S/N	Signal-to-Noise
SNC	Surveillance, Navigation, Communication
STAR	Standard Arrival Routes
STC	Satellite Tracking Center
STOL	Short Takeoff and Landing

GLOSSARY (continued)

TACAN	Tactical Air Navigation
T&E	Test and Evaluation
TCA	Terminal Controlled Airspace
TOA	Time of Arrival
TRACAB	Terminal Radar Approach/Tower Cab
TRACON	Terminal Radar Approach Control
TRSA	Terminal Radar Service Areas
TRW	Thompson Ramo Wooldridge
TSC	Transportation Systems Center
TX	Texas
VFR	Visual Flight Rules
VHF	Very High Frequency
VMC	Visual Meteorological Conditions
VOR	Very High Frequency Omni-Directional Range
VORTAC	Very High Frequency Omni-Range TACAN
VVOR	Virtual VOR
2D	Two Dimensional
3D	Three Dimensional
4D	Four Dimensional

1. INTRODUCTION

This volume presents a detailed description of the subsystems that comprise the Satellite-Based Advanced Air Traffic Management System (SAATMS). The Surveillance Subsystem is presented in Section 2, the Navigation Subsystem in Section 3, the Communications Subsystem in Section 4, the Data Processing Subsystem in Section 5, the Airport Subsystem in Section 6, and the details of the electronics required to implement each subsystem are presented in Section 7. Sections 2 through 6 include detailed descriptions of the subsystem mechanizations, the rationale for their selection, and the expected performance of each subsystem. Section 7 presents block diagrams and performance characteristics of each equipment. Particular emphasis has been placed on the integrated avionic hardware. In general, the details of the analyses and assumptions underlying the data presented in this volume can be found in Volume IX of this report.

2. SURVEILLANCE SUBSYSTEM

The SAATMS surveillance subsystem is an air-to-satellite-to-ground, asynchronous, multilateration system which provides high speed, accurate, and reliable user location data. The proposed asynchronous system design has been analyzed in detail and found to be a valid solution to the surveillance problem.

The surveillance system will track a large number of aircraft within the satellite system coverage boundary. Altitude limits and the degree of dispersion within the coverage boundary have no effect on the system operation. There are no regions of high or low accuracy such as exist with ground based systems. The system accuracy is a slowly changing function until the outer boundary of the satellite system coverage is reached.

There are only two factors which affect the growth potential of the selected surveillance scheme. The ultimate number of users is bounded by multi-access noise resulting from asynchronous user surveillance pulse transmission and by ground processing capability. The former problem can be alleviated by the addition of additional surveillance channels. The latter problem only requires more ground based equipment to absorb the growth. Both of these are valid techniques for system expansion.

2.1 Surveillance Subsystem Described

Satellite multilateration techniques are utilized for surveillance data determination. Each active user in the system transmits an aircraft identification encoded surveillance pulse at a periodic rate. These pulse transmissions are unsynchronized between aircraft. These pulses are transponded by a constellation of satellites and received by a ground station.

The ground station measures the times of arrival of the pulse sequence as they are transponded from the satellites. From these data, the user's latitude, longitude, altitude, ground velocity, and heading are computed.

Figure 2.1-1 shows the general timing involved in the surveillance process. A single pulse is transmitted, transponded by a group of satellites, and received (after decoding) as a sequence of Time of Arrival (TOA) data. Since the arrival times are known, the positions of the individual satellites at the transponding times can be computed. The transponding times and positions of the satellites will allow computation of the unique position of the aircraft if four or more TOA's are received. The four signals are required since an a priori knowledge of the time of transmission is not assumed.

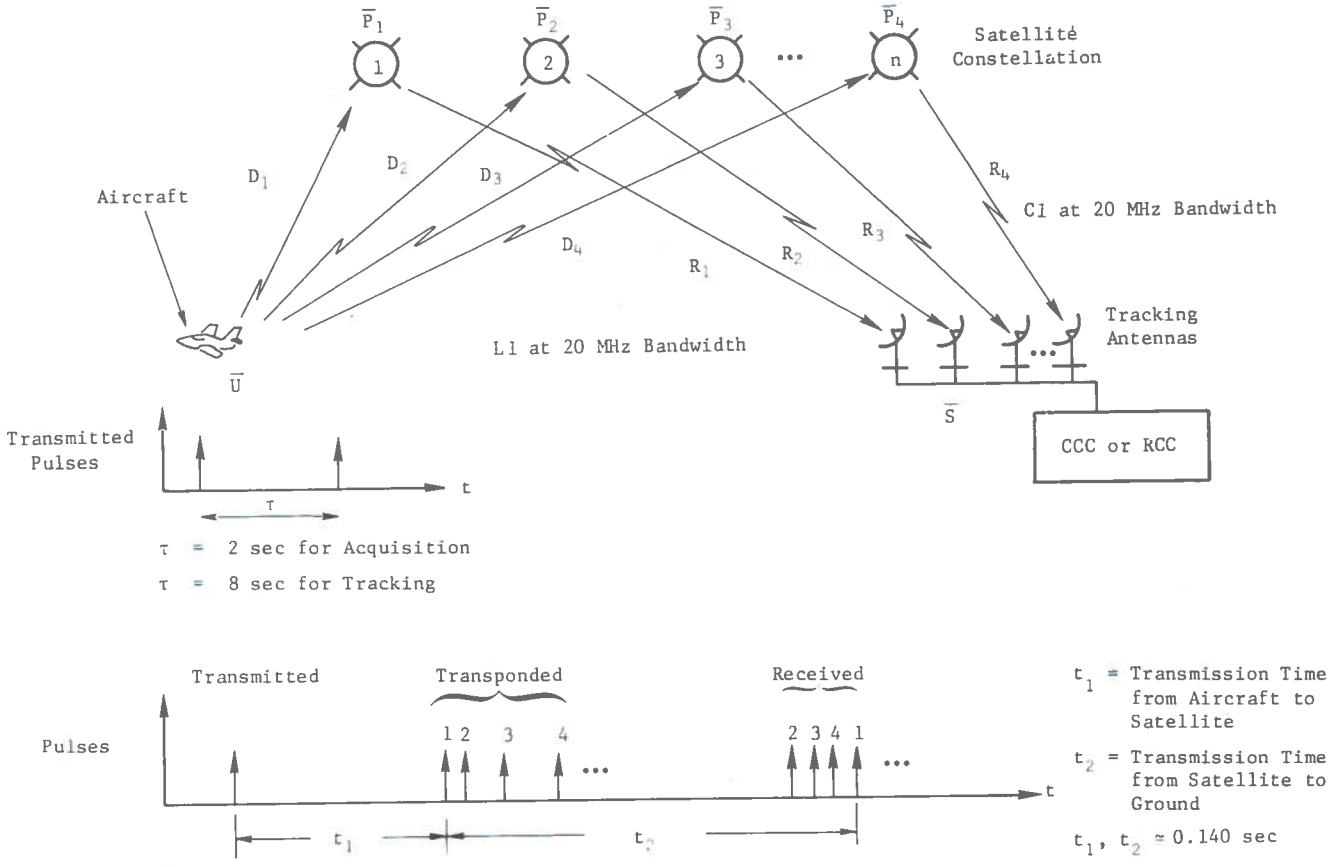

Fig. 2.1-1. Surveillance Description

Definitions: $\overline{P}_1$ through $\overline{P}_4$ = Position Vectors of Satellite (known)

$\overline{S}$ = Position Vectors of Site (known)

C = Speed of Light (known)

t_U = Time User Transmits Surveillance Pulse (unknown)

$\overline{U}$ = Position Vector of Aircraft (unknown)

$R_i = ||\overline{P}_i - \overline{S}||$

Problem: Given the time the site receives the surveillance pulses (t_{R1}, t_{R2}, t_{R3}, t_{R4}) compute $\overline{U}$.

Solution: A simplified solution can be derived from

$$t_{R1} = t_U + D_1/C + R_1/C$$
$$t_{R2} = t_U + D_2/C + R_2/C$$
$$t_{R3} = t_U + D_3/C + R_3/C$$
$$t_{R4} = t_U + D_4/C + R_4/C$$

$$\Rightarrow \quad \Delta\ell_1 = C(t_{R1} - t_{R2}) - R_1 + R_2 = D_1 - D_2$$
$$\Delta\ell_2 = C(t_{R2} - t_{R3}) + R_3 - R_2 = D_2 - D_3$$
$$\Delta\ell_3 = C(t_{R4} - t_{R3}) - R_4 + R_3 = D_4 - D_3$$

But: $D_i = ||\overline{P}_i - \overline{U}||$

Therefore, $\Delta\ell_i = D_i - D_{i+1}$ are three equations in three unknowns, i.e., the three components of the vector $\overline{U}$. A solution to $\overline{U}$ may therefore be computed.

A more complex solution based on this simplified solution is employed.

Fig. 2.1-1. (continued)

If a sequence of positions is available, the velocity and therefore the heading of the user can be computed. The velocity is in terms of ground speed since all positions and velocities are relative to the reference geoid, i.e., a mathematical description of the earth's shape used to compute geographic latitude and longitude.

In practice, the mechanization that is employed is substantially more complex than the simple explanation given. In principle, the system operates exactly as indicated.

The asynchronous air-to-satellite-to-ground configuration was selected based on the simplicity of the ground receiving sites, its low altitude remote area coverage, low user equipment costs, and the low communication requirements for surveillance. Any alternate system approach is substantially more complex and restrictive than the selected system. Further, the selected system is feasible.

In the SAATMS design study, a substantial amount of the effort was directed toward three aspects of the surveillance subsystem; the RF links and the identification coding scheme, the mechanization equations to be used, and the performance of the subsystem. Although other aspects of the subsystem certainly are important, these three areas essentially delineate the system and its potential.

2.2 Detection Assures Proper Surveillance

The surveillance RF link, identification, and detection scheme employed assures that all CONUS users can be surveyed with high probability. This can be achieved regardless of the asynchronous nature of the surveillance pulse transmission.

The essential problem with the selected mechanization lies in the multi-access noise. The aircraft transmit pseudo-noise encoded, spread spectrum, identification pulse sequences. The satellite receives pulse sequences from users in a random fashion and retransmits a data stream consisting of a large number of individual pulses. The ground based receiver processor must accept this data stream and reconstruct individual aircraft identification sequences and TOA's. For each individual identification sequence, all other sequences may be considered to be noise. This is generally referred to as multi-access noise.

A detailed study of the multi-access noise problem has indicated that this problem is not severe and the asynchronous air-to-satellite-to-ground system is feasible. Experimental validation of these results, however, has not as yet been accomplished.

The aircraft identification code consists of three pseudo-noise (PN) pulses as shown in Fig. 2.2-1. Each 40 μsec PN pulse consists of 400 chips of 100 nsec each. The interspacing between the first and second pulses and between the second and third pulses can be set in increments of 100 nsec. With the selected PN structure, there are 2^{400} possible codes of which 2^4 codes with good autocorrelation and cross-correlation properties are used. There are also 2^4 unique interpulse spacings between the first and second and the second and third pulses. The PN code sequence was used both to lower user power requirements and to increase timing accuracy relative to other coding schemes.

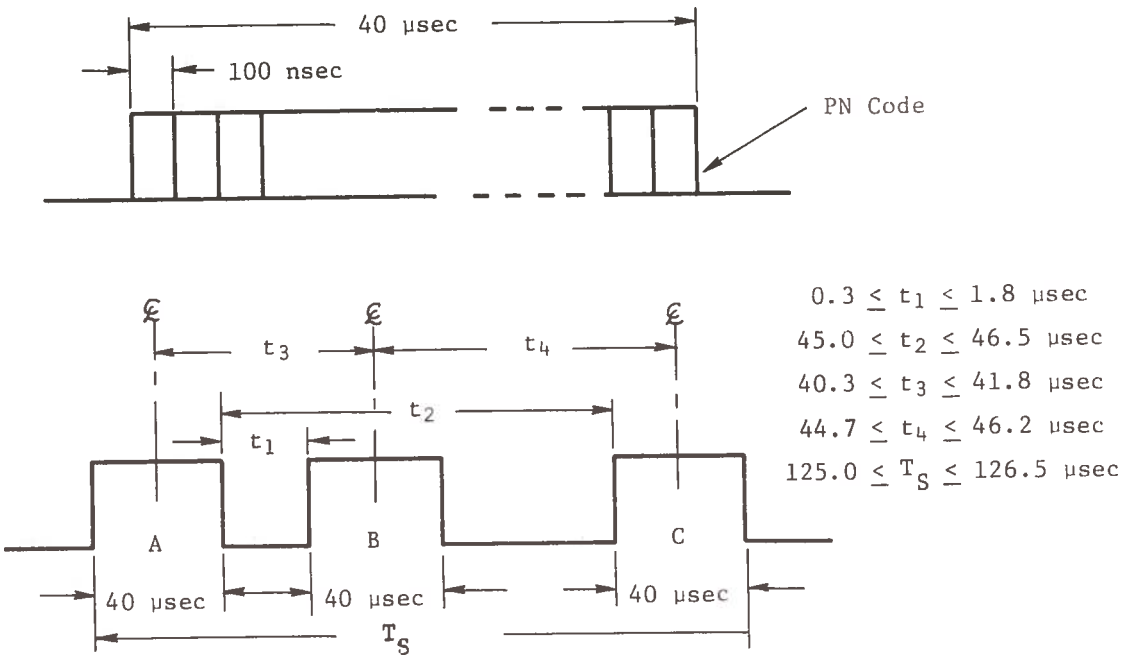

Fig. 2.2-1. Aircraft Surveillance Identification Coding

The aircraft ID code thus consists of an A pulse code, an A-B pulse spacing, a B pulse code, a B-C pulse spacing, and a C pulse code. With the assumed structure, there are $2^4 \times 2^4 \times 2^4 \times 2^4 \times 2^4 = 2^{20} = 1{,}048{,}576$ possible ID codes.

The ground receivers used with this coding structure contain Analog Matched Filters (AMF) that detect individual PN coded pulses. A post-detection processor combines the pulses into ID code sequences and associates the TOA of the first pulse with the ID code. The response of the AMF to a correctly coded PN pulse is shown in Fig. 2.2-2.

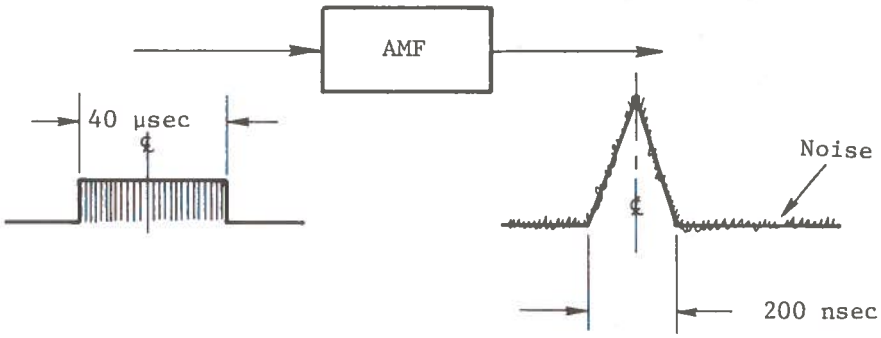

Fig. 2.2-2. AMF Operation

The output of the AMF is constrained to be above a reference threshold for pulse recognition to be acknowledged. Two factors can cause a failure of the pulse to be recognized. The signal from an aircraft can be weak due to a high user-to-satellite range (because a satellite is in a low gain orientation

with respect to the user's antenna pattern) or other factors that reduce the signal energy. An excessive amount of multi-access noise may occur during an interval, leading to false pulse decoding or missed detection. Note that false pulse detection can occur as well as missed detection.

There are a number of events that can occur as a result of the pulse detection scheme and the recombination of pulses into ID codes. These events include:

(1) Missed Detection - Failure to detect one or more pulses results in failure to detect the ID code.

(2) Phantom Detection - Pulses can be combined to yield an ID code that was not transmitted.

(3) Ambiguous Detection - More than one closely spaced ID code is detected.

(4) Unambiguous Detection - Only one ID code is properly detected.

Each of these events has a meaning with respect to the reception of signals from a single satellite.

The missed detection case has only a slight effect on the surveillance problem as a short-term phenomenon. A basic factor in the selected surveillance mechanization is that a given user-to-satellite link is dispensible. If detection is missed in one channel, the 7 to 10 other channels available with the redundant satellite constellation will still provide sufficient data. A severely disadvantaged user with an extremely high missed detection rate in all channels will cause surveillance to be lost. This possibility is reduced by requiring that tracking acquisition be made and the user informed prior to entry into the system. Subsequent in-flight failures will be detected based on track update times.

The phantom signature problem results from inauspicious combinations of overlapping surveillance signals and by false detection of real pulses or random detection of non-transmitted pulses. Phantom signatures can result from any coding scheme of this type having more than one PN pulse per identification code.

Figure 2.2-3 shows the phantom ID's that can occur using a three-pulse ID sequence, assuming no more than two signals are present for detection. Note that incommensurate A-B and B-C pulse spacing is employed so that, for example, if an A pulse combines with a valid ID sequence in the B time slot, the B pulse will be placed outside the possible C pulse time region.

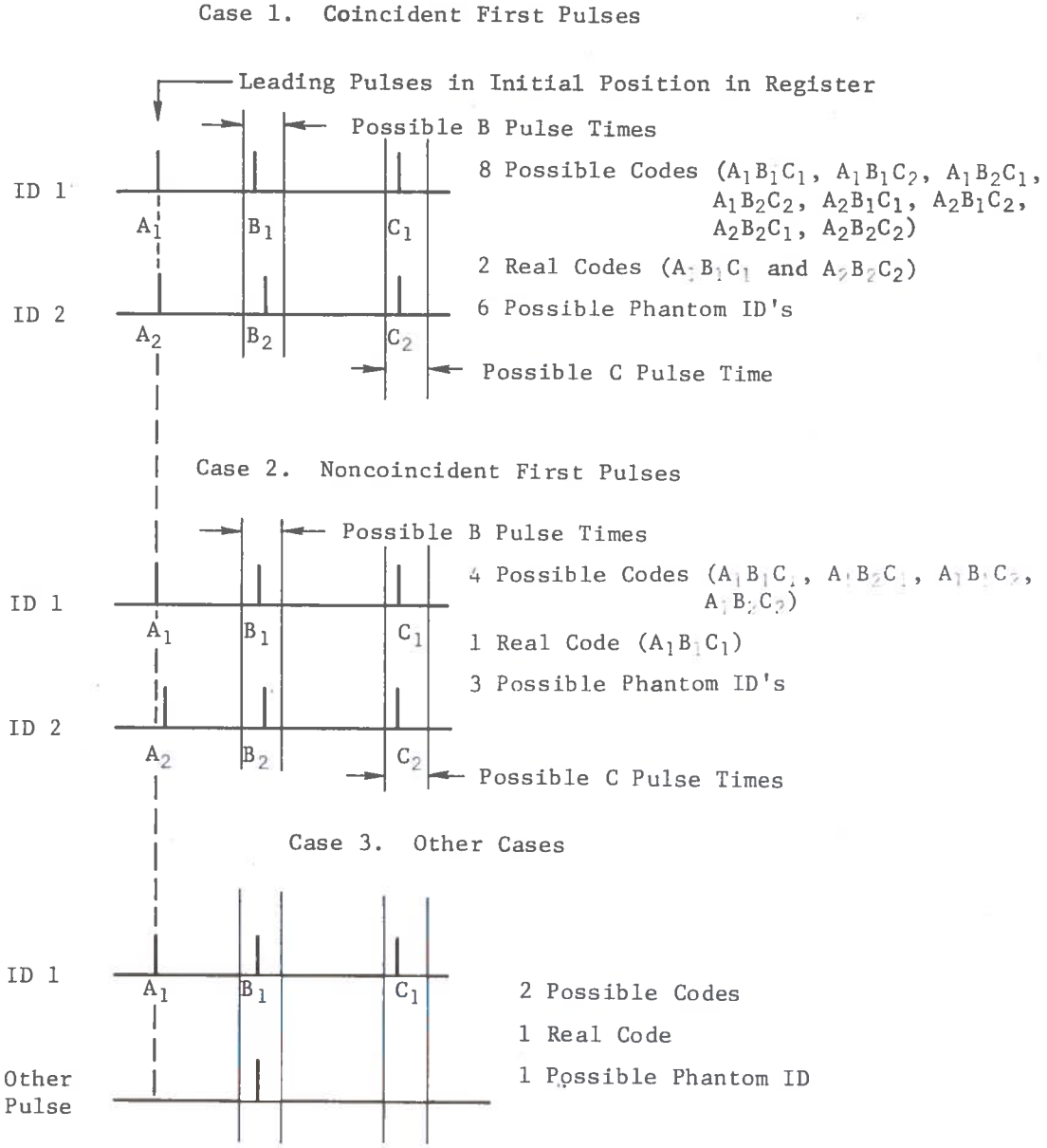

Fig. 2.2-3. Three-Pulse Code Phantom ID's

Even if phantom ID's are detected, the effect on the surveillance system is slight. The system software will reject the data if the ID has not been assigned. If the ID is valid and the aircraft is not being tracked, multiple satellite detections over a sequence of transmission times are required before the phantom ID would be accepted. This is unlikely since the acquisition surveillance rate is 0.5 Hz rather than the 0.125 Hz tracking rate and, therefore, the phantom rate from acquired aircraft cannot result in acquisition of a phantom aircraft. If the ID is valid and the aircraft is being tracked, the data are acceptable only if the phantom data occurs at the correct time and the true associated data do not occur.

The likelihood of phantom ID's reaching the surveillance data are extremely slight. The effect of phantom ID on the surveillance data is, even then, only a temporary increase in surveillance position error. Phantom ID problems are not an asynchronous surveillance system problem for the select system coding and mechanization scheme.

Ambiguous detection can occur due to phantom ID's (unlikely) or due to multipath effects. If ambiguous detection occurs during the acquisition phase, no effects on the initial surveillance position will result. Because only four TOA's are used for the position computation associated with acquisition, the presence of a single ambiguous detection will result in the selection of some other links for the TOA data. Ambiguous detection during tracking is unlikely due to window tracking, but the effect of simply eliminating the data is the same as for a missed detection.

During the tracking phase, received ID/TOA data are subjected to window tracking. After the ID/TOA data are received, the data are tested to see if they occur $8 \pm \delta$ sec after the last data. Here δ is selected to account for the maximum time uncertainty due to aircraft and satellite motion and measurement uncertainties . If unambiguous detection occurs, the next window time is set at $8 \pm \delta$ sec later. If ambiguous or missed detection occurs, the window is increased to $\pm 2\delta$ and finally $\pm 3\delta$ for the second occurrence. If the window is $\pm 3\delta$, ambiguous detection caused no change in the window; missed detection causes loss-of-lock for the channel.

The probability of unambiguous detection is a fundamental measure of the air-to-satellite-to-ground surveillance system. A mathematical model of the satellite surveillance scheme was developed to guide the selection of the coding scheme and RF link parameters. This model also allows evaluation of the selected system. Although a number of different aspects of the surveillance system were studied (see Ref. 1), only the effect of the number of PN pulses in an identification sequence (n) and the number PN codes per pulse (Cn) will be considered here. (The references for this section are presented in Section 2.5.)

The effect of varying n, the number of pulses per ID sequence, causes two conflicting events with respect to unambiguous detection. Clearly, if n is increased, the S/N ratio required to achieve a given performance level decreases since the energy is increased (analogous to post-detection integration radar systems). Conversely, increasing n causes more pulses for a given user population, thereby increasing the multi-access noise.

The performance sensitivity of the model to the number of codes per PN pulse was extremely small. An arbitrarily small number of codes (16) was planned. This eases the problem of finding codes with good orthogonality properties, i.e., good autocorrelation and cross-correlation properties. These correlation properties are expected to have large impacts on the actual performance.

The model used assumed that no coherent, i.e., no absolute phase reference, AMF's are used to detect individual pulses. This technique is used, rather than whole sequence detection, because of the difficulty in mechanizing whole sequence identification and because of phase and frequency instability in long codes.

The model also assumed that the multi-access noise to any AMF was band-limited, Gaussian, white noise. The assumption was made to obtain a relationship between noise and pulse detection probability statistics. Some evidence that as much as a 6 db error may result from this assumption has been noted (Ref. 2). That study was based on a particular coding scheme which is not representative of the selected scheme. The applicability of that analysis to the selected coding scheme is uncertain. This area requires further study to settle the uncertainty in the selected assumption.

The number of active aircraft (N_A), the surveillance pulse repetition interval (T_{ave}), the bandwidth of the system, and the average received energy per pulse also were modeled. The multi-access noise was assumed to be independent of the omni-present thermal noise, and both noises are combined to yield the total background noise.

The results of the model runs on the probability of unambiguous detection for the three-pulse code is shown in Fig. 2.2-4. Here the lower bound on probability of unambiguous detection is plotted versus S/N ratio. For a 13 db S/N ratio, this probability exceeds 0.998. This assumes that four out of four satellites are required to achieve error-free detection.

The selected power budget to achieve the required S/N ratio plus margin is shown in Table 2.2-1. This budget is based on a geosynchronuous satellite. The effect of varying n for this budget is shown in Tables 2.2-2 and 2.2-3 for 35,000 and 100,000 active users, respectively.

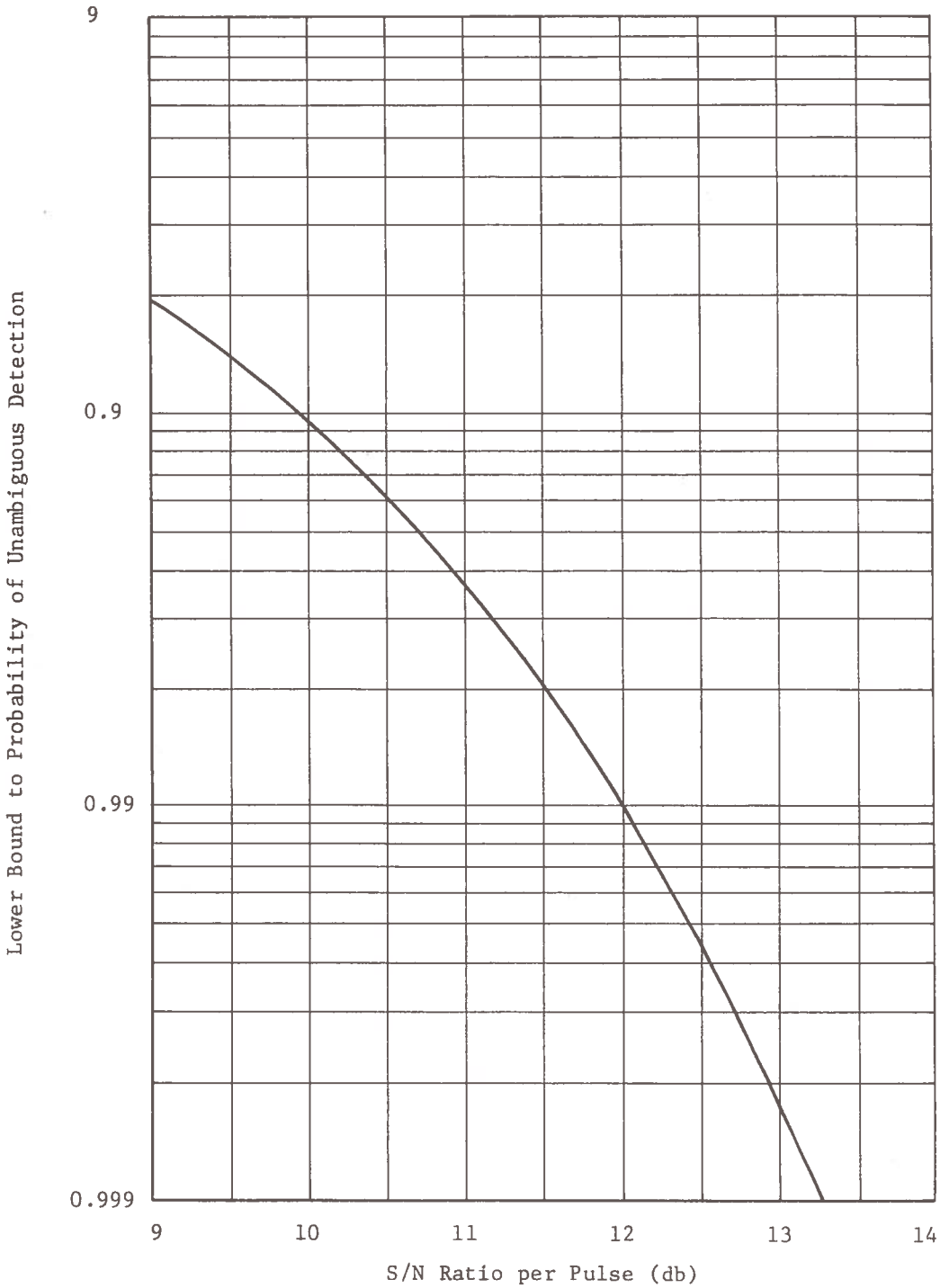

Fig. 2.2-4. Probability of Unambiguous Detection

Table 2.2-1. Surveillance Uplink (L1) Power Budget for Geostationary Satellite Channel

Parameter	Power
Transmitted Energy Per Pulse (2 kw for 40 μsec)	-11.0 dbj
Aircraft Antenna Gain	4.0 db
Satellite Antenna Gain (10 deg beam; 70 percent Efficiency)	24.6 db
Pointing Losses	1.0 db
Miscellaneous Losses (Plumbing = 1 db, Attenuation = 1 db)	2.0 db
Path Loss (f = 1.6 GHz, d = 26,000 mi)	189.0 db
Received Signal Energy per Pulse	-174.4 dbj
Effective Multi-Access Noise Power Density	-204.2 dbw/Hz
($N_A = 3.5 \times 10^4$ aircraft, $\frac{n}{T} = \frac{3 \text{ pulses}}{5 \text{ sec}}$, Bandwidth = 20 MHz)	
Receiver Noise Density	-201.0 dbw/Hz
Total Background Noise	-199.3 dbw/Hz
Downlink Degradation (100 w Transmitted Power; 10 ft ground antenna)	0.1 db
Detection Loss (Limiter and Decorrelation)	2.0 db
S/N Ratio/Pulse	22.8 db
Required S/N Ratio	13.0 db
Margin	9.8 db

Table 2.2-2. Effect of n for 35,000 Users

n	Multi-Access Noise (db/Hz)	Background Noise (db/Hz)	S/N Ratio per Pulse (db)	Required S/N Ratio (db)	Margin (db)
2	-206.0	-199.8	23.3	14	9.3
3	-204.2	-199.3	22.8	13	9.8
4	-203.0	-198.9	22.3	12.5	9.8
5	-202.0	-198.5	22.0	12.2	9.8

Table 2.2-3. Effect of n for 100,000 Users

n	Multi-Access Noise (db/Hz)	Background Noise (db/Hz)	S/N Ratio per Pulse (db)	Required S/N Ratio (db)	Margin (db)
2	-202.4	-198.6	22.1	14	8.1
3	-200.6	-197.8	21.3	13	8.3
4	-198.4	-196.5	20.0	12.5	7.5
5	-197.4	-195.5	19.3	12.2	7.1

It should be noted that the constellation GDOP nominal studies were performed using an equivalent S/N ratio of 16.0 db. This is 6.8 db less than the available S/N ratio of 22.8 for 35,000 users and 5.3 db less for 100,000 users. The GDOP visibility results are, therefore, very conservative for the assumed RF power budget and multi-access noise assumptions. Even if the effect of the multiple access noise is off by several db, there appears to be several db margin available before the onset of even minor surveillance degradation. The S/N margin can be further increased by using multiple beam antennas at each satellite. If two beams are used, each with twice the gain of the single beam case, the S/N ratio increases by approximately 1.5 db.

2.3 Surveillance Mechanization Concept

The mechanization and software requirements for the surveillance subsystem have been investigated and a unique solution to the problem has evolved. A method has been proposed which will allow the application of filtering techniques to a large number of users without the usually attendant computer complexity. This method provides substantially improve accuracy over the more usual deterministic surveillance mechanization.

Figure 2.3-1 is a block diagram of the surveillance subsystem mechanization concept. Five major elements have been identified as containing the bulk of the software requirements, as follows: the TOA correction software, the acquisition algorithm, the surveillance tracking algorithm, the regional gain and calibration algorithm, and the acquisition correlator. This latter task and the other bookkeeping functions are considered in detail in a later section.

The TOA corrector includes all pre-processing of the TOA data for use in surveillance tracking. This includes correcting the signals for delays due to ionospheric and tropospheric effects, due to downlink pseudo-range adjustments arising from satellite motion, and due to calibrated equipment. In addition, the corrector processes signals for window tracking consideration prior to using the data as inputs to the tracking filter.

The acquisition position computer contains the software mechanization required to enter a newly acquired aircraft into the surveillance system. Since no prior estimate of the entering aircraft's position is available, the function performed by this algorithm is to initialize the aircraft position on the basis of measured TOA's. A whole value algorithm based on an explicit closed form solution to the hyperbolic position determination equation is used in this mode. This mode allows extremely rapid acquisition to take place since only four TOA measurements are required.

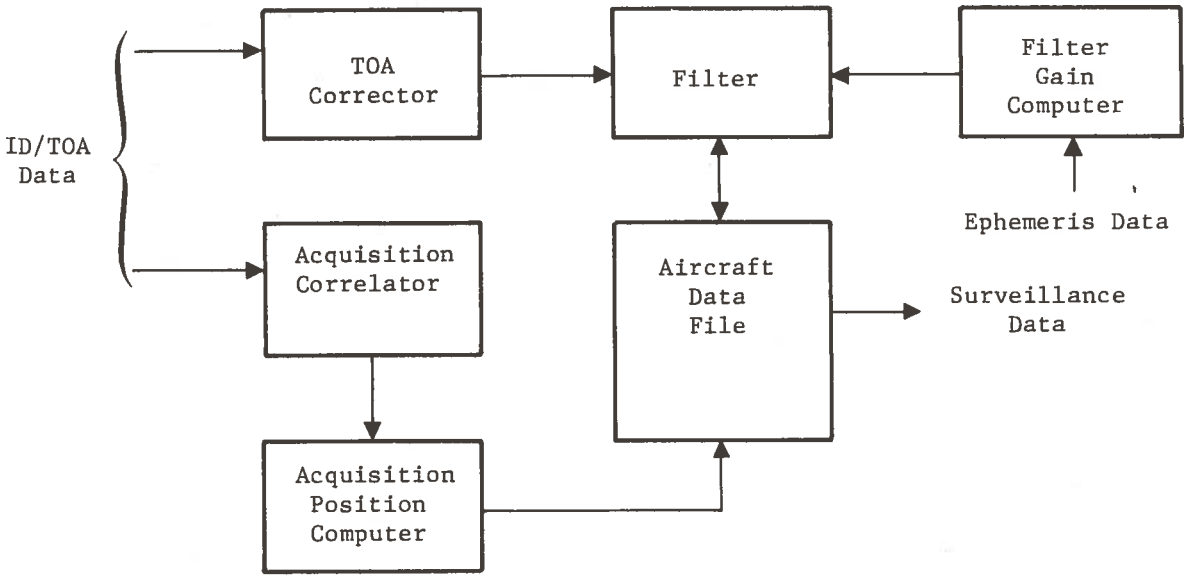

Fig. 2.3-1. Surveillance Mechanization Block Diagram

The primary task of surveillance is to keep the aircraft state vector (vector of positions and velocities) updated. A suboptimal Kalman recursive filter was selected due to its inherent accuracy. The filter processes scalar-valued TOA difference measurements since the filter size can thus be fixed regardless of the number of visible satellites. This algorithm is well suited for optimally combining successive position estimates, providing optimal velocity estimates, and providing for variable satellite visibility.

The more usual method of updating the aircraft state vector is to use the method selected for the acquisition mode. This deterministic method suffers from several disadvantages with respect to the proposed method. The basic deterministic algorithm employs only four TOA measurements per update. Since more than four satellites are always visible, the excess information is simply ignored. The state vector computed by the deterministic solution does not include velocity states. An outboard filter or curve fitting routine must be implemented to estimate the velocity states.

A major modification to the deterministic filter is required to achieve the same state vector from the basically overdetermined data set available. This requires a substantial amount of software. This same criticism also applies to the normal filter routine due to the amount of data storage required to implement the usual filter algorithm. A modification to this normal routine will allow substantial software simplification.

In practice, it is known that the convergence of the Kalman estimate state vector is not very sensitive to the Kalman gain matrix. An approximation to the correct gain matrix primarily affects the transient performance of the filter. This factor can be utilized to substantially reduce the complexity of the Kalman filter routine.

Since the Kalman gain matrix is determined by the user-satellite geometry, a single set of gains can be computed for all aircraft in a given geographic region. This is possible since the gain matrix is a weak function of the user's location within restricted geographic regions. Further, the gains do not change rapidly with time. Since a major portion of the Kalman algorithm software is involved in the computation of the proper gains, a substantial speed and storage processing gain can be achieved at a slight cost in accuracy.

To compensate for correlated system errors in high density airspace, a calibration station concept is employed. This routine corrects certain errors such that improved absolute surveillance accuracy can be achieved.

2.3.1 Surveillance TOA Model

Figure 2.3-2 depicts the geometry of a typical surveillance signal path for a pulse emitted by the aircraft and received by the ground tracking system. The user transmits a pulse at time τ_n when at position $\underline{P}(\tau_n)$. This pulse is transponded by a satellite at time T_n later and received and measured by the ground system at a still later time, T_{gn}. The measured time of arrival is related to the pulse transmission time, the refraction delays, and the scalar transmission distances corresponding to the uplink and downlink signal paths by Eq. (1) and (2).

$$T_{gn} = T_n + \eta_{gn} + \frac{1}{C} \; || \; \underline{S}(T_n) - \underline{R}_g(T_{gn}) \; || \tag{1}$$

$$T_n = \tau_n + \eta_n + \frac{1}{C} \; || \; P(\tau_n) - \underline{S}(T_n) \; || \tag{2}$$

where

T_{gn} = Time-of-arrival at ground station

T_n = Time the signal was transponded by the satellite

τ_n = Time the pulse was emitted by the aircraft

η_{gn} = Downlink refraction delays due to the ionosphere and troposphere

η_n = Uplink refraction delays due to the ionosphere and troposphere

$\underline{S}(T_n)$ = Satellite position vector at time τ_n when pulse is transponded

$\underline{R}_g(T_{gn})$ = Ground receiving antenna position vector at time of signal reception. (This position vector is constant in the earthfixed coordinate frame in which surveillance computation will be performed.)

C = Propagation speed of light

$\underline{P}(\tau_n)$ = Position vector of aircraft at time τ_n pulse is emitted

$|| \; \underline{S}(\tau_n) - \underline{R}_g(T_{gn}) \; ||$ = Range between satellite at τ_n and ground antenna at τ_{gn}

$|| \; \underline{P}(\tau_n) - \underline{S}(T_n) \; ||$ = Range between aircraft at time τ_n and satellite at time τ_n

$|| \; ||$ = Euclidian norm of the vector

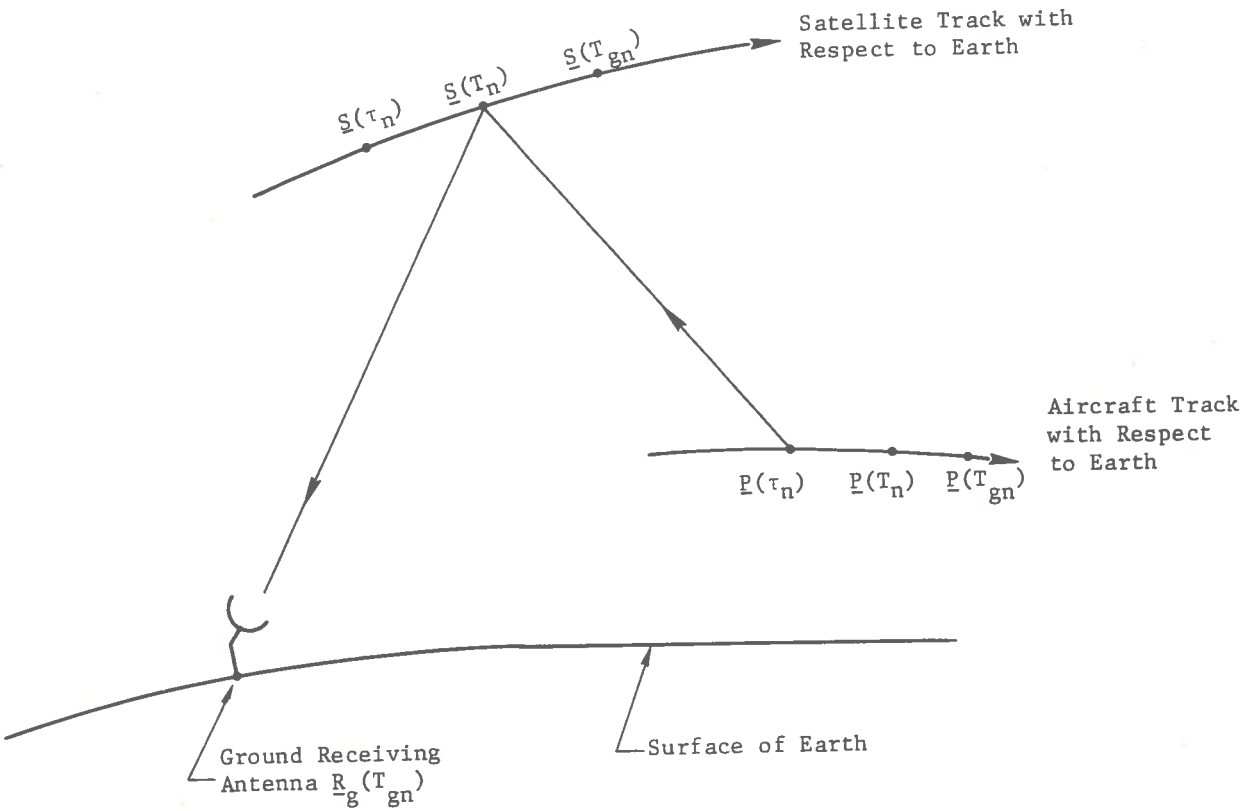

Fig. 2.3-2. Geometry of Surveillance Signal Path

Assuming a set of K satellites visible to a given aircraft, there will be K equations of the form of Eq. (1) and (2). The unknown parameters are the three components of aircraft position $\underline{P}(\tau_n)$, the initial pulse transmission time τ_n, and the time the signal is transponded from the satellite, T_n. Together, there are five parameters and two equations per measurement. This is reduced to one measurement equation and four parameters by eliminating T_n.

Equations (1) and (2) are combined to yield a single measurement equation with T_{gn} related directly to the uplink and downlink transmission distances. Thereby, in effect, the unknown pulse transponding time T_n is eliminated. This is accomplished not without a certain amount of pre-processing computation. For satellites at synchronous altitudes, a valid approximation (less than 1 ft) to T_n is obtained by solving Eq. (1) as follows:

$$T_n \simeq T_{gn} - \eta_{gn} - \frac{1}{C} P_{gn} + \frac{P_{gn}\, \underline{L}_n^T}{C^2}\, \dot{\underline{S}}(T_{gn}) \tag{3}$$

where

$$P_{gn} \equiv || \underline{S}(T_{gn}) - \underline{R}_g(T_{gn}) || = \text{Pseudo downlink signal path length at measurement time } T_{gn}$$

$$\underline{L}_n \equiv \frac{\underline{S}(T_{gn}) - \underline{R}_g(T_{gn})}{(||\underline{S}(T_{gn}) - \underline{R}_g(T_{gn})||)} = \text{Unit direction vector of downlink path}$$

$$\dot{\underline{S}}(T_{gn}) = \text{Velocity of satellite computed from ephemeris at } T_{gn}$$

Substituting Eq. (3) into Eq. (2), the measurement equation is given by Eq. (4) (where T_n has been eliminated).

$$T_{gn} - \eta_{gn} - \frac{1}{C} P_{gn} + \frac{P_{gn}\, \underline{L}_n^T}{C^2}\, \dot{\underline{S}}(T_{gn}) = \tau_n + \eta_n + \frac{1}{C} || \underline{P}(\tau_n) - \underline{S}(T_n) || \tag{4}$$

Equation (4) is next cast into a slightly different form. By transposing the known terms, both measurable and computable on the left side and the unknown terms τ_n and $\underline{P}(\tau_n)$ on the right side, one can write the equation as

$$T_{S_n} = \tau_n + \frac{1}{C} \left\| \underline{P}(\tau_n) - \underline{S}(T_n) \right\| \tag{5}$$

where the left side is the measured and/or computed term.

$$T_{S_n} = T_{gn} - \eta_{gn} - \eta_n - \frac{1}{C} P_{gn} + \frac{P_{gn} \underline{L}_n^T}{C^2} \dot{\underline{S}}(T_{gn}) \tag{6}$$

This is the desired measurement equation basic to the present surveillance problem. It is assumed the refraction delays are modeled and computed during the signal preprocessing mode. The unknown parameters to be estimated at this point are the three components of the position vector and the initial pulse transmission time, τ_n. All other parameters in this equation are either measured or computed during preprocessing. As can be seen in this equation, the preprocessing software can be considerable. It includes correcting the TOA measurable for refraction delays, downlink signal transmission time, and motion of satellite during downlink transmission time. This latter correction contributes about 3,000 ft to the range equation; therefore, it cannot be ignored in the measurement model.

2.3.2 Acquisition Algorithm

Having developed the basic measurement equation connecting the TOA to aircraft position, the next problem is to consider computational techniques required for obtaining position. This section considers the algorithm to be used during the acquisition phase.

In the initial phase when the aircraft first enters the surveillance system, no a priori estimate of its position is available to the system. To determine initial position, a whole value algorithm based on a closed form solution to a set of equations obtained from Eq. (5) is used. Suppose there is a set of K satellites transponding a given aircraft pulse. This results in the K equations (Eq. 7).

$$\begin{aligned}
T_{S_{n1}} &= \tau_n + \frac{1}{C} \left\| \underline{P}(\tau_n) - \underline{S}_1(T_{n1}) \right\| \\
T_{S_{n2}} &= \tau_n + \frac{1}{C} \left\| \underline{P}(\tau_n) - \underline{S}_2(T_{n2}) \right\| \\
&\vdots \qquad\qquad \vdots \qquad\qquad \vdots \\
T_{S_{nk}} &= \tau_n + \frac{1}{C} \left\| \underline{P}(\tau_n) - S_k(T_{nk}) \right\|
\end{aligned} \tag{7}$$

where $T_{S_{ni}}$ $(i = 1, 2, \ldots, k)$ is obtained from Eq. (6).

In the particular case of just four measurements, Eq. (7) is deterministic, reducing to a problem of solving four equations in the four unknowns $\underline{P}(T_n)$ and τ_n. Closed form solutions are available for this special case. The particular solution considered here is given by Puri using time-of-arrival differences. Figure 2.3-3 gives the complete acquisition algorithm based on this solution.

Denoting satellite number one as a reference, three TOA differences can be computed from Eq. (7) relative to the reference satellite.

$$
\begin{aligned}
d_1 &= T_{S_{n1}} - T_{S_{n2}} = \frac{1}{C} \left\| \underline{P}(\tau_n) - \underline{S}_1(T_{n1}) \right\| - \frac{1}{C} \left\| \underline{P}(\tau_n) - \underline{S}_2(T_{n2}) \right\| \\
d_2 &= T_{S_{n1}} - T_{S_{n3}} = \frac{1}{C} \left\| \underline{P}(\tau_n) - \underline{S}_1(T_{n1}) \right\| - \frac{1}{C} \left\| \underline{P}(\tau_n) - \underline{S}_3(T_{n3}) \right\| \qquad (8) \\
d_3 &= T_{S_{n1}} - T_{S_{n4}} = \frac{1}{C} \left\| \underline{P}(\tau_n) - \underline{S}_1(T_{n1}) \right\| - \frac{1}{C} \left\| \underline{P}(\tau_n) - \underline{S}_4(T_{n4}) \right\|
\end{aligned}
$$

where $T_{S_{ni}}$ $(i = 1, 2, 3, 4)$ are obtained from Eq. (6)

These are the so-called hyperbolic position fix equations. The position vector $\underline{P}(\tau_n)$ is uniquely determined from this set provided that the four satellite positions are not coplanar.

To solve this set for $\underline{P}(\tau_n)$, Eq. (8) is transformed into the following equation, originally derived by Puri.

$$
\underline{A}_i \cdot P_1 \underline{L}_1 = P_1 d_i - \frac{1}{2} (d_i^2 - \underline{A}_i^2) \qquad (9)
$$

where

i = (2, 3, 4)

$\underline{A}_i$ = $\underline{S}_1(T_{n1}) - \underline{S}_i(T_{ni})$ where $i = 2, 3, 4$

$\underline{S}_i(T_{ni})$ = Position of satellite i at the time it transponds

$\underline{S}_1(T_{n1})$ = Reference satellite position at the time it transponds

P_1 = Range from aircraft to reference satellite (to-be-determined)

P_i = Range from aircraft to the i^{th} satellite

$\underline{L}_1$ = Unit direction vector from aircraft to reference satellite

$$\equiv \frac{\underline{S}_1(T_{n1}) - \underline{P}(\tau_{n1})}{(||\underline{S}_1(T_{n1}) - \underline{P}(\tau_{n1})||)} \quad \text{Unknown (to be determined)}$$

$$d_i = C(\tau_{S_{n1}} - T_{S_{nj}}) \quad \text{where } j = 2, 3, 4$$

From Eq. (9), the following system of three equations in the three unknowns $P_1\underline{L}_1$ can be obtained.

$$\begin{aligned} A_2 \cdot P_1\underline{L}_1 &= P_1 d_1 - \frac{1}{2}(d_2^2 - A_2^2) \\ A_3 \cdot P_1\underline{L}_1 &= P_1 d_3 - \frac{1}{2}(d_3^2 - A_3^2) \\ A_4 \cdot P_1\underline{L}_1 &= P_1 d_4 - \frac{1}{2}(d_4^2 - A_4^2) \end{aligned} \tag{10}$$

This set is solved for $P_1\underline{L}_1$ from which aircraft position is obtained. Let the components of the vector $P_1\underline{L}_1$ be defined as

$$\underline{P}_1 \equiv P_1\underline{L}_1 \equiv \begin{bmatrix} P_{1x} \\ P_{1y} \\ P_{1z} \end{bmatrix} \tag{11}$$

The set in Eq. (10) is written as the matrix equation.

$$\begin{bmatrix} A_{x1} & A_{y1} & A_{z1} \\ A_{x2} & A_{y2} & A_{z2} \\ A_{x3} & A_{y3} & A_{z3} \end{bmatrix} \begin{bmatrix} P_{1x} \\ P_{1y} \\ P_{1z} \end{bmatrix} = P_1 \begin{bmatrix} d_1 \\ d_2 \\ d_3 \end{bmatrix} - \frac{1}{2} \begin{bmatrix} d_1^2 - \underline{A}_1 \cdot \underline{A}_1 \\ d_2^2 - \underline{A}_2 \cdot \underline{A}_2 \\ d_3^2 - \underline{A}_3 \cdot \underline{A}_3 \end{bmatrix} \tag{12}$$

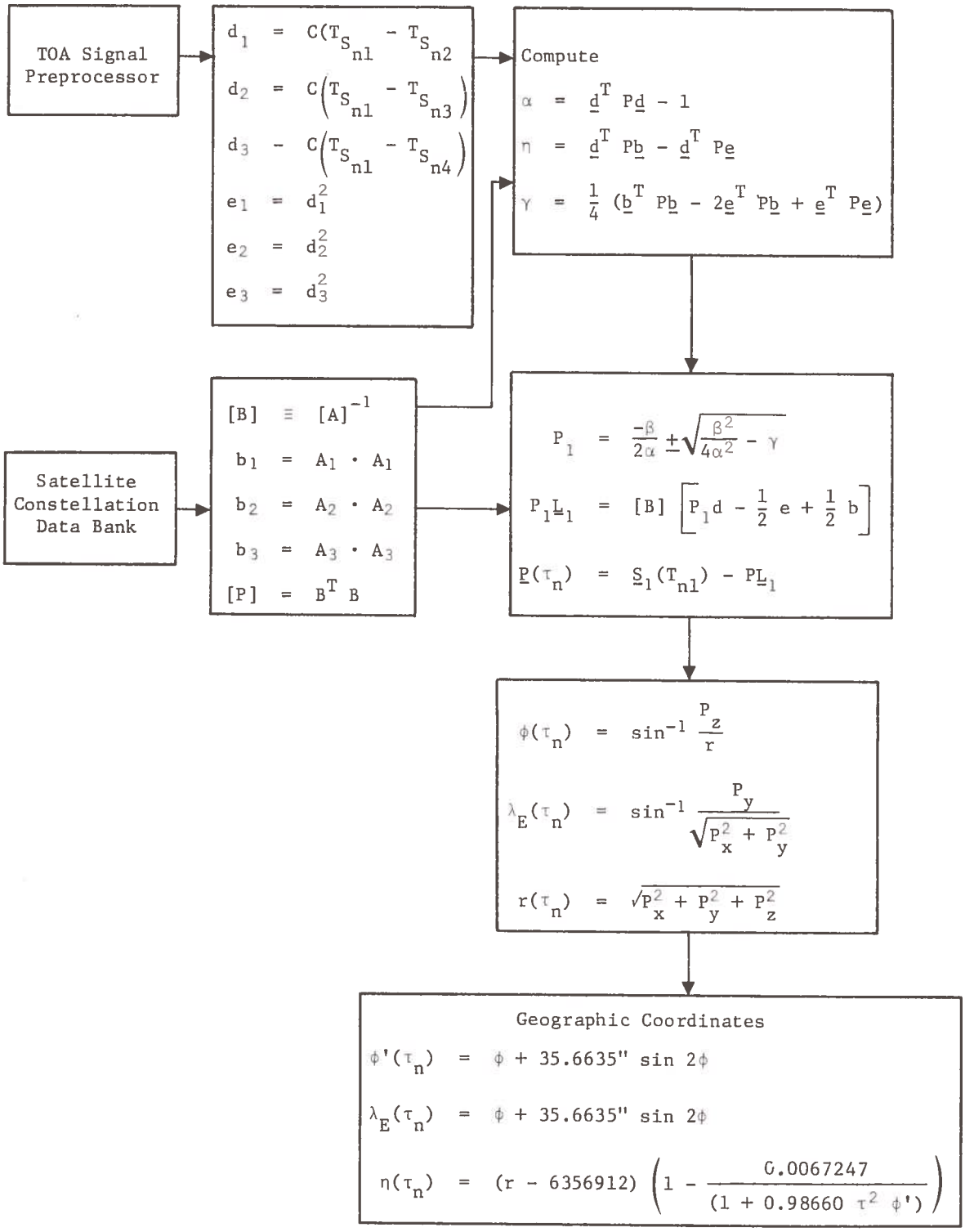

Fig. 2.3-3. Surveillance Acquisition Algorithm

Or more simply as

$$[A]\,\underline{P}_1 = P_1\underline{d} - \frac{1}{2}\,\underline{e} + \frac{1}{2}\,\underline{b} \tag{13}$$

$\underline{P}_1$ is then obtained from Eq. (13).

$$\underline{P}_1 = [A]^{-1}\,[P_1\underline{d} - \frac{1}{2}\,\underline{e} + \frac{1}{2}\,\underline{b}] \tag{14}$$

where

$$[A]^{-1} = \frac{1}{\underline{A}_1 \cdot \underline{A}_2 \times \underline{A}_3}\left[\underline{A}_2 \times \underline{A}_3 \,\middle|\, \underline{A}_3 \times \underline{A}_1 \,\middle|\, \underline{A}_1 \times \underline{A}_2\right] \tag{15}$$

The scalar magnitude of $\underline{P}_1$ is obtained from solving the quadratic

$$\alpha P_1^2 + \eta P_1 + \gamma = 0 \tag{16}$$

where

$$\alpha = \underline{d}^T P\underline{d} - 1$$

$$\eta = \underline{d}^T P\underline{b} - \underline{d}^T P\underline{e}$$

$$\gamma = \frac{1}{4}\,(\underline{b}^T P\underline{b} - 2\underline{e}^T P\underline{b} + \underline{e}^T P\underline{e})$$

This yields the solution

$$P_1 = \frac{-\beta \pm \sqrt{\beta^2 - 4\alpha\gamma}}{2\alpha} \tag{17}$$

where the sign ambiguity is easily resolved.

Having determined P_1, its vector value is determined from Eq. (14). Finally, position is obtained from

$$\underline{P}(T_n) = S_1(T_{n1}) - P_1\underline{L}_1 \tag{18}$$

If the satellite coordinates are expressed in the earth centered fixed frame, the geocentric latitude ϕ and east longitude λ_E are obtained from the following:

$$\phi(\tau_n) = \sin^{-1} \frac{P_z}{r}$$

$$\lambda_E(\tau_n) = \sin^{-1} \frac{P_y}{\sqrt{P_x^2 + P_y^2}} \qquad (19)$$

$$r(\tau_n) = \sqrt{P_x^2 + P_y^2 + P_z^2}$$

where

P_x, P_y, P_z are the components

$\underline{P}(\tau_n)$ is the earth centered fixed frame

The corresponding geographic latitude and altitude are obtained from standard formulas of the oblate earth.

When the set in Eq. (7) is overdetermined, that is, when more than four measurements are available, the redundancy can be utilized to provide a solution with better accuracy. This is accomplished by partitioning the set of measurements into groups of four. Each group is simply averaged, and the Puri method is applied to the partitioned set. Puri's original solution can be shown to be singular when the satellites are in a coplanar configuration. The poorly conditioned geometry of this configuration is minimized by partitioning. Furthermore, random measurement TOA errors are reduced by averaging.

2.3.3 Surveillance Tracking Algorithm

The Kalman mechanization depends upon linearizing the TOA measurement, Eq. (5), with respect to a nominally estimated aircraft position. Let $\underline{P}^*(\tau_n)$ be the predicted aircraft position vector. Then Eq. (5) is written as

$$T_{S_n} = \tau_n + \frac{1}{C} \left\| \underline{P}^*(\tau_n) + \underline{P}(\tau_n) - P^*(\tau_n) + \underline{S}(T_n) \right\| \qquad (20)$$

Assuming the error in the estimate, $\underline{P}(\tau_n) - \underline{P}^*(\tau_n)$, is relatively small, the following equation is obtained upon linearizing Eq. (20).

$$\hat{T}_{S_n} \simeq \tau_n + \frac{1}{C} \left|\left| \underline{P}^*(\tau_n) - \hat{\underline{S}}(T_n) \right|\right| + \frac{1}{C} \underline{U}_n^T \left[\underline{P}(\tau_n) - \underline{P}^*(\tau_n)\right] \tag{21}$$

where

$$\underline{U}_n = \frac{P^*(\tau_n) - \hat{\underline{S}}(T_n)}{(||P^*(\tau_n) - \hat{S}(T_n)||)} = \text{unit direction vector between the satellite and the aircraft}$$

$(\hat{\ })$ = Symbol used to denote computed or estimated value

The computational and measurement errors associated with $\hat{T}_{S_n}$ are not shown. Adding a subscript k to denote the particular satellite type can be expressed as

$$\hat{T}_{Sn_k} = \tau_n + \frac{1}{C} \left|\left| \underline{P}^*(\tau_n) - \hat{\underline{S}}_k (T_{n_k}) \right|\right| + \frac{1}{C} \underline{U}_{n_k}^T \left[\underline{P}(\tau_n) - P^*(\tau_n)\right]$$

The unknown parameters in this equation are τ_n and the coordinates of $P(\tau_n) - P^*(\tau_n)$. To simplify the surveillance algorithm, τ_n is eliminated by differencing $\hat{T}_{Sn_k}$ with two measurements. This yields the equation

$$\hat{T}_{Sn_k} - \hat{T}_{Sn_{k+1}} = \frac{1}{C} \left|\left| \underline{P}^*(\tau_n) - \hat{\underline{S}}_k (T_{n_k}) \right|\right| - \frac{1}{C} \left|\left| \underline{P}^*(\tau_n) - \hat{\underline{S}}_{k+1} (T_{n_{k+1}}) \right|\right|$$

$$+ \frac{1}{C} \left(\underline{U}_{n_k}^T - \underline{U}_{n_{k+1}}^T \right) \left[\underline{P}(\tau_n) - \underline{P}^*(\tau_n)\right] \tag{23}$$

Transferring the known parameters on the left side, this equation is written in the form

$$y_n = M_n X_n + \varepsilon_n \tag{24}$$

where

$$y_n = \hat{T}_{Sn_k} - \hat{T}_{Sn_{k+1}} - \frac{1}{C} \left\| P^*(\tau_n) - \hat{S}_k\,(T_{n_k}) \right\| + \frac{1}{C} \left\| \underline{P}^*(\tau_n) - \hat{\underline{S}}_{k+1}\, T_{n_{k+1}} \right\|$$

$$M_n = \left[\frac{1}{C} \left(\underline{U}^T_{n_k} - \underline{U}^T_{n_{k+1}} \right) 0\ 0\ 0 \right]$$

$$X_n = \begin{matrix} \underline{P}(\tau_n) - \underline{P}^*(\tau_n) \\ \underline{V}(\tau_n) - \underline{V}^*(\tau_n) \end{matrix}$$

ε_n = Random measurement error of zero mean

$\underline{V}(\tau_n) \equiv$ Aircraft velocity

$\underline{V}^*(\tau_n) \equiv$ Predicted aircraft velocity

The transition equation for the state X_n is modeled as

$$X_n = \phi_{n_{n-1}} X_{n-1} + \underline{U}_n$$

$$\phi_{n_{n-1}} = \left[\begin{array}{c|c} I_z & \Delta T_n I_z \\ \hline 0_z & I_z \end{array} \right]$$

$$\Delta T_n = T_n - T_{n-1} \qquad (25)$$

$$\underline{U}_n = \begin{bmatrix} \underline{0} \\ W_n \end{bmatrix}$$

$\underline{W}_n$ = Random uncorrelated aircraft velocity error of zero mean

The Kalman estimation equations are developed from the more easily understood maximum likelihood estimator. Given the following equations

$$y_n = M_m X_n + \varepsilon_n \tag{26}$$

$$\hat{X}'_n = X_n + \Delta \hat{X}'_n \tag{27}$$

Where Eq. (26) is the scalar measurement equation obtained from the TOA difference computed in Eq. (23), $\hat{X}'_n$ is the predicted state, and $\Delta\hat{X}'_n$ is the error in the prediction. Combining these equations into a single equation

$$\begin{bmatrix} Y_n \\ \hat{X}'_n \end{bmatrix} = \begin{bmatrix} M_n \\ I \end{bmatrix} X_n + \begin{bmatrix} \varepsilon_n \\ \Delta\hat{X}'_n \end{bmatrix} \tag{28}$$

This set is always overdetermined with respect to the number of parameters in X_n. Assuming the prediction error $\Delta\hat{X}'_n$ is a zero mean, uncorrelated, random variable, a maximum likelihood estimate of Eq. (28) is obtained as follows. Writing the overdetermined set in the form

$$Y^*_n = M^*_n X_n + \varepsilon^*_n$$

The maximum likelihood estimator is

$$\hat{X}_n = \left[M^{*T}_n \; W \; M^*_n\right]^{-1} M^{*T}_n \; W \; y^*_n \tag{29}$$

By substituting in Eq. (28), this equation reduces to

$$\hat{X}_n = \left[M^T_n \; C^{-1}_{\varepsilon_n} \; M_n + C^{-1}_{\Delta\hat{X}'_n}\right]^{-1} \left[M^T_n \; C^{-1}_{\varepsilon_n} \; y_n + C_{\Delta\hat{X}'_n} \; \hat{X}'_n\right] \tag{30}$$

where

$$C_{\Delta\hat{X}'_n} = E(\Delta X'_n \; \Delta X'^T_n)_{6\times6}$$

$$C_{\varepsilon_n} = E(\varepsilon_n \varepsilon^T_n) = \text{scalar for single TOA differences measurement}$$

$$M_n = \frac{1}{C}\left(\underline{U}^T_{n_k} - \underline{U}^T_{n_{k+1}} \quad 0 \quad 0 \quad 0\right)_{1\times6}$$

Equation (30) shows how a predicted estimate of the state $\hat{X}'_n$ is optimally combined with the measurable, y_n. This form is undesirable for an algorithm if the number of measurables in the vector y_n is less than the rank of X_n. In the present mechanization, the rank of y_n is one and the rank of X_n is six. Therefore, Eq. (30) is transformed as follows. It can be shown that the matrix in Eq. (30) is equivalent to

$$\left[M_n^T C_{\varepsilon_n}^{-1} M_n + C_{\Delta\hat{X}'_n}^{-1}\right]^{-1} M_n^T C_{\varepsilon_n}^{-1} = C_{\Delta\hat{X}'_n} M_n^T \left[M_n C_{\Delta\hat{X}'_n} M_n^T + C_{\varepsilon n}\right]^{-1} \qquad (31)$$

The latter matrix formulation is obviously simpler when y_n is a scalar.

Substituting Eq. (31) into Eq. (30), the estimation equation reduces to Eq. (32) and is the Kalman gain filter.

$$\hat{X}_n = (I - K_n M_n)\, \hat{X}'_n + K_n y_n \qquad (32)$$

where

$$K_n = C_{\Delta\hat{X}'_n} M_n^T \left[M_n C_{\Delta\hat{X}'_n} M_n^T + C_{\varepsilon_n}\right]^{-1}$$

$$C_{\Delta\hat{X}'_n} = \phi_{n_{n-1}} C_{\Delta\hat{X}_{n-1}} \phi^T_{n_{n-1}}$$

$$C_{\Delta\hat{X}_n} = (I - K_n M_n)\, C_{\Delta\hat{X}'_n}$$

Note here that the inverse matrix is a scalar, hence essentially no matrix inversion is required in this formulation.

Recognizing that the set of equations must be computed for each aircraft, it becomes obvious the software requirements for surveillance can be enormous. Thus, every effort was made to seek simplification of the equations. One simplification which appears to have considerable promise is to simplify the Kalman gain update routine. Indeed, if the gain matrix is held constant with time and over some geographic area, this in itself will effect a tremendous software savings.

From Eq. (32), the gain matrix update is written as

$$
\begin{aligned}
M_n &= \left[\begin{array}{c|ccc} \frac{1}{C}\ \underline{U}^T_{n_k} - \underline{U}^T_{n_{k+1}} & 0 & 0 & 0 \end{array}\right] \\
C_{\Delta\hat{X}'_n} &= \phi_{n_{n-1}}\, C_{\Delta\hat{X}_{n-1}}\, \phi^T_{n_{n-1}} \\
K_n &= C_{\Delta\hat{X}'_n}\, M^T_n \left[M_n\, C_{\Delta\hat{X}'_n}\, M^T_n + C_{\varepsilon_n}\right]^{-1} \\
C_{\Delta\hat{X}_n} &= (I - K_n M_n)\, C_{\Delta\hat{X}'_n}
\end{aligned}
\tag{33}
$$

For a given satellite pair, k and k+1, the elements of M_n will remain nearly constant a fairly wide interval of time and over a large ground area. This is apparent upon drawing the unit direction vectors to scale for synchronous altitude satellites. Since the measurement covariance error C_{gn} is assumed to be constant in the mechanization for all measurements, the gain matrix K_n can be approximated as a constant matrix for any given satellite pair. These values are stored in a gain matrix bank and used for all aircraft flying in the geographic area during this time interval. Periodically, the gains must be updated because the relative configuration of the satellite constellation appearing over the ground area will have changed.

It would appear that both position and velocity can be estimated via this suboptimal Kalman filter. The velocity estimates, however, will tend to have longer settling time to reach steady-state values primarily because they depend upon the time-rate-of-change of the TOA measurements.

Justification of why this suboptimal mechanization will work for the surveillance problem can be given qualitatively. In general, small changes in the gains from their correct values do not affect the convergence of the estimation to the true state. It only increases the settling time to reach steady state. Furthermore, the gains are primarily a function of the unit direction vectors from the aircraft to a given satellite. For synchronous satellites, these vectors are nearly constant over a fairly large ground area (typically 200 nmi square) and over a wide range in time (typically several minutes) and, hence, change very slowly with time and position. Taking advantage of this fact, a suboptimal Kalman mechanization would use constant gain values based on area, the particular satellite, and time. Thus, two aircraft in the same region transmitting to the same satellite essentially use the same gains.

The implications of this simplification as it applies to the surveillance problem is obvious. Needless to say, a tremendous saving in software is possible for updating the surveillance data of a large number of aircraft. Furthermore, processing speed is enhanced because the gain computation can be performed off line, independent of any given aircraft.

The gains are computed open loop as a function of time for different predetermined grid areas. For each grid area, a certain number of K satellites will be visible for some nominal length of time. This time is a function of the periodicity of the satellite constellation appearing in this grid. For each satellite, a 6×1 gain matrix is computed, giving a total of K×6 gain matrixes per area for the visible portion of the constellation. The size of this matrix will vary as the number of visible satellites varies.

2.3.4 Calibration Mechanization

One final consideration regarding the present surveillance mechanization is noted here. In an area where air traffic density is high, the corresponding requirement on separation standards is considerably more severe than during the enroute flight phase. This, in turn, imposes a requirement on the surveillance system to hold fixes to an even higher accuracy than can be achieved by the presently mechanized surveillance algorithm.

The surveillance algorithm has been simplified to provide high speed updates on a large number of aircraft. To achieve this, certain systematic correlated errors (for example, the satellite ephemeris uncertainty) have not been modeled in the state estimation equations. Rather, in the error analyses, it has been shown that during the enroute flight phase, the estimation errors resulting from these systematic error sources are entirely acceptable. It is in the terminal area where the errors become unacceptable.

The problem of enhancing the surveillance accuracy around the terminal was studied. A solution which appears to have promise is the use of ground calibration stations in the vicinity of the terminals. These calibration stations (whose positions are known very precisely) would transmit coded pulses in the same way as the aircraft. The surveillance subsystem measures the TOA's and processes them for station state estimation via the surveillance algorithm. These are compared with the a priori known state and the difference between estimated and known is applied as bias offsets to the aircraft state estimations in the same vicinity.

Let subscript c denote calibration station. Using the acquisition algorithm, Fig. 2.3-3, the surveillance system provides the calibration station error Xcn. From this estimate in the steady state, the station position and velocity errors are obtained.

$$\hat{X}_{cn} \equiv \begin{bmatrix} \hat{\underline{P}}_c(\tau_n^*) - \underline{P}_c(\tau_n^*) \\ \hat{\underline{V}}_c(\tau_n^*) - \underline{V}_c(\tau_n^*) \end{bmatrix} \equiv \begin{bmatrix} \Delta\underline{P}_c(\tau_n^*) \\ \Delta\underline{V}_c(\tau_n^*) \end{bmatrix} \tag{34}$$

This error estimate is given in the same earth centered frame coordinate system used by the aircraft. Subtracting this bias from the aircraft state estimate, the following new aircraft state is obtained.

$$\begin{aligned} \underline{P}(\tau_n) &= \hat{\underline{P}}(\tau_n) - \Delta\underline{P}_c(\tau_n^*) \\ \underline{V}(\tau_n) &= \hat{\underline{V}}(\tau_n) - \Delta\underline{V}_c(\tau_n^*) \end{aligned} \tag{35}$$

The bias offset vector $\Delta\underline{P}(\tau_n^*)$ and $\Delta\underline{V}_c(\tau_n^*)$ are periodically updated at arbitrary times τ_n^* to account for relative motion of the satellite constellation over the ground station. It is assumed that, nominally, the time τ_n is close to τ_n^* in order to prevent the bias estimates from "aging" relative to each other.

The theory on which this bias offset is based is that the same set of correlated systematic unmodeled errors affect both aircraft and the calibration station in the same way. Using the calibration stations to compute the offsets "off-line" provides a means for compensating the effect of unmodeled errors in aircraft surveillance without unduly loading the software.

2.4 Surveillance Performance

The accuracy of the surveillance system is essential to system operation and overall system performance. Since the user control algorithms are directly based on the surveillance data, the surveillance accuracy impacts system safety (through conflict intervention) and system capacity (through transition and arrival control algorithms).

The system surveillance accuracy is composed of both relative accuracy and absolute accuracy. The relative accuracy takes into account that two closely spaced aircraft have highly correlated errors. Thus, the absolute accuracy of the measured position relative to the ground is different from the relative accuracy. The relative accuracy is important from a safety standpoint since it determines how close aircraft may be spaced before a potential conflict can result.

This section of the report describes the approach taken to determine the relative and absolute surveillance accuracies. The results are summarized in Table 2.4-1. A detailed discussion of the results and a complete description of the models used to obtain the accuracy data are presented in Volume IX.

Table 2.4-1. Surveillance Subsystem Performance

	Absolute Error (1-σ)	Relative Error (1-σ)
Along-Track Position	36 m	6 m
Cross-Track Position	115 m	7 m
Vertical Position	48 m	4 m
Along-Track Velocity	<1 m/sec	<1 m/sec
Cross-Track Velocity	<1 m/sec	<1 m/sec
Vertical Velocity	<1 m/sec	<1 m/sec

2.4.1 Approach to the Analysis

A description of the surveillance mechanization has been presented in the previous paragraphs. A specific filter design has been assumed for this analysis.

The surveillance accuracy is affected by satellite ephemeris errors, atmospheric model residual errors in the L-band uplink and C-band downlink, system inaccuracies in measuring TOA's, aircraft dynamics, and the use of a suboptimal filter. An analysis of the surveillance system was performed using a particular realization of the suboptimal filter.

The covariance analysis of the surveillance subsystem was accomplished using an existing error analysis program, State Space Analysis of Multisensor Systems (SAMUS). A separate definition of the system and filter states is allowed using this program. Both system and filter covariances and cross covariance can be computed when a suboptimal filter is employed.

The use of a dual state vector implies that separate models and a priori statistics for the system and filter states be employed. Since the system state models are a function of the aircraft dynamics, a scenario was selected for analysis purposes. Satellite visibility models were used that are based on the RF link energy loss similar to that employed for GDOP analysis.

2.4.2 Modeled Errors and A Priori Statistics

The error sources involved in the satellite surveillance consist of those physical effects which lead to user-to-satellite-to-ground timing errors. The list of potentially significant errors include the following:

(1) Aircraft dynamics

(2) Residual ionospheric and tropospheric delays on the L-band uplink

(3) Satellite location errors

(4) Satellite transponding delays

(5) Residual ionospheric and tropospheric delay on the C-band downlink

(6) Speed of light uncertainty

(7) Ground clock errors

(8) Ground site location errors

(9) TOA measurement errors

Most of these errors lead to absolute position errors in surveillance. With the exception of aircraft dynamics and TOA measurement errors, all of these effects are highly correlated for two closely spaced users.

Representative statistics for both the system and filter were selected for error analysis purposes.

The dynamic model assumed for the aircraft state is a very simple model that is representative of an aircraft in straight and level flight. The aircraft velocity states are driven by a random walk noise. This leads to a position error over the time between observations.

The residual atmospheric delays on the L-band uplink are based on empirical studies as noted in Volume II, Section 2.4.2.2.2 Exactly the same assumptions are made for the surveillance uplink as are made for the L-band downlink used for satellite range tracking.

The satellite location error model was derived from the satellite range tracking estimation and prediction model of Volume II, Section 2.4.2. Each of the 15 satellites is characterized by a covariance of position and velocity states. The model propagates these covariances to surveillance transponding times. When a satellite is visible, the correlated uplink and downlink line-of-site errors are translated to equivalent aircraft position uncertainties. The effect of the satellite covariances are thus transformed to equivalent aircraft position covariances for error analysis purposes.

The C-band downlink atmospheric delay models are based on the same empirical studies previously mentioned for the L-band uplink. The modeled values differ because of the frequency differences between these links.

The satellite transponding delay arises from finite times between the time the surveillance pulse is received and the time it is retransmitted. Since all satellites will have approximately the same delays, the overall effect is slight. The transponding delay error is assumed to be a white measurement error.

The speed of light uncertainty is approximately 1/3 parts per million. However, since this effect is correlated to the same effect modeled in satellite range tracking, the net effect on surveillance is small. A separate error of 2 m is accounted for outside of the system error model.

The ground clock errors result from random variations and uncertainties in the high precision atomic clocks. The errors include a bias offset, a clock drift (or frequency offset), a random walk phenomenon, and a flicker noise or fractional Brownian motion effect. The assumed errors are the same as assumed in Volume II, Section 2.4.2.2.2, for the range tracking clock.

The ground site location errors are estimated during satellite range tracking. The initial covariances assumed during range tracking (see Volume II, Section 2.4.2.2.2) are substantially reduced during the range tracking estimation. Only the residual effects are assumed for this analysis.

The TOA time measurement error is extremely small for the surveillance situation. The time measurements are made at the leading and trailing edges of the compressed pseudo-noise pulses leading to a 10 nsec quantization level referenced to the center of the compressed pulse. This error is treated as a white measurement error.

There is only one potential error source that is not correctly modeled in the state model for the surveillance error analysis. This error source arises from the formation of TOA differences as the filter observable rather than the use of TOA measurements as the observable. This leads to a somewhat higher surveillance estimation error than would normally be the case if this effect were correctly modeled.

The basic error is easily visualized by assuming that each group of satellite returns were batch processed to yield a single estimate. If n satellite returns are received, it is easy to show that the covariance of the measurements is

$$E\left\{y_n\, y_n^T\right\} = \sigma^2 \begin{bmatrix} 2 & -1 & & & & & \\ -1 & 2 & -1 & & & 0 & \\ & -1 & 2 & & & & \\ & & & \ddots & & & \\ & & & & 2 & -1 & \\ & 0 & & & -1 & 2 & -1 \\ & & & & & -1 & 2 \end{bmatrix}_{(n-1 \times n-1)} \tag{36}$$

where the variance of the individual measurements are assumed to be σ^2. If the correlation between samples is ignored, the covariance would be $2\sigma I$, where I is an (n-1 × n-1) identity matrix. Clearly, in the batched process case, the use of the the inverse of the covariance matrix of Eq. (36) as a weighting matrix would yield a better estimate in the least-squares sense than an unweighted estimator.

It is not obvious that this principle extends to the case of the Kalman filter. If the effort is expended to derive the Kalman filter from the recursive least-squares estimator, it is easy to show that the principle invoked in the batch process argument will extend to the recursive least-squares and the Kalman filters. Extension of the argument to an optimal Kalman filter is obvious.

In the case of the suboptimal filter, it is obvious that the filter estimate can be no better than the estimate using a fully optimal estimation model. Clearly, ignoring the correlation of the sequential measurements will lead to a model less optimal than the true model. Therefore, the suboptimal filter will yield slightly higher estimation errors than would be the case for the correct model.

The system state vector a priori models and their statistics are summarized in Table 2.4-2.

The suboptimal Kalman filter for the surveillance mechanization is very simple. It consists of three position error states and three velocity error states. In the selected mechanization, the position error states are assumed to be a random walk which accounts basically for the position uncertainty of the aircraft due to satellite position uncertainties. The velocity error states are also driven by a random walk to account for aircraft maneuvering. This model leads to additional aircraft uncertainty between measurements due to the aircraft dynamics.

The values selected for the driving noises for the filter are a compromise. The values are larger than required for an aircraft on straight, level flight but less than for a maneuvering aircraft. The initial covariance for the position is an estimate of the initial uncertainty in the acquisition position determination. The velocity covariance assumes the aircraft is stationary during the acquisition phase.

The filter state vector a priori models and their statistics are summarized in Table 2.4-3.

2.5 References

1. C72-1206.1/201, Preliminary Technical Report, System A Concept Definitions, Advanced Air Management System (AATMS), DOT-TSC-508, December 1972

2. Draft Memorandum, System A Multiple Access Noise Simulation, Electromagnetic Technology Office, DOT-TSC, February 28, 1973

Table 2.4-2. Surveillance State Models and A Priori Statistics

Error Source	Model Type	Driving Noise RMS Value	Initial Covariance
Aircraft Dynamics			
Position - Along Track	Constant	-	40 m
- Cross Track	Constant	-	40 m
- Vertical	Constant	-	40 m
Velocity - Along Track	Random Walk	$0.22\ \sqrt{t}$ m/sec	-
- Cross Track	Random Walk	$0.22\ \sqrt{t}$ m/sec	-
- Vertical	Random Walk	$0.22\ \sqrt{t}$ m/sec	-
L-band Uplink Residual Delays			
Ionospheric		$2.8 \csc \sqrt{E^2(t) + (18°)^2}$ m	-
Tropospheric		$0.3 \csc E(t)$ m	-
Satellite Errors	Complex		
Position - Radial			
- Tangential			
- Normal			
Velocity - Radial			
- Tangential			
- Normal			
Transponding Delay	White Noise	2 m	-
C-band Downlink Residual Delays			
Ionospheric			
Tropospheric			

Table 2.4-2. (continued)

Error Source	Model Type	Driving Noise RMS Value	Initial Covariance
Clock Errors			
Bias Offset	Constant	-	10^{-6} sec
Drift Rate	Constant	-	10^{-9}
Random Walk	Random Walk	$10^{-10}\sqrt{t}$ sec	
Flicker Noise	Complex	1.33×10^{-12} t sec	
Site Location Errors (per axis)	Constant	-	3 m
TOA Measurement Errors	White Noise	1 m	-

Table 2.4-3. Surveillance Filter State Error Model A Priori Statistics

Error Source	Model Type	Driving Noise RMS Value
Position Error		
Level Axes	White	30 m
Vertical Axis	White	30 m
Velocity Error		
Level Axes	Random Walk	1.0 $\sqrt{t}$ m/sec
Vertical Axes	Random Walk	0.5 $\sqrt{t}$ m/sec
Measurement Noise	White Noise	10 m

3. NAVIGATION SUBSYSTEM

The SAATMS navigation subsystem provides two different types of navigation to users. For users with the requirement for high accuracy navigation, a satellite-to-air, synchronous, multilateration system is provided. For other users, a navigation system using surveillance data is provided.

The satellite based navigation system has been analyzed in detail and found to be a high accuracy method of achieving navigation position and velocity. This system is fully independent of the surveillance subsystem and provides all altitude coverage throughout the domain of the satellite coverage. There are no regions of high and low accuracy as exist with ground based systems or time degradations as exist with inertial systems. The system is also unaffected by the number of users since the user's role in navigation is entirely passive.

The low cost user's navigation is based on active transmission to the user of navigation signals. The content of the data is derived from surveillance position data and requested flight path data obtained from the user's flight plan. This system is called virtual VOR (VVOR) due to its operational similarity to VOR. The system is saturable since communication loading increases with the number of users. The main advantage of this system is the low cost of avionics relative to satellite navigation.

3.1 Satellite Navigation Subsystem

The satellite navigation subsystem employs active transmission (by all satellites in the constellation) of navigation timing and ephemeris data pulses. The satellite-transmissions are synchronized and the equipped user receives the navigation data at a periodic rate from each satellite. These data are used by the aircraft navigation processor to compute the aircraft position and velocity.

The individual aircraft employs a pseudo-range, multilateration algorithm using a suboptimal Kalman filter for navigation. Pseudo-range in this context results from the measurement of the satellite-to-user timing (or range) based on the user's estimate of time rather than true time.

Figure 3.1-1 shows the general timing involved in the navigation process. The navigation timing pulses are generated at the satellite. The ephemeris data are relayed from the ground via the satellite over the same channel. These data include the position of the satellite and timing error in the satellite timing pulse for the preceding timing pulse. This timing error allows the user to synchronize his clock with the system master time.

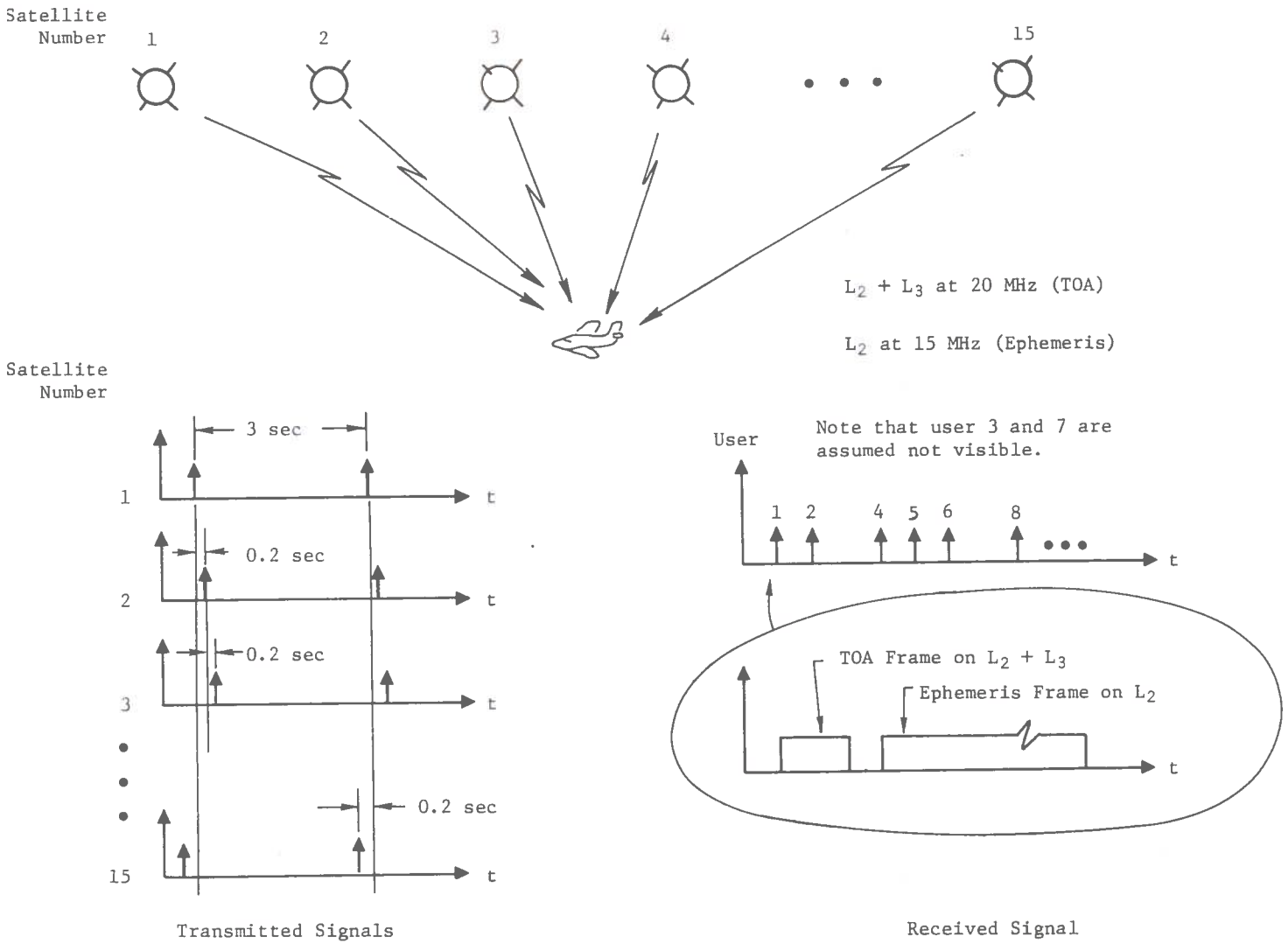

Fig. 3.1-1. Navigation Timing Diagram

Given an estimate of the master time, the TOA of the pulse can be measured. If the positions of four satellites are known and the times of arrival of their signals are measured, both the position of the user and his timing error can be estimated. If a sequence of positions is available, the velocity of the user and his heading can be computed. The velocity and heading are with respect to the ground since all satellite positions are given in an earth fixed frame.

In practice, the mechanization is more complex than this, if for no other reason than that the satellite transmissions are not all simultaneous. Further, the TOA receptions are not periodically received since all satellites are never visible to any given user. The basic principle of trilateration is merely extended for the selected mechanization.

The satellite-to-air navigation mechanization was selected due to its simplicity and passive nature. Alternate systems tend to require demand-sensitive communications loading.

In the following sections, the RF link, the mechanization equations, and the performance of the satellite navigation subsystem will be discussed.

3.1.1 Navigation Waveform and Link Analysis

The navigation signal is composed of two distinct portions: a timing frame and an ephemeris frame. The timing frame is used for TOA measurement by the aircraft. The ephemeris frame is used for transmission of the satellite position and timing error data.

The TOA frame consists of seven Pseudo-Noise (PN) pulses. Each PN pulse is a 40 μsec (400 chip/pulse, 100 nsec/chip) spread-spectrum pulse. The structure of the frame is shown in Fig. 3.1-2. Each satellite transmits a TOA frame each 3 sec. The satellites generate the TOA pulses using their on-board clocks.

The particular structure selected for the TOA frame has several advantages. Not only is there an energy gain through Analog Matched Filter (AMF) detection, but only four of the seven PN codes in the TOA frame need be detected to yield unambiguous TOA timing.

The ephemeris data are transmitted via the ground-to-aircraft digital data link using a separate PN code. The aircraft receives the ephemeris data pulses approximately 50 μsec ($\pm$50 μsec) after the last TOA pulse. The data are transmitted by the RCC on four separate ground-to-aircraft digital data channels.

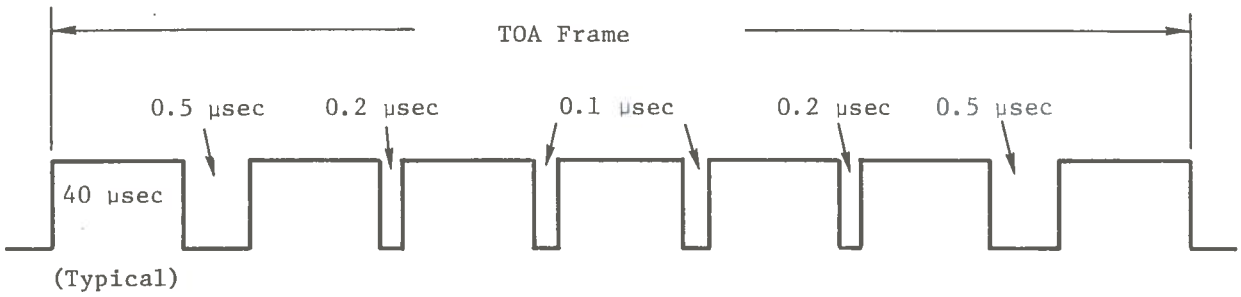

Fig. 3.1-2. TOA Frame

The satellite which transmitted the TOA pulses is used as a relay for the ephemeris data. The ephemeris frame is separated from the TOA frame by 50 $\pm$ 50 µsec. These data are transmitted from the ground and simply relayed by the satellite. The ephemeris data are encoded in the same manner as the ground-to-aircraft data, thus allowing common user decoding equipment to be employed for communication and navigation data. See Section 5.2.1.4 for a complete description of the ephemeris encoding scheme.

The L- and C-band links used for navigation are both time shared and spectrum shared with ground-to-aircraft digital data links. The TOA frame uses a 20 MHz L-band spectrum which is also used by the four 5 MHz digital data channels (3 RCC channels and 1 ACC channel). The ephemeris frame uses 15 MHz of this L-band spectrum which is utilized by the three RCC channels. The ephemeris data uplink shares the 20 MHz C-band spectrum used for RCC-to-satellite relay of digital data.

The navigation signal transmission time for both the ephemeris and TOA frames is shown in Table 3.1-1. The ephemeris data are the satellite's estimated position vector in an earth center fixed frame and the estimated error in the satellite's time with respect to master time. The satellite estimations of position are compared to the predicted transmission times thus eliminating the need for user interpolation of ephemeris data. These data

are quantized to one meter. The clock error allows up to 1 msec error in the satellite clock before it must be reset and provides 10 nsec resolution. With 129 bits required for position and 17 for timing and allowing for error detection pulses, it is estimated that 61 information frames of 53.6 μsec will be required.

Table 3.1-1. Navigation Signal Time Requirement

Event	Time (μsec)
TOA Frame	281.4
TOA Frame Guard Time	100.0
Ephemeris Sync Time	121.2
Ephemeris Data	3269.6
Total	3772.2

Since the navigation signals are both time and spectrum shared with the ground-to-air digital data links, the ground has the primary time-sharing responsibility for the system. Each RCC and the ACC's must control their transmissions such that there is no signal overlap due to time share errors. Several different types of problems can occur.

Transmission of a navigation pulse and its associated ephemeris data takes place for each satellite on a periodic basis. Normally, one or two satellites are so far into the southern hemisphere that no navigation data are required and digital communications can occur throughout the navigation time. If the communications and navigation function is from the same satellite, very little time need be devoted to switching between functions.

When navigation signals are to be provided from a different satellite than the communications function, it is necessary to provide guard times between the events. This guard time prevents signal overlap in the user's avionics. The total guard time is a function of the satellites involved and their relative spacing. The maximum guard time is about 32 msec and the average value is about 19 msec.

For the case of the ACC's, the digital data transmissions need only be silent during the time the navigation data are being received within its local area. Since the propagation times are very short over the coverage region, only about 1 msec guard time is required.

With average guard plus navigation times of 19 + 4 = 23 msec each 200 msec, the digital data must be silent about 11.5 percent of the time. For the case of the ACC's, about 2.5 percent silent time is required.

It should be noted that an error in the system that would result in overlapping signals is not disastrous. Overlapping signals cause only an increase in the effective noise power (multi-access noise) since separate AMF's are employed for communications, TOA pulses, and ephemeris data.

A power budget for the navigation TOA pulses is shown in Table 3.1-2. The satellite-to-aircraft digital data link power budget is applicable for the ephemeris data pulses.

Table 3.1-2. Power Budget for Navigation (Satellite-to-Aircraft) TOA Pulses

Parameter	Units	Comments
Transmitted Energy per pulse	-14 dbj	1000 w, 40 μsec
Satellite Antenna Gain	24.6	10 deg beam
Aircraft Antenna Gain	4.0 db	-
Pointing Losses	1.0 db	-
Miscellaneous Losses	2.0 db	Plumbing, attenuation
Path Loss	189.0 db	f = 1.6 GHz, d = 26,000 nmi
Received Signal Energy	-177.4 dbj	-
Receiver Noise Density	-198.0 dbω/Hz	-
Detection Losses	2.0 db	-
S/N Ratio per pulse	18.6 db	-
Required S/N Ratio	11.0 db	4 out of 7 pulses
Margin	7.6 db	-

3.1.2 Satellite Navigation Mechanization Concept

The mechanization and software requirements for the satellite navigation concept have been investigated and a viable solution to the problem has been found. The method selected is a suboptimal Kalman filter operating with scalar TOA observations. The filter can be mechanized at several levels of complexity depending on the user's accuracy requirements and willingness to acquire the required processing capability.

The basic satellite navigation mechanization elements are shown in Fig. 3.1-3. The TOA measurement is made with respect to the user's clock (pseudo-range measurements). The data are corrected for user and satellite clock errors and for ionospheric and tropospheric delays. The corrected TOA is then made available to the filter mechanization.

The Kalman filter mechanization is based on linearization of the nonlinear multilateration equations about the estimated user's position. Therefore, the Kalman filter is designed to estimate errors in the system state vector rather than the whole value state vector. The whole value state vector is extrapolated independent of the filter. Each time a TOA is available, the estimated state vector error is used to reset (or update) the state vector.

The best estimate of the system state vector is provided to the navigation computation element. This element accepts user inputs (such as waypoint data) and provides display and steering data to other user avionics systems.

The differences between levels of complexity in the users' equipment are in the size of the system state vector and the complexity of the navigation computation element. Clearly, there is a minimum acceptable state vector size. This would include three orthogonal position error states, two level velocity error states, and the user's clock error states. This simple state vector could be expanded to include vertical velocity, a more comprehensive user's clock model, and other error states. The navigation computation element essentially performs an RNAV computation role as well as a data formatting role. Other avionics system inputs can also be implemented. An example would be to provide true air speed and heading inputs which would allow computation of wind speed and direction. There is a wide choice available in the complexity of the navigation processing that is dependent only on the user's willingness to afford the equipment.

3.1.2.1 Basic Navigation Problem

The basic navigation problem can be visualized by considering the basic transmission and reception of timing pulses. Assume that the K^{th} satellite transmits a pulse at time t_{SK} and the user receives the pulse at t_{UK}. Now the user's estimate of the reception time is

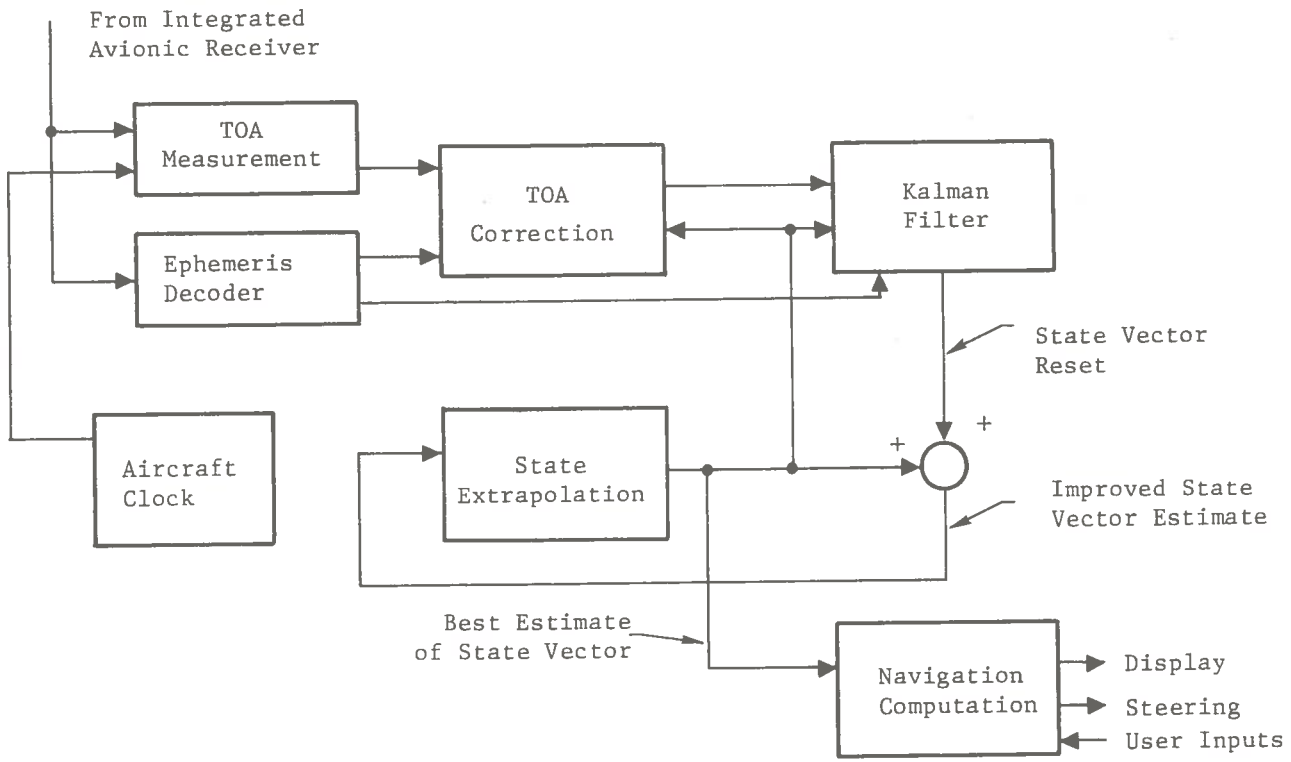

Fig. 3.1-3. Satellite Navigation Mechanization Concept

$$t_{UK} = t_{SK} + (1/C)\ R_K + t_D + t_C + \eta_K \qquad (1)$$

where

C = Speed of light

R_K = Satellite to user range

t_D = User's clock error

η_K = Measurement error noise

The user to satellite range is

$$R_K = || \bar{\rho}_{SK} - \bar{\rho}_{UK} || \qquad (2)$$

where

$\bar{\rho}_{SK}$ = Position vector of satellite

$\bar{\rho}_{UK}$ = Position vector of user

$|| \ ||$ = Euclidian Norm

Clearly, this equation is nonlinear in terms of the user's position since

$$R_K = \sqrt{(X_{SK} - X_{UK})^2 + (Y_{SK} - Y_{UK})^2 + (Z_{SK} - Z_{UK})^2} \qquad (3)$$

This is in terms of X, Y, and Z components of the satellite and user's position vectors in some given orthogonal coordinate system.

Given that the satellite's position, time of arrival, and an estimate of the atmospheric delay are known, there remain three user position terms and a clock error term which are unknown. If four simultaneous equations of the form of Eq. (1) were available, it would be possible to compute the four unknowns. Here, the measurement error term would lead directly to a position uncertainty.

There are a number of obvious problems in using the preceding deterministic approach to the navigation problem. One such problem is that the satellite transmission times are not simultaneous. This can be rectified by including the user velocity to obtain a sequence of the form

$$R_1 = || \bar{\rho}_{S1} - \bar{\rho}_{U1} ||$$

$$R_2 = || \bar{\rho}_{S2} - [\bar{\rho}_U + \bar{v}_U (t_{S2} - t_{S1})] ||$$

$$\vdots$$

$$R_n = || \bar{\rho}_{SN} - [\bar{\rho}_{U1} + \bar{v}_U (t_{SN} - t_{S1})] || \qquad (4)$$

Clearly, this introduces more unknowns (since the user's velocity is also unknown), but it affords the use of nonsimultaneous satellite transmissions. The user's states must be expanded to include three velocity states in addition to the three position and clock states.

Note that this formulation requires more observables than the previous four to yield a deterministic solution. Further, this formulation assumes a constant user velocity. These equations are, as before, nonlinear in position but are also nonlinear in velocity.

At this point, it is helpful if the problem is linearized. Consider that the system state is defined to be the vector of unknowns, $\underline{X}$. The state vector will be assumed to be

$$\underline{X} = \hat{\underline{X}} + \tilde{\underline{X}} \tag{5}$$

where

$\hat{\underline{X}}$ = An a priori estimate of the system state

$\tilde{\underline{X}}$ = The error in the system state estimate

Clearly,

$$\hat{t}_{UK} = t_{SK} + F(\bar{\rho}_{SK}, \underline{X}) + t_D + \eta_K \tag{6}$$

where $F(\bar{\rho}_{SK}, \underline{X})$ is a nonlinear function of the satellite position vector and the system state vector. This function can be expanded in a Taylor series about the estimated state vector yielding

$$\hat{t}_{UK} = t_{SK} + F(\bar{\rho}_{SK}, \hat{\underline{X}}) + \nabla_{\underline{X}} F \, \tilde{\underline{X}} + t_D + \eta_K \tag{7}$$

where $\nabla_{\underline{X}} F$ is a sensitivity vector and the higher order terms in the expansion are ignored.

Equation (7) can now be placed in a vector form so that

$$\underline{\hat{t}}_{UK} = \underline{t}_{SK} + \underline{F}(\bar{\rho}_{SK}, \hat{\underline{X}}) + A \, \tilde{\underline{X}} + \underline{t}_D + \underline{\eta}_K \tag{8}$$

where A is a matrix composed of the row vectors $\nabla_{\underline{X}} F$. Clearly, if a determined set of equations is available and A is nonsingular, then

$$\tilde{\underline{X}} = A^{-1} [\underline{\hat{t}}_{UK} - \underline{t}_{SK} - \underline{F}(\bar{\rho}_{SK}, - \hat{\underline{X}}) - \underline{t}_D - \underline{\eta}_K] \tag{9}$$

The bracketed term on the right side of Eq. (9) is in reality the difference between the time the pulse was received and the time it would be received if the system state estimate were exact.

The development to this point has neglected a certain complexity in several factors. Essentially, Eq. (9) explains how the problem is formulated as a linear equation by expansion of the nonlinear equation about the estimated state. In point of fact, several system states must be modeled to account for the other system errors.

It should be noted at this point that the system states and the state vector for the filter are not the same. The system states are equations involving the aircraft position, velocity, and clock. The filter states are errors in these states, and additional states required to model system noise.

The system states can be modeled in a number of coordinate systems. For example, the X, Y, Z orthogonal coordinates may be an earth centered fixed coordinate system; a latitude, longitude, altitude coordinate system; or any other convenient set. A generic X, Y, Z coordinate set will be considered here. The clock model assumes that the clock reset will be made as appropriate. The state equation propagation is then

$$
\begin{aligned}
X_{n+1} &= X_n + \dot{X}_n \, (t_{K+1} - t_K) \\
Y_{n+1} &= Y_n + \dot{Y}_n \, (t_{K+1} - t_K) \\
Z_{n+1} &= Z_n + \dot{Z}_n \, (t_{K+1} - t_K) \\
\dot{X}_{n+1} &= \dot{X}_n \\
\dot{Y}_{n+1} &= \dot{Y}_n \\
\dot{Z}_{n+1} &= \dot{Z}_n \\
B_{n+1} &= B_n + \dot{B}_n \, (t_{K+1} - t_K) \\
\dot{B}_{n+1} &= \dot{B}_n
\end{aligned}
\tag{10}
$$

or

$$
\underline{X}_{n+1} = \phi \, (t_{K+1}, \, t_K) \, \underline{X}_n \tag{11}
$$

Here, the system velocity states (X, Y, Z) and clock bias rate ($\dot{B}$) are assumed constant.

The filter state model is used to compute errors in these states. Since the filter state model is based on a differential equation that includes stochastic models that account for system noise propagation, the filter state model is larger than the system state model. Neglecting for the moment the actual estimation process, assume that an estimate is made. The state model is updated by

$$\underline{X}_K^+ = \underline{X}_K^- + \Delta S \, \hat{\underline{\tilde{X}}}_K \tag{12}$$

where ΔS is a system reset matrix. The reset matrix properly distributes the estimated filter state element into corrections to the system states. The filter estimates are then updated using

$$\hat{\underline{\tilde{X}}}_K^+ = \hat{\underline{\tilde{X}}}_K^- - \Delta F \, \hat{\underline{\tilde{X}}}_K^- \tag{13}$$

The matrix ΔF accounts for the control (or reset) applied to the state equations that must now be removed from the filter states.

For the selected mechanization, the system states and the time of state are held constant. Each time a TOA is received, the filter state is updated. The system reset and control matrices are used to update the system and filter states. The system state time is updated to the corrected TOA time. The state propagation for the navigation computational element will then take place outside of the state vector storage element. This allows simpler timing to be involved in the estimation cycle.

3.1.2.2 Filter State Model

The derivation of the filter state model is the crux of the navigation mechanization development. This model is based on a state and measurement model of the general form

$$\underline{\tilde{X}}_K = \phi \underline{\tilde{X}}_{K-1} + G\underline{U}_K \tag{14}$$

$$\underline{y}_K = M_K \underline{\tilde{X}}_K + \underline{N}_K \tag{15}$$

where

ϕ = Filter state propagation matrix

G = Noise distribution matrix

$\underline{y}_K$ = Observation vector

M_K = Measurement matrix

$\underline{N}_K$ = Observation noise

The system state vector model and the measurement model are used to mathematically describe the relationship between system errors and the observables. The only observable for this problem is the TOA measurement. Identification and modeling of those phenomena that affect the errors in the TOA measurement is the basis of the filter development.

The general Kalman filter equations will be presented first and then will be related to the specific problem at hand.

The following specific quantities will be defined first.

$\hat{\underline{\tilde{X}}}_n$ = Estimate of the system error at time t_n given measurements through time t_n

$\hat{\underline{\tilde{X}}}'_n$ = Extrapolated or predicted estimate of the system error at time t_n given measurement through time t_{n-1}

$\underline{y}_n$ = Observed measurement at time t_n

$\hat{\underline{y}}_n$ = Predicted measurement at time t_n

b_n = Filter weighting at time t_n

ρ^*_n = Filter covariance matrix

$$= E\left\{ (\underline{\tilde{X}}_n - \hat{\underline{\tilde{X}}}'_n)\ (\underline{\tilde{X}}_n - \hat{\underline{\tilde{X}}}'_n)^T \right\}$$

$P_n = E\{(\underset{\sim}{X}_n - \hat{\underset{\sim}{X}}_n)\ (\underset{\sim}{X}_n - \hat{\underset{\sim}{X}}_n)^T\}$

F = Error model description matrix where $\phi = \exp(-F\Delta t)$

$U = E\{\underline{U}_K\ \underline{U}_K^T\}$

$R = E\{\underline{\eta}_K\ \underline{\eta}_K^T\}$

$\Delta t = t_n - t_{n-1}$

The discrete Kalman Filter equations are

$$\hat{\underset{\sim}{X}}_o = \underline{0} \tag{16}$$

$$\hat{\underset{\sim}{X}}_{n+1} = \phi(\Delta t)\ \hat{\underset{\sim}{X}}_n \tag{17}$$

$$\hat{\underset{\sim}{Y}}_{n+1} = M\ \hat{\underset{\sim}{X}}'_n \tag{18}$$

$$\hat{\underset{\sim}{X}}_{n+1} = \hat{\underset{\sim}{X}}_{n+1} + b_{n+1}\ (y_{n+1} - \hat{y}_{n+1}) \tag{19}$$

$$P^*_{n+1} = \phi(\Delta t)\ P_n\ \phi(\Delta t) + N(\Delta t) \tag{20}$$

$$N(\Delta t) = \int_0^{\Delta t}\int_0^{\Delta t} \phi\ G\ U\ G^T\ \phi^T\ d_{\tau 1}\ d_{\tau 2} \tag{21}$$

$$b_{n+1} = P^*_{n+1}\ M^T[M\ P^*_{n+1}\ M^T + R]^{-1} \tag{22}$$

$$P_{n+1} = (I - b_{n+1} M) P^*_{n+1} \tag{23}$$

$$P_o = E\{\underset{\sim}{X}_o \underset{\sim}{X}_o^T\} \tag{24}$$

Full development of the filter state model requires a substantial knowledge about the error processes.

There are a number of factors which will affect the predicted measurement at time $t_n(\underline{\hat{y}}_n)$. Clearly, position errors will affect this value as will velocity errors through propagation into position errors. Satellite clock errors will also affect the predicted TOA. A less obvious error source is signal delay in transition through the ionosphere and troposphere.

The clock error model is an attempt to replicate those phenomena physically observed in crystal controlled clocks. The error model consists of a bias offset, a frequency drift, and a random fluctuation. Empirical results have indicated that the random fluctuations consist of a random walk plus flicker noise which can be modeled as a fractional Brownian motion. The selected models for navigation consist of a two-state model of the form of a bias plus drift model.

The ionospheric and tropospheric effects cause a diurnal variation in signal delays. The mean value of this effect is modeled as a function of electron densities, transition angles, and other factors. These errors are used to correct the received TOA's. The residual effects serve as system noise but are not modeled in the selected mechanization.

The selected state vector is

$$\underset{\sim}{x} = \begin{bmatrix} x \\ y \\ z \\ \dot{x} \\ \dot{y} \\ \dot{z} \\ b \\ \dot{b} \end{bmatrix} \begin{matrix} \left.\begin{matrix} \\ \\ \end{matrix}\right\} \text{Position Errors} \\ \left.\begin{matrix} \\ \\ \\ \\ \end{matrix}\right\} \text{Velocity Error} \\ \text{Bias Error} \\ \text{Drift Error} \end{matrix} \tag{25}$$

More complex mechanizations are possible by inclusion of the neglected effects.

In the selected mechanization, the position and velocity states are driven by random walk noise and the clock states are assumed constant over the interval between observations. The state transition matrix thus accounts only for aircraft dynamics. The initial covariance of the system states is a simple diagonal matrix. The measurement matrix associated with the state vector is

$$M = \left[\left(\frac{1}{C}\right)\frac{\partial R}{\partial x} \quad \left(\frac{1}{C}\right)\frac{\partial R}{\partial y} \quad \left(\frac{1}{C}\right)\frac{\partial R}{\partial z} \quad 0 \quad 0 \quad 0 \quad 1 \quad T \right] \tag{26}$$

The range functions are determined by the satellite ephemeris data, the estimated location of the users at the TOA time, and the coordinate system selection. The measurement noise is assumed to be a white noise process due to quantization errors and fluctuation in RF time delays prior to measurement of the TOA.

3.1.2.3 TOA Corrections

Correction to the raw measured TOA data must be accomplished prior to its use in the filter. These corrections remove the major biases due to the user and satellite clock errors and atmospheric delays. The ephemeris data include a clocking error which allows synchronization of the user's clock with master system time.

The satellite transmits a signal at time t_S which is not at master time zero. The user's clock measures t_U when the pulse is received. The time required is given from Eq (9) as

$$t_F = \hat{t}_U - t_s - F(\rho_S, \hat{\underline{X}}) - t_D \tag{27}$$

where

$\hat{t}_U$ = Measured clock time

t_s = Satellite clock error from ephemeris error

$F(\bar{\rho}_S, \hat{X})$ = A nonlinear function

t_D = Atmospheric delay

The nonlinear function $F(\bar{\rho}_S, \hat{\underline{X}})$ is approximated by computing

$$t_C = B + \dot{B}(\hat{t}_U - t_n) \tag{28}$$

where t_n = time of last state vector update.

$$t_a = \hat{t}_U - t_C \tag{29}$$

$$\hat{\underline{X}}(t_a) = \phi(t_a - t_n)\, \hat{\underline{X}}(t_n) \tag{30}$$

$$F(\bar{\rho}_S, \hat{\underline{X}}) = 1/C \,||\, \bar{\rho}_S - \bar{\rho}_U(t_a) \,|| + t_C \tag{31}$$

The atmospheric delay is computed based on empirical formulas similar to those discussed in Volume II, Section 2.4.2.

The corrected time value is then provided to the filter as

$$\underline{y}_{n+1} = t_F \tag{32}$$

The measurement provided to the filter amounts to the difference between the measured and the predicted TOA.

3.1.2.4 Filter Equations

The filter equations given in Eq. (16) through (24) may now be specialized to the particular case under consideration. First, note that the entire filter state vector is used to reset the system states each cycle. Thus,

$$\hat{\underset{\sim}{X}}_n = \underline{0} \tag{33}$$

$$\underset{\sim}{y}_{n+1} = \underline{0} \tag{34}$$

This results in the simple equation

$$\hat{\underset{\sim}{X}}_{n+1} = b_{n+1}\, \underline{y}_{n+1} \tag{35}$$

where b_{n+1} is a vector of dimension 8×1.

The system transition matrix is

$$\phi = \begin{bmatrix} 1 & 0 & 0 & t & 0 & 0 & 0 & 0 \\ 0 & 1 & 0 & 0 & t & 0 & 0 & 0 \\ 0 & 0 & 1 & 0 & 0 & t & 0 & 0 \\ 0 & 0 & 0 & 1 & 0 & 0 & 0 & 0 \\ 0 & 0 & 0 & 0 & 1 & 0 & 0 & 0 \\ 0 & 0 & 0 & 0 & 0 & 1 & 0 & 0 \\ 0 & 0 & 0 & 0 & 0 & 0 & 1 & 0 \\ 0 & 0 & 0 & 0 & 0 & 0 & 0 & 1 \end{bmatrix} \tag{36}$$

The noise distribution matrix is

$$G = \begin{bmatrix} G_x & 0 & 0 & 0 & 0 & 0 & 0 & 0 \\ 0 & G_y & 0 & 0 & 0 & 0 & 0 & 0 \\ 0 & 0 & G_z & 0 & 0 & 0 & 0 & 0 \\ 0 & 0 & 0 & G_x^{\bullet} & 0 & 0 & 0 & 0 \\ 0 & 0 & 0 & 0 & G_y^{\bullet} & 0 & 0 & 0 \\ 0 & 0 & 0 & 0 & 0 & G_z^{\bullet} & 0 & 0 \\ 0 & 0 & 0 & 0 & 0 & 0 & G_B & 0 \\ 0 & 0 & 0 & 0 & 0 & 0 & 0 & G_B^{\bullet} \end{bmatrix} \qquad (37)$$

The matrix U, which is the covariance of the system driving noise, is a unity matrix with the scaling requirements implicit in G. The initial covariance is a diagonal matrix with the individual elements equal to the a priori selected variances of the associated states. These quantities are sufficient to allow completion of the mechanization.

3.1.3 Satellite Navigation Performance

The accuracy of the satellite navigation is of fundamental importance in providing users with the data necessary for flight conformance. Although the navigation accuracy can be segregated into errors that lead to relative and absolute navigation inaccuracies, only the total or absolute accuracy is of importance. This stems from the system philosophy of distributed (or user responsible) flight conformance. While the use of calibration stations for navigation is possible, they have not been incorporated in the SAATMS concept since they would only improve the absolute accuracy. The improvement, however, would not be great enough to permit satellite navigation to replace instrument landing systems. Further, system F&E and O&M costs would be greatly increased with little improvement in system performance.

This section of the report describes the approach, models, and results of the navigation analysis performed to date. The results are summarized in Table 3.1-3. A complete description of the results and the analysis is presented in Volume IX.

Table 3.1-3. Navigation Subsystem Performance

	Absolute Error (1-σ)
Along-Track Position	29 m
Cross-Track Position	66 m
Vertical Position	29 m
Along-Track Velocity	< 1 m/sec
Cross-Track Velocity	< 1 m/sec
Vertical Velocity	< 1 m/sec

3.1.3.1 Approach to Analysis

A description of the navigation mechanization, including a description of the Kalman filter has been presented in the preceding paragraphs. This filter mechanization has been analyzed in detail to determine the navigation accuracy for a specific filter design.

The satellite navigation accuracy is affected by satellite ephemeris errors, atmospheric model residual delays, user inaccuracies in measuring TOA's, aircraft dynamics, and the use of a suboptimal filter rather than the full system model filter. The use of the suboptimal filter forces several design compromises that are required to implement a practical filter.

The analysis of the satellite navigation mechanization is a covariance analysis based on the use of a suboptimal filter. This analysis is based on the use of an existing error analysis program, State Space Analysis of Multisensor Systems (SAMUS). For the navigation analysis, the system error states and the filter states are defined. SAMUS propagates both the system and estimation covariances and the system/estimation cross covariances. This allows a complete analysis of the estimation error even though the filter states differ from the system states.

The use of this dual state vector requires that the a priori statistics associated with both the system and the filter be defined. Since the system states are a function of the assumed flight path, a scenario was selected for performance evaluation. Satellite visibility also affects the navigation error analysis. This fact was accounted for by using the same visibility criteria employed for GDOP calculations. A modification of the RF link energy computations were included.

3.1.3.2 Modeled Errors and A Priori Statistics

The error sources involved in satellite navigation account for all known physical effects which can lead to satellite-to-user time errors. The list of potentially significant errors includes

(1) Satellite location errors

(2) Satellite clock errors

(3) Residual ionospheric and tropospheric delays

(4) Speed of light uncertainty

(5) User clock errors

(6) Aircraft dynamics

(7) TOA measurement quantization

To perform the error analysis, sets of representative statistics for both the system and the filter must be assumed. The system error states and a priori statistics will be discussed first.

The satellite location errors and the satellite clock errors are estimated during satellite range tracking. Since both errors are estimated concurrently, these errors are correlated. Each satellite was therefore assumed to be characterized by a position error. Since the satellite ephemeris are estimated and then predictions made based on this estimate, a high degree of correlation exists from one navigation position transmission time to the next.

The system satellite model consists of a six-state model of position and velocity covariances that are propagated to each time in the orbit the satellite transmits. Independent propagations are employed for each of the 15 satellites in the system. When a satellite is visible, the position covariance of the satellite is used to compute the equivalent effect on the aircraft covariances (based on the line-of-sight from the aircraft to satellite). Thus, the satellite covariance is translated into an equivalent position uncertainty in the aircraft.

The quantization errors in the satellite position and timing amount to $1/\sqrt{12}$ meter rms per axis and $10/\sqrt{12}$ nsec rms, respectively. These errors are treated as measurement errors.

The residual ionospheric and tropospheric delays are based on empirical studies as noted in Volume II, Section 2.4.2.2.2. Exactly the same errors are assumed here as were assumed for range tracking.

The speed of light uncertainty was not used in the navigation state model. Since the effect on navigation is almost fully correlated to the effect during satellite tracking, no provisions need be made in the navigation analysis. A separate rms speed-of-light induced position uncertainty of 1 meter rms was added outside of the covariance analysis to account for the uncorrelated portion of this effect.

The error model for the user's clock is composed of four separate effects. The user attempts to synchronize his clock to the master time but makes an initial error. This time bias is an initialization error but is quickly estimated. The user's crystal oscillator has a frequency offset which produces a clock or time drift rate. The selected value of this parameter is representative of the frequency accuracy obtainable with a moderately priced oscillator. The two remaining terms in the clock model are a random walk error and a flicker noise. The random walk term arises from a white noise at the frequency level. The flicker noise is a fractional Brownian motion term that has been empirically observed (see Volume II, Section 2.4.2.2.2). Neither of these terms can be prespecified in procuring oscillators. Typical values were selected for purposes of this analysis.

The aircraft dynamics may be modeled at several levels. The method selected for this study is to drive the velocity state with a random walk noise that leads to a position error over the time between observations. This method was based on straight and level flight scenarios.

The TOA quantization term is the rms error in digitizing the TOA data. This is treated as a measurement noise.

The initial covariance states are important in the transient response of the system. Since the steady-state response of the system was desired and not the transient response, somewhat arbitrary values were selected for all of the preceding errors. An attempt was made to select values representative of system initialization at an airport.

Table 3.1-4 lists the models selected for the system state errors.

Table 3.1-4. System State Error Model A Priori Statistics

Error Source	Type Model	Driving Noise RMS Value	Initial Covariance
Satellite Error Model	Complex		
Radial Velocity			
Normal Velocity			
Tangential Velocity			
Radial Position		15 m min - 20 m max	
Normal Position		7 m min - 55 m max	
Tangential Position		60 m min - 90 m max	
Ephemeris Quantization			
Position (per axis)	White Noise	$1/\sqrt{12}$ m	-
Time	White Noise	$10/\sqrt{12}$ nsec	-
Residual Ionospheric Delay		$2.8 \csc \sqrt{E^2(6) + 18°)^2}$ m	-
Residual Tropospheric Delay		0.3 csc E(t)	-
User's Clock Errors			
Bias Offset	Constant	-	1 μsec
Drift Rate	Constant	-	10^{-6} t sec
Random Walk	Random Walk	$4 \times 10^{-10} \sqrt{t}$ sec	0
Flicker Noise	Complex	1.33×10^{-12} t sec	0
User's Dynamic Errors			
Position Along Track	Constant	-	40 m
Position Cross Track	Constant	-	40 m
Position Vertical	Constant	-	40 m
Velocity Along Track	Random Walk	$0.22 \sqrt{t}$ m/sec	-
Velocity Cross Track	Random Walk	$0.9 \sqrt{t}$ m/sec	-
Velocity Vertical	Random Walk	$0.22 \sqrt{t}$ m/sec	-
TOA Quantization	White Noise	$30/\sqrt{12}$ m	-

The suboptimal filter model is an eight-state vector model. The model contains three position error states, three velocity error states, a clock bias error state, and a clock drift error state. This model is attempting to reproduce the effects of the 102-element system state vector. Most of the missing state vector terms involve the satellite position error states. It is desired to form a filter model which will nominally replicate the system model during all normal system operating conditions.

The suboptimal filter is at best a design compromise. It is desired to design the filter for the smallest practical error during normal steady-state flight and still be able to handle the maneuvering aircraft case. The user position error states are used to absorb the satellite position and atmospheric delay states. The effects of aircraft dynamics are included as velocity error driving noises. The clock error states are prevented from converging too rapidly by assuming driving noise.

The model selected for the user position error is a random walk driving noise. This model is an attempt to produce the effect of the satellite errors on the system. The velocity error states are similarly selected to have random walk driving noises. The value of noise is an attempt to compromise between a dynamically stable and maneuvering aircraft situation. The random walk noise models for the clock states are an attempt to free-up these states so that the gains are high enough to preclude divergence of these states.

The models selected for the filter state model are as given in Table 3.1-5.

3.2 Virtual VOR Navigation Subsystem

The Virtual VOR (VVOR) subsystem is based on transmission of navigation quantities to users. The navigation quantities are derived by the ground based system elements using the user's surveillance data and the user's requested flight plan data. The navigation data are transmitted to the user using the ground-to-air digital data link.

3.2.1 Mechanization Description

Two different forms of VVOR navigation are available to users dependent on the type of steering information desired. The accuracies of the two methods are substantially different but the inherent flexibility of the less accurate method is higher. Neither form of the VVOR equations requires any degree of sophistication in the user avionics.

Table 3.1-5. Filter State Error Model A Priori Statistics

Error Source	Type Model	Driving Noise RMS Value	Initial Covariance
User's Position Error			
Along Track	Random Walk	67 $\sqrt{t}$ m	50 m
Cross Track	Random Walk	67 $\sqrt{t}$ m	50 m
Vertical	Random Walk	67 $\sqrt{t}$ m	50 m
User's Velocity Error			
Along Track	Random Walk	0.45 $\sqrt{t}$ m/sec	2 m/sec
Cross Track	Random Walk	1.8 $\sqrt{t}$ m/sec	2 m/sec
Vertical	Random Walk	0.45 $\sqrt{t}$ m/sec	2 m/sec
Clock Errors			
Bias Offset	Random Walk	22×10^{-10} $\sqrt{t}$ sec	1 μsec
Drift Rate	Random Walk	10^{-7} $t^{3/2}$	10^{-6}
Measurement Error	White Noise	10 m	-

The first option provides a system similar to present VOR system operations. In this option, the user may select any arbitrarily located VVOR site as a desired destination. The steering data that are provided to the user consist of the bearing and range from his present position to that VVOR site. The user may change to other available sites at his option.

The advantage of this option is in the flexibility of changing VVOR sites at any given time. This allows full option to return to any VVOR site (e.g., an airport) from any point. The disadvantage is that the cross-track errors are a function of the range to the selected VVOR site. This type of option is most useful for flight within a local area rather than cross country flights.

For long distance flights, a second option is provided. In this option, a sequence of VVOR sites is entered which defines a sequence of great circle paths between VVOR sites. In this option, the steering needle is driven by the distance-off-track rather than heading. This allows flight path conformance to the selected great circle path. Distance to the selected VVOR site is also provided.

The advantage of this option is that it allows the user to conform, with a high degree of precision, to a given flight path. The cross-track error is independent of distance from the VVOR site. The disadvantage of this option is that it presumes a specific preselected route will be flown. Revisions to the preselected route can, of course, be made in flight.

The mechanization of both VVOR forms is based on great circle flights. Figure 3.2-1 shows the geometry involved for either option. Here (ϕ_i, λ_i) represents the terminal VVOR site for the desired flight leg and (ϕ_p, λ_p) represents the user's present position. The flight leg desired for the second option is the great circle path from $(\phi_{i-1}, \lambda_{i-1})$ to (ϕ_i, λ_i). The VVOR sites are defined as a set of latitude/longitude coordinates.

3.2.2 Bearing Range Mechanization

The bearing range mechanization is based on simple spherical trigonometry. Let θ_A be the spherical angle from the user's position to the VVOR destination. From Fig. 3.2-1,

$$X = \cos(\theta_A) = \cos(90 - \phi_p)\cos(90 - \phi_i) + \sin(90 - \phi_p)\sin(90 - \phi_i)\cos(\lambda_i - \lambda_p) \quad (1)$$

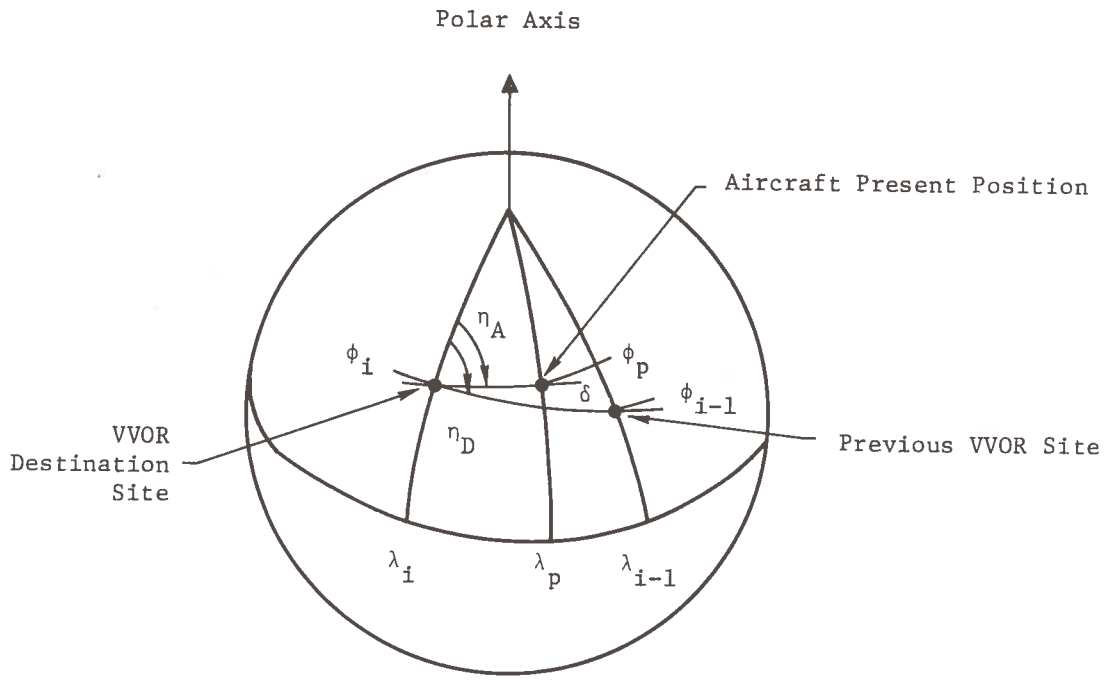

Fig. 3.2-1. VVOR Geometry

$$\theta_A = \cos^{-1}(X) \tag{2}$$

$$\eta_A = \sin^{-1}\left[\frac{\sin(90 - \phi_p)\sin(\lambda_i - \lambda_p)}{\sin\Theta_A}\right] \tag{3}$$

$$R_{TG} = a\theta_A \tag{4}$$

where

R_{TG} = Range to go

a = Earth's radius

η_A = Bearing angle

The values (ϕ_p, λ_p) are the surveillance positions propagated from the last state vector time to the present time. The quantities η_A and R_{TG} are then computed and transmitted to the user.

3.2.3 Cross-Track Deviation Method

The cross-track deviation method is slightly more complicated than the bearing range method but is still based on spherical trigonometry. The quantities θ_{Di}, the spherical angles between VVOR sites, are computed once as

$$\theta_{Di-1} = \cos^{-1} \{ \cos (90 - \phi_i) \cos (90 - \phi_{i-1}) + \sin (90 - \phi_i) \sin (90 - \phi_{i-1}) \cos (\lambda_i - \lambda_{i-1}) \} \quad (5)$$

The distance between VVOR sites, η_{Di}, is similarly precomputed as

$$\eta_{Di} = \sin^{-1} \{\sin (90 - \phi_{i-1}) \sin (\lambda_i - \lambda_{i-1})/\sin \theta_{Di}\} \quad (6)$$

The quantities θ_A and η_A are computed each update time exactly as previously given in Eq. (2) and (3). The range-to-go (R_{TG}) is computed using Eq. (4). The cross-track error is then computed using

$$R_{XT} = a \sin^{-1}[\sin \theta_A \sin (\eta_D - \eta_A)] \quad (7)$$

The quantities η_A, R_{TG}, and R_{XT} are then transmitted to the user.

3.2.4 VVOR Performance

The VVOR performance is predominately a function of the update rate of the equations and only a weak function of surveillance accuracy. Both mechanizations may be characterized by an R_{TG} error (δR_{TG}) and a cross-track error (δR_{XT}).

The range-to-go error is a function of the aircraft velocity and update rates. If a 0.1 mile quantized R_{TG} value is transmitted to the user, the surveillance error is negligible compared to the system accuracy. The R_{TG} error increases linearly between update times. Both mechanizations exhibit similar performance. The bounding range error as a function of aircraft velocity is shown in Fig. 3.2-2. This assumes that the aircraft is flying directly toward the VVOR site, which leads to a worst-case R_{TG}.

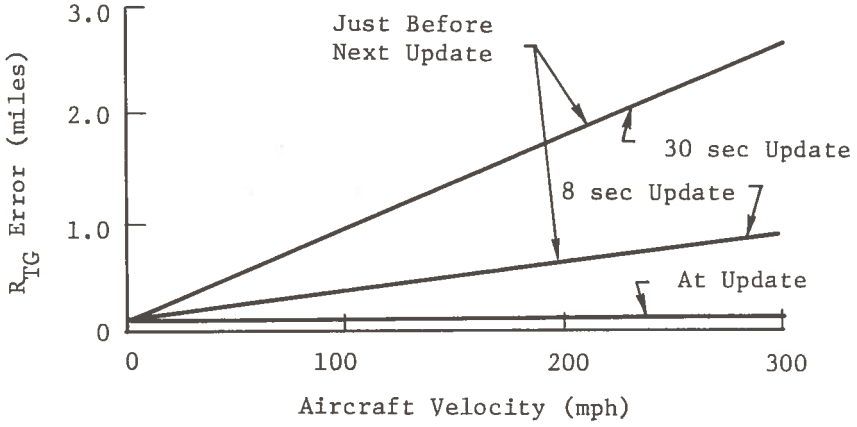

Fig. 3.2-2. Bounding VVOR Range-to-go Error

The cross-track performance of the two mechanization options differs substantially. The cross-track performance of the bearing range mechanization is directly a function of range. The cross-track deviation allows much better cross-track accuracy.

Assuming that the user fly to null his steering needle and that a heading accuracy of 1 deg is provided, the cross-track uncertainty of Fig. 3.2-3 is achievable using the bearing range mechanization. This uncertainty is relative to where the pilot assumes he is, rather than an error from a given ground track.

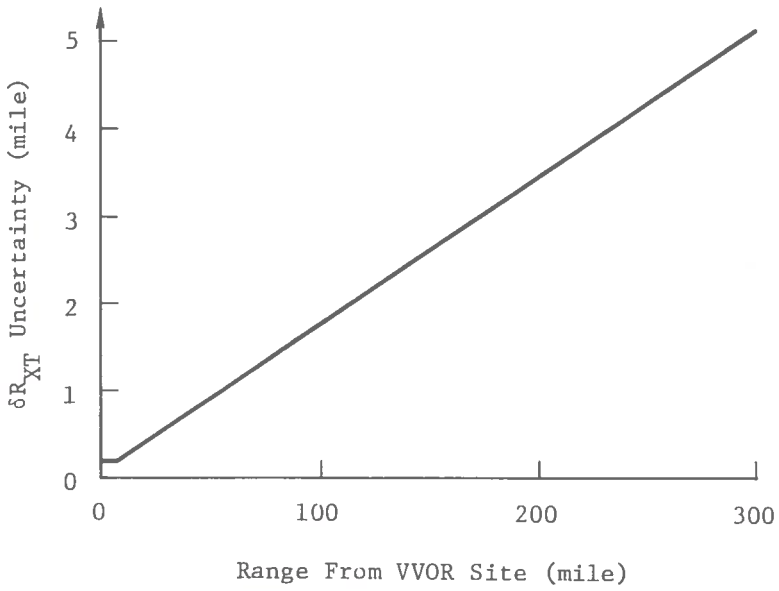

Fig. 3.2-3. Option One Cross-Track Uncertainty

The cross-track error for the second option is range independent. Assuming that the user is flying to null the steering needle, the cross-track error is dependent only on the cross-track distance quantization of 0.1 mile. The ability to null the steering needle will probably introduce some uncertainty in cross-track errors between updates. Total error of 0.2 miles is probably realizable with a position uncertainty of 0.1 mile at update times.

4. COMMUNICATIONS SUBSYSTEM

The SAATMS design concept employs an integrated communications subsystem that interconnects all ground based system elements and ties user aircraft to the controlling ground jurisdictions. The major features of the subsystem include several unique items that enhance the integrated communications capability.

The subsystem is based on the premise that integrated user avionics will be of primary importance in achieving a cost effective system design. For this reason, a single transmission-reception band (L-band) is employed for all information dissemination to or reception from user aircraft. All user communications (as well as surveillance and navigation) system data interfaces are in the L-band spectrum (1535 to 1660 MHz).

The interface between the users and the ground jurisdictions is primarily via satellites with supplementary direct ground-to-air interfaces at airports. The satellite relayed communications insures continuous coverage at all altitudes within the satellite system boundary. A user within the system is always assured that communications links are present regardless of his geographic position within CONUS. At airports where communications loading is highest, supplementary direct line-of-sight links are used to relieve the satellite communications load.

By defining the system as primarily a digital data system with voice backup, the system is conducive to automation. Digital data links allow a degree of flexibility, speed, and backup to be implemented in conjunction with the automation routines. The voice option enhances safety by allowing human intervention in the event of automation or equipment failures.

The system is designed to require relatively few user frequency changes for the primary digital links. The small number of voice and digital frequency changes assures that a minimum of user induced errors will either occur or persist.

The ground-to-ground communications subsystem allows for extremely large amounts of data transfer between sites. The subsystem is satellite based and allows direct links to be implemented throughout the system. There are no remote sites except in a geographic sense.

In the following paragraphs, an overall description of the communications system will be presented. This will be followed by a detailed description of each link.

4.1 Communications System Description

The RF links used to interconnect the various system elements are shown in Fig. 4.1-1. This diagram indicates the links by functions. The links of interest in this section are the digital, voice, and ground-to-ground links.

Table 4.1-1 shows the communications links. All links involving aircraft are at L-band (1535 to 1660 MHz) to permit an integrated avionics design. Links not associated with aircraft are at C-band (5000 to 5280 MHz) primarily because of the spectrum availability. Except for airport to user line-of-sight links, all communication is via satellite.

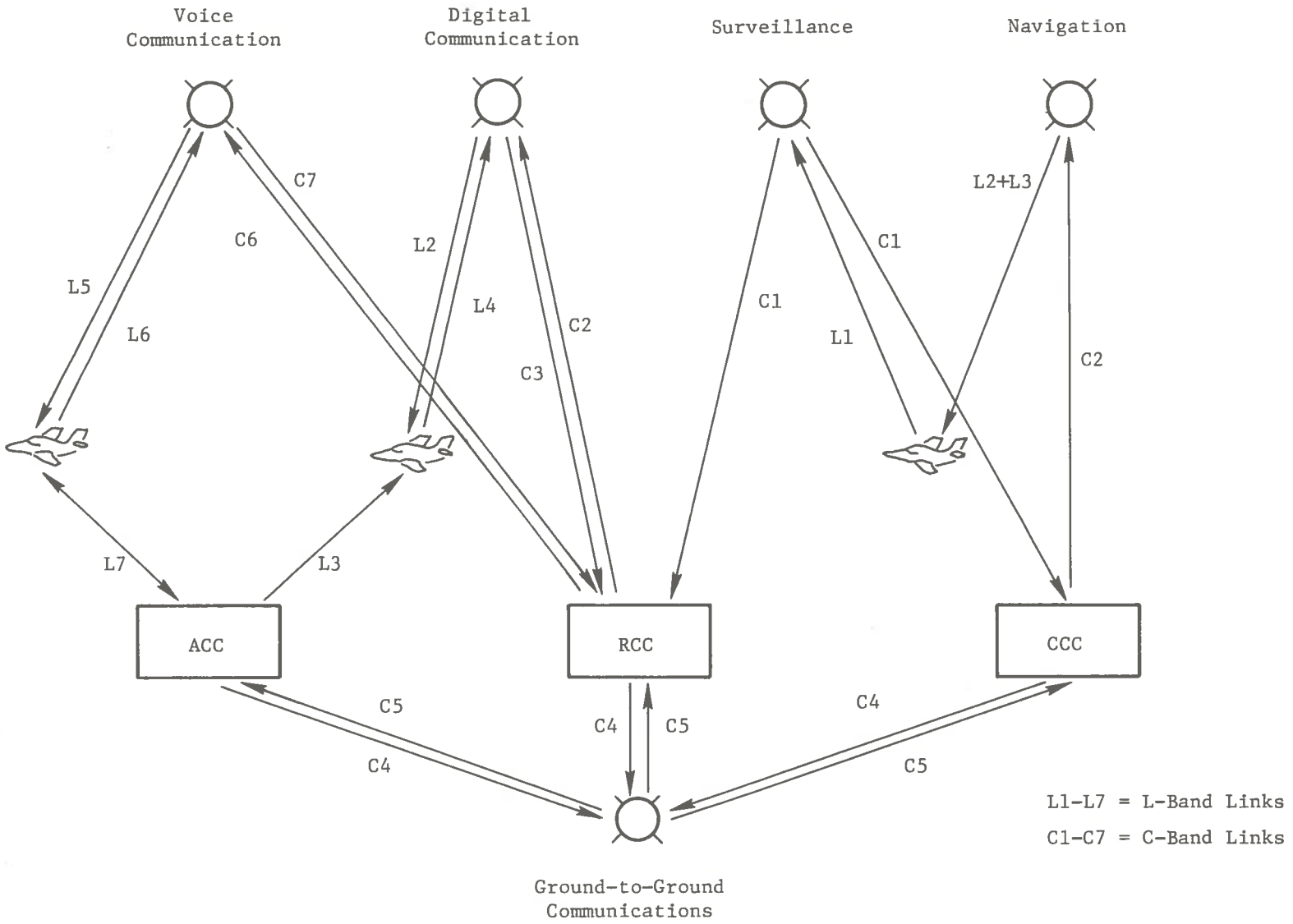

Fig. 4.1-1. System RF Link Interconnection

Table 4.1-1. Communications RF Links

Function	Path	Band	Bandwidth MHz	Number of Channels	Single Channel Bandwidth MHz	Comments
A-G Digital Data	A-S	L4	15	1	15	Asynchronous, with Aircraft ID's as basic element in PPM code
	S-G	C3	15	1	15	
G-A Digital Data	G-S	C2	15	3	5	Discrete address, time ordered, shared with navigation function
	S-A	L2	15	3	5	
	T-A	L3	5	1	5	
Voice Links	G-S	C6	3.75	150	0.025	Ground-air two-way voice links
	S-A	L5	3.75	150	0.025	
	A-S	L6	3.75	150	0.025	
	S-G	C7	3.75	150	0.025	
	T-A	L7	10	400	0.025	Line-of-sight two-way voice links
	A-T	L7	10	400	0.025	
G-G Digital Data	G-S	C4	3	600	0.005	Employs four Equatorial satellites for 2400 channel capacity
	S-G	C5	3	600	0.005	

Notes: A = Aircraft
S = Satellite
G = Ground
T = ACC's
PPM = Pulse Position Modulation
Total Spectrum = 55 MHz at L-band and 46 MHz at G-band

To accommodate a relatively high degree of automation, digitally encoded message data are assumed for the majority of the air-ground and ground-ground communications. The air-ground communication relies on wideband, high speed, digital channels, thus reducing the number of required channels and frequency changes. The possibility of losing air-ground communications due to frequency error is practically eliminated.

Digital data from aircraft-to-ground are transmitted via a spread-spectrum, random access channel. The aircraft transmits its unique ID as the basic component of a Pulse Position Modulation (PPM) scheme. The ID has the same waveform structure as the surveillance ID to allow integrated equipment. The RCC in whose region the aircraft is located is responsible for message decoding. If the data are intended for an airport, the RCC must relay the decoded message via the ground-ground links. Approximately 100 kilobits/sec (kbs) can be accommodated before the channel becomes multi-access limited (i.e., the average multi-access noise power becomes larger than the satellite receiver thermal noise power). The spectrum occupancy is 15 MHz each at L-band and C-band.

Digital data from ground to aircraft are transmitted via four separate channels. Each channel occupies a 5 MHz bandwidth and operates at 93 kbs. Three channels are used by the RCC's and these channels are satellite relayed. One channel is time shared by all ACC's, which have a digital data capability. The airport channel is a line-of-sight link and widely separated airports use the channel simultaneously. The total spectrum occupancy for ground-to-aircraft digital data is 15 MHz of a 20 MHz channel at L-band and 15 MHz at C-band. The 15 MHz channel is shared with the navigation function which uses the entire 20 MHz spectrum about 6 percent of the time. This 6 percent includes the necessary guard (or dead) times in changing fuctional use for the channel.

There is a total of 150 air-ground voice channels which are relayed via satellite. There are also 400 line-of-sight voice channels between ACC's and aircraft. Thus, a total of 550 two-way voice channels exist. The channels are spaced 25 kHz apart. The spectrum occupancy is 17.5 MHz at L-band and 7.5 MHz at C-band.

Air-air communication is provided by the line-of-sight voice links which are not satellite relayed. In very special cases, the RCC could relay messages via satellite between aircraft very widely separated. An additional air-to-air mode is available for navigation data interchange as accessory to support the air-to-air collision avoidance.

Ground-to-ground information transfers are handled by 2400 digital channels. Each channel operates at up to 2.4 kb. Four of the geostationary satellites are used as relays with each satellite capable of relaying 600 channels. The channels are the same in each satellite and space diversity is used to permit simultaneous use (by different users) of the same frequency in all four satellites. The spectrum occupancy is 6 MHz at C-band.

4.2. Ground-to-Aircraft Digital Link

There are four separate ground-to-aircraft digital links; three for RCC-to-aircraft usage and one for ACC-to-aircraft usage. These channels are time shared with the navigation function which demands about a 6 percent duty cycle. The characteristics of the channels include a 5 MHz bandwidth which allows a 93 kbs transmission rate (46.5 kbs information rate), a pulse position modulation encoding scheme based on 40 μsec PN codes, and redundant transmission.

The coding scheme employed uses three components per message: synchronization, address, and message. The basic coding scheme is shown in Fig. 4.2-1. The basic coding scheme is structured on a 40 μsec, 400 nsec/chip, 100 chip/pulse PN encoded pulse. This is the same type code used for navigation data transmittal to aircraft. Only one code is required for all functions.

At the beginning of any transmission, synchronization is achieved by transmitting three PN codes separated by 0.4 μsec. The sync pulses alert aircraft that an address is forthcoming. Following the sync frame, there is a four pulse address frame. This is followed by an information frame.

The coding scheme used by the address and information frames allows five binary bits (2^5) to be encoded per pulse. Within a coding frame of 53.6 μsec, there are 32 distinct time slots where the PN code can be positioned. The first coding frame starts 0.4 μsec after the last sync pulse. A coding frame always begins and ends with an empty 0.4 μsec timeslot. This restricts address and information PN codes to a 0.8 μsec spacing to prevent confusion with sync pulses.

With four coding frames per address frame, there are $2^5x2^5x2^5x2^5$ or 2^{20} unique addresses possible. This corresponds to the 2^{20} possible surveillance ID codes. Aircraft communications processors are thus only required to decode those information frames specifically addressed to the correct ID. The information frames immediately follow the address frame and contain a variable number of bits depending on the message type.

Each 5-bit PPM information frame symbol is transmitted twice and a simply implemented two-out-of-two decoding algorithm is used. More sophisticated decoding algorithms can be used if they prove cost effective. With the two-out-of-two algorithm, threshold detection is used and a single pulse position must exceed the threshold both times. Retransmission is requested if no position within a frame or if more than 1 position per frame exceeds threshold. With 14 db S/N ratio ($P_d = 0.9999$, $P_f = 3x10^{-3}$), the probability of correctly decoding a symbol is approximately 0.9995. The probability of an undetected symbol error is approximately $6x10^{-8}$. By using an error detecting frame at the end of each message (a modulo 32 check), the probability of accepting a 100 bit message (20 pulses) with an undetected error is approximately $6x10^{-14}$.

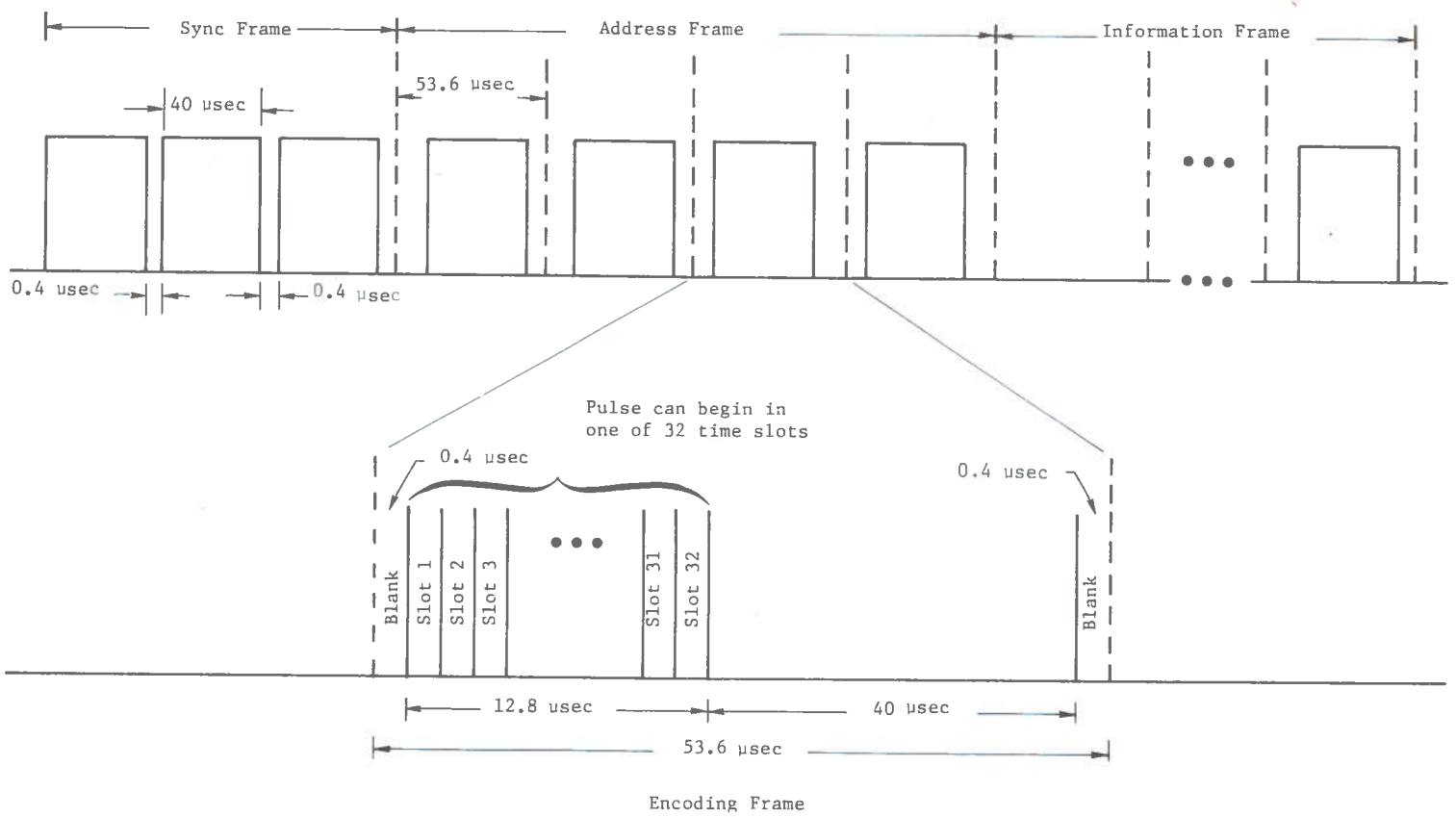

Fig. 4.2-1. Ground-To-Air PPM Digital Communication Scheme

Three of the ground-to-aircraft digital channels are satellite relayed and used by the RCC's. The two RCC's have exclusive use of one channel each and time share the third channel. All three satellite relayed channels have uplink frequencies at C-band and downlink frequencies at L-band.

The downlink (i.e., satellite-to-aircraft) is the critical RF link in the satellite relayed channels. Table 4.2-1 contains a power budget for this link. The uplink has approximately 24 db more S/N ratio, primarily because of the large ground antenna gain (45 db).

Table 4.2-1. Satellite-to-Aircraft Digital Data Link (L2) Power Budget

Parameter	Units	Comments
Transmitted Energy	-17 dbj	500 w, 40 μsec pulses
Satellite Antenna Gain	30.6 db	5 deg beam
Aircraft Antenna Gain	4.0 db	150 deg beam
Pointing Losses	2.0 db	
Miscellaneous Losses	2.0 db	Plumbing = 1 db Attenuation = 1db
Path Loss	189.0 db	f = 1.6 GHz d = 26,000 miles
Received Energy per Pulse	-175.4 dbj	
Receiver Noise Power Density	-198.0 dbw/Hz	
Uplink Degradation	0.1 db	50 w; 15 ft ground antenna
Detection Losses	2 db	
S/N Ratio per Pulse	20.3 db	
Required S/N Ratio	14 db	10^{-7} undetected symbol error
Margin	6.3 db	

All airports with digital data capability time share the remaining channel. Since an ACC jurisdictional area extends only about 5 miles, the links are line-of-sight. The time available to each airport would be roughly proportional to need. To ensure no interference from adjacent airports, a maximum guard time of approximately 600 sec is necessary each time the channel is switched to a different airport. Assuming 50 switches/sec, about 3 percent of the channel is consumed by dead time (in addition to the 5 percent dead time needed for navigation). Airports separated by approximately 100 miles can use the channel simultaneously. If an average of 140 airports use the channel simultaneously, the total airport-to-aircraft digital capability is approximately 600 kbs.

As an example of the time sharing between airports, suppose the channel is divided into 100 equal time slots of 10 msec each. Each time slot occurs once per second. A small airport might need only one time slot. Every second it could transmit approximately

$$(46.5 \text{ kbs})(9.4 \text{ msec}) \approx 435 \text{ bits}$$

A high density airport might be assigned nine time slots. Every second it could transmit approximately

$$(46.5 \text{ kbs})(89.4 \text{ msec}) \approx 4150 \text{ bits}$$

4.3 Aircraft-to-Ground Digital Link

To minimize the aircraft avionics cost, digital data from aircraft-to-ground are transmitted via a random access channel. The aircraft transmits a unique ID of similar structure to the surveillance ID (i.e., 3 PN pulses of 40 μsec duration). The ID is used as the basic component of a 7-bit PPM scheme. The ID is transmitted once per frame and the ID start time within the frame is chosen from 128 time slots. Each time slot is 0.1 μsec and each frame is 139.4 μsec. The first 0.1 μsec of each frame is not used so that the end of any pulse is separated from the beginning of the next pulse by at least 0.1 μsec. At the beginning of any transmission, the ID is transmitted three consecutive times for synchronization (see Fig. 4.3-1).

Since the channel is random access, an aircraft can transmit digital messages at any time. Since each frame is 139.4 μsec and contains seven bits, information is transferred at the rate of approximately 50 kbs.

The RCC in whose region the aircraft is located is responsible for the decoding. Signals from three satellites are used in a majority decoding scheme. An RCC would normally use the returns from one geostationary and two geosynchronous satellites to obtain triangular coverage. The aircraft's wide antenna beamwidth and the multiple satellite coverage should provide sufficient protection against aircraft banks. If the message is intended for an ACC, the RCC must relay the decoded message via the ground-ground communications link.

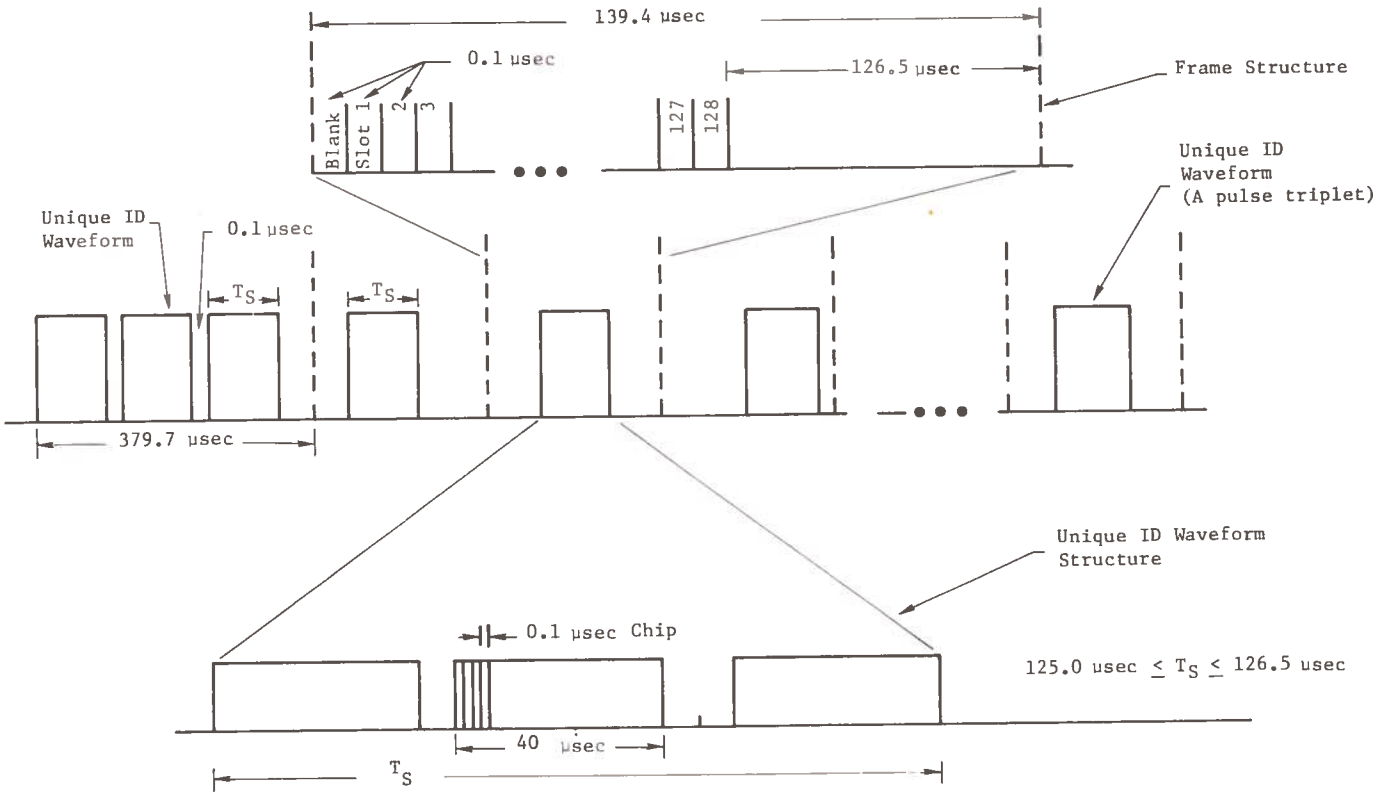

Fig. 4.3-1. Aircraft-to-Ground PPM Digital Communication Scheme

The power budget for the aircraft-to-ground digital data link is shown in Table 4.3-1. The total information rate relayed by the satellite is assumed to be 35 kbs. The effect of increased information rates, because of more bits per aircraft or simply more aircraft, is shown in Table 4.3-2.

With 13 db S/N ratio per pulse from each of three satellites, it is estimated that symbol error rates of approximately 10^{-5} can be attained.

Table 4.3-1. Aircraft-to-Ground Digital Data Link Budget

Parameter	Units
Transmitted Energy per Pulse (2 kw, 40 usec)	-11 dbj
Aircraft Antenna Gain (Curved Turnstile, 150 deg Beamwidth)	4 db
Satellite Antenna Gain (5 deg Beam)	30.6 db
Pointing Losses	2.0 db
Miscellaneous Losses (Plumbing, Attenuation)	2.0 db
Path Loss (f = 1.6 GHz, d = 26,000 miles)	189.0 db
Received Signal Energy per Pulse	-169.4 dbj
Multi-Access Noise (3.5×10^4, $\frac{1 \text{ bit/sec}}{\text{aircraft}}$, $\frac{1 \text{ pulse}}{7 \text{ bits}}$, 15 MHz Beamwidth)	-208.2 dbw/Hz
Receiver Noise Density	-201.0 dbw/Hz
Total Background Noise	-200.2 dbw/Hz
Downlink Degradation (30 w transmitted, 15 ft ground Antenna)	0.1 db
Detection Losses	2.0 db
S/N Ratio per Pulse	24.7 db
Required S/N Ratio	13.0 db
Margin	11.7 db

Table 4.3-2. Effect of Total Information Rate on Aircraft-to-Ground Digital Data Link Margin

Total Information Rate (10^3 bits/sec)	Multi-Access Noise (dbw/Hz)	Margin (db)
35	-208.2	11.7
70	-205.2	11.1
105	-202.2	10.0
140	-199.2	8.5
175	-196.2	6.5
210	-193.2	4.0

4.4 Ground-Aircraft Voice Links

Two types of voice links are planned between aircraft and the ground. One is a two-way link between the RCC's and aircraft which is directed through a satellite relay; and the other is a direct line-of-sight link between airports and aircraft. Transmissions to and from the RCC occur in C-band, and transmissions to and from the aircraft are performed at L-band.

The modulation technique used for all of the voice transmissions is narrowband FM with each transmission requiring 10 kHz of bandwidth. Frequency division multiplexing is used to support the multitude of voice channels. The center frequencies of the individual voice channels are spaced by 25 kHz. The number of channels available for use by an aircraft will depend upon the type of aircraft involved and will range from 20 to 550. Each RCC is provided with 75 voice channels. The number of channels an airport has is dependent upon its location and traffic density.

Four of the geostationary satellites will be capable of relaying 25 channels each. These channels would all be distinct. The other 50 channels would be relayed by the geosynchronous satellites. Each geosynchronous satellite relays a set of 25 channels. Thus, at any instant, a maximum of two geosynchronous satellites serve as voice relays.

Power budgets for the various voice links are provided in Tables 4.4-1, 4.4-2, and 4.4-3.

Table 4.4-1. Aircraft-Satellite Voice Link (L5 and L6) Power Budget

Parameter	Units	Comments
Transmitted Power	16 dbw	40 w
Aircraft Antenna Gain	4 db	150 deg beam
Satellite Antenna Gain	30.6 db	5 deg beam
Pointing Losses	2.0 db	
Miscellaneous Losses	2.0 db	
Path Loss	189.0 db	f = 1.6 GHz d = 26,000 miles
Received Power	-142.4 dbw	
Receiver Noise Density	-201 dbw/Hz	-198 dbw/Hz for aircraft
Carrier-to-Noise Density	58.6 db-Hz	
Required Carrier-to-Noise	46 db	Phase-locked FM, 10 kHz IF
Margin	12.6 db	9.6 db for satellite-to-aircraft

Table 4.4-2. Ground-Satellite Voice Link (C6 and C7) Power Budget

Parameter	Units	Comments
Transmitter Power	0 dbw	1 w (Required for the uplink; 100 mw required for the downlink)
Ground Antenna Gain	45 db	15 ft antenna
Satellite Antenna Gain	24.6 db	10 deg beam
Pointing Losses	1.0 db	
Miscellaneous Losses	2.0 db	
Path Losses	198.9 db	f = 5 GHz d = 26,000 miles
Received Power	-132.3 dbw	
Receiver Noise Density	-201 dbw/Hz	
Carrier-to-Noise Density	68.8 db-Hz	
Required Carrier-to-Noise	45 db	Phase-locked FM, 10 kHz IF
Margin	22.8 db	Reduced to 12.8 db for satellite-to-ground

Table 4.4-3. Line-of-Sight Air-Ground Voice Link (L7) Power Budget

Parameter	Units	Comments
Transmitted Power	3 dbw	2 w
Aircraft Antenna Gain	-3 db	
Ground Antenna Gain	0 db	
Miscellaneous Losses	2 db	
Path Losses	133 db	f = 1.6 GHz, d = 40 miles
Power Received	-135 dbw	
Receiver Noise Density	-198 dbw/Hz	
Carrier-to-Noise	63 db-Hz	
Required Carrier-to-Noise	46 db	Phase-locked FM, 10 kHz IF
Margin	17 db	

4.5 Air-to-Air Digital Links

The air-to-air digital links are used to support the interchange of navigation information for performing the airborne collision avoidance function. This mode is implemented only by controlled aircraft. These data are transmitted asynchronously.

The avionics would be modified to include this capability. The transmission frequency would be at L-band and would occupy two of the many voice channels available to the system.

Aircraft will transmit their derived navigation data at a rate of approximately once every 4 sec. Assuming 100 bits of information (see Table 4.5-1), 40 μsec pulses, and 1 bit per pulse, each transmission is then 4 msec. With 200 aircraft in a region, an aircraft will receive messages an average of once every 20 msec. The probability that a given message is received without any overlap is approximately 0.67.

Fortunately, when overlaps do occur, the near/far phenomenon will allow useful information to be extracted. The smaller the separation between aircraft, the larger the probability that useful information will be exchanged. For example, the path loss advantage of a signal traveling 3 miles over another traveling 30 miles is 20 db.

Table 4.5-1. Approximate Estimate of Message Length

Message	Approximate Estimate
Latitude	16 (1 $\widehat{\text{sec}}$ out of 17 deg)
Longitude	16 (1 $\widehat{\text{sec}}$ out of 17 deg)
Altitude	9 (100 ft out of 50,000 ft)
ID	20 (1 out of 10^6)
Intent	8 (1 out of 256)
Velocity	12
Total	81 bits ≈ 100 bits

4.6 Ground-Ground Digital Links

The ground-ground communication links interconnect the various ground elements of the system. For example, the links are used to transmit surveillance data, handoff messages, and traffic information from RCC to airport. All data are assumed routed through one of four geostationary satellite relays.

Exclusive use of geostationary satellites as relays is possible because ground terminals, unlike aircraft, have no antenna pointing problem. Four satellites are used instead of only one because space diversity can be utilized to permit simultaneous use of the same frequency channel. Thus, for the same spectrum, four times as many channels are available.

The digital data are transmitted by bi-phase modulation at 2400 bits per sec. Frequency division multiplexing is utilized to multiplex many channels within a total system bandwidth.

Each RCC is provided with approximately 1200 channels for both the transmit and receive modes. The number of channels assigned to an airport is dependent upon its need but four channels might be typical. The total bandwidth occupancy for the ground-to-ground transmission system is 6.0 MHz.

Table 4.6-1 contains a power budget for the satellite-to-ground RF link (downlink). The ground-to-satellite link (uplink) is similar except that the transmitted power is increased to 2 w.

Table 4.6-1. Satellite-Ground Link (C4 and C5) for Ground-to-Ground Communication

Parameter	Units	Comments
Transmitted Power (from Satellite)	-10 dbw	100 mw; increased to 2 w in ground-to-satellite link
Satellite Antenna Gain	30.6 db	5 deg beam
Ground Antenna Gain	45.0 db	15 ft Antenna, 0.85 deg beam
Pointing Loss	1.0 db	
Miscellaneous Losses	2.0 db	
Path Loss	198.9 db	f = 5 GHz, d = 26,000 miles
Received Power	-136.3 dbw	
Receiver Noise Power Density	-198.0 dbw/Hz	
Noise Bandwidth	33.8 db	
Uplink Degradation	0.1 db	
S/N Ratio per Bit	28.0 db	
Required S/N Ratio	12 db	$P_e = 10^{-6}$
Margin	16 db	

5. DATA PROCESSING SUBSYSTEM

The data processing subsystem is that portion of the SAATMS design concept concerned with the computations required to implement the system functions and services. The data processing subsystem is resident in the CCC, the two RCC's, and the ACC's. Interconnection of the subsystem is achieved through the ground-to-ground communications links of the communications subsystem

This section of the report is directed toward defining the major aspects of the processing subsystem. The processing functions are described, processing speed and processing memory requirements are estimated, and the hardware and software requirements are estimated. The processing subsystem is highly dependent on the level of system automation desired. This section assumes a certain achievable automation level.

The general data processing subsystem requirements are first summarized. The individual requirements for CCC, RCC's, and the ACC's are then described in detail. The basic processing categories discussed include surveillance, user, control, flow planning, satellite tracking, communication, and executive processing.

The terms used in this section are as follows:

AMF	Analog Matched Filters
APE	Any Pulse Enable
CP	Checkpoint
CPU	Central Processing Unit
FT	First Time
GFT	Greater Than First Time
IOP	Input/Output Processing
IPS	Instruction per Second
ROM	Read Only Memory
STC	Satellite Tracking Center
WPS	Words per Second

5.1 Data Processing Subsystem Summary

A block diagram of the processing requirements for SAATMS is shown in Fig. 5.1-1. The majority of these are real time processing functions that result in the issuance of a communication to the user or to ground based elements. The communications include commands/advisories to operations personnel; i.e., pilots or control system operating personnel, as well as to other elements in the processing subsystem.

The magnitude of the data processing subsystem requirement can be seen in the summary of the processing listed in Table 5.1-1. In this table, lines 1 through 4 are surveillance; lines 5 through 7 and 10 and 11 are user control; lines 8 and 9 are flow planning; lines 12 and 13 are satellite tracking; lines 15, 20, and 21 are communication; and the rest of the lines are executive and miscellaneous processing.

The surveillance processing includes those functions necessary to detect and quantify aircraft surveillance signals, acquire newly entered aircraft, compute surveillance data, and maintain files of aircraft data and status. These tasks are performed with a combination of special purpose and general purpose computers due to the speed and demand level requirements. These tasks are performed for as many as 20,000 active users at each RCC. The CCC provides complete backup of this function for either or both RCC's and is sized for a 35,000 active user capability.

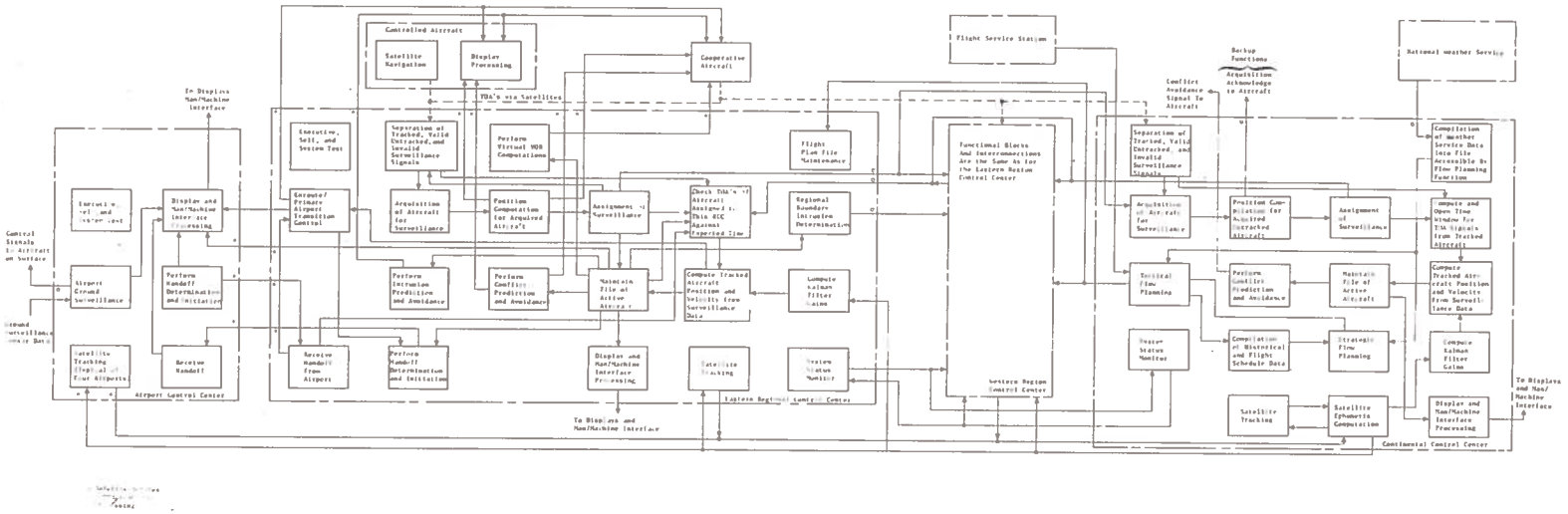

Fig. 5.1-1. SAATMS Data Processing Top Functional Diagram

Table 5.1-1. Summary of SAATMS Data Processing

Function	Location Where Performed	Processing Speed (IPS)	Processing Requirements			Method of Mechanization
			Memory (Words) Data	Program	Input/Output Usage (WPS)	
1. Aircraft surveillance ID conversion and filtering	RCC CCC (Backup of RCC's)	4,000,000 4,000,000	65,000 65,000	7,000 7,000	100 100	Combination of special purpose parallel, associative, and general purpose processing
2. Computation of positions of newly acquired aircraft	RCC CCC (Backup of RCC's)	250,000 250,000	32,000 32,000	1,000 1,000	300 300	General purpose processing
3. Compute positions of tracked aircraft	RCC CCC (Backup of RCC's)	3,400,000 5,000,000	500 500	700 800	3,000 6,000	General purpose processing
4. Maintain file of active aircraft	RCC CCC (Backup of RCC's)	353,000 620,000	2,200,000 3,200,000	500 500	7,500 7,500	General purpose processing
5. Conflict prediction and avoidance	RCC CCC (Backup of RCC's)	150,000 260,000	Included in active aircraft file	300 300	34,000 50,000	General purpose processing
6. Intrusion prediction and avoidance	RCC	50,000	250,000	200	3,000	General purpose processing
	CCC	90,000	500,000	300	6,000	
7. Handoff determination and initiation	RCC	21,500	1,000 100,000 Auxiliary	300	30,000	General purpose processing
	CCC	43,000	2,000 200,000 Auxiliary	400	50,000	General purpose processing
8. Strategic flow planning	CCC	200×10^6/run	16,000 + 15×10^6 Auxiliary	1,000	180×10^6/run	General purpose processing in batch mode

Table 5.1-1. (Continued)

Function	Location Where Performed	Processing Speed (IPS)	Processing Requirements			Method of Mechanization
			Memory Data	(Words) Program	Input/Output Usage(WPS)	
9. Tactical flow planning	CCC	200,000	300,000	700	1.5×10^6	General purpose processing
10. Associated data compilation	CCC	50×10^6/run	16,000 +15×10^6 Auxiliary	1,000	200×10^6/run	General purpose processing
11. Virtual VOR	RCC	170,000	26,000 +234,000 Auxiliary	200	5,000	General purpose processing
	CCC	300,000	45,000 +405,000 Auxiliary	300	9,000	General purpose processing
12. Transition and arrival control	RCC	10×10^6	700,000 +2,100,000 Auxiliary	20,000	22,000	General purpose processing
	CCC	17×10^6	1,250,000 +3,750,000 Auxiliary	35,000	40,000	General purpose processing
13 Satellite tracking	STC STC/RCC STC/CCC STC/ACC	1,000 1,000 1,000 1,000	100 100 100 100	200 200 200 200	100 100 100 100	General purpose processing
14. Satellite position prediction	CCC	200×10^3	11,500	500	200	General purpose processing
15. Navigation processing	Controlled aircraft	50×10^3	1,000	1,000		Small general purpose processor in aircraft
16. Communications processing	RCC CCC ACC	120×10^3 120×10^3	15,000 15,000	2,000 2,000	22,500 22,500	General purpose processing
17. Display and man/machine interface processing	RCC CCC ACC	500×10^3 800×10^3	150,000 250,000	20,000 30,000	15,000 30,000	General purpose processing

Table 5.1-1. (Continued)

Function	Location Where Performed	Processing Speed (IPS)	Processing Requirements			Method of Mechanization
			Memory (Words) Data	Program	Input/Output Usage (WPS)	
18. System and self-test	RCC CCC ACC Controlled aircraft	100,000 150,000 10,000 1,000	5,000 7,000 200 50	10,000 15,000 2,000 500	100 100 10 1	General purpose processing
19. Executive programs	RCC CCC ACC Controlled aircraft	1,000,000 1,000,000 20,000 5,000	4,000 6,000 200 50	50,000 60,000 10,000 500	- - - 100	General purpose processing
20. Ground traffic surveillance and control	ACC	50,000 (maximum)	4,000	1,000	100	General purpose processing
21. User to ground communication ID conversion and filtering	RCC CCC	4,000,000 4,000,000	65,000 65,000	7,000 7,000	100 100	Combination of special, associative, and general purpose processing
22. User to ground communication decoding and message assembly	RCC CCC	250,000 250,000	32,000 32,000	1,000 1,000	10,000 10,000	General purpose processing

The user control processing includes the generation of control commands and advisories for active users and transfer of data between jurisdictional areas. The user control processing is, in general, based on the surveillance data generated by the surveillance processing subsystem. User control processing is essentially located at RCC's and ACC's, with RCC backup at the CCC. The user control processing is generally parallel, real time computation performed in general purpose (GP) computers.

The satellite tracking processing includes satellite tracking preprocessing and satellite emphemeris estimation and prediction. The preprocessing data manipulation occurs at STC's. These data are collocated at the CCC, RCC's, and ACC's. This GP processing represents a very small computational load and will probably share collocated facility processing equipment. The prediction and estimation routine is accomplished at the CCC using real time, general purpose computers.

The flow planning processing is performed in the batch mode on a processor located at the CCC. The functions include strategic flow planning, tactical flow planning, traffic demand data processing, and weather and system status dissemination.

The communications processing functions include all those data formatting and routing functions required to interconnect the system elements. The processing is performed by GP computers with the exception of user-to-ground communications. This latter function requires special purpose parallel and general purpose processing similar to surveillance data acquisition.

The executive and miscellaneous functions include executive programs, display and man/machine interface programs, and system and self-test programs. For completeness, the aircraft navigation and ACC ground traffic surveillance and control are also included. These processing functions are all general purpose computer functions.

The general philosophy behind the system design has been discussed previously. No particular claims for the optimality of some of the automation algorithms are made. The automation functions described are feasible and serve the purpose of sizing the data processing subsystem. The majority of the efforts in the design were directed toward the SAATMS specific special purpose hardware. Feasible solutions to these areas are critical, and viable solutions have been identified.

5.2 CCC Data Processing

The CCC data processing includes those functions used throughout the system; Fig. 5.2-1 shows these functions. These CONUS oriented functions comprise three groups. The first group of CCC data processing functions consists of those functions that are performed only at the CCC.

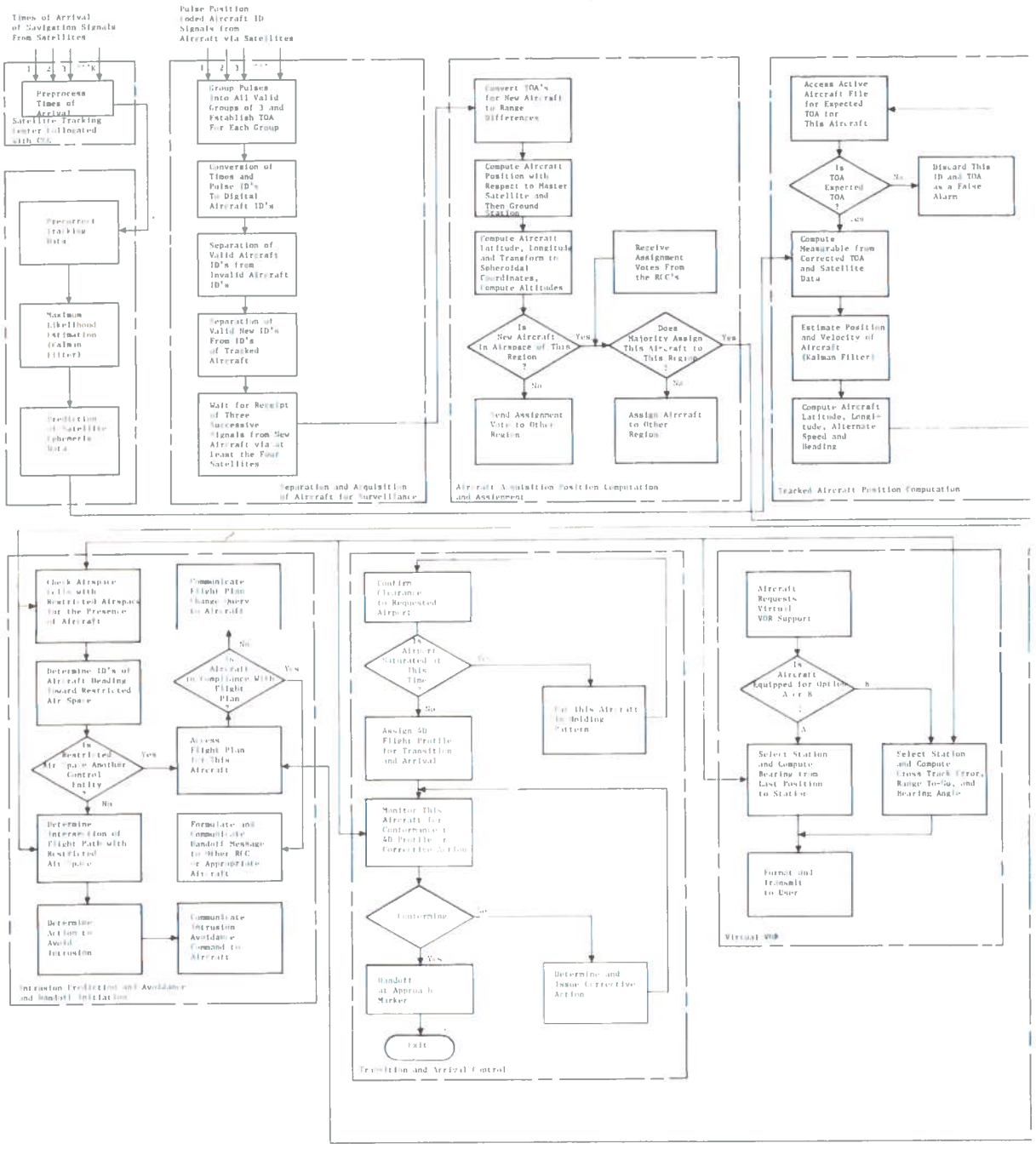

Fig. 5.2-1. CCC Data Processing Top Functional Diagram

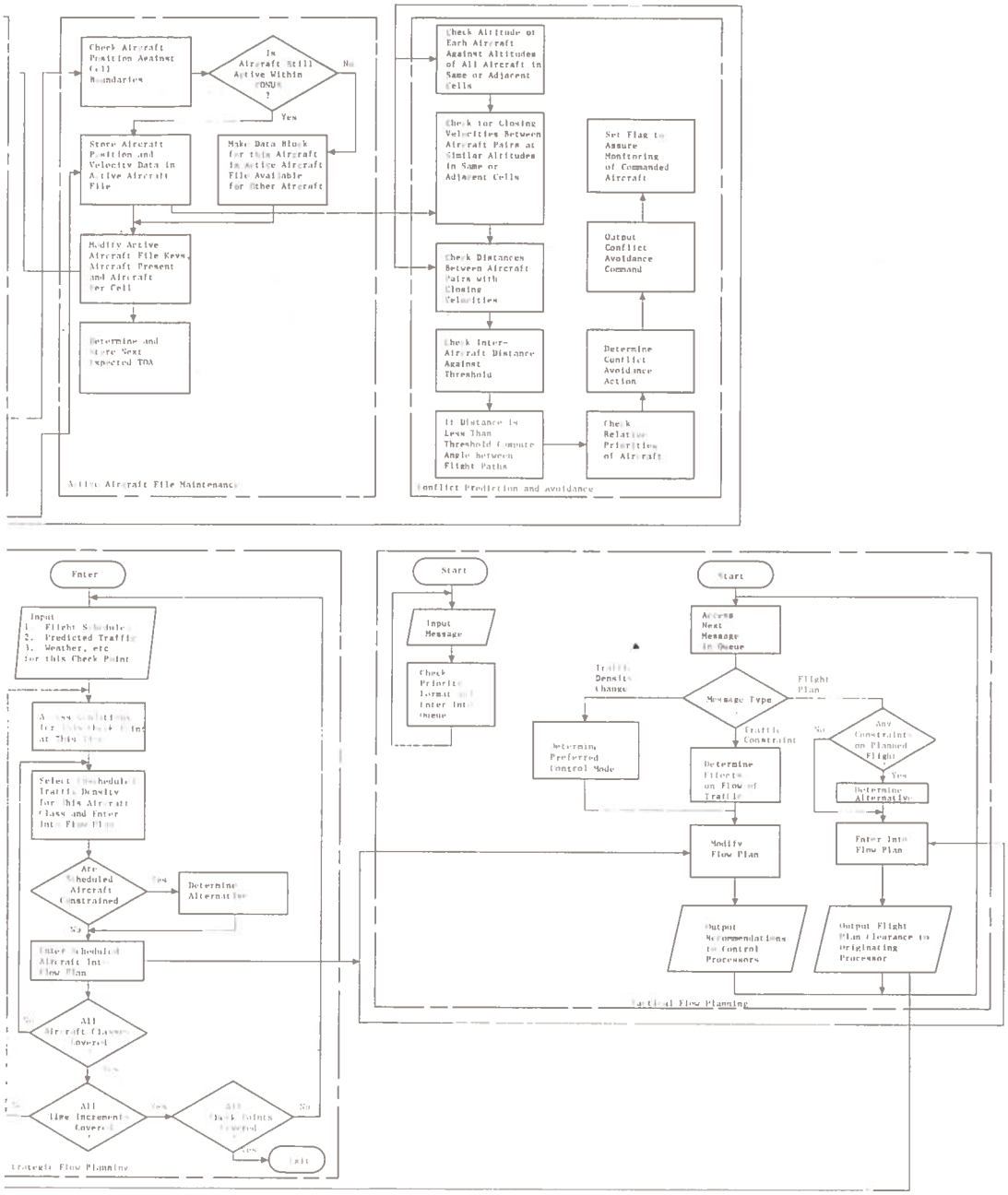

Fig. 5.2-1. (Continued)

The second group of CCC data processing functions consists of those real time functions that are normally performed for each region by an RCC. These functions are also performed for both regions by the CCC as system backup. That is, in case an RCC fails or an RCC function is unavailable for some reason, the functions are performed by the CCC on a backup basis. In addition to providing real time near instantaneous backup for the RCC functions, this redundancy in the system provides a means of achieving an early operational capability since the CCC will be completed before the RCC's. Thus, an aid to a phased transition from the then existing system to the SAATMS is provided.

The third group of CCC data processing functions consists of service and executive functions. Each of these categories of functions are discussed separately in the following paragraphs.

5.2.1 Functions Performed Only at the CCC

The CCC performs those functions that are necessary to plan and maintain the flow of controlled and cooperative aircraft throughout CONUS. These necessary functions include

(1) Strategic flow planning

(2) Tactical flow planning

(3) Compilation of weather service data into a file for accessing by the flow planning functions

(4) Compilation of historical flight data as a function of time and weather conditions

(5) Compilation of flight schedules

(6) Satellite orbit computations

5.2.1.1 Strategic Flow Planning

A functional diagram for strategic flow planning is shown in Fig. 5.2-1. The results of strategic flow planning consist of tables of words which list the numbers of aircraft of each of the four classes that are expected to pass through each checkpoint (CP) during each of M time increments. These tables of words are assembled by first estimating the unscheduled aircraft that will pass through a CP and then adding to it the traffic that is scheduled, taking into consideration the forecast weather and other constraints such as runway closures.

For each time increment at each CP, the predicted weather is accessed and is used in turn to access the predicted unscheduled traffic that will pass through during this time increment. Traffic of each aircraft class is entered into the flow plan and a check is made to determine if any traffic of that class is scheduled for that CP at that time. If traffic of that class is scheduled, tests are made to determine the effects of wind, other weather conditions, and other traffic constraints on the scheduled traffic and, after passing these tests, the scheduled traffic is entered into the flow plan. If, under predicted wind conditions, aircraft of a certain class will not be able to maintain schedule, the resulting delay is computed and that aircraft class is again subjected to the tests to determine the effect of constraints or traffic. If aircraft of a certain class are precluded by weather, congestion, or other constraints from passing a CP, an attempt is made to find an alternate CP and, if found, that aircraft class is subjected to the tests to determine the effect of constraints on traffic at the alternate CP. The number of occurrences of requirements for an alternate CP is not expected to be high.

Figure 5.2-2 shows the strategic flow planning functions in sufficient detail to allow the derivation of data processing requirements; i.e., central processor use, memory, main frame and auxiliary memory, and input/output use.

The data necessary for assembly of these flow plan tables include the following which are entered into the processor from the auxiliary memory for each CP prior to its being planned.

(1) Predicted wind and other weather conditions and planned constraints on traffic flow such as runway closures. For each time increment, one 32-bit word containing the following data is required; wind speed and direction, weather type, duration of weather, and other constraints. The filing order of these data will be sequential according to time, thus facilitating their access by sequential indexing.

(2) An array of predicted unscheduled traffic versus aircraft class, time, and weather. The data in this array, consisting of one 8-bit byte per aircraft class, time, and weather type will be derived from historical records of actual unscheduled traffic through this CP at similar times and under similar weather conditions. These data will be filed according to time and weather. Random access to them can be had by computing a displacement address from the time and weather type and combining this displacement with the starting address of the array to obtain the address of the desired quantity.

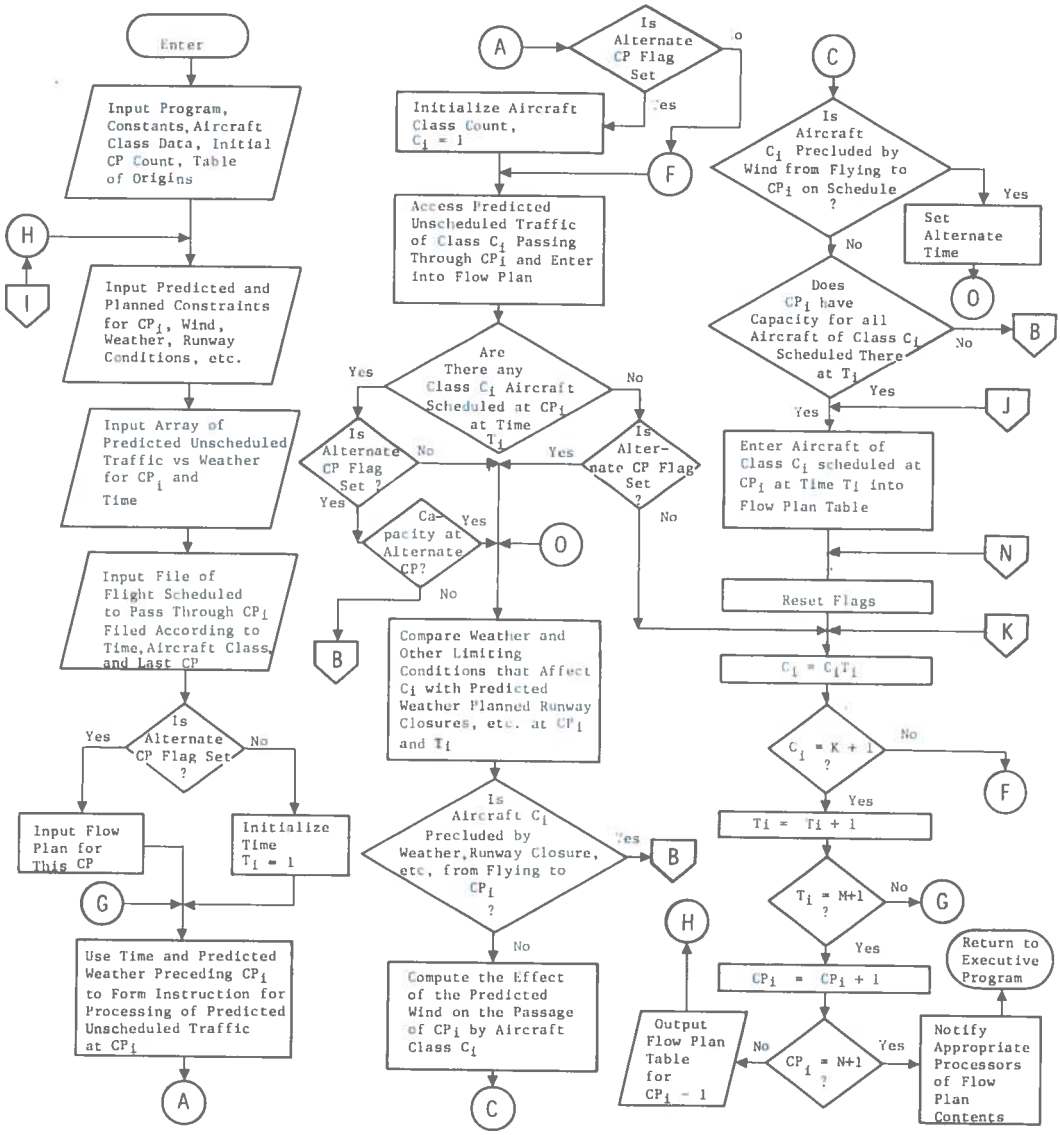

Fig. 5.2-2. Strategic Flow Planning

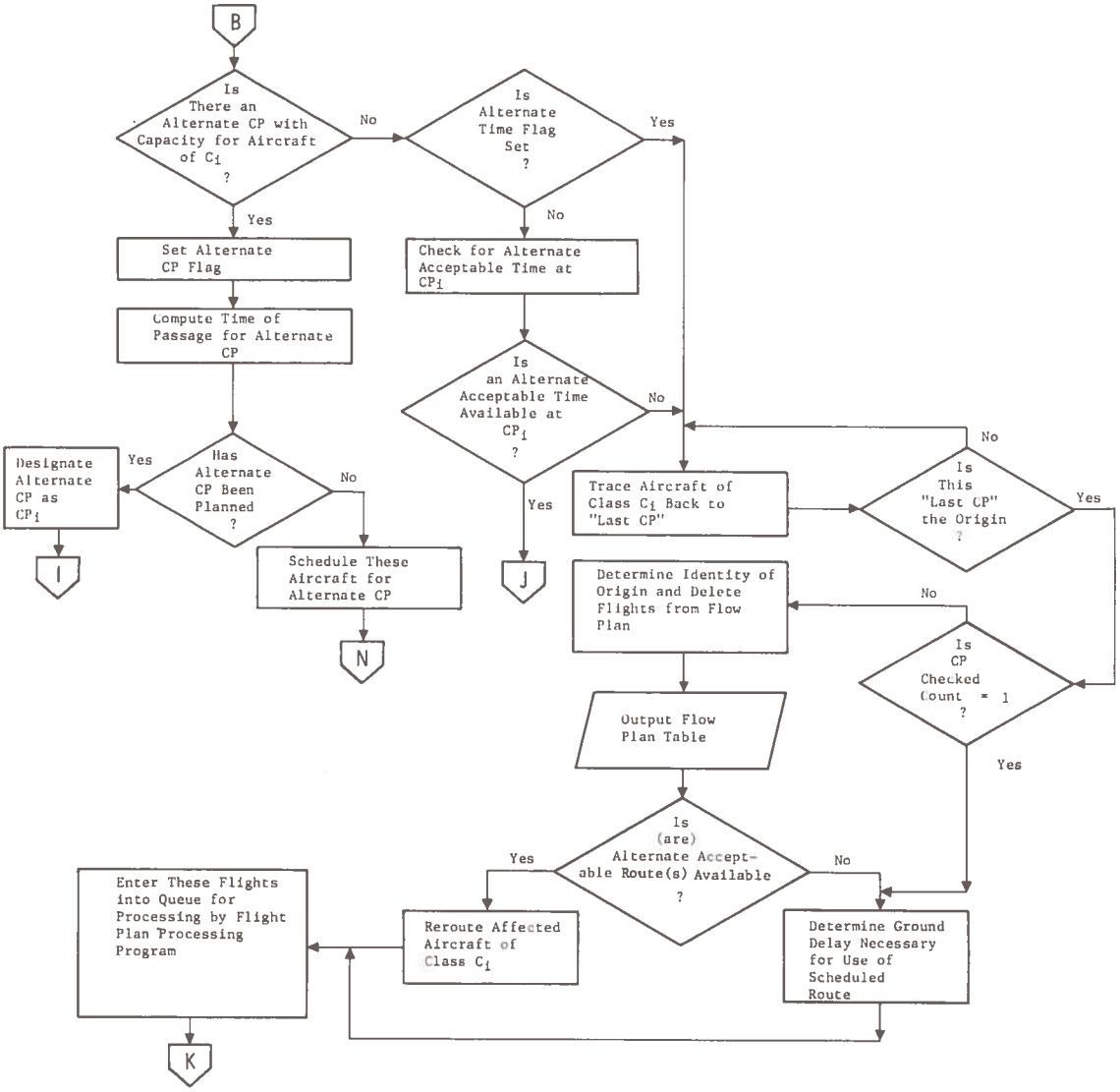

Fig. 5.2-2 (Continued)

(3) A file of flights that are scheduled to pass through this CP. For each aircraft class, time increment, and last CP, one 32-bit word containing the following data is required: quantity of aircraft, distance and direction from last CP, and indications of the allowable delay and the next CP. The schedule files for the CP's will be assembled by means of another program which will use as inputs all periodic flight schedules defined in terms of CP passage times. Addressing of the schedule file data will be by means of a base plus displacement scheme with the latter computed from the aircraft class, time, and last CP.

The relatively long interval that elapses between strategic flow planning runs indicates that this function can be treated similarly to a batch operation and can be run during off-hours, e.g., early morning prior to the daily inception of heavy air traffic. Thus, the amount of data processing hardware required at the CCC is minimized with no degradation of system performance.

With 4000 CP's planned and the number of time intervals over which they are planned equal to 100, typical data processing requirements for strategic flow planning are

(1) 200×10^6 instructions per run

(2) 200×10^6 words input or output per run

(3) 15×10^6 words of auxiliary, e.g., disk storage

(4) 16×10^3 words of main memory

It can be seen that this function tends to require a large number of central processor instructions, a large number of input/output operations, and a large off-line auxiliary memory. This function can be readily performed by means of hardware similar to that used for real time and on-line functions as long as it is done during a different time period than the real time and on-line functions.

5.2.1.2 Tactical Flow Planning

The flow plan that results from the strategic flow planning function is the basis on which short-term changes to aircraft flow in an area are taken into consideration. The types of changes that will affect a flow plan include

(1) Unplanned increases or decreases in traffic density

(2) Constraints or traffic flow such as closed airports or runways, winds, and other weather conditions

(3) New flight plans

(4) Changed or cancelled flight plans

The latter two items, the process of updating flow plans and clearing flight plans or changes thereto, are two facets of one task.

A functional diagram for the tactical flow planning task is presented in Fig. 5.2-1. The results of tactical flow planning consist of recommendations to control processors, modifications to flow plans, and flight plan clearances (with or without changes). As in strategic flow planning, constraints on traffic such as wind, weather other than wind, and airport and runway closures are taken into consideration.

Entering the messages that initiate tactical flow planning actions into the flow planning processor can be a rather large task in itself. One or more processors may be assigned to this task. One hardware mechanization, as indicated in Fig. 5.2-2, would have a front end processor performing message processing and placing the messages in a queue in the memory that is accessible to the main processor.

In addition to the input messages, performance of the tactical flow planning function requires data on predicted weather and other constraining conditions and the strategic flow plans. The volume of these data is large and thus most likely be stored in the auxiliary memory.

Each message that is received is first processed to determine its priority. Any necessary formatting is done and the message is queued on the basis of its priority. Then, as each message comes up, it is tested for type. Here three general types have been assumed: (1) traffic density changes, (2) traffic constraints, and (3) flight plan initiations or changes.

A message that describes a change in traffic density, either up or down, results in a recommendation to the affected control processor(s) that tighter or looser control is to be exercised. Also, the flow for the affected CP's is replanned and the changed plans are disseminated to the appropriate control processors.

A message that indicates an added constraint on traffic at certain CP's results in replanning of traffic at and/or around those CP's. Removal of an existing constraint results in file searches to determine traffic that was rerouted, and the replanning of traffic flow to use preferred routes or destinations.

A message that describes a new flight plan or a change to an existing flight plan results first in tests to determine whether it is new, cancelled, or changed. If it is a cancellation, the flow plan is modified. If it is a new or changed plan, constraints and capacity at each planned CP are checked and if necessary, alternate legs, destinations, or times are selected. In either case, the flight plan clearance or modification is transmitted to the requester and the changed flow plan is transmitted to the affected control processors.

Figure 5.2-3 shows the tactical flow planning function in sufficient detail for derivation of processing requirements.

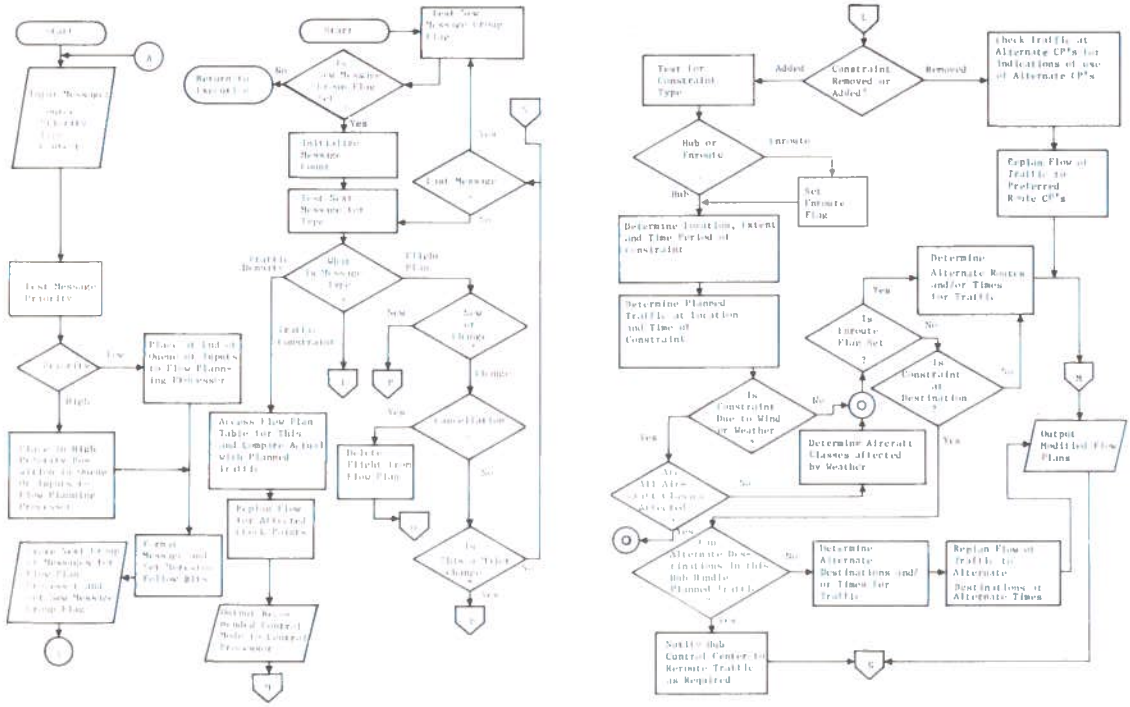

Fig. 5.2-3. Tactical Planning Flow

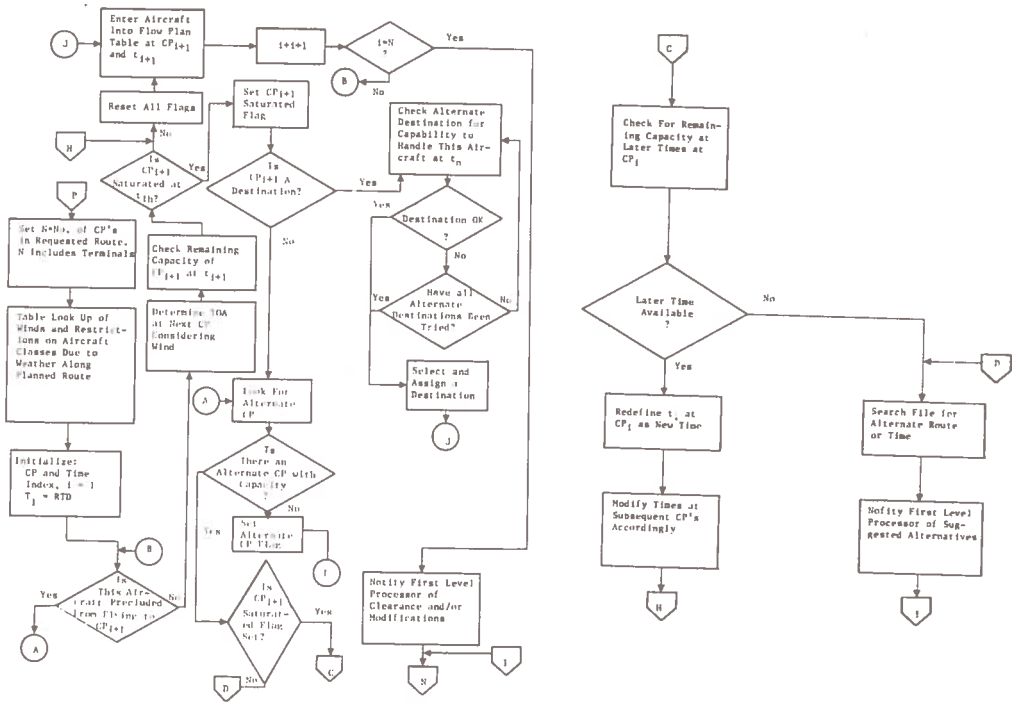

Fig. 5.2-3 (Continued)

Tactical flow planning being an on-line function will require the dedication of certain hardware capabilities to its needs. With the rate of messages and therefore the rate of tactical flow planning actions equal to 150 per second, typical data processing requirements for this function are

(1) 200×10^3 instructions per second

(2) $1\text{-}5 \times 10^6$ words input or output per second

(3) 300×10^3 words of main memory

5.2.1.3 Data Compilation Functions

Under strategic flow planning above, mention was made of the data input requirements. Hardware and software must be provided to compile these data into formats which correspond to both the stragetic and tactical flow planning software and hardware. The required data compilation tasks (those for weather service data, historical flight data, and flight schedules) will be performed off-line in a more or less batch mode. Multiple use of data processing hardware can be accomplished with no degradation or real time or batch functions by using hardware, normally used for real time functions, during off-hours for the performance of these data compilation tasks.

5.2.1.4 Satellite Tracking and Ephemeris Computation

Performance of data processing associated with the tracking of satellites for the purpose of acquiring and correcting the present position of each satellite is a function that does not fall into one of the categories previously presented. While it is a necessary function, it is not a demanding function for control processor, input/output processor, and memory capabilities. Thus, the satellite tracking function can be performed at all locations where needed: CCC, RCC's, and the ACC's. The data processing capability that will exist at these locations can be used for this function. The number of data processors tends to be minimized by this collocation of functions.

To estimate the orbits of the satellites from the corrected tracking data, however, involves the use of a large (48-element) state vector which processes the data in this vector with a recursive maximum likelihood estimation algorithm (a Kalman filter). The outputs of this filter, which are computed only at the CCC, are used to predict future satellite positions and velocities. These data are used by the RCC's to determine the positions of aircraft. The data are also used to perform satellite navigation functions.

The data processing equipments for satellite tracking and ephemeris computations are

(1) 170×10^3 instructions per second

(2) 12×10^3 words of main memory

The input/output traffic for these functions is on the order of 10 words per second.

5.2.2 Functions Performed at the CCC to Back Up the RCC's

The CCC must include the capability to perform those functions that are primary to an RCC but which must be backed up if the RCC fails. These backup functions will be performed for the entire CONUS in parallel with the RCC's. If one or both RCC's is down due to failure or some other cause, the backup functions are continued in a normal manner.

The backup functions performed at the CCC include

(1) Acquisition of aircraft for surveillance

(2) Computation of positions of newly entered aircraft

(3) Computation of positions of tracked aircraft

(4) Maintenance of file of active aircraft

(5) Conflict prediction and avoidance

(6) Intrusion prediction and avoidance

(7) Handoff determination and initiation

(8) Virtual VOR

(9) Transition and arrival control

5.2.3 Service and Executive Functions

The following functions must be performed whenever the CCC is operating:

(1) Communications processing

(2) Display and man/machine interface processing

(3) System and self-test

(4) Executive functions

When the CCC is substituting for one or both RCC's, the display and man/machine interface processing functions will allow the operations personnel to control the appropriate airspace.

5.2.4 CCC Processing Hardware Organization

Figure 5.2-4 shows a configuration for data processing hardware that is capable of performing the functions listed in Table 5.1-1. A discussion relevant to Fig. 5.2-4 can be found in Section 5.3.

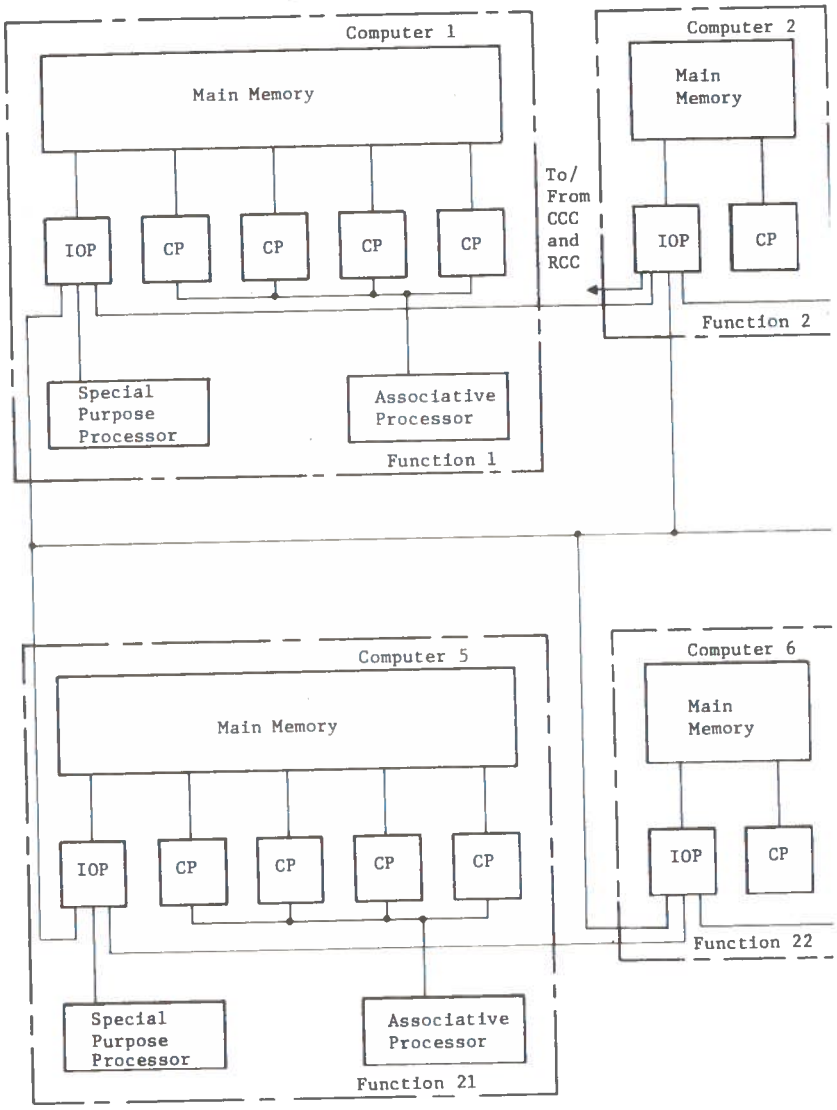

Fig. 5.2-4. CCC Processing Hardware Block Diagram

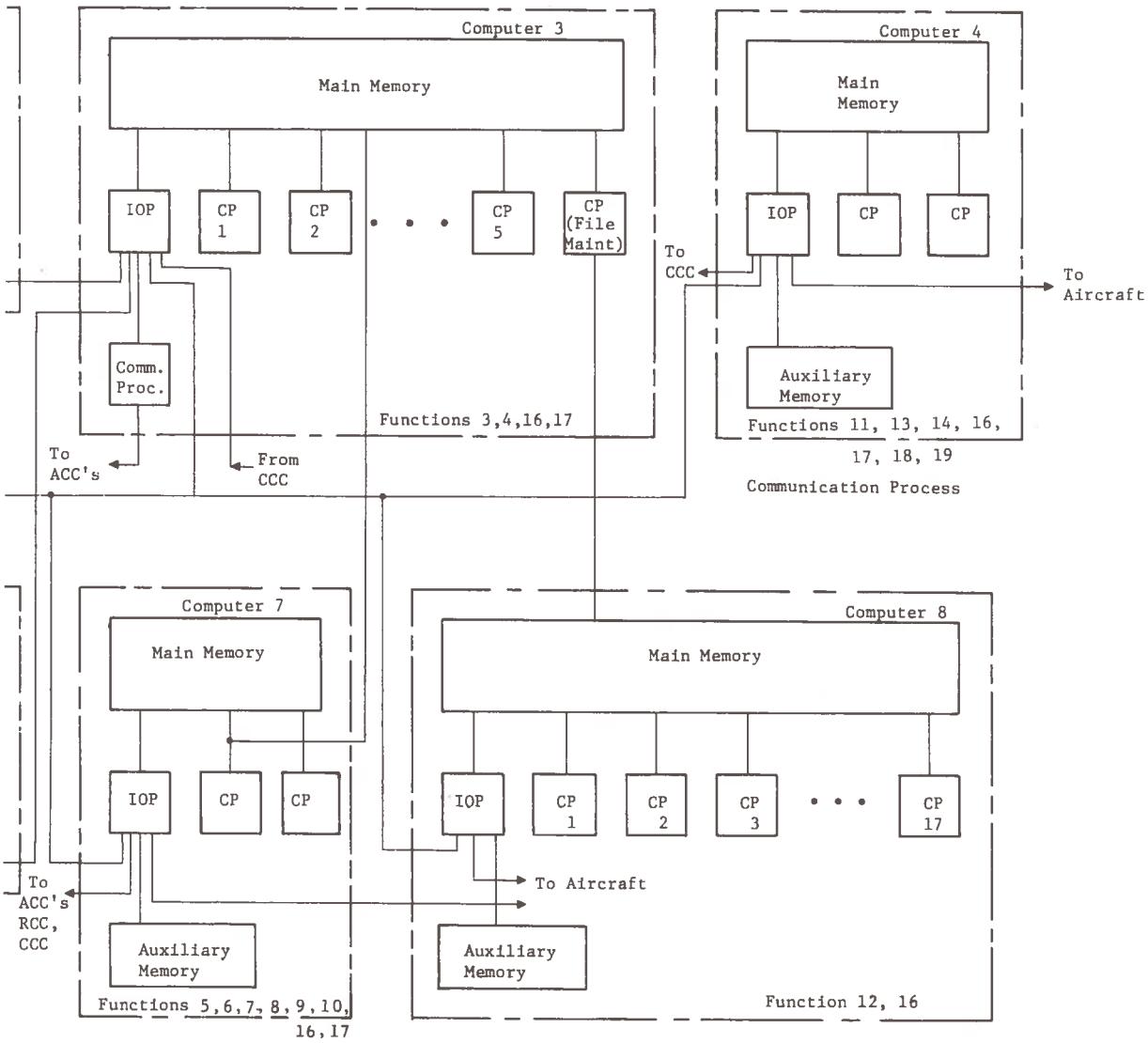

Note: The function numbers are those listed in Table 5.1-1

Fig. 5-2.4 (Continued)

5.3 RCC Data Processing

Figure 5.3-1 shows the data processing functional block diagram for an RCC. The principal data processing functions to be performed at an RCC include:

(1) Acquisition of aircraft surveillance signals, filtering of these signals to separate new ID's from tracked aircraft ID's, TOA computation of newly acquired aircraft position, and assignment of primary surveillance responsibility

(2) Computation of tracked aircraft position

(3) Maintenance of a file of active aircraft

(4) Prediction of conflicts between aircraft and determination of the required action for avoidance

(5) Prediction of impending intrusions into controlled airspace; airport airspace, or restricted regions, and determination of the required action to avert such intrusions

(6) Determination of a need for a handoff to the other RCC region or airport and performance of a handoff to or from other airspace.

(7) Computation, for those cooperative aircraft that request them, of area navigation commands by means of the Virtual VOR mechanization

(8) Computations related to entry of aircraft into, exit of aircraft out of, and control of aircraft while within transition airspace between airport airspace and enroute airspace

5.3.1 ID/TOA Decoding and Preprocessing

The SAATMS concept uses periodic surveillance signals from all active aircraft in CONUS that include an identification code. L-Band surveillance signals are transmitted to satellites for conversion to C-Band and for retransmission to the CCC and RCC's. At each of these control centers, up to 12 C-Band controllable antennas track each of the visible satellites. The received signals are translated and sent to a bank of 16 Analog Matched Filters (AMF) for detection. The identification signal is shown in Fig. 5.3-2.

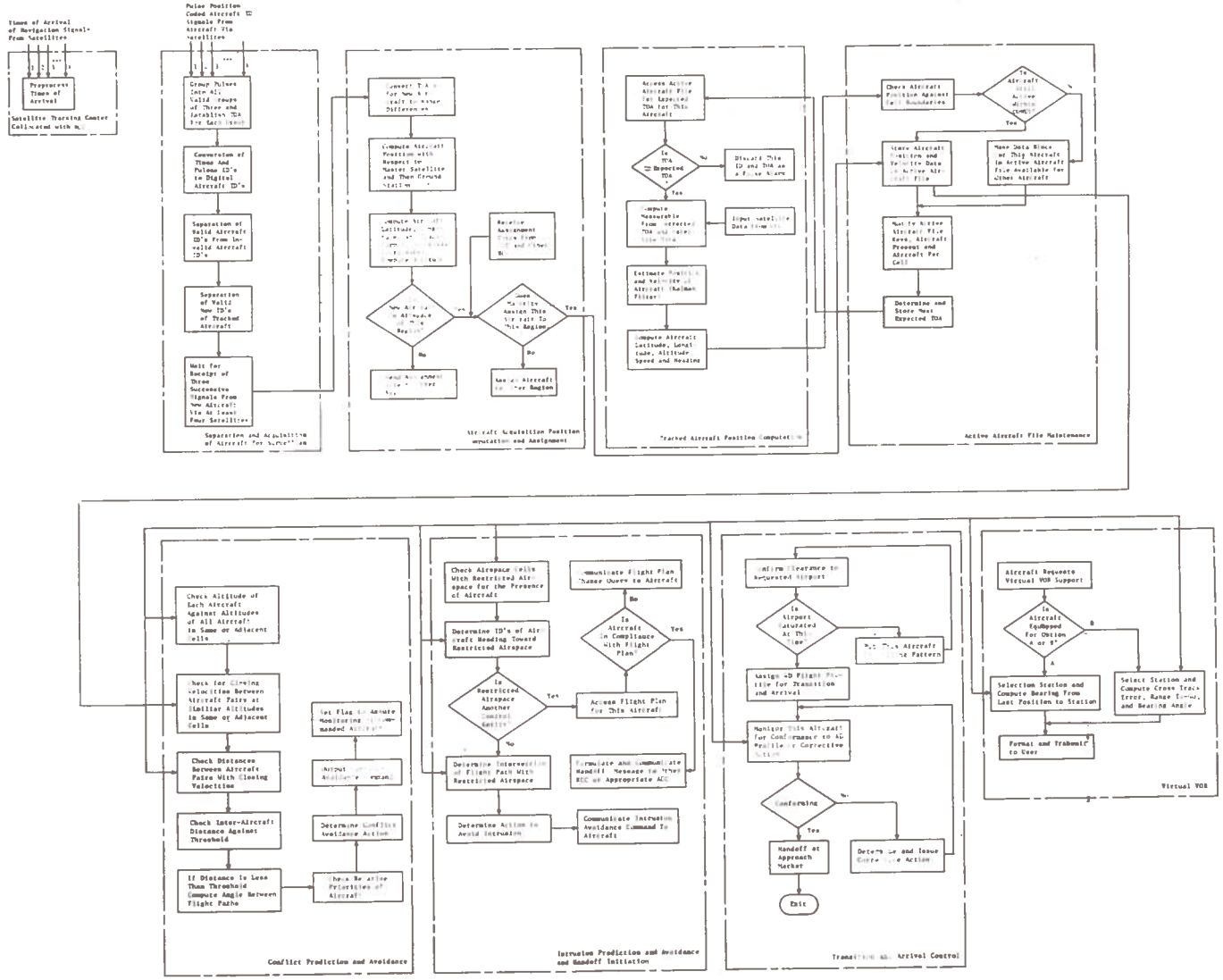

Fig. 5.3-1. RCC Data Processing Top Functional Diagram

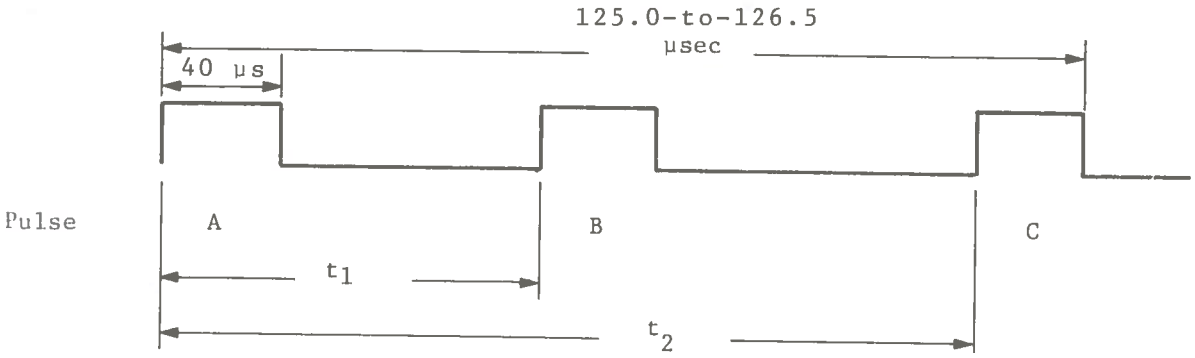

where: $t_1 = T_1 + \Delta t$

$t_2 = T_2 + \delta t$

T_1 and T_2 are nominal pulse position times

Δt and δt are times in increments of 100 nsec assigned for each identification

Fig. 5.3-2. Aircraft ID Signal Format

Each of the three pulses is pseudo-noise modulated. The second and third pulses will be positioned in time relative to the first. Sixteen code combinations and 16 relative positions for the pulses provides a total identification capability of $[(2^4)(2^4)(2^4)(2^4)(2^4)] = 1{,}048{,}576$.

As noted, these pulses are processed through AMF's. The 40 μsec pulse widths are then compressed into 100 nsec pulses.

The surveillance system parameters are given as follows:

(1) Total aircraft to be identified = 10^6

(2) Active aircraft at any time = 35×10^3

(3) Update time per aircraft = 2 and 8 sec for entrance and tracking, respectively

(4) Compressed identification arrival $\leq$ 100 μsec

(5) Time to receive all satellite signals from an aircraft = 80 msec

(6) Number of satellites = 10

Acquisition is based upon receipt of the same identification number from four or more receivers for three successive identification transmissions. After the establishment of a legitimate identification, four TOA's from different receivers are used to obtain three differential TOA's. The differential TOA's, the signal velocity of propagation, and satellite positions are used to determine the aircraft location. This location data is supplied to the surveillance tracking function.

Figure 5.3-3 presents the overall surveillance concept for the CCC or RCC's.

The time alloted to extracting the identification data from the pulse trains and the characteristics of the pulse trains dictates the use of special purpose digital processing equipment to perform the function of identification processing.

As noted earlier, the received signals are time compressed in matched filters and shaped to provide 100 nsec pulses. These pulses are routed to shift registers forming a 100 μsec sample of the received codes. The processing problem is to associate the three pulses which form legitimate identifications and assign a TOA upon doing so.

One concept for performing the pulse association process is shown in Fig. 5.3-4 and 5.3-5. The 100 μsec sample is dynamically stored in shift registers and updated every 100 μsec. The ends of the 16 shift registers are logically OR'd to initiate the identification processing each time a possible A pulse occurs. This signal is used with two others generated by examining the time slots corresponding to the B and C pulse position. If all three are present, an aircraft identification is required; if not, this pulse is not an A pulse and no further action occurs.

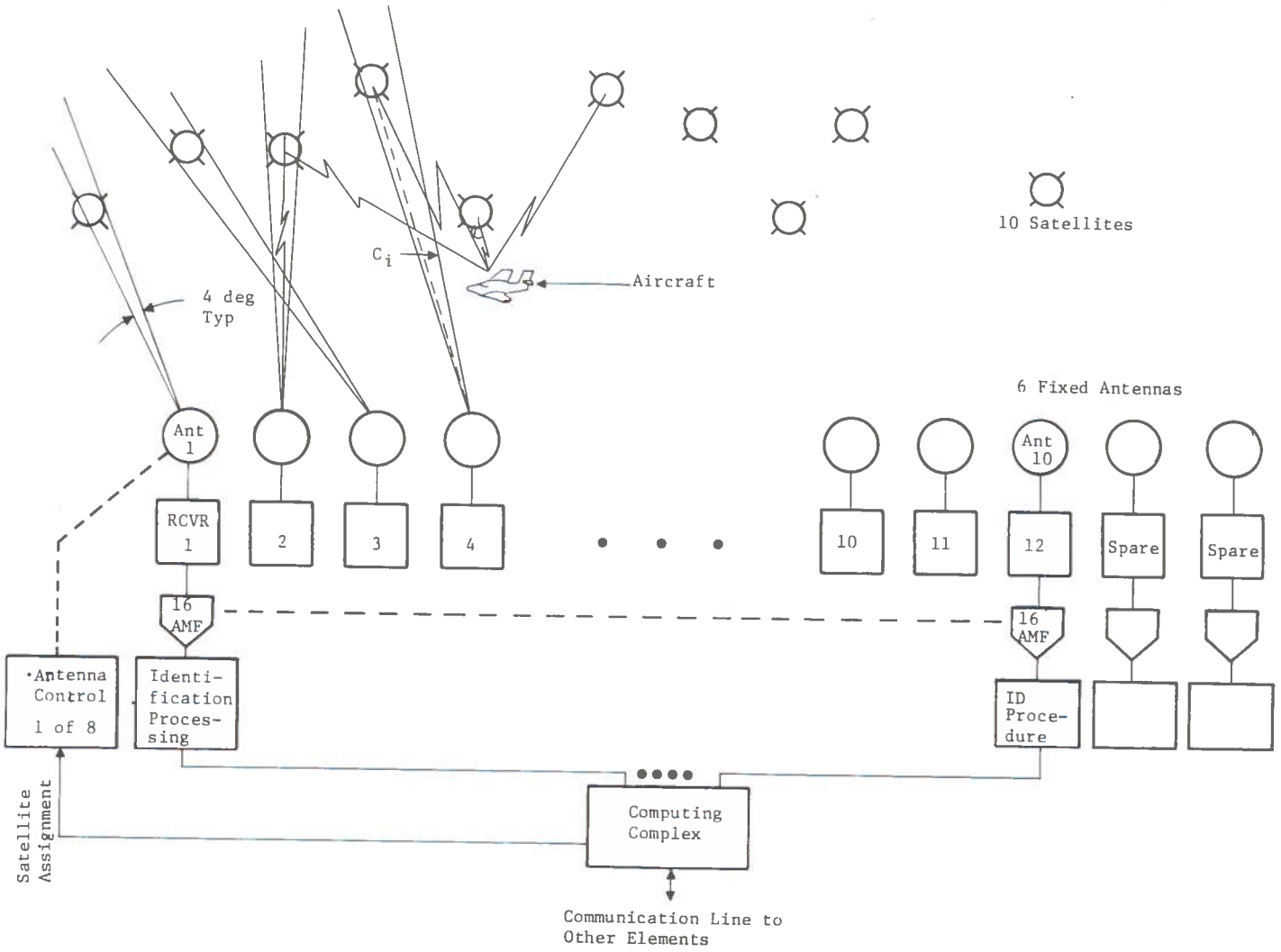

Fig. 5.3-3. Surveillance Subsystem Organization for CCC or RCC

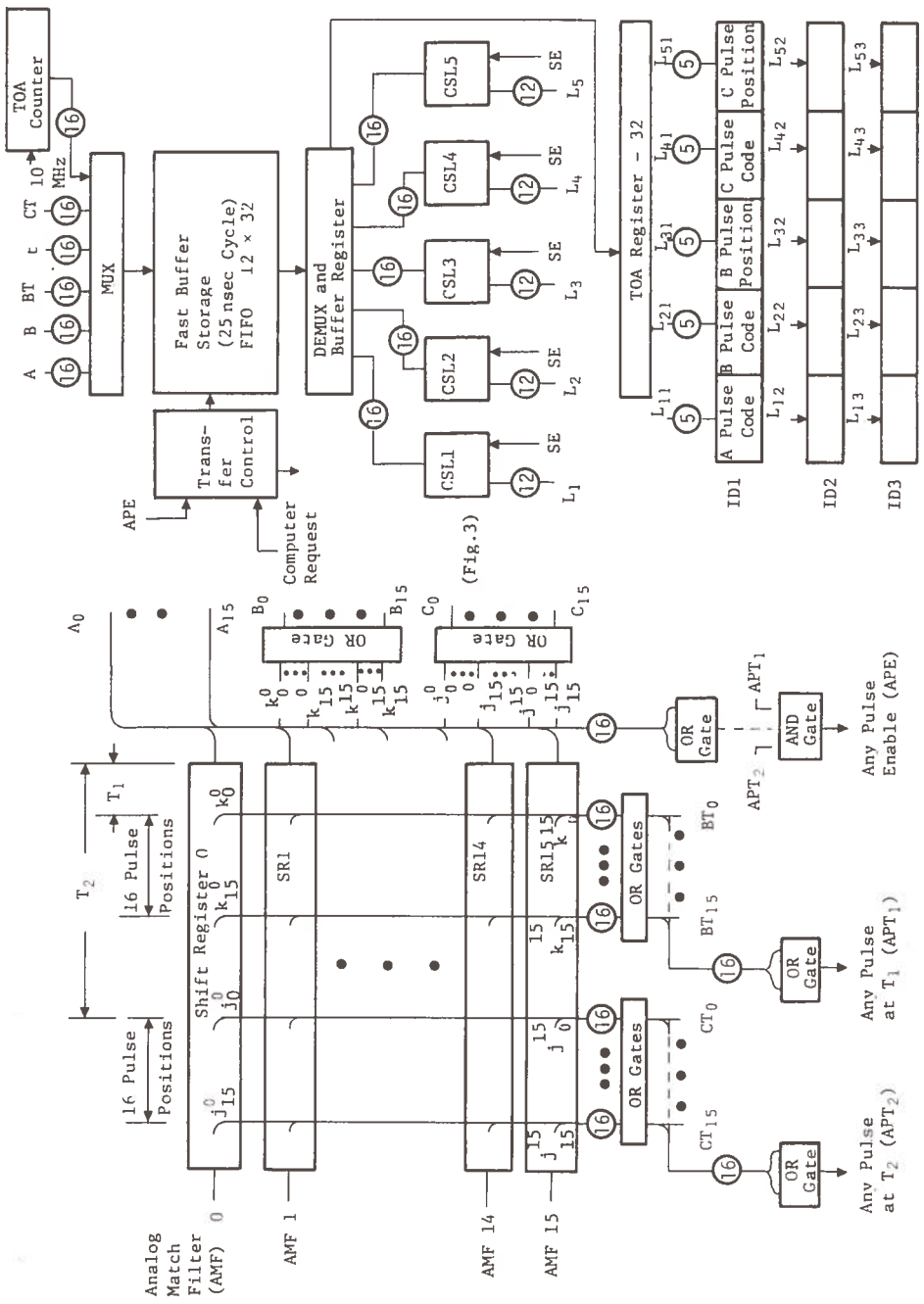

Fig. 5.3-4. Identification Processing

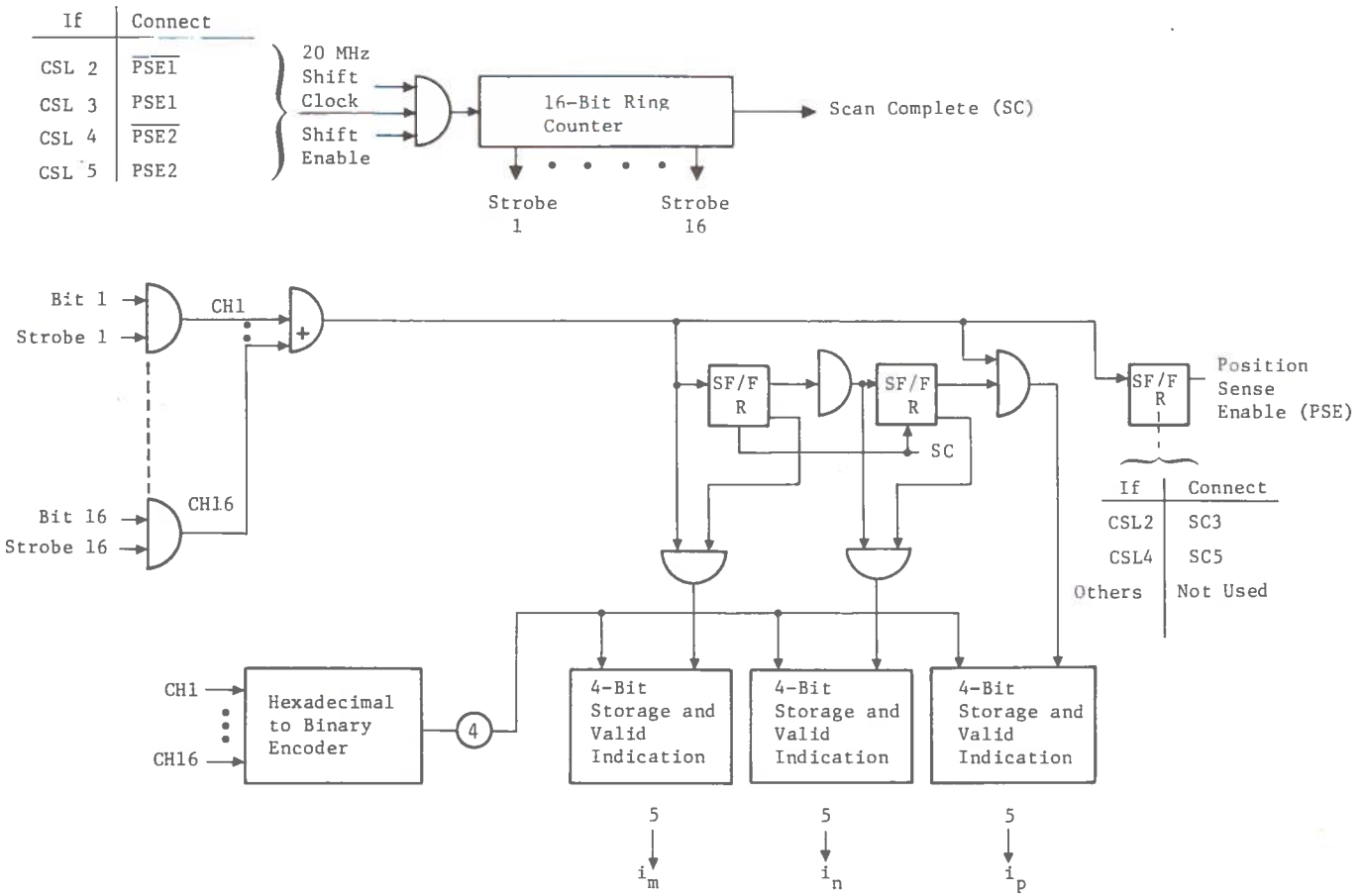

Fig. 5.3-5. Code Segment Logic (CSL)

The sensing of a possible identification (A, B, and C pulses present) results in immediate transfer of the pulses in the shift registers to a fast buffer storage whose function is to store a snapshot of the pulses in the shift register. The pulses and their corresponding TOA's must be stored within 100 nsec. A nominal method using a 12-word by 32-bit, 25 nsec buffer is shown in the upper right portion of Figure 5.3-4.

The transfer control contains the timing and logic to address and control the loading and unloading of the buffer in response to legitimate Any Pulse Enable (APE) signals or requests from the computing complex.

The rapid storage provides the ability to process multiple valid or possible identifications received within a short time. The following cases are considered to be of reasonably high probability of occurrence as to warrant processing provisions:

(1) Multiples of three identification sets received during a 100 μsec interval

(2) Two concurrent A pulses due to multiple identification or false alarms due to noise or previous pulse trains

(3) Single A pulses and multiples of up to three B and/or C pulses for each

(4) Double (concurrent) A pulses and multiples of up to three B and/or C pulses

(5) Three successive A pulses within 100 nsec of each other with up to three B and/or C pulses for each.

The worst of these, item (4), results in 18 possible combinations of identification to be analyzed by computer processing to segregate legitimate returns from false alarms.

The buffer thus provides a means of capturing the identification pulses under the above situations. The rest of the identification processing is concerned with formatting the identification pulse in binary and associating the B and C pulse codes with their respective pulse times. As shown in Fig. 5.3-4, the information is transferred from the buffer storage through a demultiplexing network to Code Segment Logic (CSL). (Five CSL's are shown. Alternately, a design using two could be employed at the sacrifice of processing time.) The outputs of the CSL's are directed to identification registers prior to transfer to the computer complex for further processing.

The CSL design is shown in Fig. 5.3-5 and consists of scanning logic with conversion to binary and storage of the resultant code segments. A fifth output bit per segment is shown to indicate a valid zero is stored. Logic is included to permit the association between the pulse code and position. The 20 MHz clock provides a scanning capability of 50 nsec per step. It takes a maximum of two complete scans to convert the pulses. This results in a conversion time range of 0.8 to 1.6 μsec.

A design for precise TOA requirements and recombination with ID's is not shown here, but is required.

The considerations involved in the identification of a new aircraft are shown in Fig. 5.3-6.. When a new set of possible identifications (maximum of 18 as noted earlier) is received, it is first compared with known aircraft. Known aircraft here include previously acquired, nonissued, and calibration identities. These will be eliminated from consideration with the remainder providing the input to the surveillance tracking function. They must then be compared with the remainder file of unknown aircraft for all of the other "R" receivers. A record of the numbers of comparisons must be noted.

If the number of receivers which have an identification corresponding to the one being processed is fewer than four, it is because (1) the other receivers have not received the signal via their satellites or (2) this is a false alarm. In order to determine which, the TOA of each receiver's identification must be examined to see if 80 msec (the maximum transmission time expected between an aircraft code emission and its receipt via a remote satellite) has elapsed. If so, and fewer than four receivers have identified that aircraft, the data must be removed from the file. If not, the identity information must be saved for later comparisons.

If the receiver number is greater than or equal to four, this identification must be compared with a table of possible new aircraft. This table is the accumulation of identifications received by four or more receivers over a given time period. A further detection requirement is that at least four of these receivers must process the identical code for three consecutive bursts. Thus, if any of the stored possible identifications have elapsed times exceeding 6 sec, they must be eliminated from that file.

If all detection/criteria are met, the identification being processed represents a new aircraft. The processing exits to that activity for handling new identification. This includes the setting of the appropriate files and assignment for routing control.

It is apparent that a large quantity of information must be examined in order to extract the unknown from the false alarm and known aircraft.

It is evident, by the surveillance procedure defined to this point, that all active aircraft must be examined during the 8 sec basic burst interval. Table 5.3-1 illustrates a typical distribution of aircraft identification codes for a receiver.

Assuming 10 receivers are used, approximately 500,000 identifications must be compared with a known aircraft file within 8 sec. This amounts to 16 μsec per comparison if these are done sequentially. If performed in parallel,16.0 μsec can be allotted for each comparison.

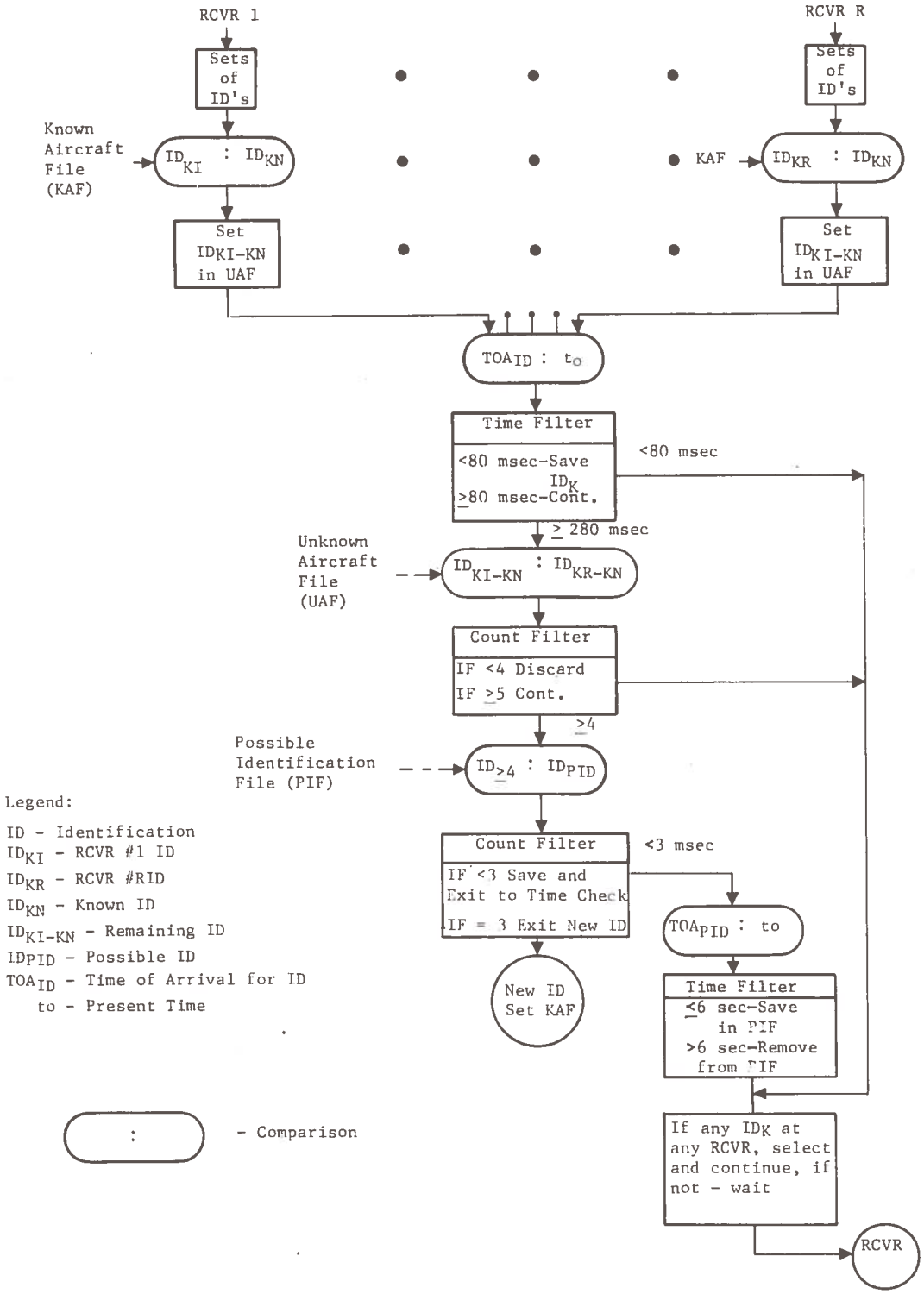

Fig. 5.3-6. New Aircraft Identifcation Flow Diagram

Table 5.3-1. Distribution of Aircraft Identification

Identifications/100 μsec	Total Aircraft (%)	TOA's	Possible Identifications
1	85	29,750	29,750
1 plus 1 false alarm pulse	5	1,750	3,500
2	9	3,150	12,600
3	1	350	6,300
Total		35,000	52,150

These times represent an average and include that amount needed to access the data and update the file. It is reasonable to expect that unless the data are processed at the fastest rate expected some buffering is required. The size of the buffer is interrelated with the speed at which comparisons can be made.

There are a number of concepts which could be developed to accomplish these comparisons. These could encompass various direct and associative addressing schemes. One reasonable approach is to provide a memory which has a bit assigned to the indication if the identification is known. The identification itself would be the address of this bit. A memory of 32,000 × 32 bits would supply the total storage needed to contain this activity status. Further, with rapid memory accessing possible and projected, it is reasonable to assume that such a file will be fast enough to perform the comparison in real time.

Figure 5.3-7 is the flow chart of the front end processor computational functions. Its primary function of separating the known identifications from the unknown is shown in more depth since the majority of the computer requirements are derived from this chart. The data processing requirements are

(1) 4,000,000 Instructions per Second (IPS)

(2) 80,000 words of main memory

The output result of the front end processing will be those identifications which are considered unknowns and include the false alarms. If the approximate 17,000 identifications per receiver remaining were to be conveyed to the next filter action (i.e., the comparison between receiver unknown files), a substantial amount of computing still would be required.

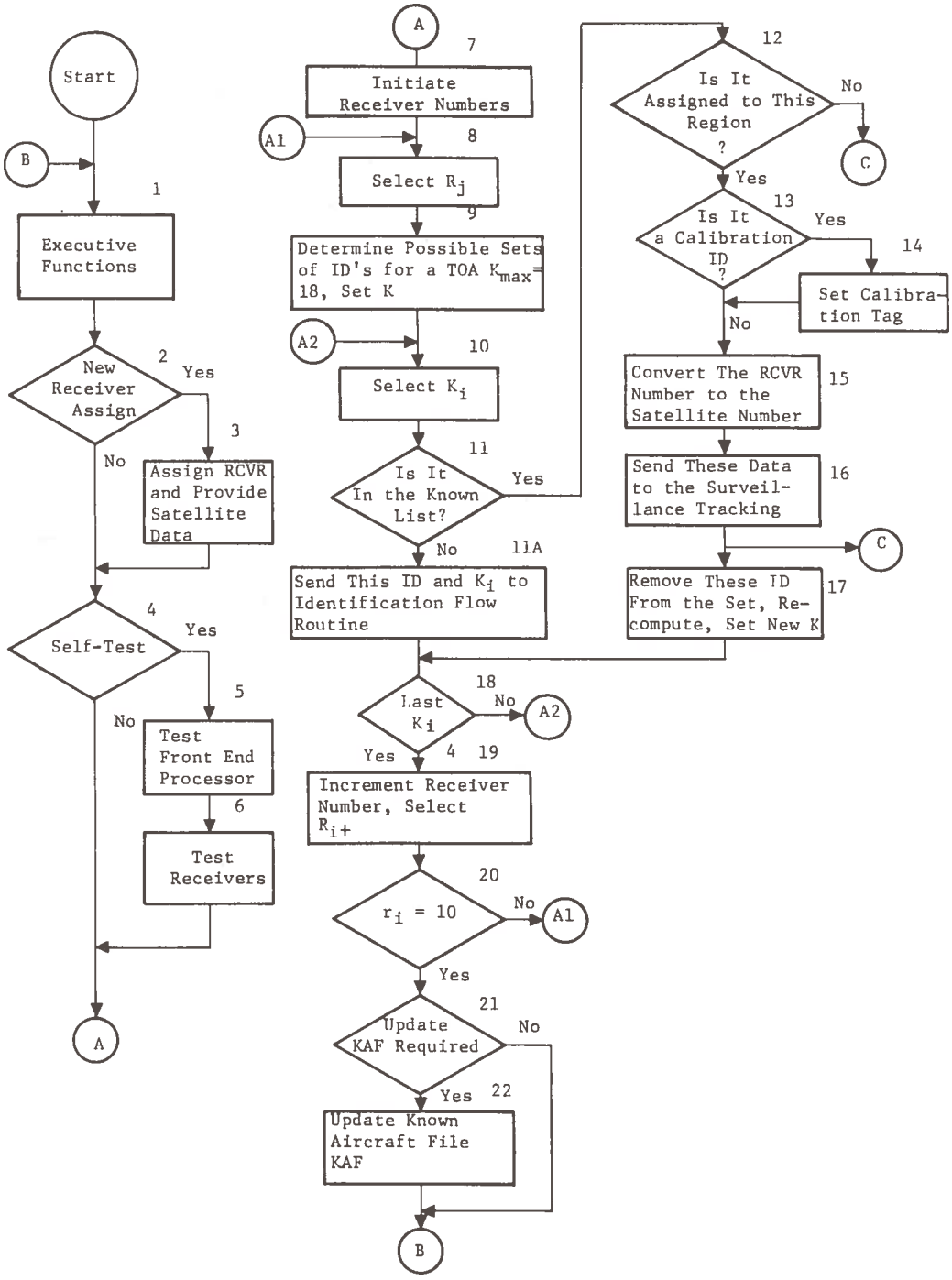

Fig. 5.3-7. Flow Diagram - Front End Processing

It is possible, however, to reduce the number which must be compared. One method would be to revise the received ID set when an identification is made by removing that one from the set and redetermining a new set based upon the remaining codes. This approach may result in the elimination of a possible new identification for one or even a few burst intervals. However, the likelihood of all receiver's replicating ambiguous identifications is extremely remote. Therefore, new aircraft would probably be quickly entered into the system. Also, since no return acknowledge signal is transmitted until the aircraft does enter, no danger to the system operation is possible.

If the above is done and if allowances are made for replication of known and nonexisting identification, it is estimated that 4,000 identifications per receiver need further processing. Table 5.3-2 shows this analysis.

Table 5.3-2. Estimate of ID Processing Load

Type ID/100 μsec	Possible ID's	Possible ID's after Revising ID Set
1	29,750	0
1 plus 1 false alarm	3,500	0
2	12,600	3,150
3	6,300	1,400
	Subtotal	4,550
Less estimate for replicate known and unassigned		550
Total per receiver		4,000

The actual number of aircraft entering and leaving the system would be within this number. With 1,000 airports and a worst case entrance/exit time of 80 sec, about 100 new identifications per 8 sec is expected.

The number of ID's per second per receiver is 500; the number per 80 msec interval is 40. A major reduction in the number of identifications to be processed can be obtained by storing all of the same identifications from all receivers for 80 msec. After this time, only those with more than a four-receiver responses would be saved. The others would be dropped. It is expected that less than 1 percent of the possible false alarms will remain. A conservative allowance number of ID's to be further processed is estimated as four per receiver per 80 msec.

Figure 5.3-8 is a flow chart describing this processing activity. The logic for placement of data in various files and the tests for validation of an identification are presented. Also shown are methods to remove old data when

IDENTIFICATION

FLOW DIAGRAM

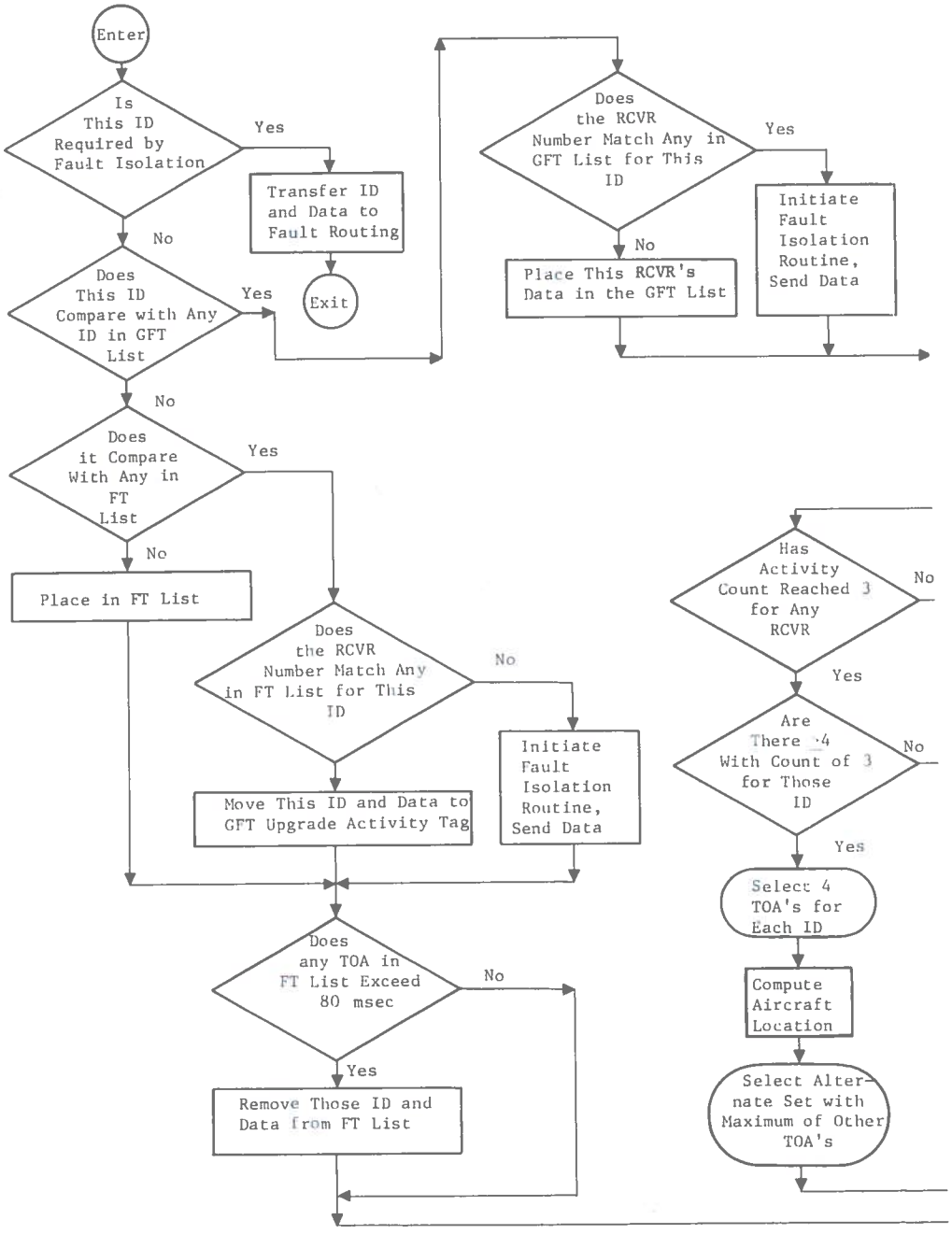

Fig. 5.3-8. Identification Flow Diagram

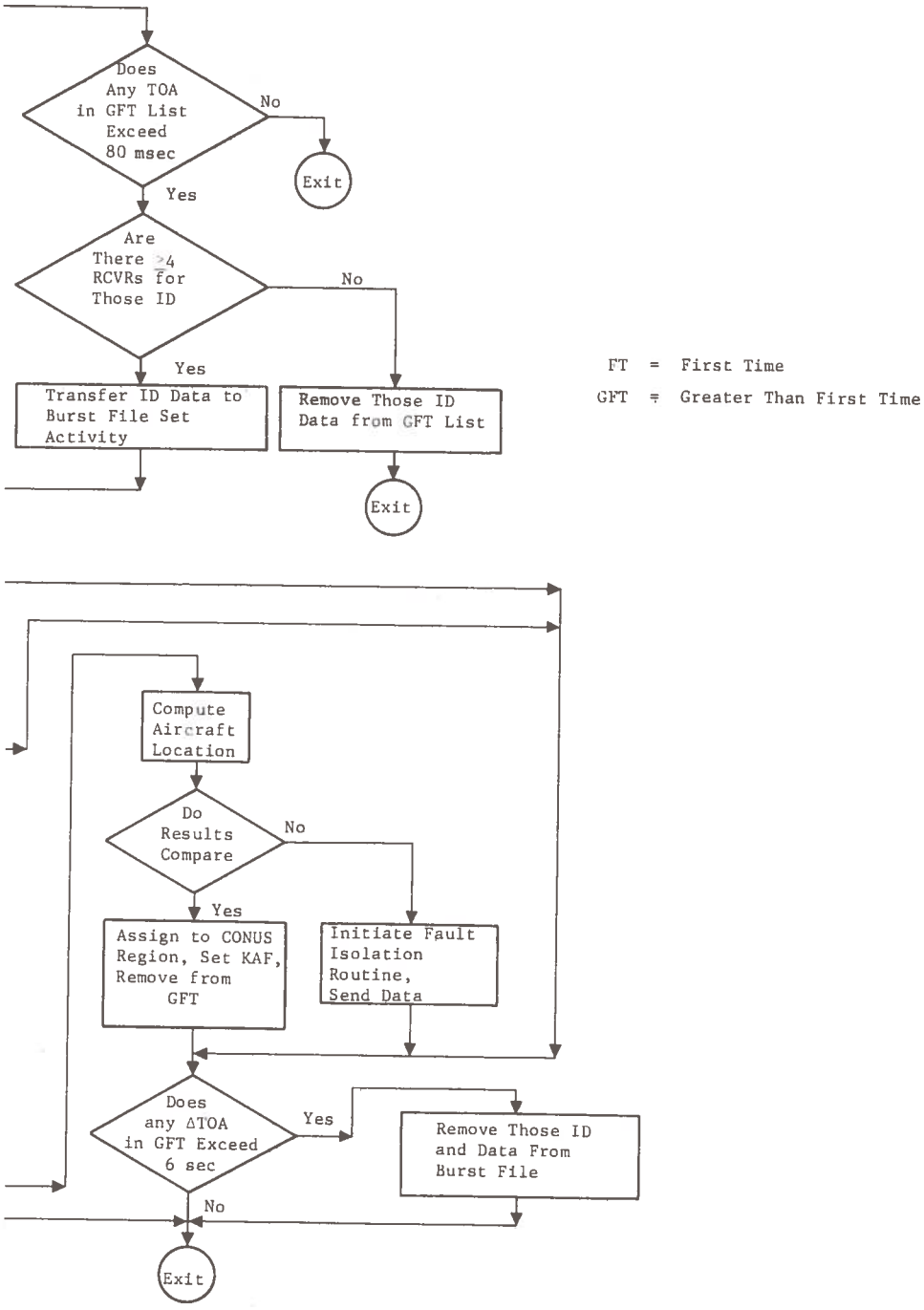

Fig. 5.3-8 (Continued)

accumulated in these files. These are based upon the various maximum receiver time allowed. As noted, the time checks are accomplished at the end of the routine and are only needed if new information is being supplied. Thus, computer performance is not consumed in making periodic file checks.

It is expected that some memory protection as file address bounding will be supplied in the computer to protect the files. File overflow or intrusion for any reason will result in notification of the executive for appropriate action.

As noted from the flow chart, a check on the location calculation is made using other TOA's of an identification (if available) to compute a second location. A comparison difference results in the executive being notified and data supplied to a fault isolation routine. This routine can further check the TOA's by accumulating these over a period of time and computing the location several ways. If required, checks can be made on the receiving and processing equipment. Should problems persist, maintenance/operations personnel can be alerted.

The final filter action of requiring three bursts from four receivers should eliminate all false alarms. If an aircraft is falsely identified as entering the system when it has not, an acknowledge command would be given to it. Since it is not active, the command would not be received or executed (i.e., change of burst rate from every 2 sec to 8 sec). The known aircraft list would be adjusted and the tracking surveillance function notified. Should the identification fail to be received, the tracking function initiates the removal from the system. This may also result in an operator alert. If it continues to be received, perhaps because of system component failure or degradation, a problem of granting entrance of the aircraft with this identification will occur. The aircraft will not receive its acknowledge command and must use some other form of communication (typically, voice) to bring this fact to the attention of the controllers.

At this point, it is worth noting that the entering and exiting of aircraft into and out of the system is worth printing out and/or placing on magnetic tape. Such recordings can be useful for flow analysis and fault isolation using reasonableness checks on time of flight and points of departure and arrival.

From the preceding discussion and flow chart, a number of files have been indicated as required for the detection and identification of new aircraft. Proper organization of these files is necessary to keep to a minimum the amount of memory and speed required.

Table 5.3-3 presents information on one possible file structure for the 80 msec file and the burst file.

Table 5.3-3. File Structures

File Name	List Name	Format	Storage Method	Size		Comments
				ID's	Slots	
80 msec	First time (FT)	ID-RCVR No.-TOA	Individual ID's in order of TOA	400	400	
	Greater than first time (GFT)	ID-RCVR No.-TOA	Grouped by identification. Within group, in order of TOA	40	400	Ten slots allocated for each possible ID.
Burst		ID-RCVR No.-TOA - Activity tags	As with GFT file	100	1,000	

Two methods considered for the 80 msec file for storing information and which show the effects of file structures on processing needs are

(1) According to identification and receiver numbers. If this were done, 4,000 slots must be provided. (A slot is defined as the memory needed to contain all information pertaining to an identification.) The earliest TOA for an identification would be the first of the block of 10 slots. Therefore, to test for $\Delta TOA > 80$ msec, the equivalent of 400 (maximum) comparisons must be made each 80 msec. An address pointing method to fill vacated slots would be required. To insert a new identification, up to 400 comparisons would be needed to establish that this is a new identification.

(2) According to whether one or more than one receiver has received an identification. The first list, the First Time (FT), would hold all received identifications which have been received only once. These would be in the sequence of their TOA. The second list is the Greater than First Time (GFT) and would hold identifications received from more than one receiver. Due to the elimination of false alarms, 800 slots are needed with this approach. The test for $\Delta TOA > 80$ msec would require 41 comparisons (40 in the GFT and 1 in the FT). A newly received ID would be compared with the GFT list first and then with the FT. With this approach, the equivalent of 440 (maximum) comparisons must be made each 80 msec. However, the average number should be less than the first approach since those that are most likely identifications are examined first.

Table 5.3-3 and Fig. 5.3-8 reflect the second file organization for the 80 msec file. Information is received at a rate of 40 identifications per receiver per 80 msec. This filtering results in an estimated two identifications per 80 msec being conveyed to the burst file.

In 2 sec, the burst file will receive 50 identifications. In the next 2 sec, half of these are expected to be true identifications (some for the first, second, or third time) and will be retained. The other from previous intervals are dropped. Each 2-sec interval should provide similar behavior. Thus, a 100 identification or 1,000 slot storage is anticipated to be a requirement.

Those identifications which have been received for a third time will be examined for four TOA's and a position calculation made. A check can be made by substituting other TOA's for all or some of the first four. The result is the ability to identify a new aircraft every 80 msec.

The files required for the surveillance function can be rearranged during processing to access by sequential addressing or not arranged and accessed by random addressing. The former requires executive overhead to maintain the location information and may involve considerable data movements. The latter can be achieved with associative methods. The conception and evaluation of the most suitable approach must be deferred for future studies.

5.3.2. Computation for Newly Acquired Aircraft

Following the selection of the proper combination of sets of three pseudo-noise pulses and associated intervening times that constitute an aircraft ID and conversion of these data to an aircraft ID, the position of that aircraft must be computed. This position computation is based on the difference in TOA of surveillance signals from a number of satellites and will be performed only after surveillance signals have been received by the satellites at least three times. In addition to the TOA's of surveillance signals for the N^{th} time, it is required that the satellite positions be known. Ephemeris data satisfy this latter requirement. Figure 5.3-9 shows a mechanization for a deterministic computation of untracked aircraft position.

The process for determining the position of an aircraft consists of converting the TOA measurements to range differences and, knowing the position of the satellites from the ephemeris data, computing the position of the aircraft.

The position determination equations are presented in Fig. 5.3-9. MOD 1 converts and corrects the time-of-arrival signals to range differences. MOD II and III combine the outputs from MOD I with the ephemeris data to arrive at the uncorrected position of the aircraft with respect to the designated "master" satellite. MOD IV then computes the aircraft position relative to the ground station and applies position calibration as required. MOD V is used to determine the aircraft's bearing, relative to true North, and the corresponding solid angle (range). MOD VI computes the latitude and longitude of the aircraft in spherical coordinates while MOD VII transforms the outputs (latitude, longitude) of MOD VI to spheroid coordinates.

When the position of an untracked aircraft has been computed, the data are used in two ways. First, they are used to determine in which of the two regional airspaces the aircraft is located. Surveillance of the aircraft is then assigned to that region. Since the initial position determination is performed by each of the two RCC's and by the CCC, the actual acceptance of an aircraft for surveillance by either of the two regions will be based on the result of a majority vote wherein the CCC and the two RCC's will each have one vote. Secondly, they are used by the CCC and the RCC to which the aircraft is assigned to initialize a maximum likelihood estimation mechanization (Kalman filter) which determines the position of tracked aircraft.

The memory, speed, and input/output demands on the central computer at each of the RCC and CCC is

(1)	Memory	32,000 of 32-bit words
(2)	Speed	250,000 instructions per second
(3)	Speed/Output	60,000 words per second

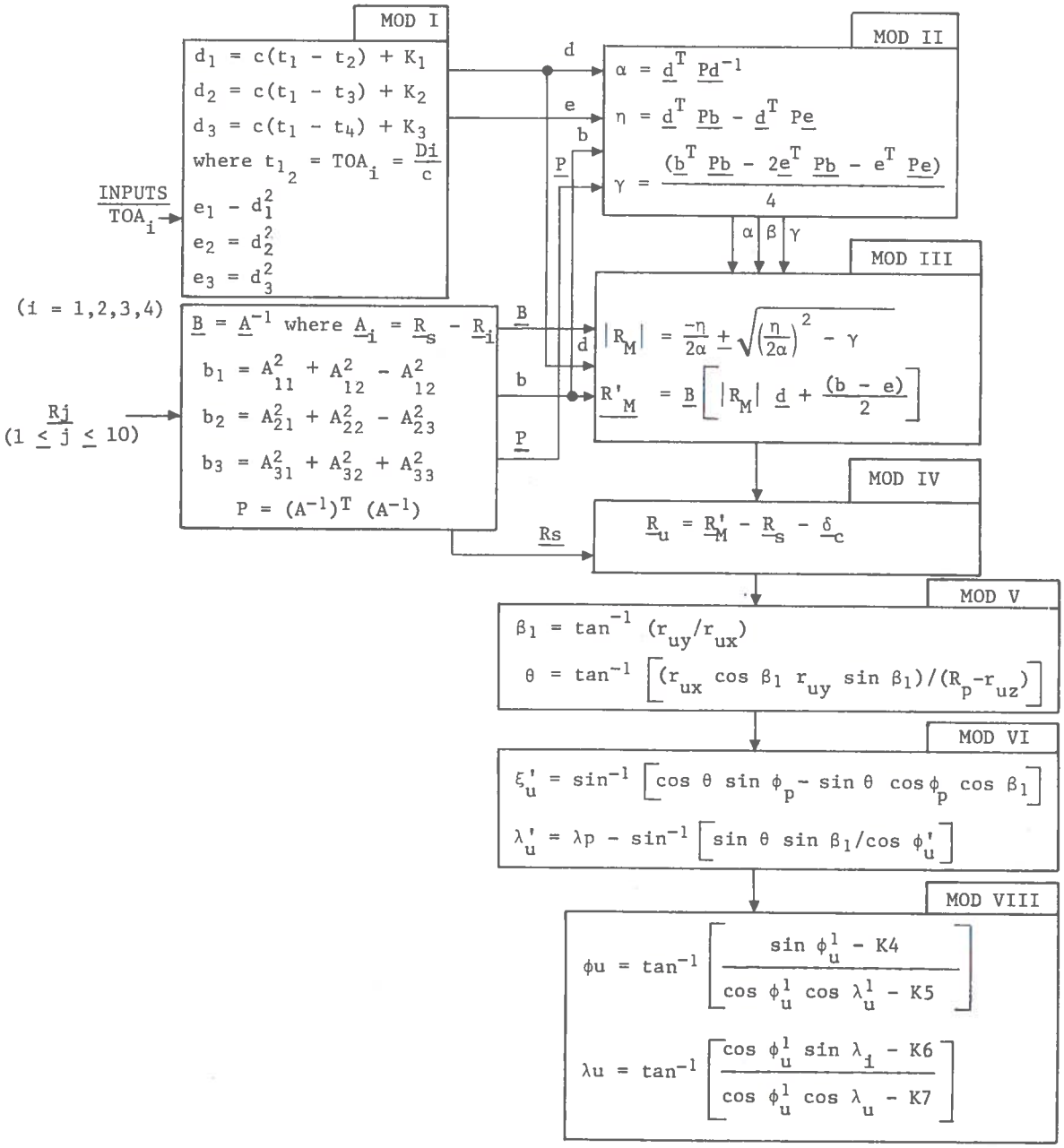

Fig. 5.3-9. Surveillance Mechanization Equations

5.3.3 Compute Position and Velocity Tracked Aircraft

Continuation of the aircraft position and velocity determining task will be done by means of a maximum likelihood estimation technique. The TOA of the last surveillance pulse group to be received from an aircraft via a satellite and the surveillance pulse group interval for that aircraft are used to define the center of a time window. The CCC and the RCC to which the aircraft has been assigned will use the window to reject false alarm data. If a surveillance pulse falls outside of the window, it is discarded as being a false alarm. Receipt and decoding of the pseudo-noise pulse group from the appropriate aircraft is performed by receivers, AMF's, and decoding hardware. One set of the previously mentioned hardware is dedicated to the receipt and decoding of pseudo-noise pulse groups from each of the satellites. The TOA's of the pseudo-noise pulse groups from the satellites and the ephemeris data for the satellites are used to establish measurables for each surveillance transmission by the appropriate aircraft. These measurables are then used in the maximum likelihood estimation filter that was initialized by means of the position data derived from the third transmission from that aircraft while it was yet untracked.

The computation of the position of tracked aircraft, since it is done for each aircraft that is currently active within the airspace of a region is a very demanding load on the data processing subsystem. Except for the filter gains which are done separately, all other surveillance computations are performed at the surveillance rate for each tracked aircraft.

If the number of satellites visible to the ground antennas is assumed to be an average of 10, and if the peak number of aircraft active within the airspace of a region is 20,000, the peak data processing requirements for the computation of the positions of tracked aircraft within the airspace of a region include

(1) 3.4×10^6 instructions per second

(2) 3.0×10^3 words input or output per second

(3) 1200 words of main memory

5.3.4 Maintain File of Active Aircraft

A central file of position, velocity, and status data on active aircraft is maintained for the use of a number of RCC real-time functions. A multiple level file is used as a means of minimizing processing by testing the status of a file entry before proceeding with further processing of the contents of that entry. Aircraft within the control region will be entered into two duplicate three-level files, as shown in Fig. 5.3-10, which will serve as the source of data for the conflict prediction, intrusion prediction, handoff, virtual VOR, and transition and arrival control functions. Duplicate files are required since access to these files during performance of the previously mentioned functions will be simultaneous and at rates that will preclude their being handled by one main memory subsystem.

However, if identical files are stored and maintained in duplicate, the central processors that compute aircraft positions will have the capability of writing these position data into memory. Processor speed capability is adequate to allow a doubling of processing rate, whereas memory speed capability probably is not.

The active aircraft file will be organized on a geographical basis; i.e., the RCC region will be divided up by a latitude/longitude grid. On the top and least detailed level for each division of the RCC region, one bit in a group of computer words will be set if one or more aircraft are present within that two-dimensional cell. The second level of the file will include an indication of the number of aircraft in each cell. The third level will contain, for each aircraft in a cell, the aircraft ID, which is used to address indirectly all required data on each active aircraft. The aircraft ID includes information on the aircraft class. Access to the aircraft ID's can be by means of a base plus displacement addressing scheme wherein the count of aircraft is added to a base address.

This approach requires that for each cell, storage be provided for aircraft ID's for the maximum number (between 2 and 16) of aircraft expected in that cell. Thus, though the number of active aircraft that can be handled is 65,536, the storage required for aircraft ID's is on the order of 16 times that number. This memory requirement could be reduced by resorting to other approaches that involve indirect addressing and/or content addressing. Selection of the most appropriate mechanization scheme should be subjected to further detailed study.

Storage within each active aircraft file as shown in Fig. 5.3-10 will be provided for two sets of data on active aircraft since new data will be entered and derived while the last set of data is being used for conflict checking. The indirect address of the appropriate file will be 16 bits, thus providing for access to 65,536 active aircraft.

Storage required for the files described above will be as follows: (assuming 32-bit words)

(1) First Level

$$\text{Number of Words} = \frac{\text{No. of Cells}}{32} = \frac{N_c}{32}$$

(2) Second Level

$$\text{Number of Words} = \frac{\text{No. of Cells}}{4} = \frac{N_c}{4}$$

(3) Third Level

$$\text{Number of Words} = 2\ [8N_c\ (\text{Average No. of Aircraft/Cell})]$$

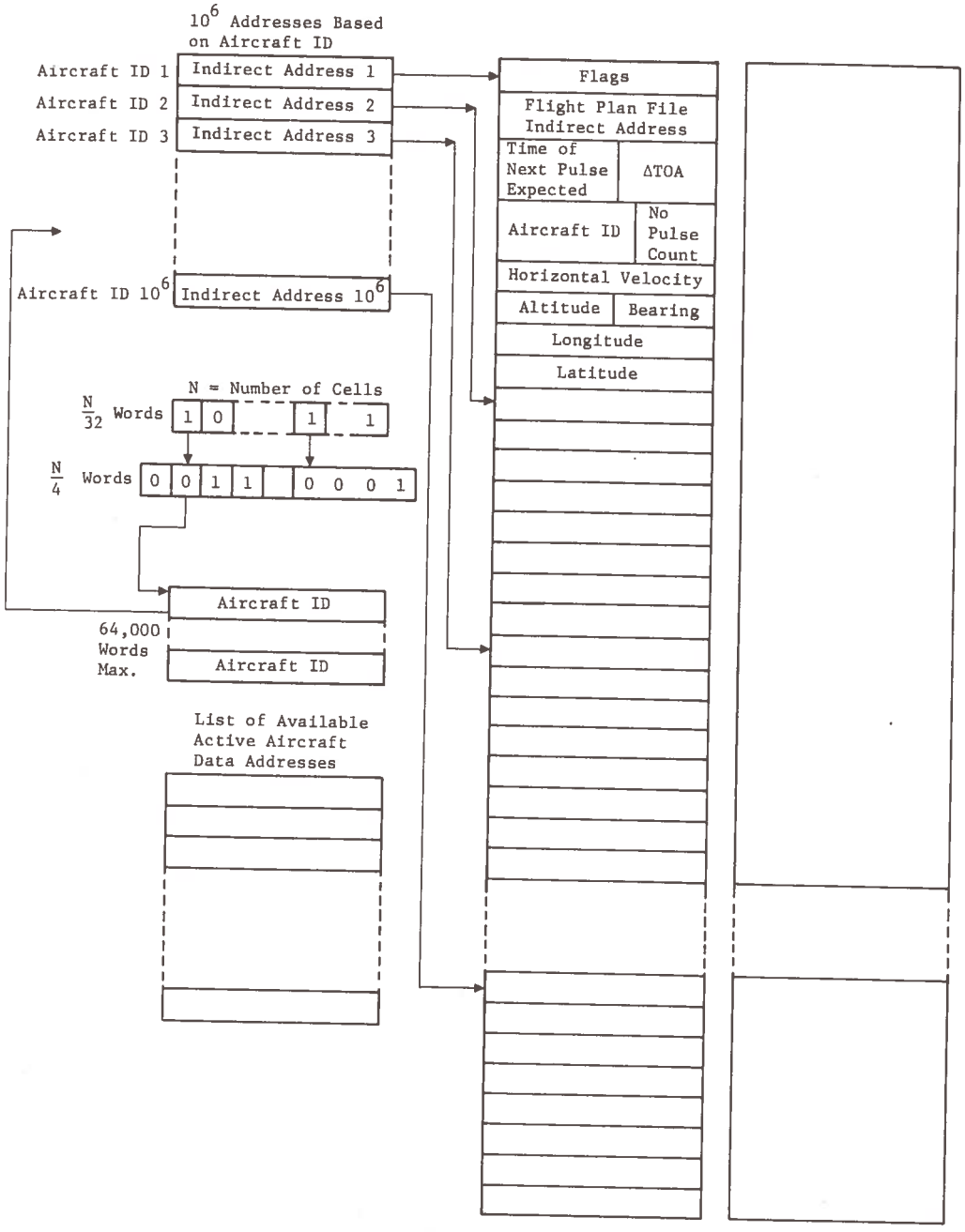

Fig. 5.3-10 Active Aircraft File Organization

Third level storage is provided for:

(a) Latitude

(b) Longitude

(c) Altitude

(d) Heading

(e) Horizontal Velocity

(f) Aircraft ID

(g) Flight Plan File Indirect Address

(h) Time of Arrival of Last Pulse Group

(i) Expected Time of Arrival of Next Pulse Group

(j) Count of Time Windows with no Pulse Group from this Aircraft

(k) Flags including

Aircraft has requested transition to airport

Aircraft is using VVOR

Aircraft has requested clearance to an airport

As an adjunct to the active aircraft file, and for use in the acquisition of aircraft, there is a file of 10^6 fast memory bytes each of which is 4-bits long. Each of these bytes contain the ID that is used to address the aircraft; one bit that indicates if that aircraft ID has been assigned to an aircraft, one bit that indicates if the aircraft with that ID is being tracked by the RCC at which the file is located, one bit that indicates if the aircraft with that ID is being tracked by the other RCC, and one bit that indicates if the aircraft with that ID is being tracked by the CCC. By making use of this fast memory file, the aircraft acquisition processor can make decisions as to whether groups of pseudo-noise pulses represent aircraft ID's that have actually been assigned and therefore are valid, if the aircraft ID has been assigned and is currently being tracked, or if it is an untracked aircraft entering the system.

When an aircraft goes out of the system, i.e., lands, goes into an Airport Control Area, or goes into the adjacent region, the aircraft ID for that aircraft must be removed from the list of aircraft active in the appropriate RCC and CCC (backup). This is done automatically if a handoff occurs, but if an aircraft leaves the system for some other reason the following capability is made use of:

(1) A 4-bit count (to 16) is maintained in the 8-word block of data stored for each active aircraft; this count is incremented each time the time window is opened for receiving surveillance if no signal is received via any of the satellites.

(2) If the count reaches a threshold of 16, the 8-word block of data is made available for use by placing its starting address in the list of available active aircraft data blocks.

(When an aircraft leaves the system under nonhandoff conditions, this fact is made known to the operator monitoring the area of interest.)

Each time an aircraft enters or leaves a cell, the aircraft count for the appropriate cell must be incremented or decremented, followed by a test of the aircraft present bit for that cell and if need be a setting or resetting of that bit.

Maintenance of the Active Aircraft File requires storage in that file of all new position and velocity data as these data are computed. Other tasks that are part of this file maintenance function are

(1) Update active aircraft file keys, i.e., the aircraft present bit and aircraft count

(2) Modification to the file of addresses available for the storage of active aircraft data blocks

Data processing requirements for the active aircraft file are

(a) 350×10^3 instructions per second

(b) 2.2×10^6 words of main memory

5.3.5 Conflict Prediction and Avoidance

Conflict prediction is based on aircraft location within cells. The entire airspace is segmented into cells. The first level file of a cell is checked. If there are aircraft present, the second level file is checked for the presence of more than one aircraft. For each aircraft within a cell, a check is made for a possible conflict with each of the other aircraft in that cell and with each aircraft in adjacent cells. The data that are required for the performance of conflict checks are stored in the third level file.

A check for a conflict between two aircraft can be performed as shown in the accompanying flow diagram, Fig. 5.3-11.

When it has been found that a conflict between two aircraft is possible, the angle between the velocity vectors for the two aircraft will be computed for use in determining the type of evasive action that should be taken. Fig. 5.3-12 is a flow diagram of an algorithm for determination of the types of action to be taken by two aircraft with an impending conflict.

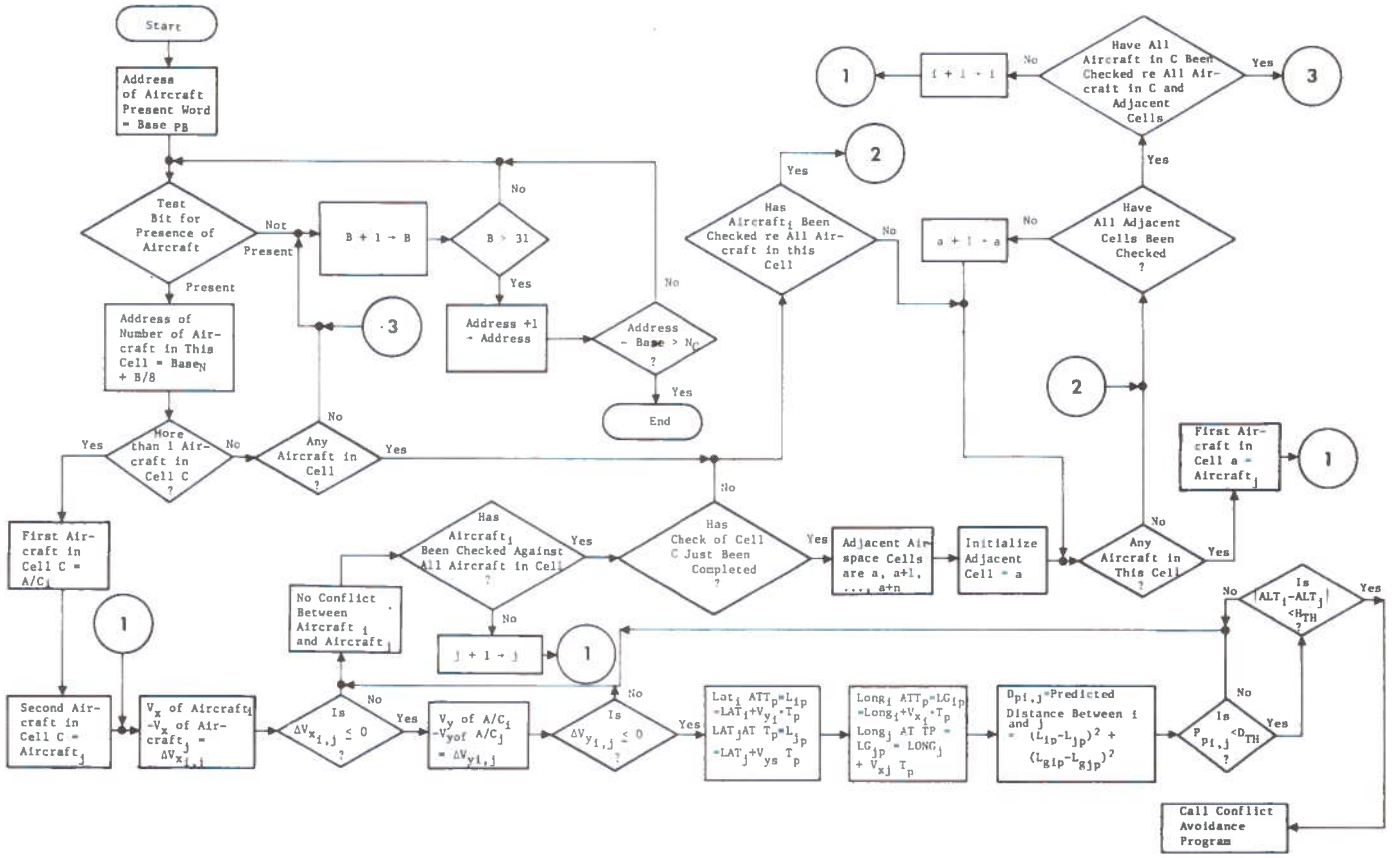

Fig. 5.3-11. Logic Flow for Predictions of Conflicts

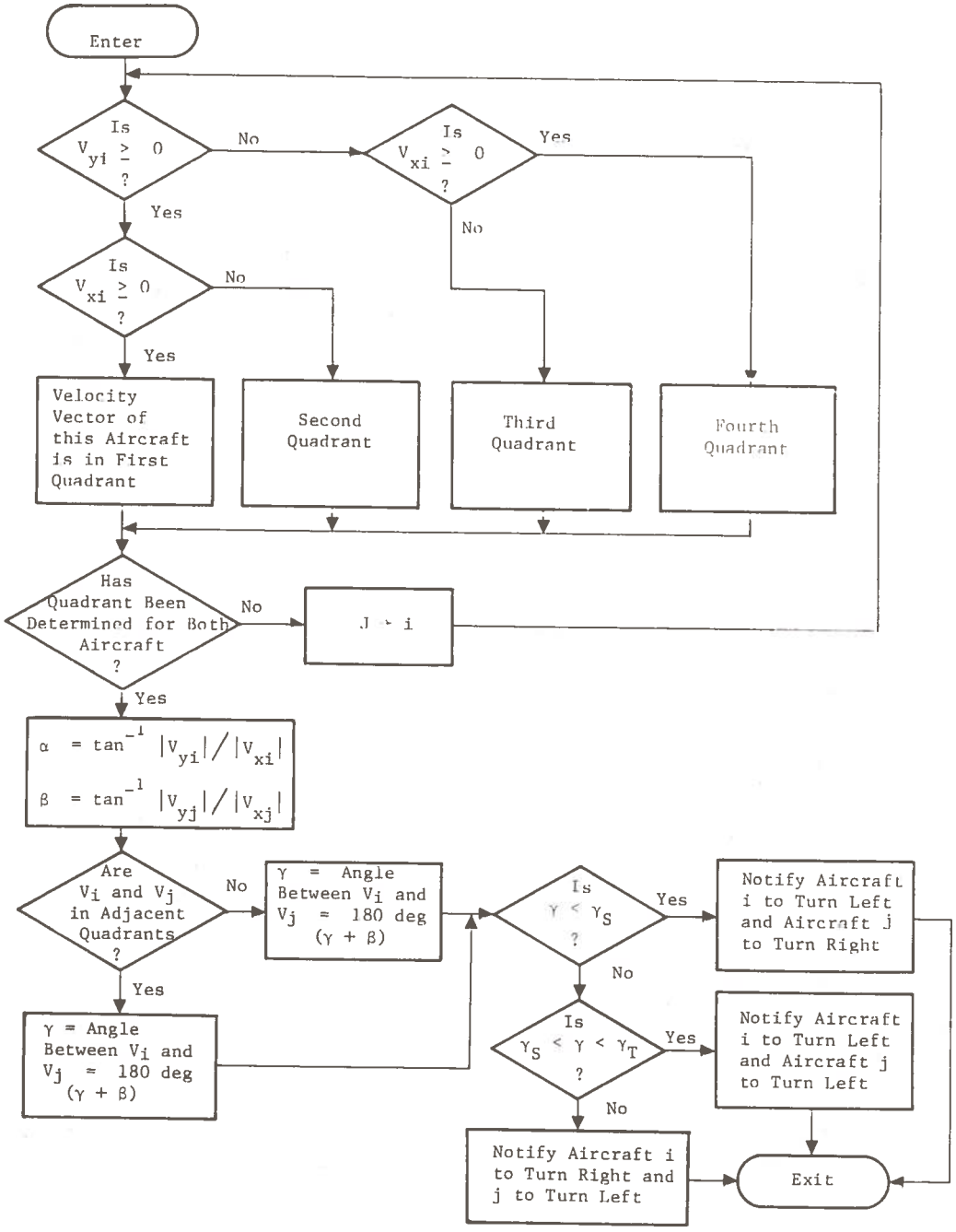

Fig. 5.3-12. Conflict Avoidance Program

The airspace cells on which the mechanization for conflict prediction is based and around which the active aircraft file is organized are of two sizes. The larger of the two sizes of cells is 30 $\widehat{\text{min}}$ (≈30 miles) on a side and is used in the less congested areas that account for 90 percent of the airspace. The smaller of the two cell sizes is 6 $\widehat{\text{min}}$ (≈6 miles) on a side and is used in the most congested 10 percent of the CONUS airspace. Most of these cells will not contain aircraft, but some will contain a number of aircraft. The data processing requirements for conflict prediction and avoidance under the conditions that 8 percent of the cells contain aircraft and 2 percent of the cells contain more than one aircraft are

(1) 150×10^3 instructions per second

(2) 34×10^3 words inputted or outputted per second

(3) 300 words of main memory (data storage is covered by the Active aircraft file)

5.3.6 Intrusion Prediction and Avoidance

This function entails the prediction of impending intrusions of aircraft into restricted airspace and the computations of means to avoid such intrusions.

The file of data on aircraft within the RCC as described in Section 5.3.5 will also be used in performance of the intrusion prediction and avoidance function. A file of the boundaries of volumes of airspace which cooperative and/or controlled aircraft are prohibited to enter will also be required. This file will be organized similar to the Active Aircraft file but will have only two levels. The first level will specify the number of restricted air space volumes in cell number(s) and specifications of the restricted airspaces therein described in terms of surfaces of constant latitude, longitude and altitude. In some cases, this may somewhat enlarge the restricted volume. In those cases, such as enroute corridors, where the altitude boundaries are surfaces of constant altitude, and ascent and descent corridors, where none of the boundaries are surfaces defined by a constant, the definition of the boundaries can be by means of the equation of the center line of the corridor (Form: $Y = Mx + B$) along with a radial dimension from that center line, and coordinates of the end points of the center line.

This function, which is diagrammed in Fig. 5.3-13 requires that each airspace cell in an RCC be looked at for (1) the presence of aircraft, (2) the number of aircraft present, and (3) the presence of restricted airspace. For each cell that includes aircraft and restricted airspace, the present position of the aircraft is extrapolated to the boundaries of the restricted airspace by using the X and Y velocity vectors. The X and Y coordinates of the intersection of the aircraft within the restricted airspace is computed.

As shown in Fig. 5.3-14, depending on the angle of approach of the aircraft velocity vector to the restricted airspace boundary, the aircraft is directed to fly left or right to avoid the restricted airspace.

INTRUSION PREDICTION

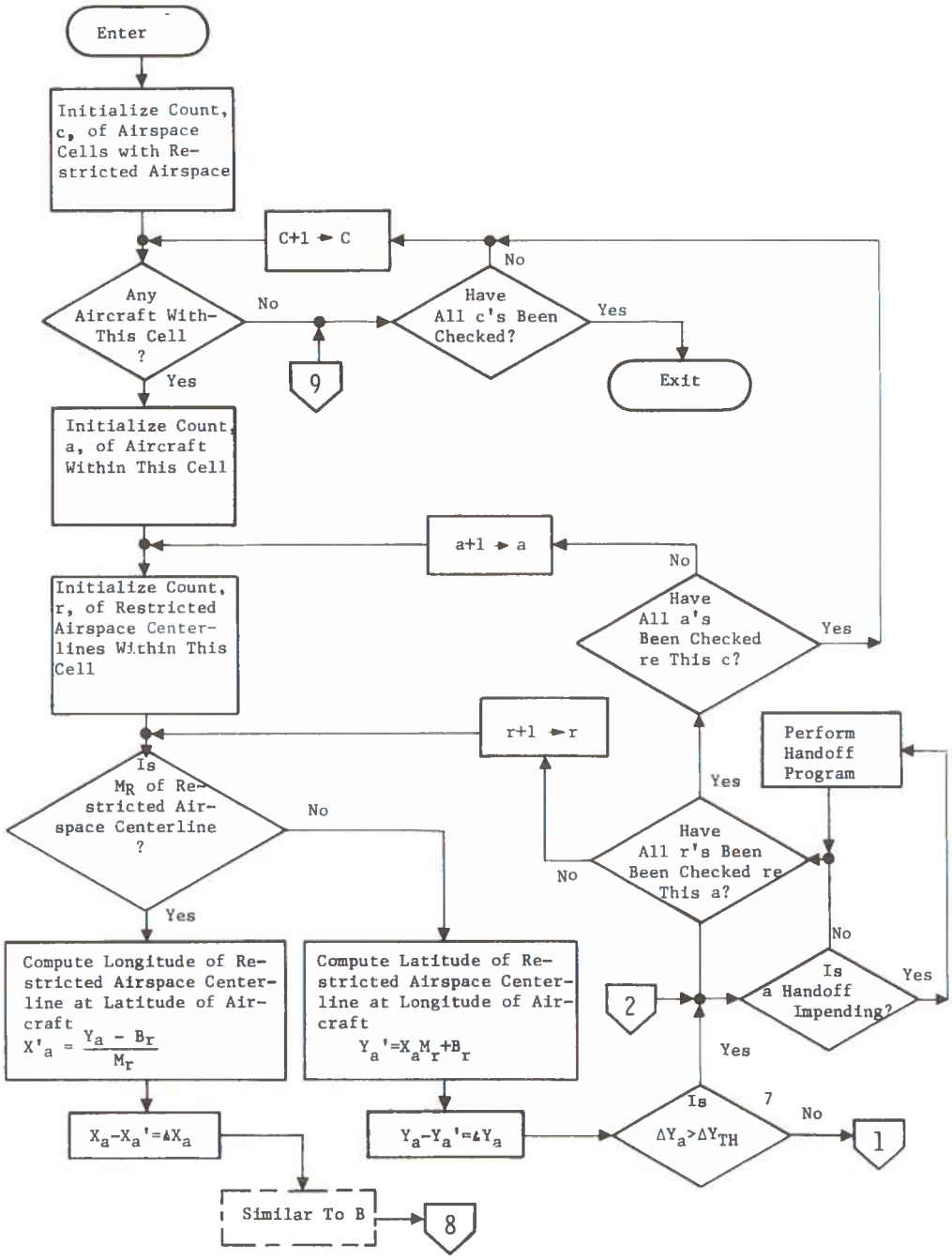

Fig. 5.3-13. Intrusion Prediction

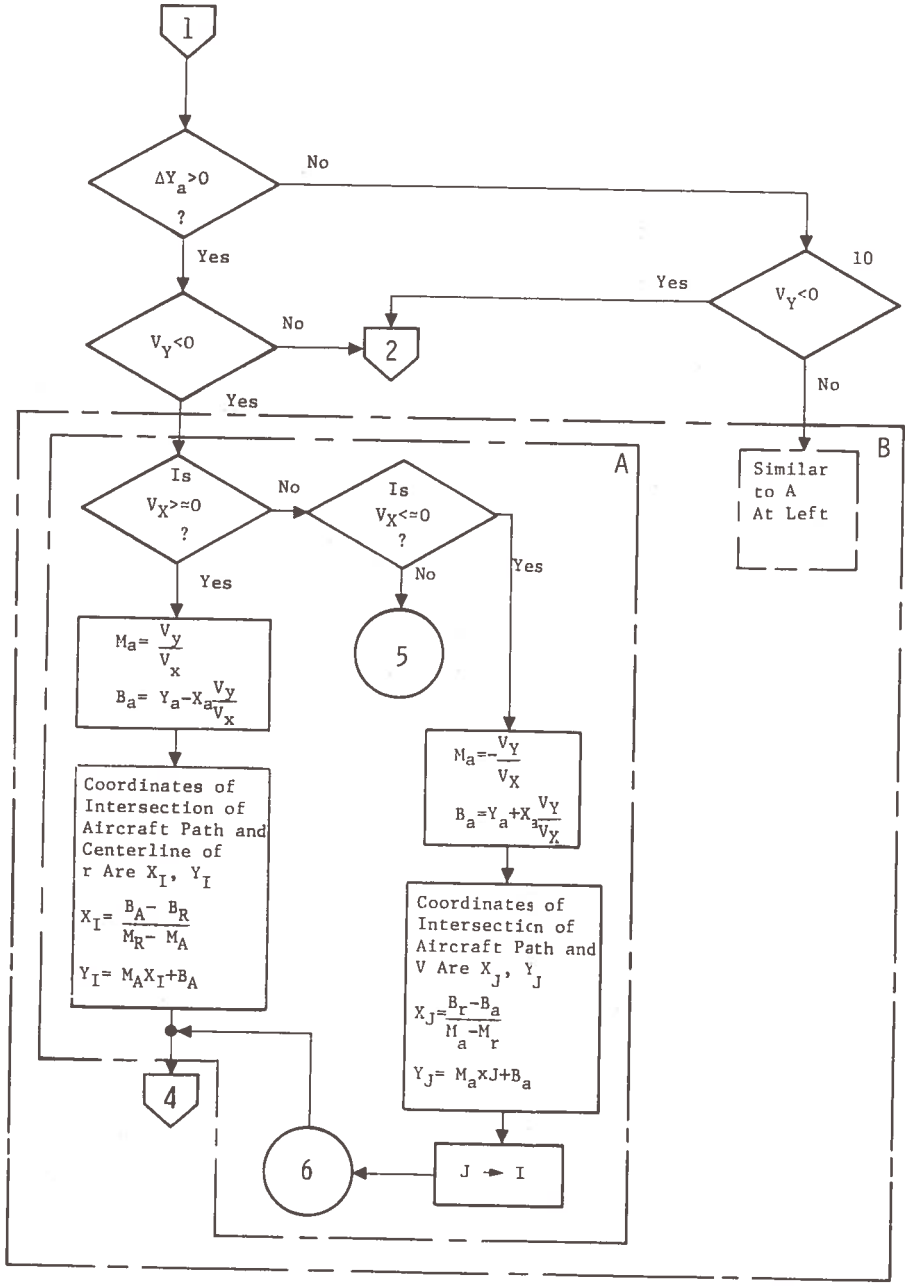

Fig. 5.3-13 (Continued)

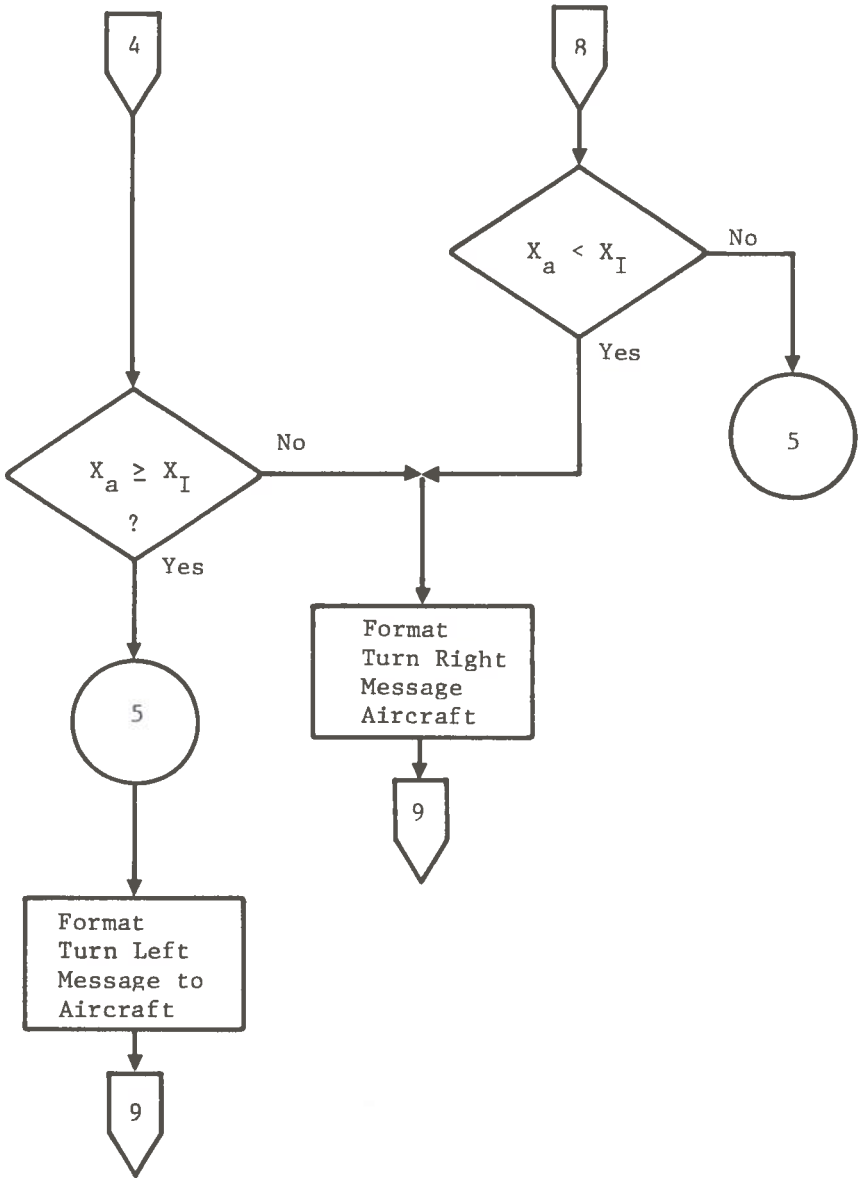

Fig. 5.3-14. Intrusion Avoidance

The data processing requirements for intrusion prediction and avoidance under the conditions that 50 percent of the airspace cells that contain restricted airspace also contain aircraft, and 25 percent of the cells that contain aircraft contain more than one aircraft are

(1) 50,000 instructions per second

(2) 25,000 words of main memory

(3) 3,000 words inputted on outputted per second

5.3.7 Handoff Initiation

Handoff is the transfer of control from one control entity to another. If the handoff decision block in Fig. 5.3-13 indicates that a handoff is required because the aircraft is approaching the boundary of the other RCC, the Handoff Program is called. The Handoff Program includes a check as to whether the aircraft's flight plan calls for it to enter the airspace of interest which may be the region controlled by the other RCC, an airport, or the transition airspace for an airport. To do this the file of flight plan data must be accessed to obtain data on whether the flight of the aircraft is planned to enter the other RCC. This accessing of flight plan data from auxiliary memory is likely to take 10 msec or more of real time. However, it does not use more than a few microseconds of central processor time and therefore does not present a significant load on the central processing capability of the data processing subsystem.

The flags that indicate active requests for transition and clearance are checked for compatibility with the aircraft position and flight plan. If there are incompatibilities, the pilot is notified.

Assuming 100 handoffs/sec (a worst case) the data processing requirements are

(1) 21,500 instructions per second

(2) 1,300 words of main memory

(3) 30,000 words inputted or outputted per second

5.3.8 Virtual VOR (VVOR) Processing

The VVOR navigation processing algorithm is mechanized to provide the user with the selection of two navigation options. The first of these two options provides the same capability and display technique offered today's aircraft flying normal VOR navigation (bearing and range). In this case the user, having selected the flight path of his choice, can fly normal radial navigation relative to any VVOR station along that path. The advantage of this method is the user's ability to position the station any place of his choice. The disadvantage of this technique is that the cross-track error increases with range from the selected points. For example, a 1 deg error at a range of 100 nmi would produce an approximate 1.75 nmi error, while at a range of 10 nmi, the cross-track error would be 0.17 nmi. Thus, this technique offers more to the user flying shorter ranges.

The second option lends itself more toward long distance navigation. In this case, the user, selects two VVOR stations of his choice, thus defining a route leg. He will then fly a great circle route from one station to the next. The instrumentation, although basically the same as that for the present VOR, will be mechanized somewhat differently. This results from driving the steering indicator with cross-track error derived as a measure of distance rather than angle; i.e., in the first option the steering needle was driven simply by the angular error between the actual radial (transmitted by the system) and the desired radial (introduced by the user). In the second option the steering indicator will be totally driven by the system wherein the error is computed in terms of distance off track. In addition, the system will also provide the user with range-to-go and bearing angle relative to true North. The advantage of this option is that it offers the user an accurate long range means for navigation. The logic flow diagram depicting the VVOR algorithm as described is given in Fig. 5.3-15.

The steering equations mechanized for the two described navigation options use the so-called great circle steering technique. The basic geometry illustrating both options and the great circle steering geometry are presented in Fig. 5.3-16.

The resulting equations for both options and the data to be transmitted by system to the user are as follows:

Option A

$$\cos \theta_A = \cos (90 - \phi_A) \cos (90 - \phi_i) + \sin (90 - \phi_A) \sin (90 - \phi_i) \cos (\lambda_i - \lambda_A)$$

$$\theta_A = \cos^{-1} \theta_A$$

$$\eta_A = \sin^{-1} \left[\sin (90 - \phi_A) \sin (\lambda_i - \lambda_A) / \sin \theta_A \right]$$

$$R_{TG} = a \, \theta_A$$

Transmit to user

Bearing Angle: η_A

Range-to-Go: R_{TG}

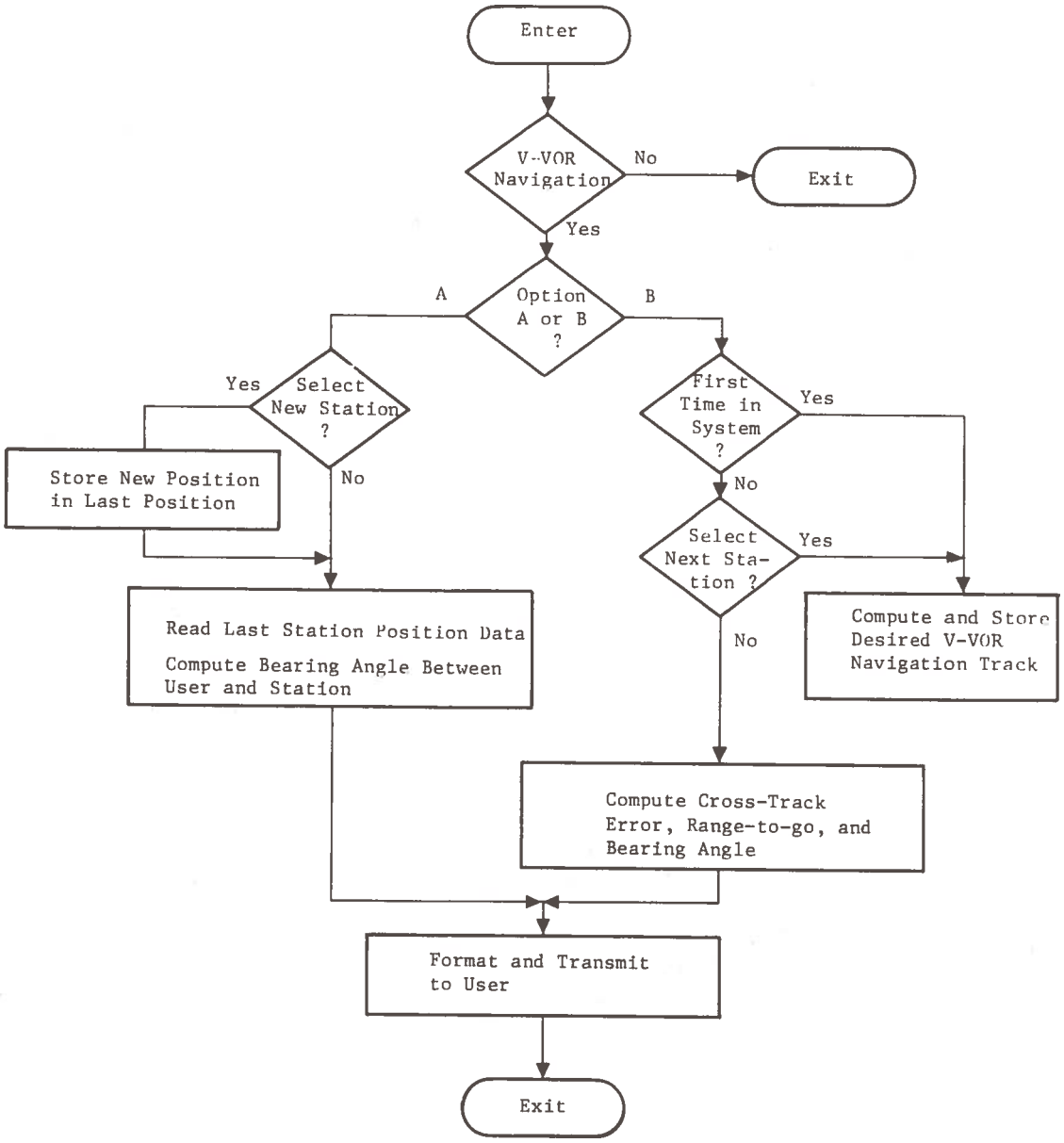

Fig. 5.3-15. VVOR Logic Flow Diagram

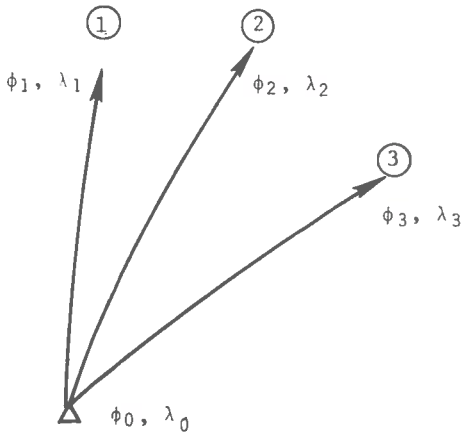

Option A: 1 or 2 or 3

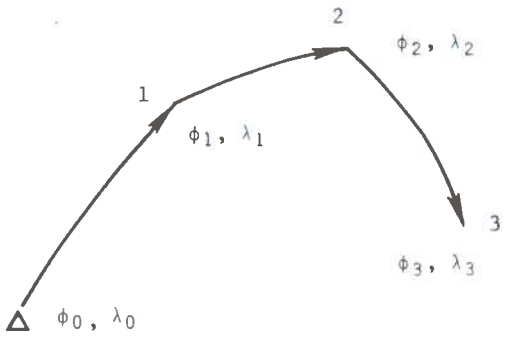

Option B: 1 and 2 and 3

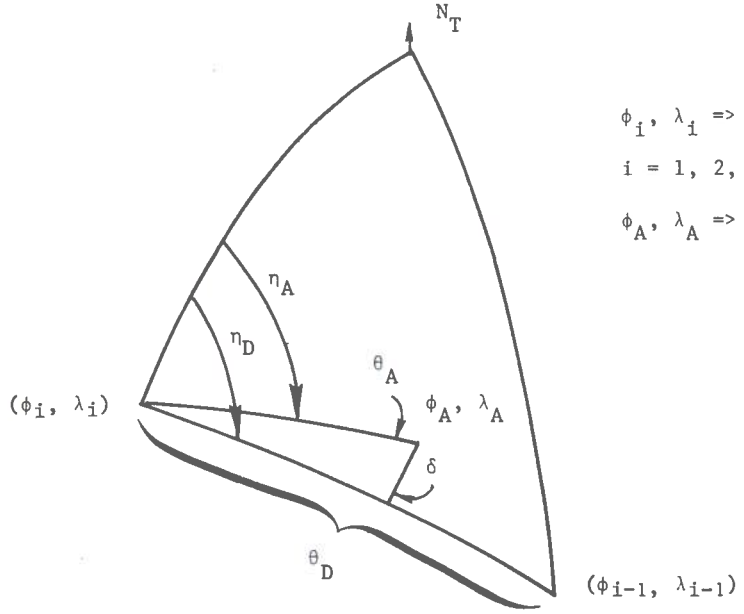

ϕ_i, λ_i => V-VOR Station

$i = 1, 2, 3, \ldots > 0$

ϕ_A, λ_A => Aircraft Position

Great Circle Steering Geometry

Fig. 5.3-16. VVOR Naviagation Geometry

Option B

$$\cos \theta_D = \cos (90 - \phi_i) \cos (90 - \phi_{i-1})$$

$$+ \sin (90 - \phi_i) \sin (90 - \phi_{i-1}) \cos (\lambda_i - \lambda_{i-1})$$

$$\theta_D = \cos^{-1} \theta_D$$

$$\cos \theta_A = \text{(See Option A)}$$

$$\theta_A = \cos^{-1} \theta_A$$

$$\eta_D = \sin^{-1} \left[\sin (90 - \phi_{i-1}) \sin (\lambda_i - \lambda_{i-1})/\sin \theta_D\right]$$

$$\eta_A = \text{(See Option A)}$$

$$\delta = \sin \theta_A \sin (\eta_D - \eta_A)$$

$$R_{XT} = a \delta$$

$$R_{TG} = a \theta_A$$

Transmit to User

Cross-track Error: R_{XT}

Range-to-Go: R_{TG}

Bearing Angle: η_A

The processing requirements in terms of Instructions Per Second (IPS) and memory storage are given below. The IPS are written in equation form as a function of the number of instantaneous users.

Option A (Update rate = once per 8 sec)

IPS = 4,000 + 10/user

Storage = 1,000 + 20/user* (32-bit words)

Option B (Update rate = once per 8 sec)

IPS = 5,000 + 20/user

Storage = 1,500 + 20/user* (32-bit words)

5.3.9 Transition and Arrival Control

The processing requirements to be applied during the transition through the arrival phase of the flight are predicated on the following criteria:

(1) Airport classification
(2) Runway configuration
(3) Runway reversals
(4) Instantaneous runway capacity
(5) Separation standards
(6) Airspace structure about the terminal area
(7) Class or type of aircraft
(8) Aircraft performance characteristics

Arrival transition and arrival control is provided for primary aircarrier airports. The concept assumes that the high density primary airport consists of three sets of parallel runways, two sets specifically designated for the aircarrier aircraft and one set for general aviation. The low density primary airport consists of one set each plus one additional aircarrier runway.

Runway configurations are considered to be unique, as they are today, for the various airports. Typically, runway reversals and the instantaneous runway capacity are considered dependent upon the local weather and/or runway conditions existing at the various airports. In essence, this implies that the processing algorithm must be capable of handling parameters which vary with conditions unique to each of the airports.

*Approximately 10 percent required on-line.

The airspace structure, relative to the aircraft's descent profile, remains constant for all airports. The specific geometric azimuth orientation of the structure is, however, considerate of the specific airport runway configuration. The structure provides for 25 arrival entry slots per major route, Fig. 5.3-17. On entry, the slots are so designed as to provide both vertical and lateral separation as a function of the aircraft's altitude and nominal performance velocity. Class segregation is dependent on the altitude and speed capability of the aircraft.

The separation standard between aircraft is considered to be fixed except for those aircraft producing extreme wake turbulence. For these aircraft an additional buffer zone is provided. The separation between aircraft will provide for a safe volume about each aircraft plus a buffer zone between them.

The class of aircraft and its performance characteristics about its nominal speed profile is the driving function for the applied 4D control law; i.e., the control to be applied must be capable of merging aircraft having significantly different speed profiles onto a single runway. The one single facet permitting a merger of these aircraft is that their speed differential, although initally large, becomes increasingly smaller as the aircraft nears the runway. Thus, if the control system can provide proper separation while speed differentials are large, as they become relatively small, in-trail merging on an approach to the runway can be easily accommodated.

The processing control algorithm monitors the aircraft for clearance to a particular airport. Once a clearance request is detected and confirmed by the user and the system, a 4D conflict-free flight plan is computed and issued to the user. The flight plan is automatically entered into the navigator which in turns computes and displays the command information necessary to fly the particular 4D flight plan. The system then surveys and computes the conformance of the vehicle to the plan. When the user exceeds certain tolerances, a discrete command is issued to the user to either fly up, fly down, turn left, turn right, speed up, or slow down. The aircraft, having reached the outer approach marker properly sequenced and in-trail is then handed off to the airport controller for landing.

The basic logic and control functions performed by the transition/arrival processing control algorithm are illustrated in Fig. 5.3-18. The File and Maintenance Program module will check for clearance requests initiated by the user. Whenever a clearance is detected and confirmed, the File and Maintenance module will route that aircraft's active data file to the particular processor performing the 4D control for the specified airport. This action constitutes handoff between enroute, transition, and arrival.

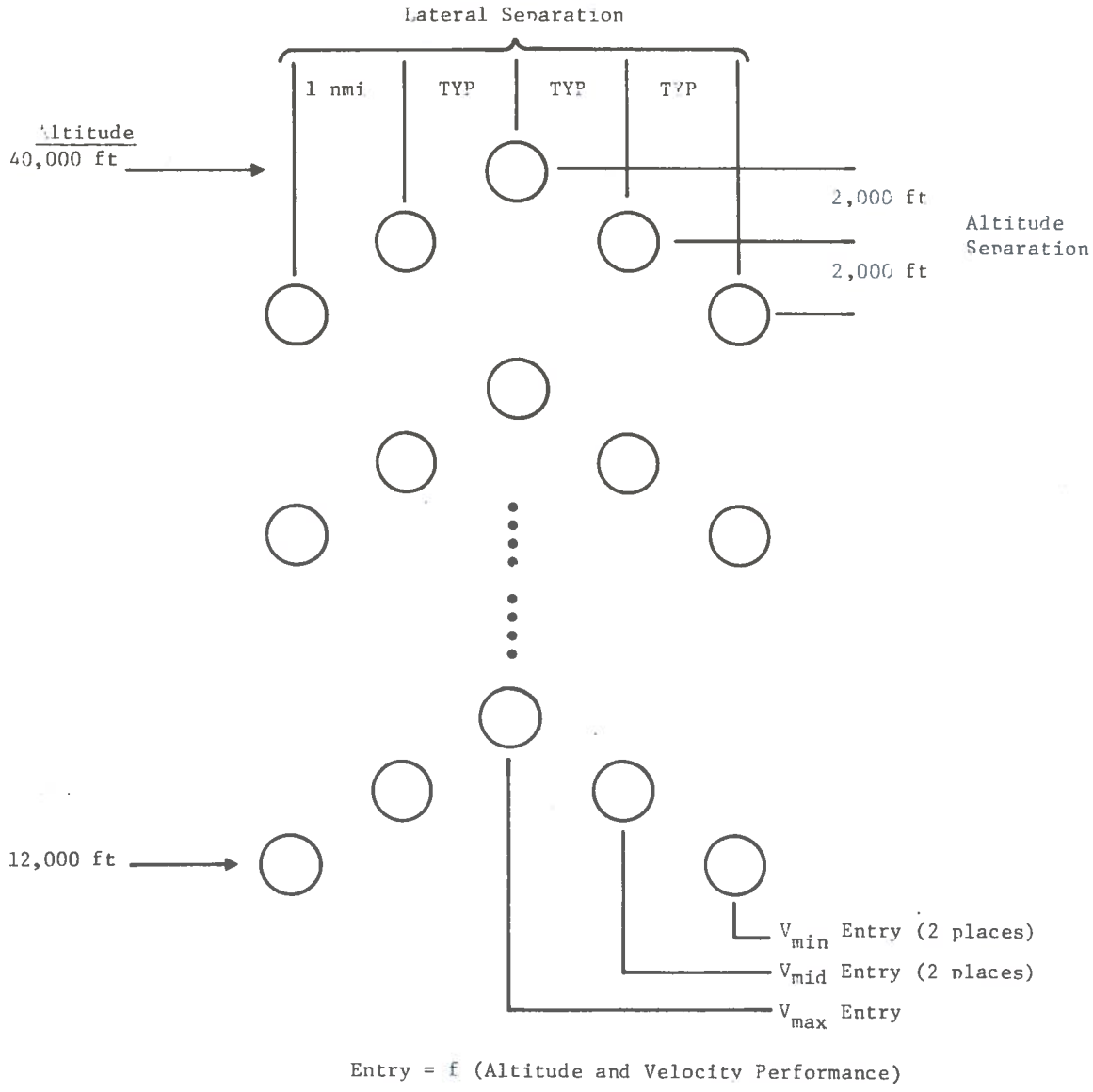

Fig. 5.3-17. Front View of Arrival Airspace Structure

FRONT VIEW OF
ARRIVAL AIRSPACE STRUCTURE

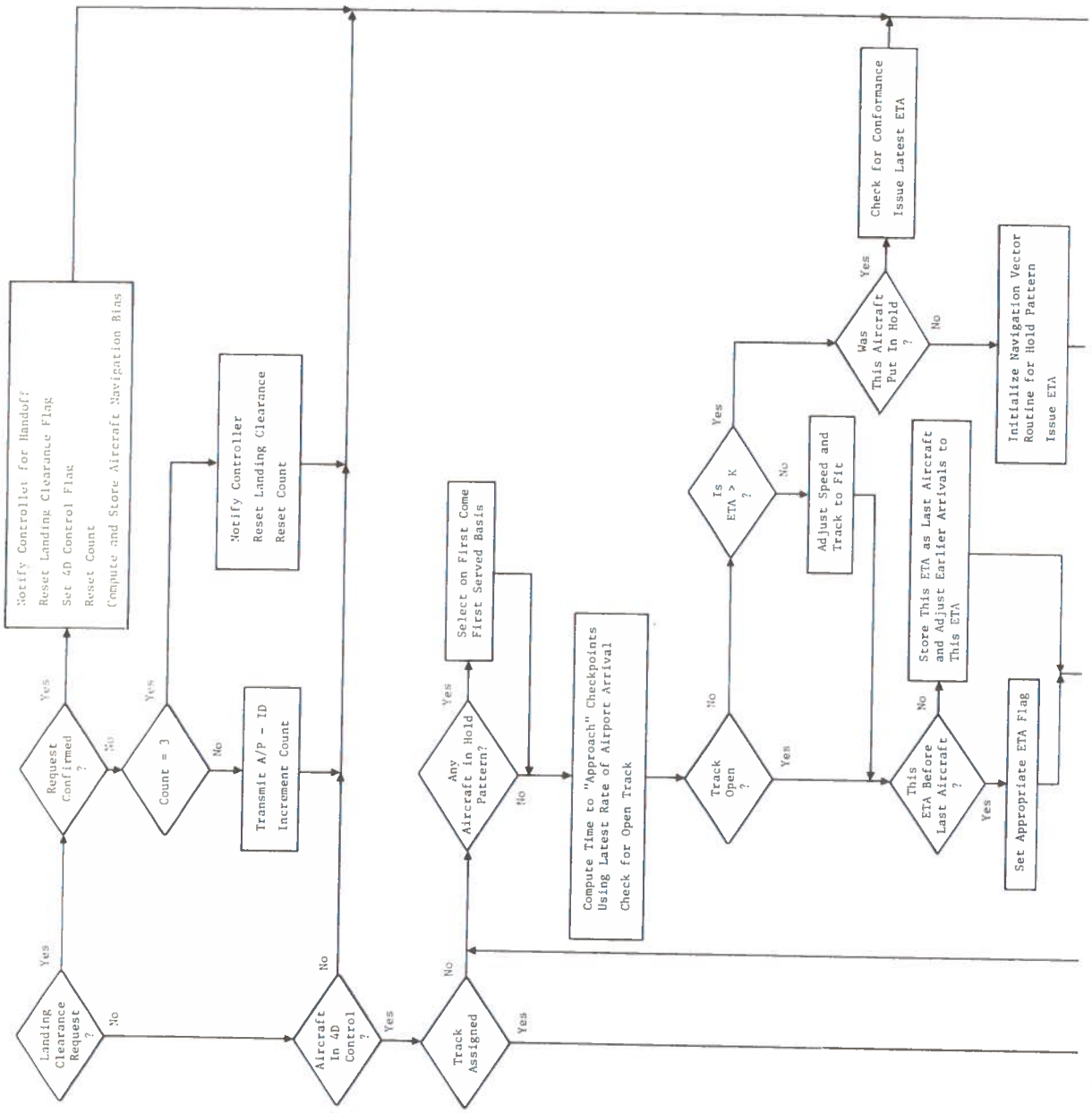

Fig. 5.3-18 Transition/Arrival Logic Flow Diagram

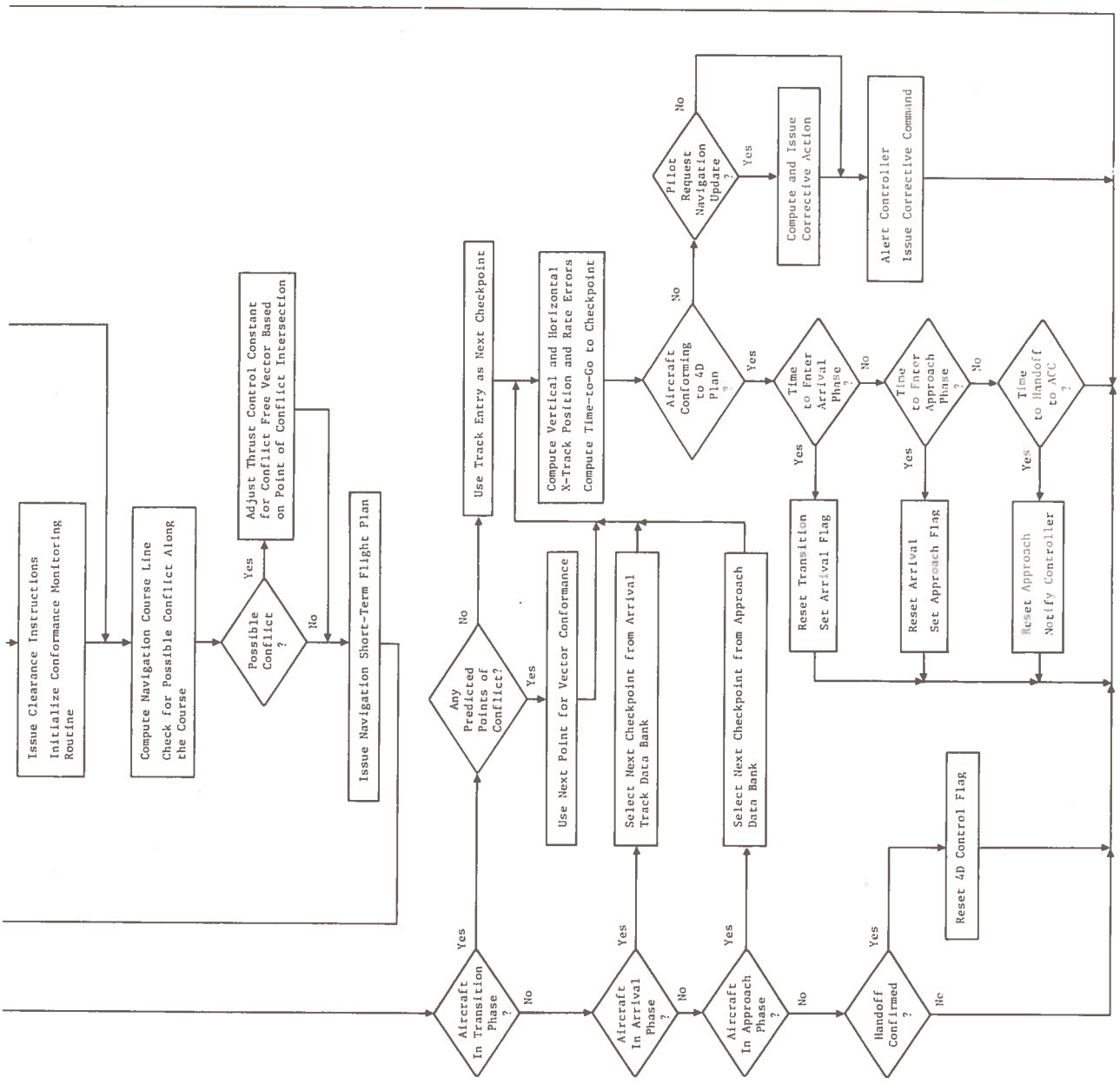

Fig. 5.3-18. (Continued)

Once the aircraft is handed off, the 4D control processor computes where the aircraft will be "n" seconds from the last point of location. Next, the aircraft's class and estimated loading factor is accessed from the flight plan file. Using these data, the velocity profile for this class vehicle is determined from a lookup table. The velocity profile contains the nominal velocity beginning at the arrival entry point with acceptable performance tolerances. Based on this nominal velocity and his present altitude, an arrival track is selected, again from a lookup table. Knowing the present velocity and the expected position in "n" seconds and the position and velocity at the arrival entry point, a great circle track and time-to-go is computed. It should be noted that the arrival tube is a predetermined 4D flight plan designed to move the aircraft from the point of entry to a point of merge on approach to the runway. The time down each tube to the approach marker will be normalized to the existing runway acceptance rate which translates into aircraft separation. Thus, once having computed the time-to-go to the arrival entry point (rounded off to the nearest separation standard) the time down the tube is added and this opening is searched for. If this time is filled, an earlier slot is searched for, keeping within the performance tolerance of the vehicle. If no slots are available, the time of the last aircraft is subtracted from this time, and depending on the difference, the aircraft is either path stretched or put in a hold pattern.

Assuming that a slot is found, the aircraft is then given a clearance to proceed to the airport. Meanwhile, the flight plan to be flown is transmitted to the aircraft and automatically read into the navigation computer. The user then switches to the landing arrival mode and navigates the aircraft in accordance with the 4D steering commands provided by the navigation processor. Note, that by translating the present position in time, a smooth maneuver can be made onto the transition track.

Once having issued the aircraft transition track, the aircraft is monitored for conformance to the issued flight plan. To do this, the vertical and horizontal cross-track error is computed as well as the rate of error. Whenever the rate of error and/or position error exceed certain boundaries, a command will be issued to the user to get him back on track. Conformance to the flight will continue until the aircraft reaches the approach marker and is handed off to the airport control center. This should occur somewhere between the 3 and 5 nmi markers.

In order to provide for conflict intervention between aircraft flying in the 4D airspace, a dimensional matrix will be structured for locating the various aircraft relative to each other. The location of the aircraft within this matrix will be updated each sample period. Thus, if an aircraft is found outside the flight plan and not responding, the aircraft flying in the immediate area can be warned and issued temporary commands for resolution of the conflict.

In summary, if aircraft fly in accordance with the issued flight plans, a conflict-free flight through the transition and arrival phase is inherent.

The basic control equations representative of the control law to be applied are given below. The geometry used in their derivation is shown in Fig. 5.3-19.

The terms for these equations are as follows:

ϕ_o, λ_o	Initial waypoint latitude, longitude
θ_D	Desired great circle track angle
η_D	Desired track bearing angle
M_{HD}	Slope of track (approximate)
n	Present update
τ_p	Time constant (used for initial waypoint)
ϕ_B, λ_B	Aircraft navigation bias error
ϕ_E, λ_E	Position of arrival track window
$\dot{\phi}$, $\dot{\lambda}$	Rate of change
R_{ED}	Range from starting point to arrival entry
t_{ED}	Time-to-go from starting point to arrival entry (normalized to separation segments)
t_{MD}	Time-to-go to approach marker (normalized to separation segments)
Δt_{MD}	Variation in t_{MD} as function of acceptable aircraft performance
V_N	Nominal aircraft airspeed
ΔV_N	Acceptable speed tolerance about nominal
τ_c	Latest airport separation segment
θ_A	Actual great circle track angle
η_A	Actual track bearing angle
δ	Cross-track angle of error
μ	Along-track angular component

Great Circle Navigation
Steering

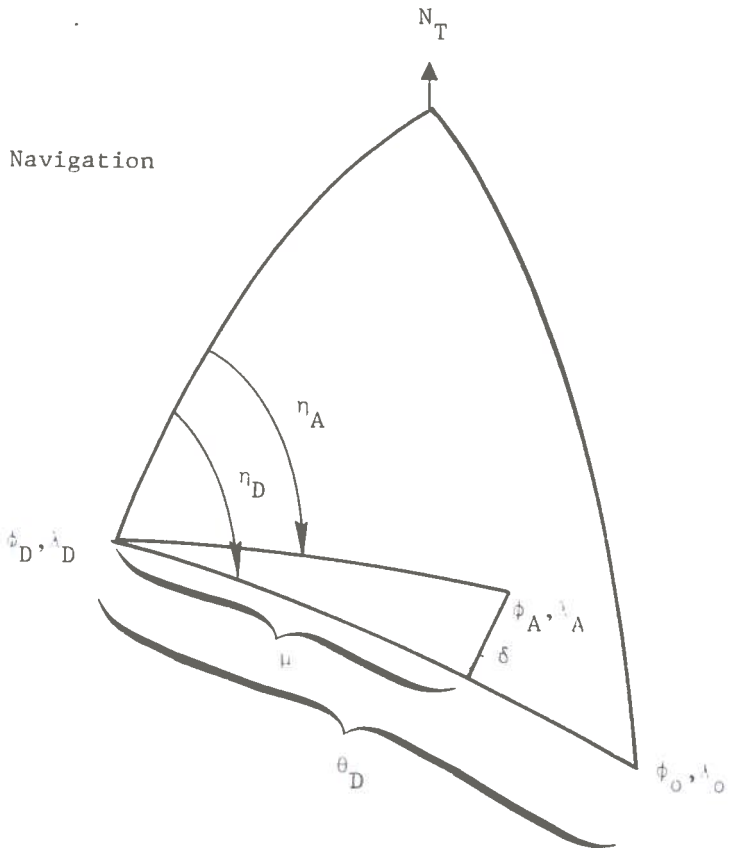

Fig. 5.3-19. General Transition Arrival Geometry

R_{XT} Cross-track error

R_{AT} Along-track component

M_{HA} Actual track slope

$\dot{R}_{XT}$ Rate of cross-track error

$\dot{R}_{AT}$ Rate of along track

V_A Aircraft ground speed

t_{TG} Actual time-to-go to next point

R_o Initial range-to-go between points

h_{DAT} Altitude as a function of actual range-to-go

$\dot{h}_{DAT}$ Desired altitude rate

h_{xt} Altitude error

h'_{xt} Altitude rate-of-error

Initial Transition Track Computations

$$\lambda_D = \lambda_E \text{ and } \phi_D = \phi_E$$

$$\lambda_o = \lambda(n + \tau_p) = \lambda(n) + \dot{\lambda}(n)\ \tau_p \pm \lambda_B$$

$$\phi_o = \phi(n + \tau_p) = \phi\ C_n + \dot{\phi}(n)\ \tau_p \pm \phi_B$$

$$R_{ED} = a\ \theta_D$$

$$t_{ED} = R_{ED} / \left[(V_N \pm V_W)\ \tau_c \right]$$

$$t_{MD} = t_{ED} + (K\tau_c)_i$$

$$\Delta t_{MD} = t_{MD} \pm R_{ED} / \left[(\Delta_{VN} \pm V_W)\ \tau_c \right]$$

$$i = 1 \text{ to } 25$$

Initial Waypoint/Track Computations

$$\cos \theta_D = \cos (90 - \phi_o) \cos (90 - \phi_D) + \sin (90 - \phi_o) \sin (90 - \phi_D) \cos (\lambda_D - \lambda_o)$$

$$\theta_D = \cos^{-1} \theta_D$$

$$\eta_D = \sin^{-1} \left[\sin (90 - \phi_o) \sin (\lambda_D - \lambda_o) / \sin \theta_D \right]$$

$$M_{HD} = \tan^{-1} \left[(\phi_D - \phi_o) / (\lambda_D - \phi_o) \right]$$

Conformance Monitoring Computations

$$\cos \theta_A = \cos (90 - \phi_D) \cos (90 - \phi_A) + \sin (90 - \phi_D) \sin (90 - \phi_A) \cos (\lambda_D - \lambda_A)$$

$$\theta_A = \cos^{-1} \theta_A$$

$$\eta_A = \sin^{-1} \left[\sin (90 - \phi_A) \sin (\lambda_D - \lambda_A) / \sin \theta_A \right]$$

$$\delta = \sin^{-1} \left[\sin \theta_A \sin (\eta_D - \eta_A) \right]$$

$$\mu = \tan^{-1} \left[\tan \theta_A \cos (\eta_D - \eta_A) \right]$$

$$R_{XT} = a \, \delta$$

$$R_{AT} = a \, \mu$$

$$M_{HA} = \tan^{-1} \left[\dot{\phi}_A / \dot{\lambda}_A \right]$$

$$\dot{R}_{XT} = V_A \sin (M_{HD} - M_{HA})$$

$$\dot{R}_{AT} = V_A \cos (M_D - M_A)$$

$$t_{TG} = \left[R_{AT} / \dot{R}_{AT} \right]$$

$$h_{DAT} = \frac{(h_D - h_o)}{R_o} \left[a \, \theta_A \right]$$

$$\dot{h}_{DAT} = \frac{(h_D - h_o)}{t_{Go}}$$

$$h_{xt} = h_{DAT} - h_A$$

$$\dot{h}_{xt} = \dot{h}_{DAT} - \dot{h}_A$$

$$\text{Fly Left/Fly Right} = f(R_{XT}, \dot{R}_{XT})$$

$$\text{Fly Up/Fly Down} = f(h_{DAT}, \dot{h}_{DAT})$$

$$\text{Slow Up/Speed Up} = f(R_{AT}, \dot{R}_{AT})$$

Conflict Avoidance Computation

The equations for Conflict Avoidance Computation are basically the same as shown in the Surveillance Mechanization Equations, Fig. 5.3-9.

The processing requirement needed to accommodate the transition/arrival control function including the display of information to the controller was estimated. The equation relating instructions per second as a function of the instantaneous aircraft including the display of information to the controlling monitor is

$$\text{IPS} = 30{,}000 + 1{,}350/\text{aircraft}$$

This figure is based on an update rate of once every 2 sec. The estimated memory storage requirements in terms of off-line and on-line storage are

(1) On-Line = 8,000 (32-bit words)

(2) Off-Line = 24,000 (32-bit words)

The on-line memory storage requirements include the operational program, the input/output, and the active display buffer. The off-line includes the aircraft velocity profiles, the short-term arrival flight plans and the corresponding required display formats.

The given requirements are defined for any one given 4D controlled airport. Thus, where two or more airports are combined into the processor a certain percentage of savings can be made. This saving would result from sharing common routines and common off-line storage information, e.g., the aircraft velocity performance data. The saving is estimated to be approximately 20 to 30 percent of the total.

5.3.10 Communications Processing

Communications processing required at each RCC (and also at the CCC) falls into two categories:

(1) Special purpose processing of aircraft-to-ground digital communications messages

(2) Processing associated with the formatting of digital data before and after communication between an RCC and other SAATMS control locations; the other RCC, CCC, ACC's, and aircraft.

5.3.10.1 Processing of Aircraft-to-Ground Digital Messages

Processing similar to that described for surveillance is required at the RCC's and CCC for air to ground digital communications. A general purpose processing capability will be required to associate the signals received from three satellites and perform error detection and correction. Figures 5.3-20 and 5.3-21 outline the general purpose processing that is required. Error detection is performed by means of majority voting whereby the seven-bit code derived from the position of a given pulse as received from three satellites is taken to be that of the majority; i.e., two or three satellites. If the value is different for all three satellites, an error is declared and retransmission by the aircraft is requested. The general purpose data processing requirements for this latter function are

(1) 250,000 instructions per second

(2) 32,000 words of main memory

5.3.10.2 General Communications Processing

The transmission of digital data between processing equipment requires that most of the processors have the capability of formatting data into messages and extracting data from message formats. In most cases, the processing load for this type of function is under 30,000 instructions per second. This can be considered essentially as overhead for these functions. However, in the case of the transmission of active aircraft file data from an RCC to the ACC's, the processing load is approximately 100,000 instructions per second and this may call for the use of a dedicated processor.

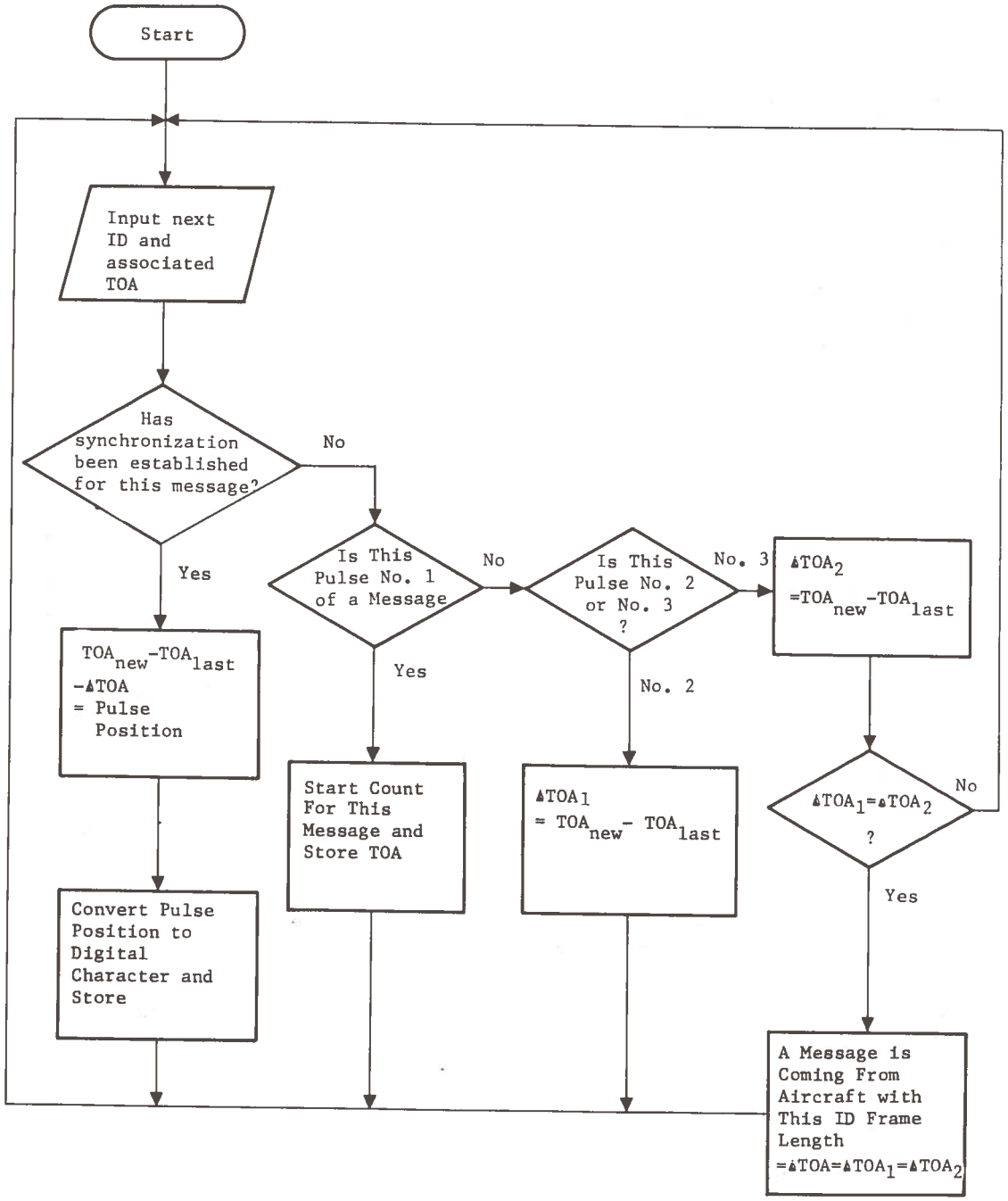

Fig. 5.3-20. Pulse Position Decoding

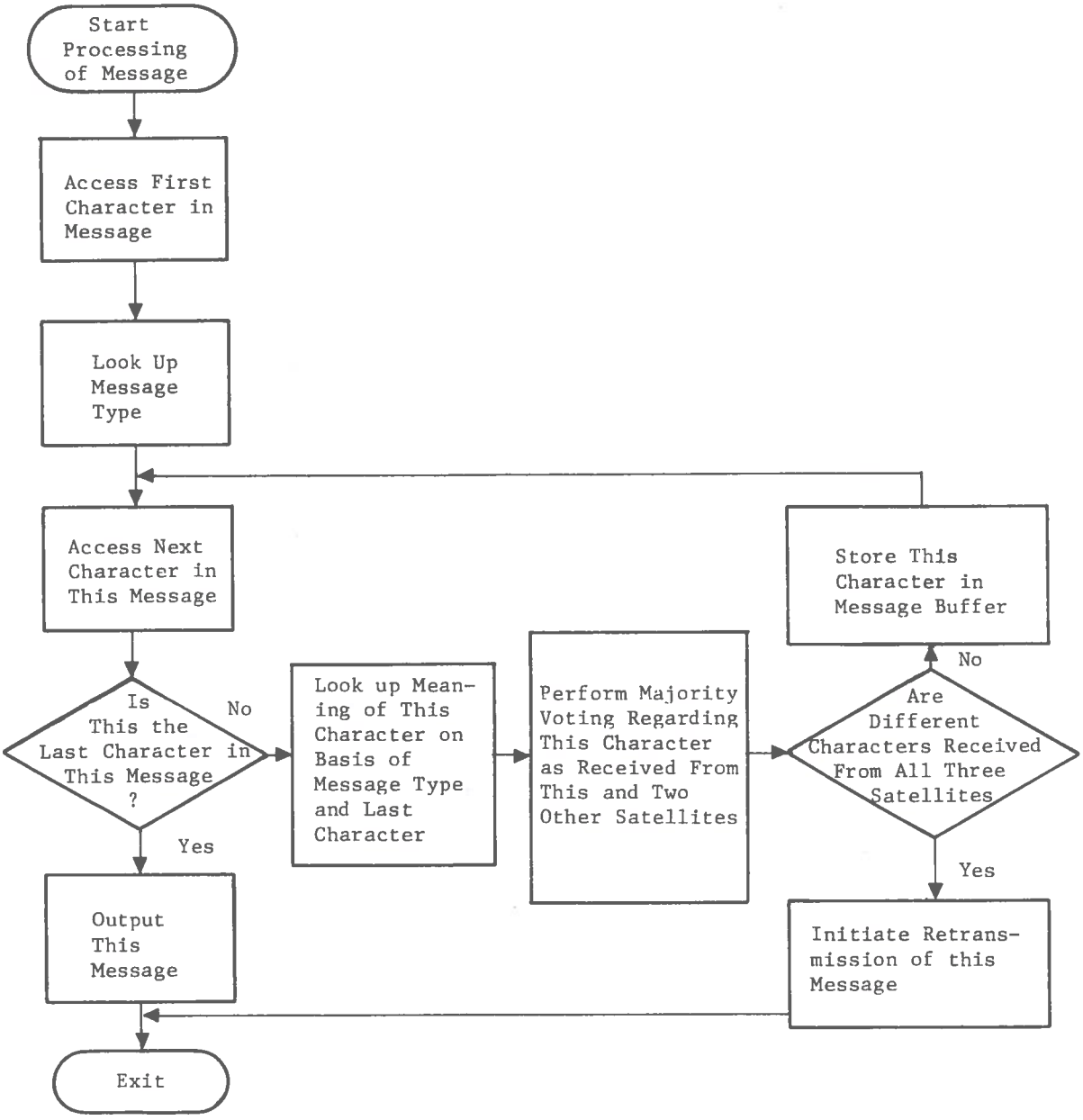

Fig. 5.3-21. Message Decoding

5.3.11 Display and Man/Machine Interface Processing

Positions of all active aircraft and other data, e.g., aircraft ID, clearance requested, VVOR in use, must be displayed at the RCC. Each position will include two displays, one of which will present an overall plan view of the sector covered by that position while the second display will be available for a close look at portions of the sector down to one cell (30 x 30 ft). In addition to the displays, each position will include a function keyboard similar to that currently used in the ARTS III system by which the operator can manage the display.

Processing for the displays will consist principally of those instructions necessary to transform aircraft position data to the coordinate system of the display of interest, and formatting these data and other data from the active aircraft file as required for use by the display subsystem. Transformation here is merely a shifting of origins and requires no trigonometric computations. Since sectors are of different sizes and the close-look display is generally on a different scale than the primary display at a given location, the equations for these transforms will probably be unique to each display.

Processing is also required for the man/machine interface; however, this function is limited by the speed at which a man can process information and react. Since man's reaction time is slow, this will not present a sizable processing load to the subsystem.

In addition to the display of active aircraft positions, there is a need for other displays at an RCC for use in the performance of tactical flow planning and for monitoring the status of the hardware elements of the system.

5.3.12 System and Self-Test Functions

System and self-test functions will include:

(1) Self-test of each computer

(2) Testing of all computers by one or more other computers in the computer complex

(3) Display of status of equipment at this location

(4) Display of status of equipment at other locations (RCC and CCC)

(5) Transfer of system status to other locations (RCC and CCC)

5.3.13 Executive Programs

The Executive Programs for data processing equipment at a location will be distributed among all computers within that location. In addition, one computer will be designated as a master for any executive functions that are used by more than one computer and can be centralized. Due to the relatively small number of programs that run in any one computer, the overhead for executive functions in all but the master computer will probably be less than 4 percent of the processing capability.

5.4 Hardware Mechanization of RCC and CCC Functions

This section will present a suggested approach to the organization of the major hardware elements required for performance of the RCC and CCC functions. The first to be presented will be the processing and memory capabilities necessary for performance of the functions, without specific consideration to fail-soft requirements. This will be followed by a brief discussion of the inherent fail-soft capabilities of the RCC processing equipment as backed up by the CCC, and the measures that will be required to satisfy the system failure-prevention requirements.

5.4.1 Basic Hardware

The hardware necessary for performance of the RCC and CCC functions falls into three general categories:

(1) General purpose data processing hardware that performs most of the required functions

(2) Special purpose parallel processing hardware that is used for the selection and separation of aircraft ID's transmitted as pseudo-noise pulse codes for surveillance and air-to-ground communications purposes

(3) Associative processing for rapid table searching.

Figure 5.4-1 is a block diagram presenting the principal features of the suggested organization of the data processing equipment in an RCC and CCC. Fig. 5.4-1 is separated into computers which include central processing (CP), main memory, and Input/Output Processing (IOP) on the basis of functions performed. The function numbers listed are those shown in Table 5.1-1. In some cases this results in a rather large amount of processing capability being interfaced with a bank of memory. In that case, the majority of the processing will be performed by moving blocks of data to the fast cache memory within the central processor. The processor will then perform a series of operations using instructions in fast Read Only Memory (ROM) within the central processor, and then store the data in the main memory. In this manner, the main memory cycle time need not be less than 500 nsec for all the computers shown in Fig. 5.4-1, except computer 1. Computer 1 has a processing throughput capability of 4,000,000 instructions per second. The achievement of this speed may require multiple processors if the state of art in component technology and architectural design at the time of implementation dictate it. Throughout, the system General Purpose Data Processor should have the capability for double word, word, half word, byte, and bit addressing.

The special purpose processors in computers 1 and 5 are as described previously in the description of Function 1. The communication processor in computer 3 will handle the relatively high volume of traffic between an RCC and aircraft. Communication processing is performed in other computers by one of the central processors.

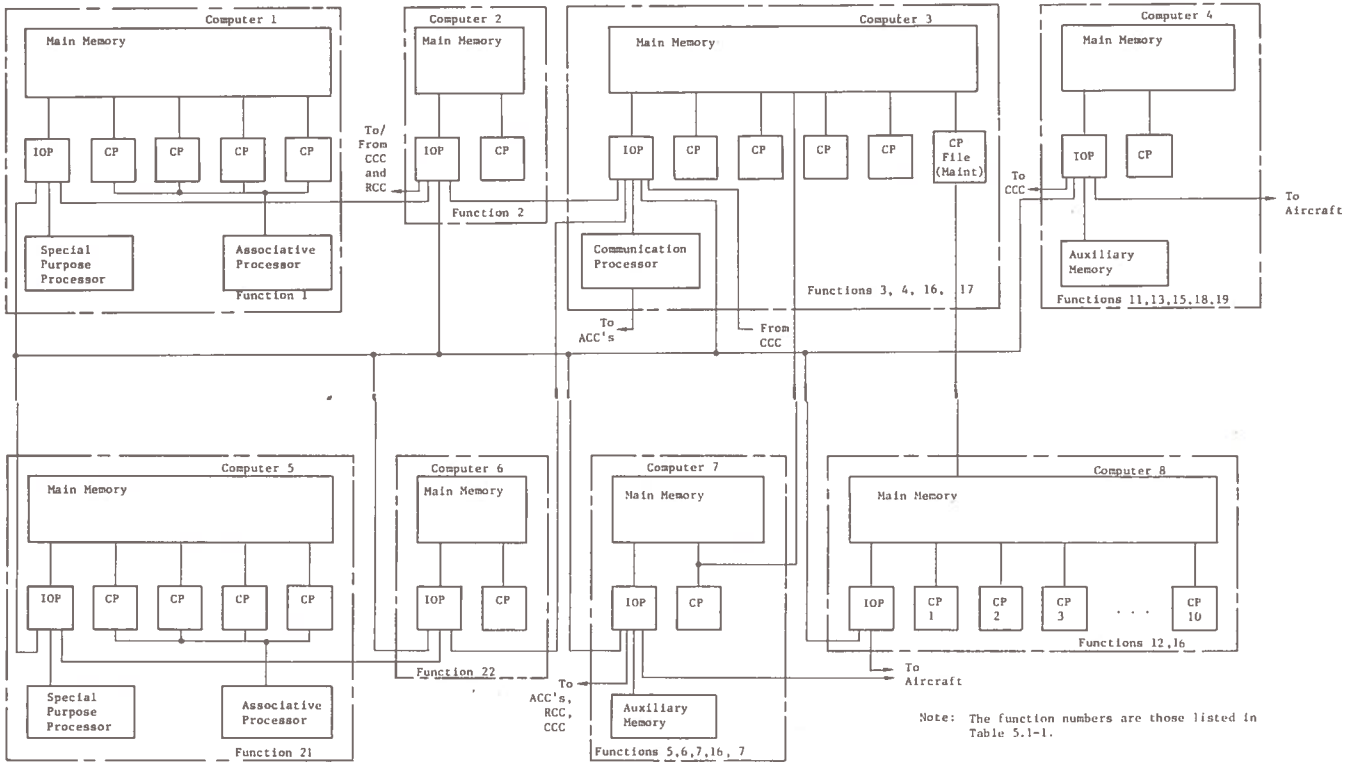

Fig. 5.4-1. RCC Processing Hardware Block Diagram

Associative, content addressable memory, processors are shown for Functions 1 and 20. As noted earlier, the sizing estimates reflect the use of an associative processor for use in the performance of Function 1. When a new identification is received by the central computer, it is sent to the associative processor for comparison to determine if it is in the FT, GFT, or B (burst) files (see Fig. 5.4-2).

These files are organized as:

(1) GFT and B: These files contain words formatted with identification, tag bits related to file type and status, and the address in the central computer's memory where the actual GFT and B files are stored.

(2) FT: This file contains words formatted with identification, tag bits, and TOA's.

The above allocation of information is beneficial in reducing the data flow between the associate processor and the central computer. Rapid search capability for the high processing rate routines can still be achieved with the reduced amount of associative logic.

The comparisons on a new identification are made immediately, and indications are provided from the associative processor to the central computer. The central computer tests these identifications and proceeds to executing the program accordingly.

5.4.2 Fail-Soft Capabilities

The CCC, being capable of performing all the functions performed by an RCC will provide a certain degree of fail-soft capability. Also, within an RCC (or CCC) the large computing capability and its modularity will allow undegraded performance of most functions. In addition to the modularity of processing, as shown in Fig. 5.4-1, the storage capability would be modularized by making the system capable of operating in a degraded mode and by removing the failed memory modules from the system.

It may, however, be necessary to provide totally redundant hardware for some functions such as those performed by Computer 1. Figure 5.4-3 shows a configuration which may be used. This organization will provide a capability for Fail Operational-Fail Safe-Fail Soft operation. Cross checking by two computers can ensure this performance.

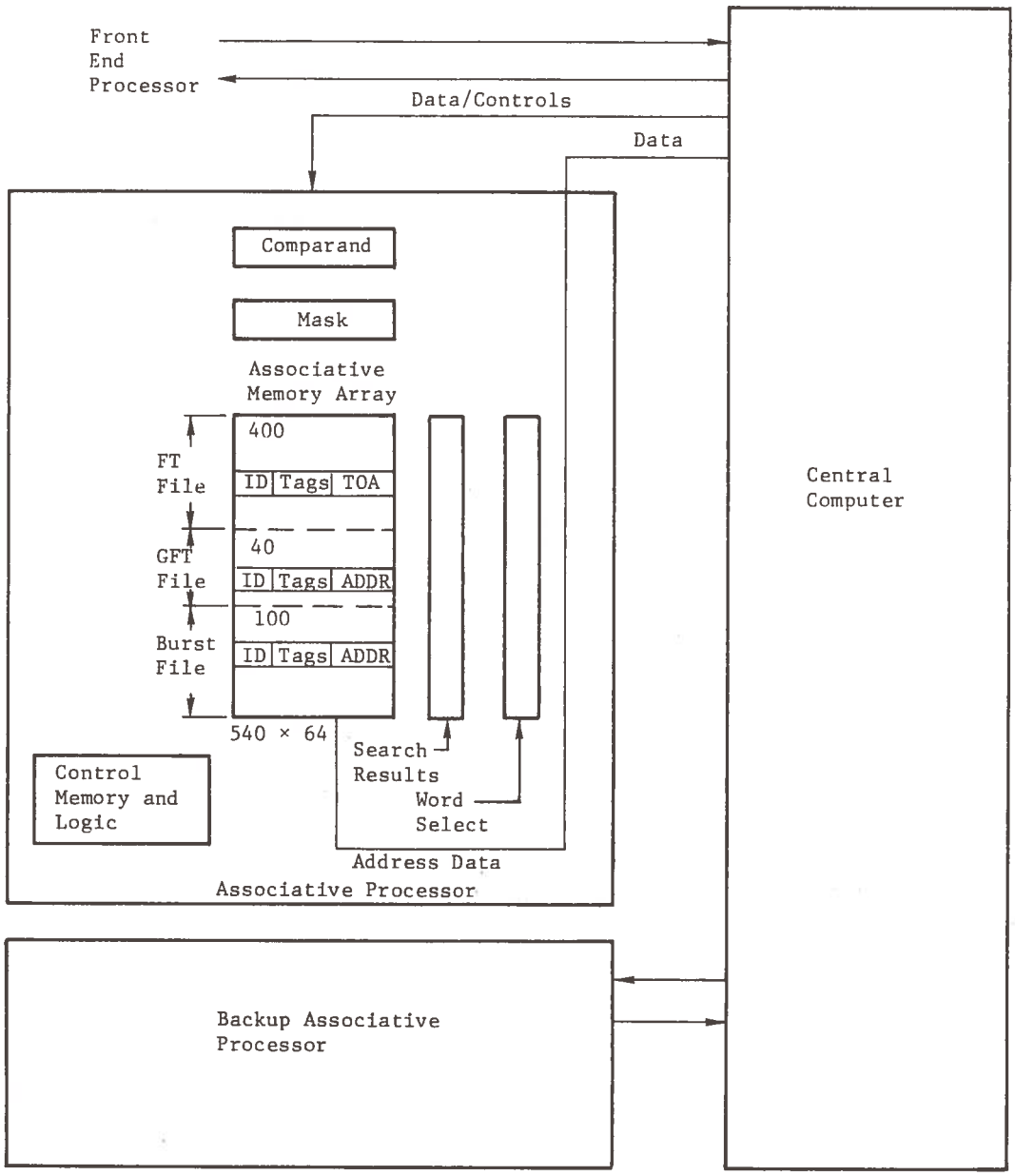

Fig. 5.4-2. Central Computer for Surveillance Identification Processing

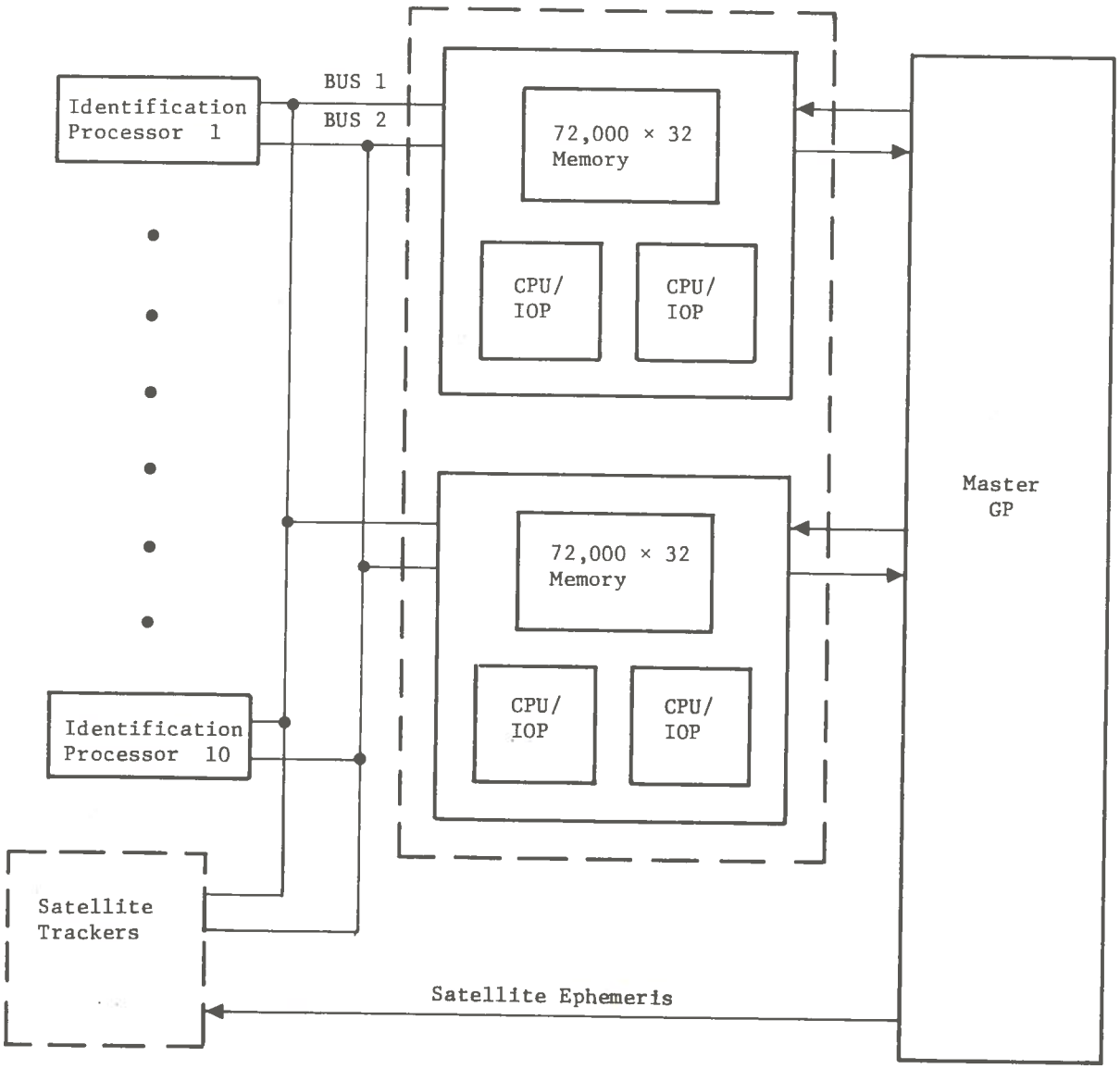

Fig. 5.4-3. Redundant Prooessor for Function 1

The associative processing capability for which no inherent hardware redundancy exists in the system, will probably have to be duplicated to assure adequate system operation.

The GP hardware present in the system can preclude system downtime by providing redundant modules of a number less than that constituting full redundancy. A similar approach is appropriate to the parallel special purpose processors used for surveillance data filtering and for user-to-RCC communications pseudo-noise pulse filtering.

5.5 Airport Control Center

Figure 5.1-1 shows those data processing functions that are required at an ACC. At each ACC a need will exist for a mini-computer to perform processing of data received from the RCC for display in the airport control tower. Processing of these data at the ACC include

(1) Communications Processing

(2) Display and Man/Machine Interface Processing

(3) Handoff Processing

(4) Compute Self-Test

(5) Compute Executive

Table 5.1-1 indicates the range of data processing requirements for these functions. At some airports the number of aircraft in the vicinity to be displayed will be in the hundreds, and at others in the tens. Thus, the range of requirements for ACC display and communications is broad. However, it is felt that a mini-computer with a capability of up to 32,000 words of main memory can handle these functions. At some small airports the main memory requirement will be as low as 8,000 words.

At the larger airports there will also be the need for processing associated with surveillance and control of aircraft on the ground. This, being a low rate function will also fit into a minicomputer along with such functions as display, communications, handoff, etc.

5.6 Processing in the Controlled Aircraft

Processing in the controlled aircraft will include two principal application functions plus executive and self-test functions. The two principal application functions are

(1) Satellite Navigation

(2) Display and Man/Machine Interface Processing

Both of these functions are associated with satellite navigation, the second merely formats the display of the first. Data processing requirements for those functions are on the order of 50,000 operations per second or less, and 2,000 words of memory. These requirements can be satisfied quite economically by a computer that utilizes high density MOS LSI for both logic and memory.

6. AIRPORT SUBSYSTEM

6.1 Airport Ground Control System - Fully Compatible with Airport and Avionics Equipment

To minimize both aircraft and airport equipment costs, a trilateration TOA scheme, similar to the satellite surveillance, is recommended for the primary SAATMS airport ground control system. The advantages to this system, particularly at large airports, are high accuracy, self-contained aircraft identifications, simultaneous tracking of all aircraft, adaptive update rates, and minimal blind spots. In addition, the technique is fully compatible with SAATMS aircraft transceivers

Ground control is accomplished using the normal aircraft three-pulse ID waveform, in this case, received by towers rather than the satellites. The towers are local to the airport and uniquely configured to maximize accuracies and eliminate blind spots. Employing local towers allows the use of the normal aircraft RF system and antenna. Although the total RF gain may be reduced by 10 db, the ranges are such that high S/N ratios can be obtained. Directional tower antennas will be used to reduce the density of received signals and, therefore, the overlap and near/far problems where signal sources close to the receiver come in stronger than do remote signals. They will also help to minimize the effects of multipaths.

The towers receive the aircraft signal and transpond the signal to the ACC. Time-of-arrival differences are measured at the ACC and the aircraft position is determined. The position data are used for two purposes. First, they are used to perform aircraft surveillance and provide separation advisories. Second, the data are retransmitted to the aircraft for navigation.

The navigation position data are retransmitted to the aircraft on the normal digital link, and the navigation mode requires no additional avionics receivers. A special navigation display would be required but can be integrated with the existing situation display.

The tower ground control system was analyzed for Los Angeles International Airport. Using a five-tower system (Fig. 6.1-1), a mean GDOP value of 1.26 was obtained. As shown in Fig. 6.1-1, four towers are located at the corners of the airport. A fifth tower was placed on the commuter terminal to account for signal blockage caused by buildings and hangars and to increase the system reliability in the event of a failure. The GDOP contours for both normal and failed operations are shown in Fig. 6.1-2 through 6.1-7.

Although this particular five-tower configuration has resulted from a comparative analysis of several tower geometries, no attempt was made to optimize the geometries. The results should be viewed as illustrative of the potential of this technique.

The estimated error budget for the trilateration system is shown in Table 6.1-1.

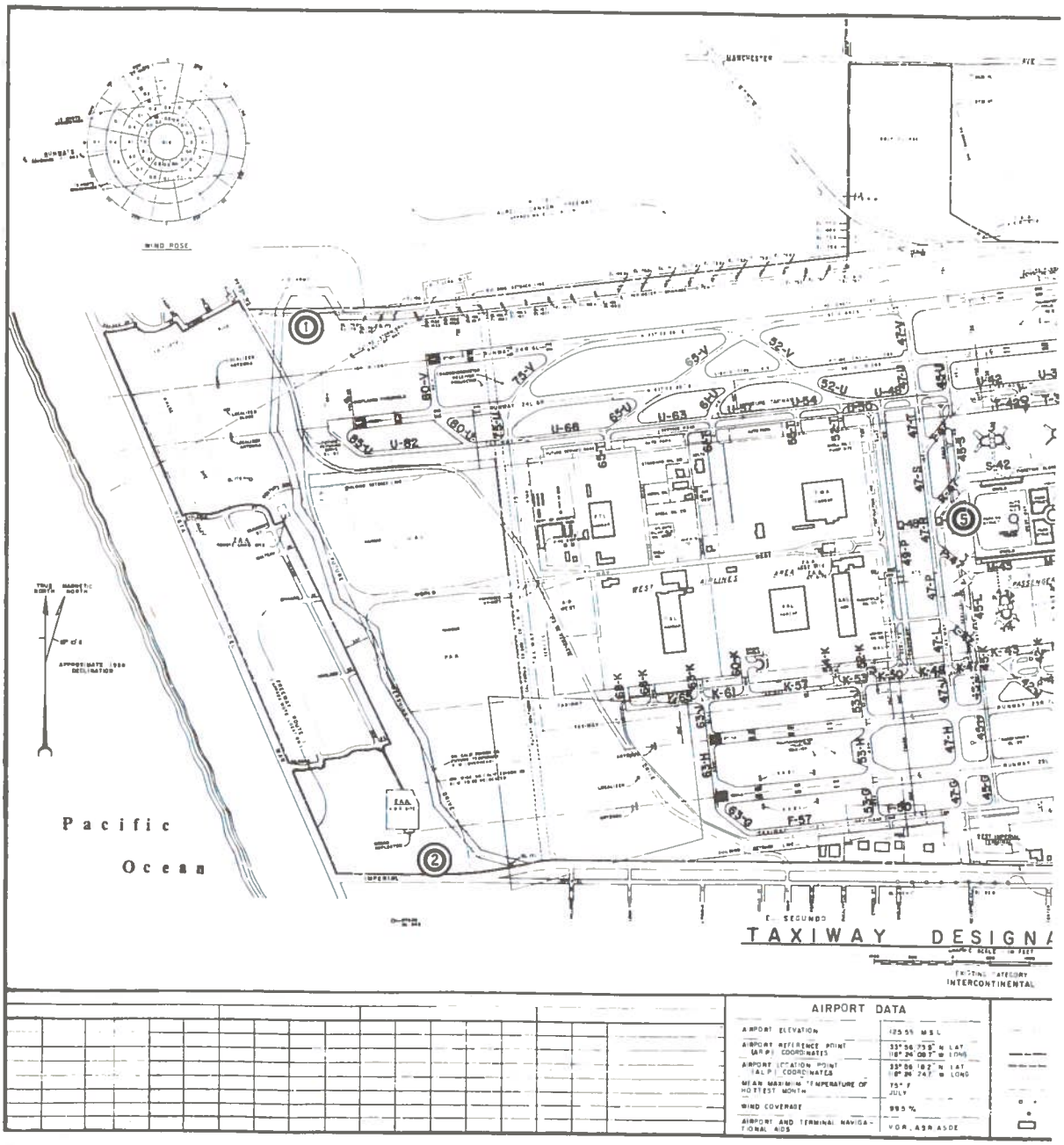

Fig. 6.1-1. Los Angeles International Airport with Proposed Tower Locations

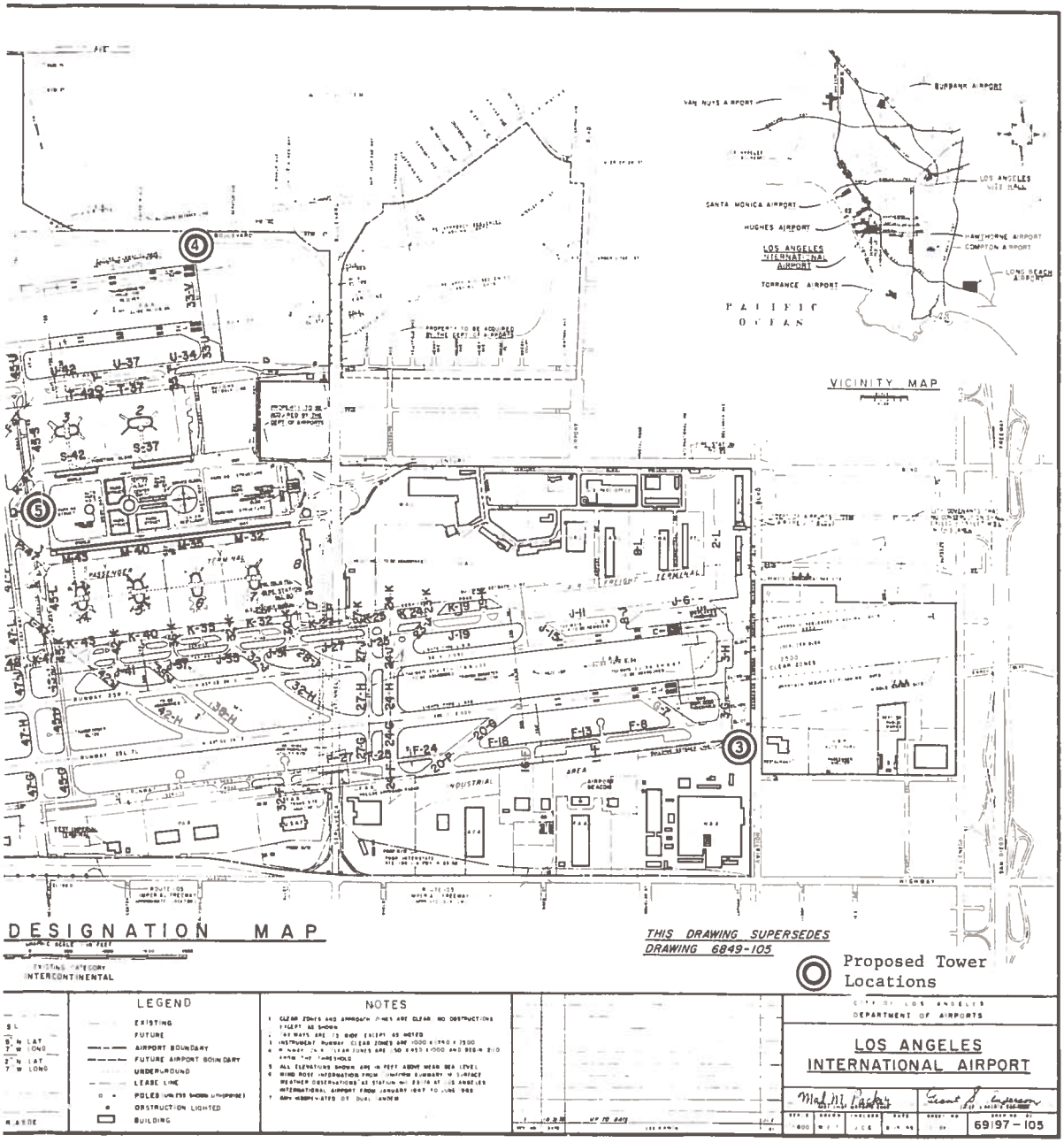

Fig. 6.1-1 (Continued)

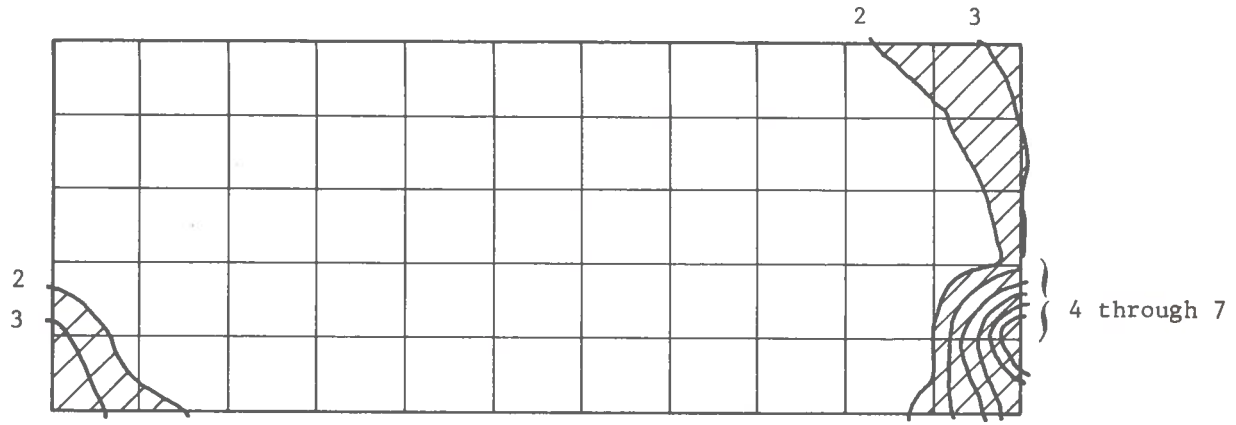

Fig. 6.1-2. GDOP Contours All Towers Operational

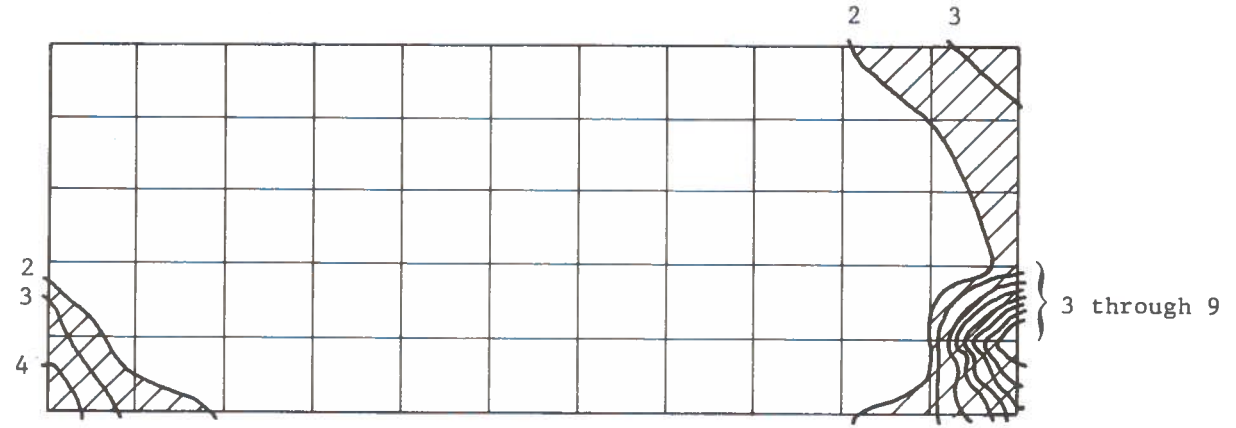

Fig. 6.1-3. GDOP Contours with Towers 1, 2, 3, and 4 Operational

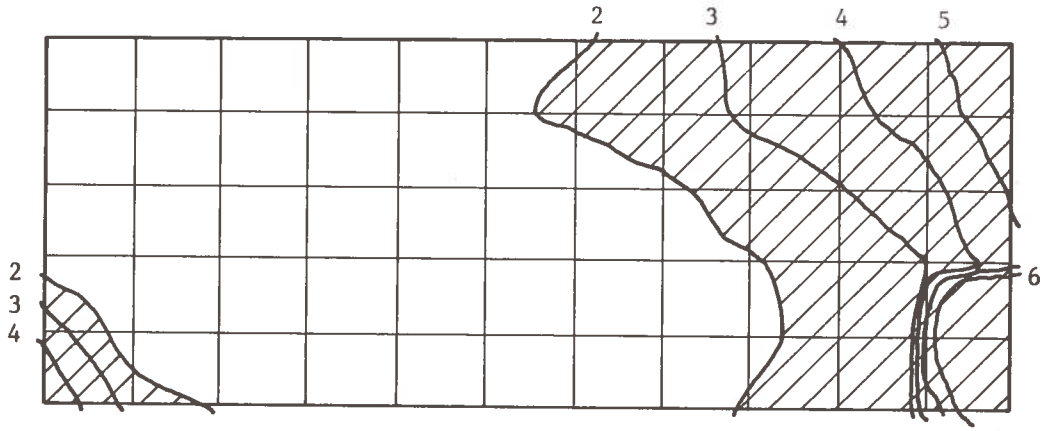

Fig. 6.1-4. GDOP Contours with Towers 1, 2, 3, and 5 Operational

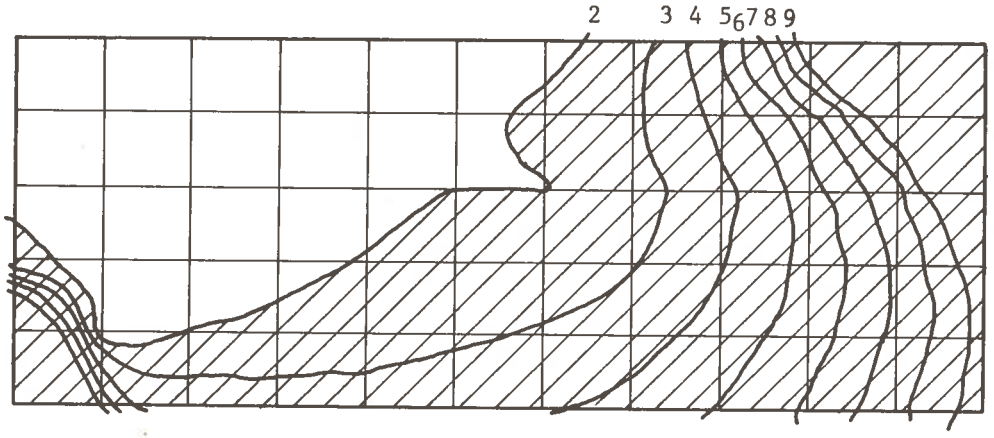

Fig. 6.1-5. GDOP Contours with Towers 1, 2, 4, and 5 Operational

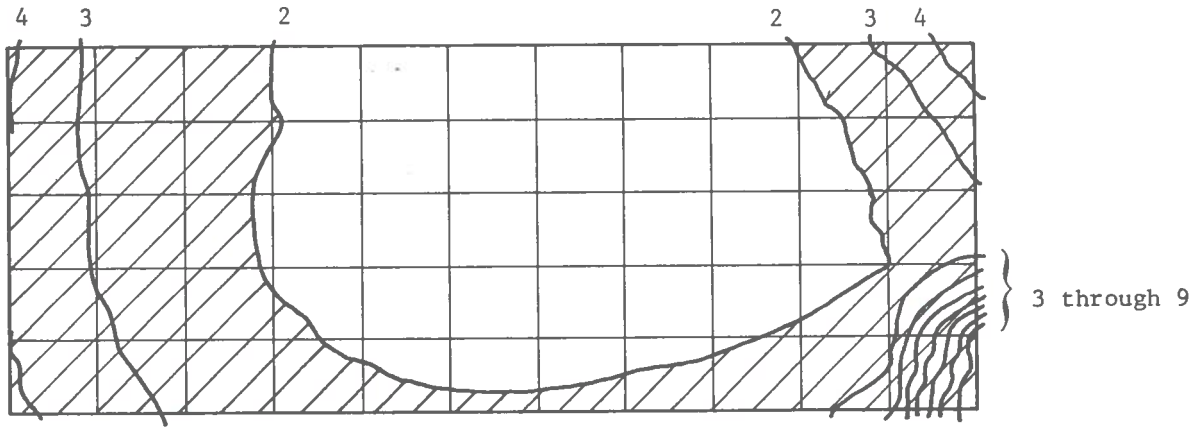

Fig. 6.1-6. GDOP Contours with Towers 1, 3, 4, and 5 Operational

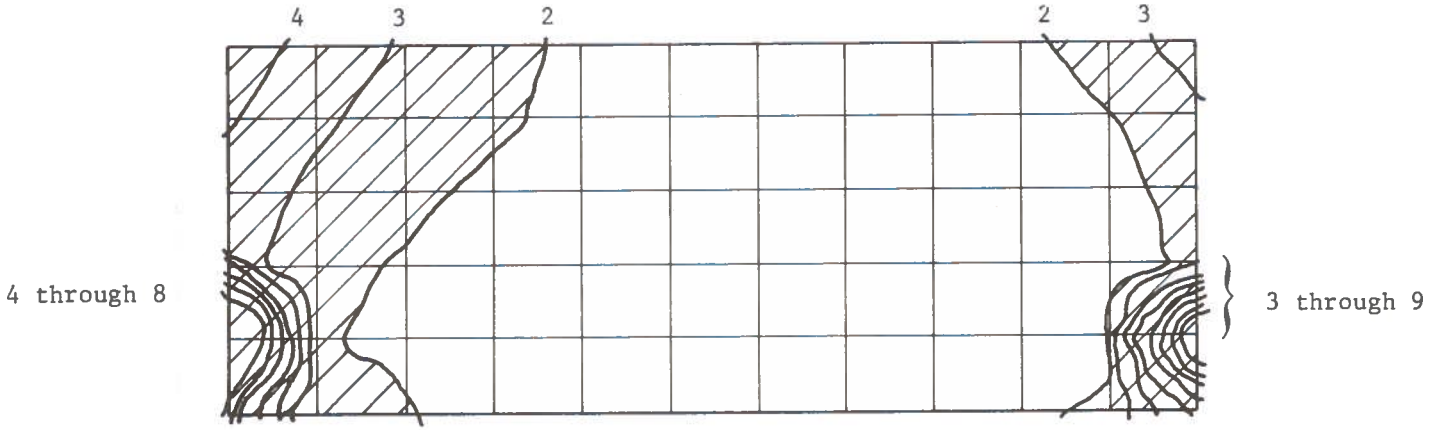

Fig. 6.1-7. GDOP Contours with Towers 2, 3, 4, and 5 Operational

Table 6.1-1. Trilateration Error Budget Source

Parameter	Error
Ranging	3 nsec
Multipath	25 nsec
Clock	10 nsec
Computation	2 nsec
Total RSS Error	27 nsec
TOA Difference Error Per Tower Pair	38 nsec
Relative Ranging Error Per Tower Pair	19 ft. ($1-\sigma$)
GDOP (Mean) = 1.26 (Normal Operation)	24 ft.

The ranging noise error is primarily a function of the bandwidth of the system and the available S/N ratio. However, due to the decreased range and, thus, the increased S/N ratio, the receiver noise error should be no greater than 3 nsec. The multipath error of 25 nsec is by far the dominant error source and is considered worst case. The wide bandwidth pseudo-noise coding technique will minimize the effects of multipath. The use of crystal clocks with a short-term stability of 10^{-8} and a long-term stability of 10^{-6} will produce an error of approximately 10 nsec. Computation errors are considered small because of the small ranges involved.

The trilateration technique is fully compatible with both the aircraft and airport equipments and can be used for both surveillance and navigation. In addition, with proper tower location, control and guidance at the ramp areas, the runways, and taxiways can be obtained.

While the trilateration scheme is, in general, suitable for ground surveillance, it is felt that an auxiliary discrete sensor technique should be used. These discrete sensors can be used at high density intersections where airport configuration creates special blind spot trouble areas or at lower class airports where a less costly surveillance scheme is desired. This technique makes use of discrete scanning infrared (IR) sensors located at critical points at the airports. The sensors detect the xenon beacon normally used on aircraft.

The lamp has the spectral intensity as a function of wavelength indicated by Fig. 6.1-8. Significantly, the intensity peaks around 0.9 microns where there is a window for infrared transmission in the atmosphere. A silicon detector response curve is also shown in Fig. 6.1-9, and it appears that the xenon lamp and silicon detector are a proper combination for the IR system.

Infrared sensors, consisting of multi-element silicon detector arrays, are placed on each side of the runway for reception of the lamp emissions (Fig. 6.1-9). The sensors on either side of the runway measure the angles to the aircraft, thereby providing sufficient information to determine aircraft position. The sensor outputs are transmitted to the ACC computer. The ACC computer determines aircraft position, transmits guidance information via RF digital data link to the aircraft, and simultaneously displays all aircraft positions.

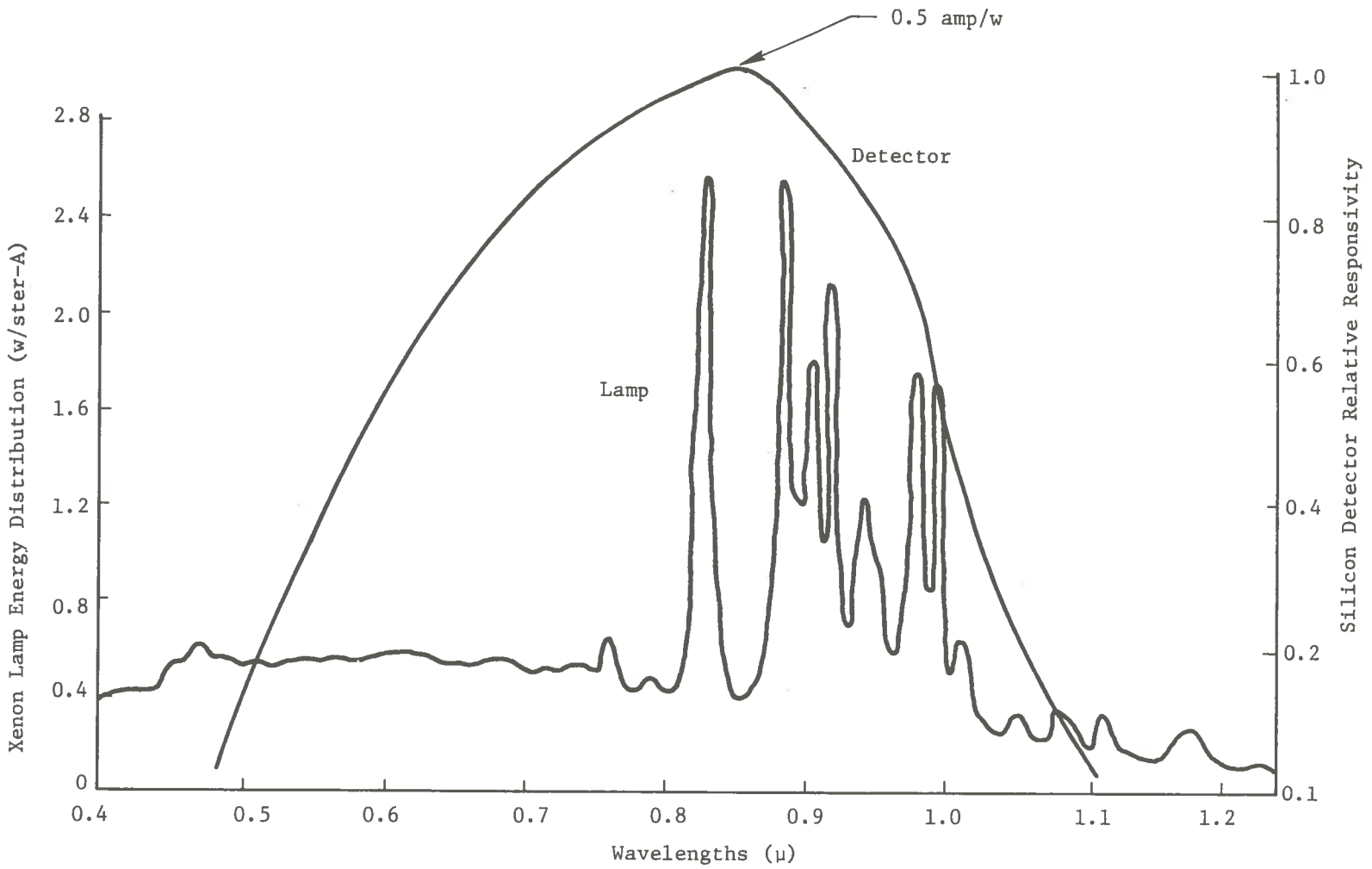

Fig. 6.1-8. Spectral Intensity of a Xenon Lamp and Spectral Response of a Silicon Detector

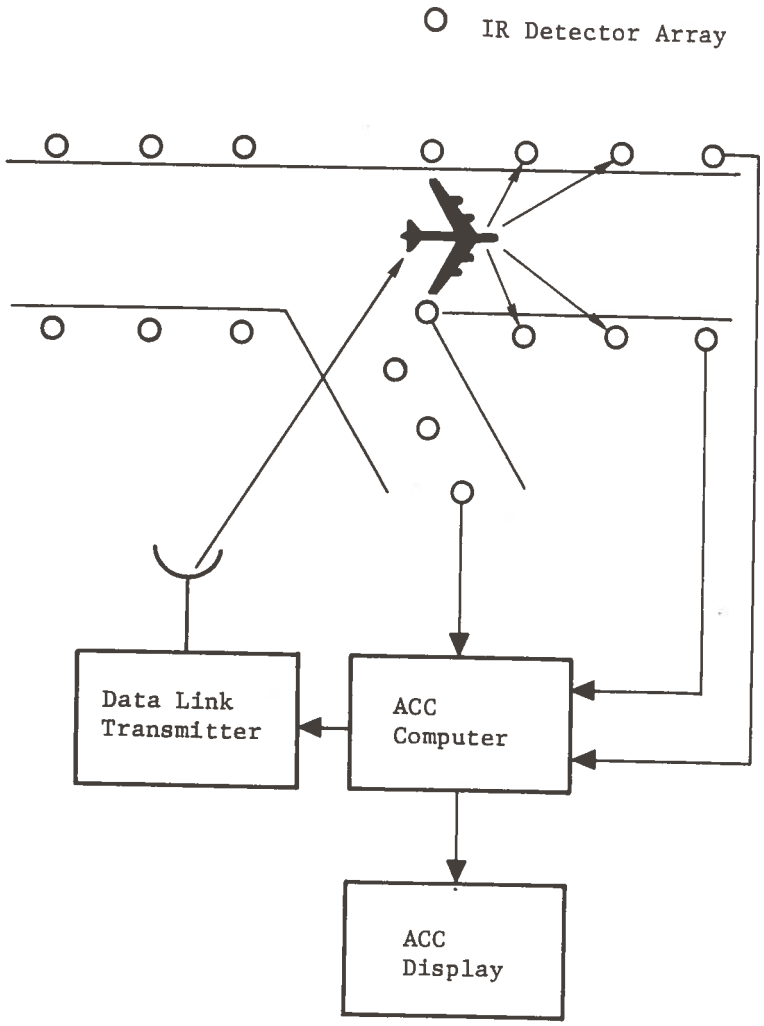

Fig. 6.1-9. Configuration for the Runway and Taxiway for the IR System

Autonetics has conducted some limited testing to investigate the range improvement factor of the IR over the visual (Fig. 6.1-10). Although the data points are limited, good correlation with the theoretical curve is obtained.

It should be noted that the theoretical improvement is better at shorter ranges. Additionally, at short ranges, the location accuracy is very good. For example, at a 200-ft distance, a 2-deg sensor can locate the aircraft beacon within 6 ft. Thus, high accuracy navigation data can be retransmitted to the aircraft. These data are particularly important in Category III conditions for keeping aircraft on runways and for indicating and directing turns. The accuracies required for these functions are probably beyond the capabilities of the trilateration scheme but well within the performance of discrete IR sensors.

The IR system has the advantages of high accuracy, low cost and high reliability. Furthermore, with the lamps located under the aircraft, the system lends itself to operation with sensors located in the housing of the center lights installed on the airport taxiway and ramp areas. This technique can also be used on ground vehicles such as cars, trucks, etc., for complete control of all airport ground traffic.

6.2 SAATMS Landing System

While the exact design of the proposed Microwave Landing System (MLS) cannot be completely specified at this time, the impact of the SAATMS navigation capability on the MLS requirements can be discussed.

The primary requirements for the MLS in the final approach, landing, and rollout phases of flight include high precision data, in all weather conditions, at low altitudes in severe multipath environments. The costs of providing these services are estimated to be quite high compared to other SAATMS services. A large part of the cost is due to the requirements for wide angle coverage and a 30 nmi range. These requirements are primarily based upon the need for metering, spacing, and curved approaches for noise abatement.

The satellite SAATMS provides high accuracy and complete coverage for the surveillance and navigation functions regardless of aircraft location. In addition, all SAATMS users will be able to fly complex RNAV routes. New airport routes can be optimized for minimum environmental impact.

The impact of these SAATMS capabilities on the MLS is considerable. First, the need for backcourse missed approach guidance is obviated since high accuracy surveillance and navigation data are available. Second, the range and azimuth requirements for the MLS can probably be reduced. For example, an azimuth coverage of $\pm$10 deg and a range of 10 to 15 nmi is probably adequate when coupled with the flexible routing capability of SAATMS. If the range is reduced, the number of simultaneous users is correspondingly reduced and the requirements on the MLS DME substantially lessened.

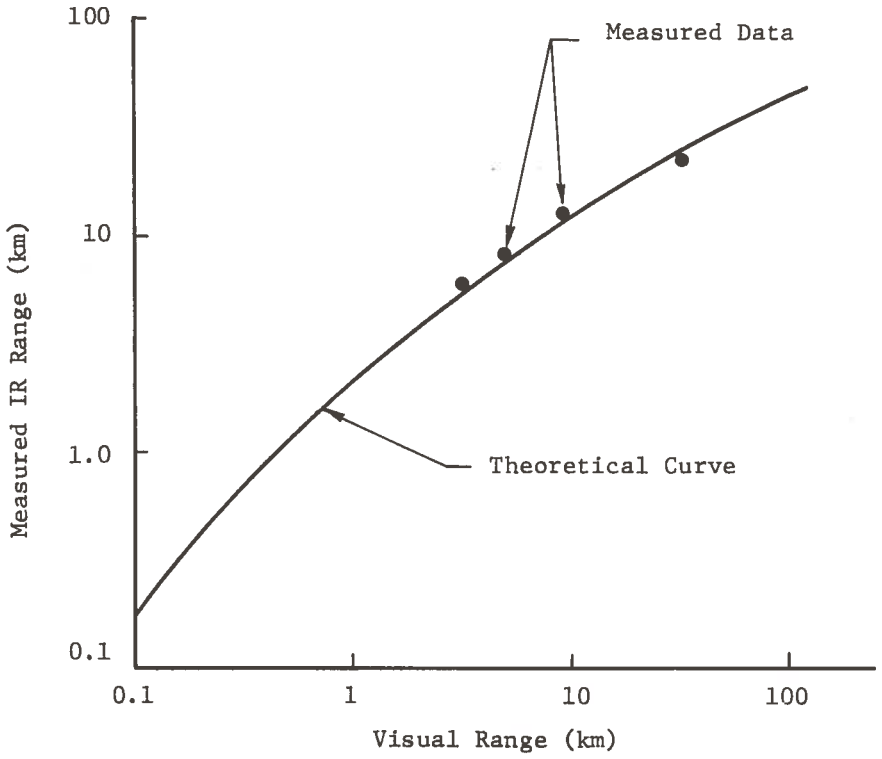

Fig. 6.1-10. IR Range Improvement

In summary, the MLS for the SAATMS has the potential of utilizing the satellite feature to substantially reduce costs. The impact of the SAATMS performance on coverage and range requirements should be addressed in detail. Besides the coverage and range considerations, the impact of waveform on user avionics costs and the possibility of integrating the MLS function with the SAATMS designs should be investigated.

7. SAATMS ELECTRONICS

The SAATMS electronics considered here consist of those equipments directly associated with communications, surveillance, and navigation and not the associative processing, display, and control hardware. The equipment considered herein are those specifically required to establish the basic structure of the system irrespective of automation levels.

7.1 Control Center Equipment

The CCC and RCC equipment are similar in most respects. This follows from the CCC backup capability for RCC functions. The major functions in the RCC and CCC are as follows:

(1) Receiving surveillance data

(2) Receiving air-to-ground digital and voice data

(3) Transmission of ground-to-air digital and voice data

(4) Transmission and reception of ground-to-ground data

(5) Satellite navigation ephemeris data insertion

(6) Receiving navigation timing data for satellite tracking

All of these functions involve RF links between the control centers and satellites.

Table 7.1-1 shows the antenna requirements for each control center. The surveillance function requires six fixed and nine steerable C-band antennas for reception of surveillance data. This allows the use of one steerable antenna as backup for either a fixed or steerable antenna. The navigation function requires four antennas to receive satellite navigation signals. These four antennas yield hemispheric satellite coverage without any steering requirements. The air-ground and ground-air links require three antennas plus one spare. The ground-air ephemeris insert requires four additional antennas with the capability to reposition within 0.6 sec to allow ephemeris insert each 0.2 sec. A completely redundant set of ground-to-ground communication antennas is provided to insure fail-operational operation.

All of the C-band antennas at the control centers are 15 ft in diameter. These provide approximately 45 db gain. The steerable antennas have a 0.2 deg pointing accuracy. The L-band antennas are electronically steerable to allow nominal pointing for navigation pulse reception.

A separate surveillance receiver as shown in Fig. 7.1-1 is associated with each of the 15 satellites. The local oscillator frequency is adjusted to remove most of the doppler shift caused by the inclined orbit satellite movement. The

Table 7.1-1. Control Center Antenna Requirements

Function	Antenna Type	Number of Antennas	Frequency Band	Usage	Spares Available
Surveillance	Fixed	6	C1	Receiving	2
	Steerable	9	C1		
Navigation	Fixed	4	L2 + L3	Receiving	-
Communication					
A-G Digital	Steerable	4	C3	Receiving	1
A-G Voice	Steerable	4	C7	Receiving	1
G-A Digital*	Steerable	8	C2	Transmitting	1
G-A voice	Steerable	4	C6	Transmitting	1
G-G Digital	Fixed	8	C4	Transmitting	4
G-G Digital	Fixed	8	C5	Receiving	4

*Includes Ephemeris Insert

A-G means air-ground; G-A means ground-air: G-G means ground-ground

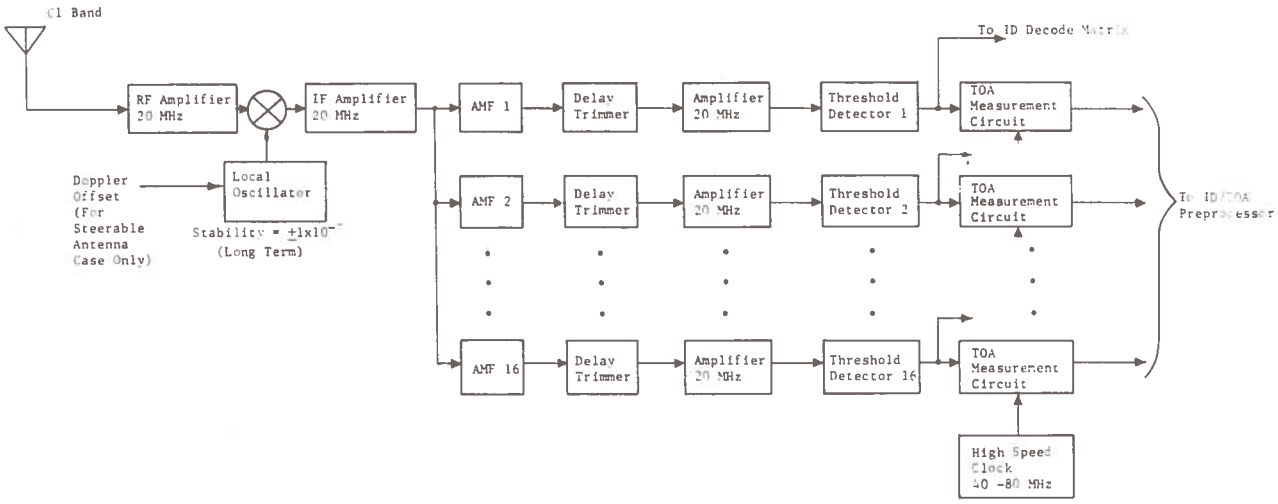

Fig. 7.1-1. Surveillance Receiver

frequency offset due to the change in carrier frequency of the uplink surveillance signal is based on the satellite's radial velocity with respect to its subsatellite point. The frequency offset due to the downlink signal can be computed exactly because of the known RCC-satellite orientation.

As discussed in Section 2.2, an aircraft surveillance ID consists of three pulses with each pulse containing one of 16 PN codes. Each of the 16 different pulse types are detected individually and a TOA is associated with each detection. The individual pulse TOA's are then combined in a processor that extracts ID's. The ID's that satisfy the correct criteria are then used as inputs to the position computation.

The diagram of the RCC receivers to accept digital data from aircraft is shown in Fig. 7.1-2. Each RCC has three such active receivers. The output from the three receivers is used to majority decode the received data. Since each aircraft transmits a unique ID, the detection circuitry is exactly as in the surveillance receiver except for the narrower bandwidth. The communications preprocessor shown in Fig. 7.1-2 must combine the outputs of the 16 individual detection circuits and form ID's. The TOA of an ID represents a pulse position carrying 7 binary (128 decimal) bits of information.

The transmitter section of the RCC-satellite-aircraft digital data system is shown in Fig. 7.1-3. The same transmitter is used for the transmission of navigation ephemeris data.

Each RCC has three transmitters for digital data excluding spares. These three transmitters are used for both digital communication and navigation ephemeris data. Four transmitters in each RCC are used by the RCC to send navigation data only.

The equipment associated with voice communication between the RCC and aircraft are shown in Fig. 7.1-4 and 7.1-5. The modulation technique is 10 kHz narrowband FM. The voice channels are frequency division multiplexed in sets of 25 with 25 kHz spacing between channels. Each set of channels is connected to the appropriate antenna. Each RCC has a total of 100 two-way channels.

The equipment associated with ground-to-ground communication is shown in Fig. 7.1-6 and 7.1-7. Data are biphase modulated at 2.4 kbs. The channels are frequency division multiplexed with 5 kHz channel spacing. An RCC has two identical sets of 600 channels which can be operated simultaneously. The separation between sets of channels is provided by separate satellite relays and separate high gain ground antennas.

The equipment associated with a Satellite Tracking Center that is collocated at the control centers is shown in Fig. 7.1-8. This L-band equipment is essentially the same as the navigation portion of an integrated user avionics package. Similar equipments are located at four ACC's in addition to the CCC and RCC's.

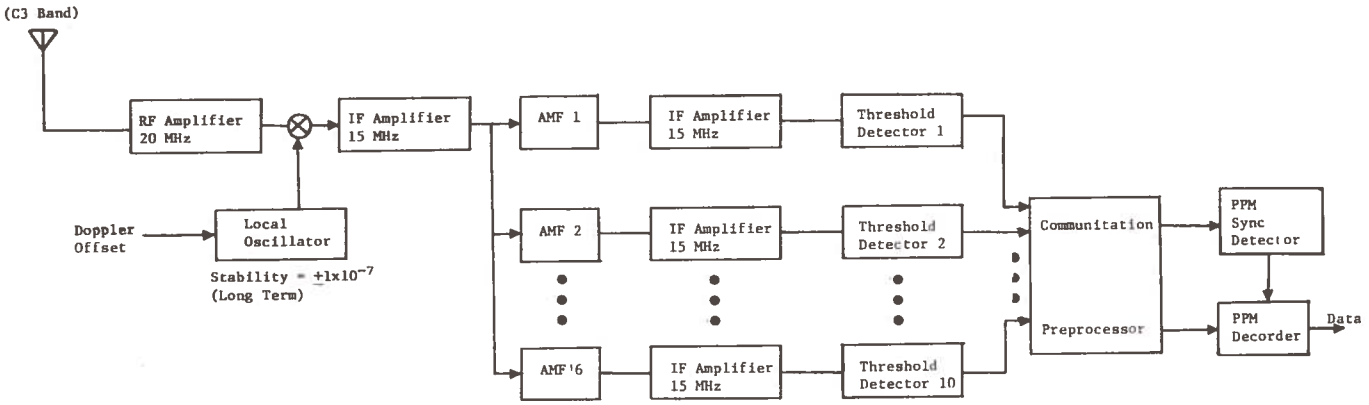

Fig. 7.1-2. RCC Digital Data Receiver, Aircraft-Satellite-RCC

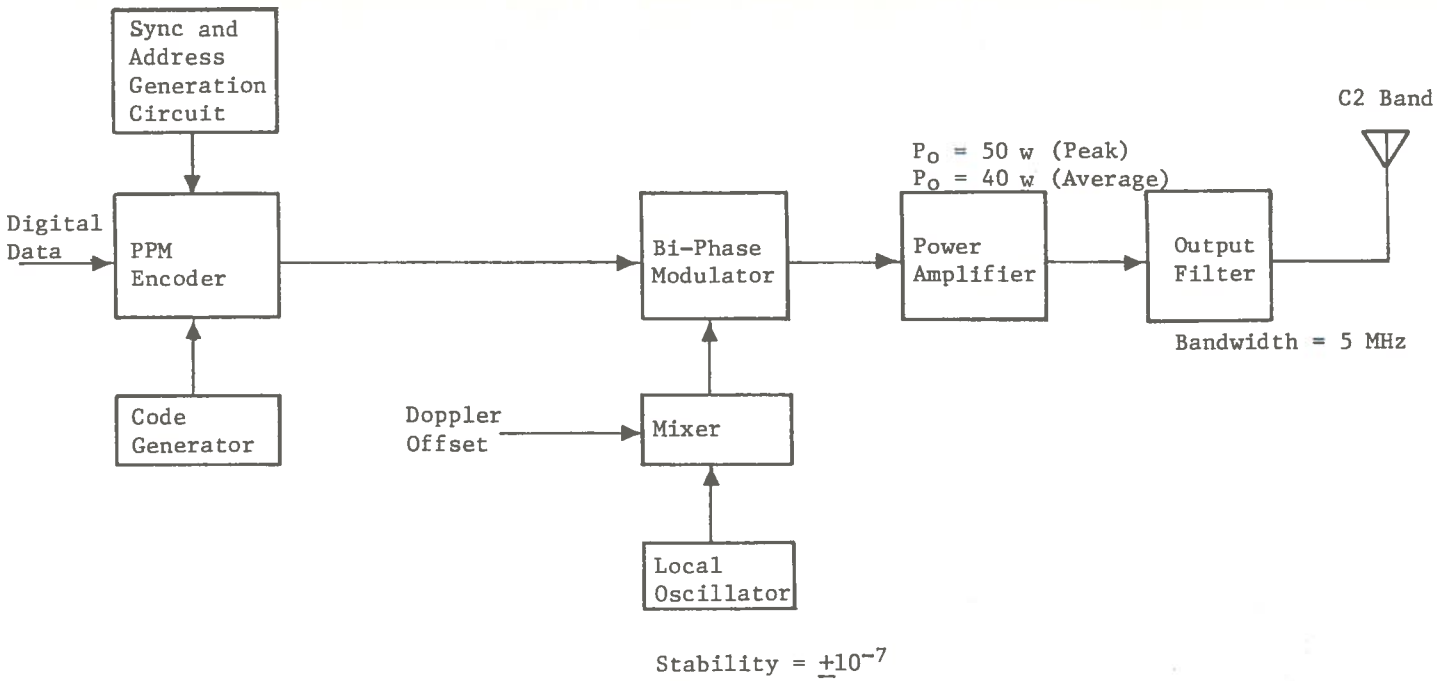

Fig. 7.1-3. RCC Digital Data Transmitter RCC-Satellite-Aircraft

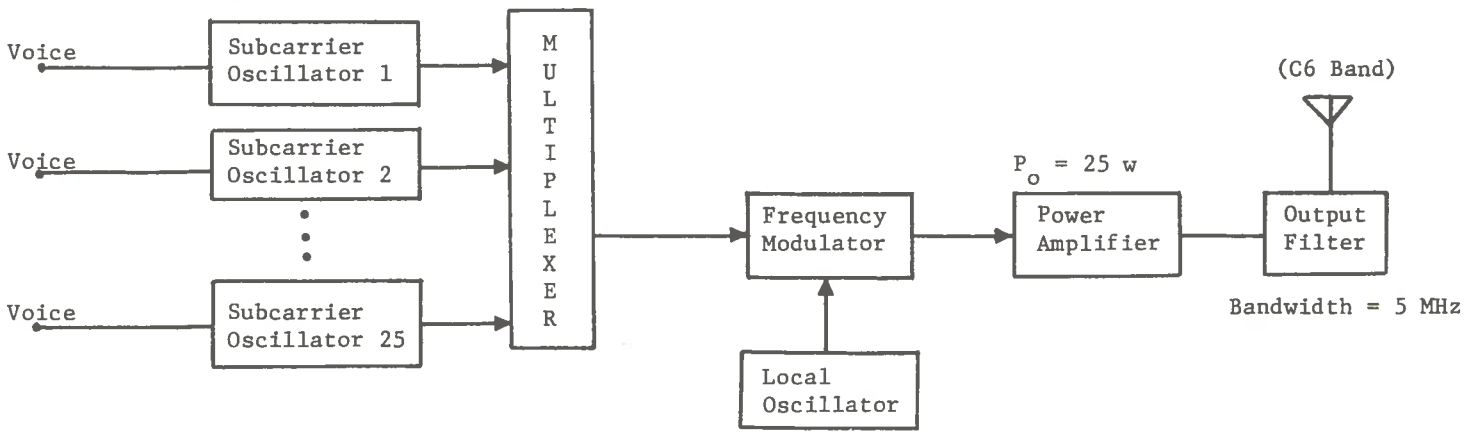

Fig. 7.1-4. RCC Voice Transmitter RCC-Satellite-Aircraft

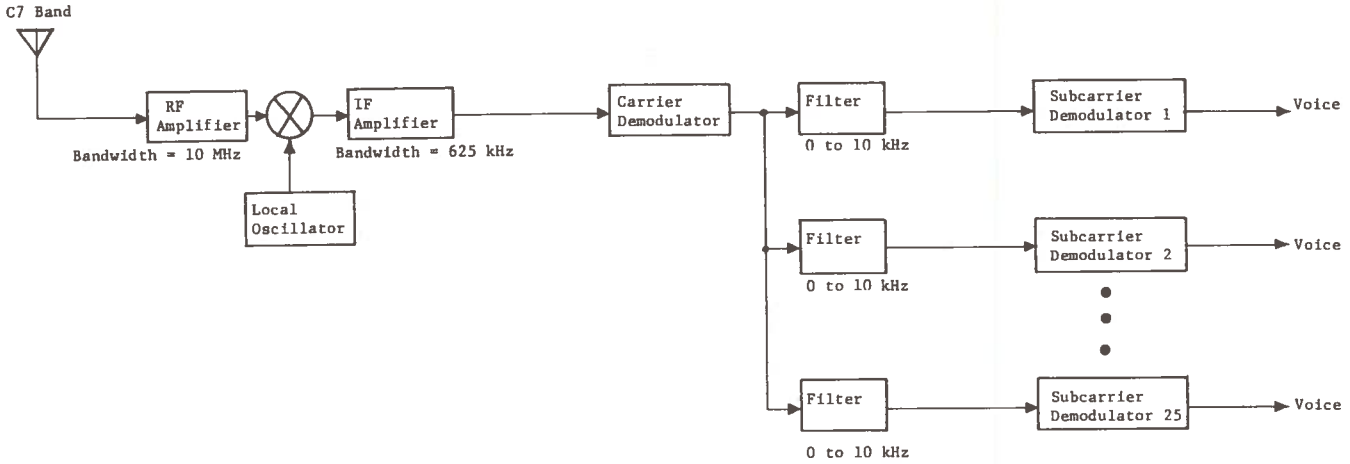

Fig. 7.1-5. RCC Voice Receiver, Aircraft-Satellite-RCC

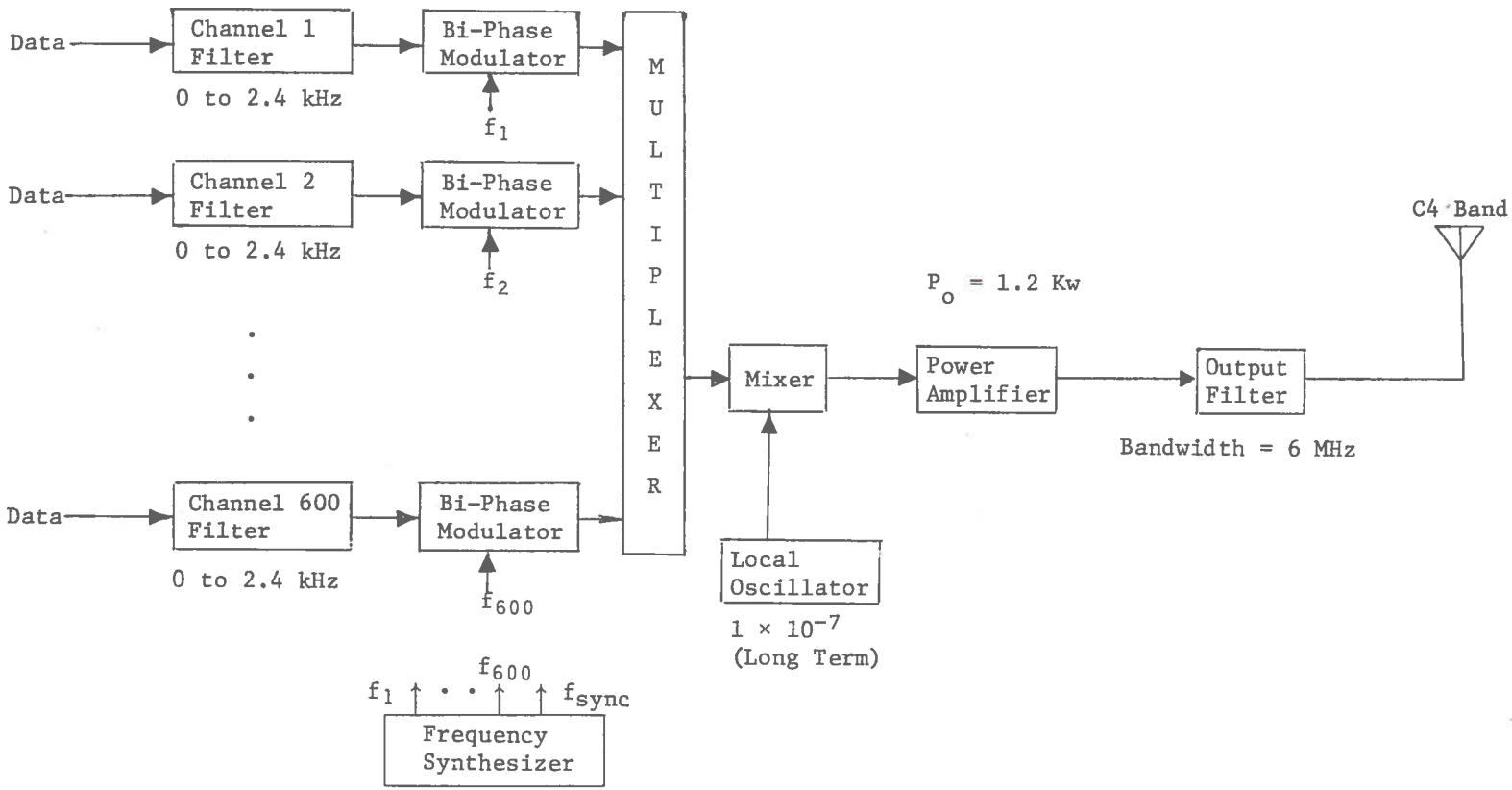

Fig. 7.1-6. RCC Digital Data Transmitter (Ground to Ground)

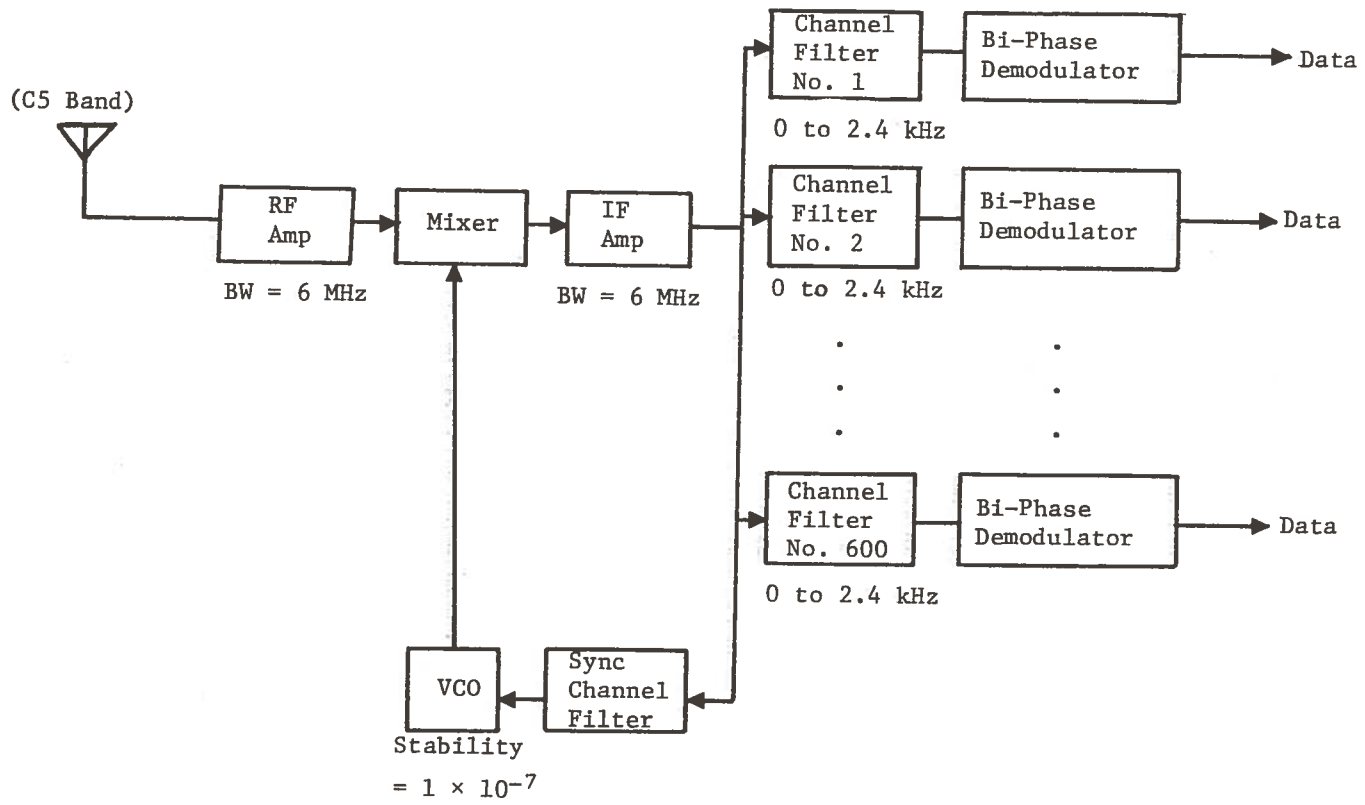

Fig. 7.1-7. RCC Digital Data Receiver (Ground to Ground)

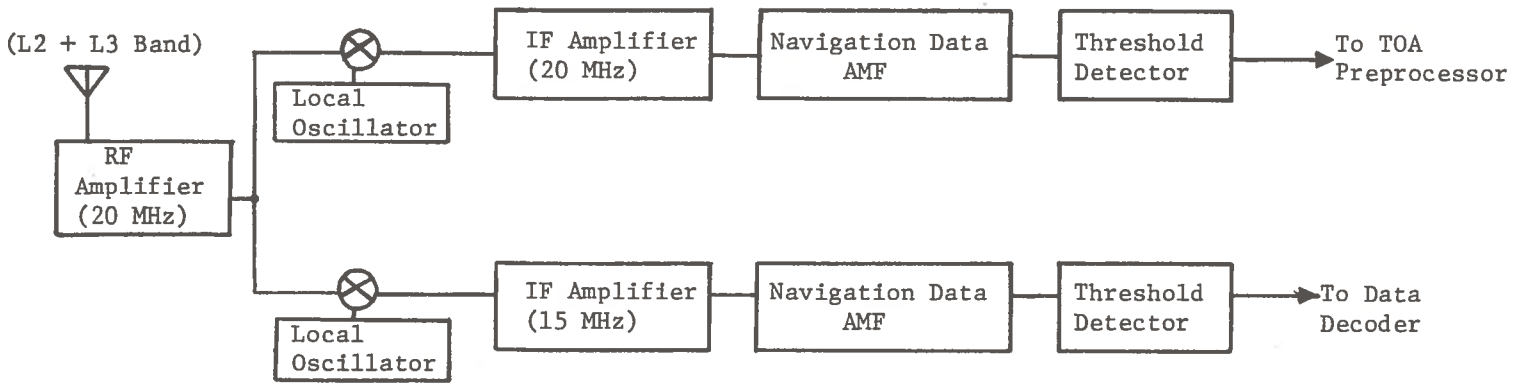

Fig. 7.1-8. Satellite Tracking Center Receiver

7.2 ACC Electronics

An ACC contains electronics equipment to support line-of-sight communication with aircraft and satellite-relayed communication with other ground terminals.

The digital data transmitter for transmissions to aircraft is shown in Fig. 7.2-1. The transmitter is the same as that shown in Fig. 7.1-3, except that the transmitted frequency is at L-band and less transmitted power is required. The differences between Fig. 7.1-3 and 7.2-1 arise because the ACC transmits directly to aircraft while the RCC transmits to a satellite relay.

The equipment to support line-of-sight voice communications between the ACC and aircraft is shown in Fig. 7.2-2 and 7.2-3. Although 50 channels are shown, the exact number of channels used by an ACC is dependent upon its location and traffic density.

The ACC electronics required for ground-to-ground communications are shown in Fig. 7.2-4 and 7.2-5. Except for the number of channels involved, Fig. 7.2-4 and 7.2-5 are identical to Fig. 7.1-6 and 7.1-7, respectively. The exact number of channels used by an ACC is dependent on its traffic density.

7.3 Satellite Electronics

The satellite relays serve as the means of providing RF links interconnecting the various widely spaced elements of the ATM system. Except for the generation of navigation time pulses, the satellite merely serves as a relay. Incoming signals are simply shifted in frequency and retransmitted.

The electronics in the four centrally located geostationary satellites are shown in Fig. 7.3-1. The inclined orbit satellites have the same electronics except for the deletion of the ground-to-ground channel. It might also be desirable to delete the voice channels from the inclined orbit satellites if sufficient confidence is gained concerning the cost of convenient input-output devices in the aircraft for digital communications. If all emergencies can be readily handled without voice, the satellite weight can be drastically reduced.

Table 7.3-1 shows the transmitted power required to support the various functions. The ground-to-aircraft voice channels require the largest proportion of average power. If the number of these channels can be reduced, the satellite power requirements will correspondingly decrease.

Each satellite requires four antennas, two each at L-band and C-band. Separate antennas are assumed for transmission and reception. The links involving surveillance and navigation time pulses require 10 deg beamwidths, while all communication links require 5 deg beamwidths. Thus, each antenna has an aperture size corresponding to a 5 deg beam and a separate feed to obtain the 10 deg coverage. The L-band antennas are approximately 8 ft in diameter and the C-band antennas are 2.6 ft in diameter.

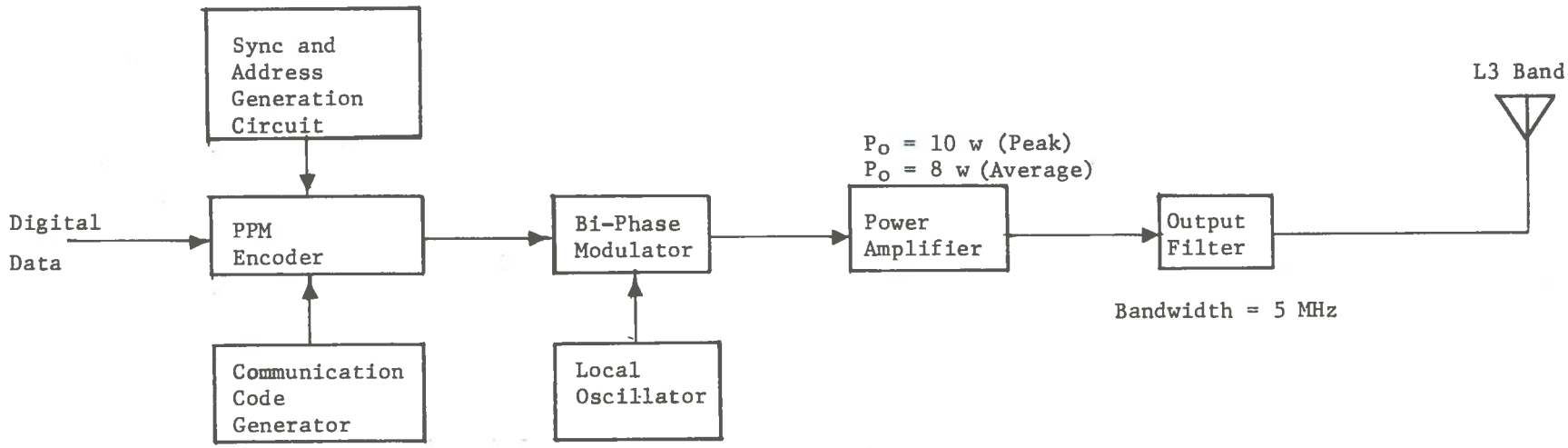

Fig. 7.2-1. Airport Digital Data Transmitter, Airport - Aircraft

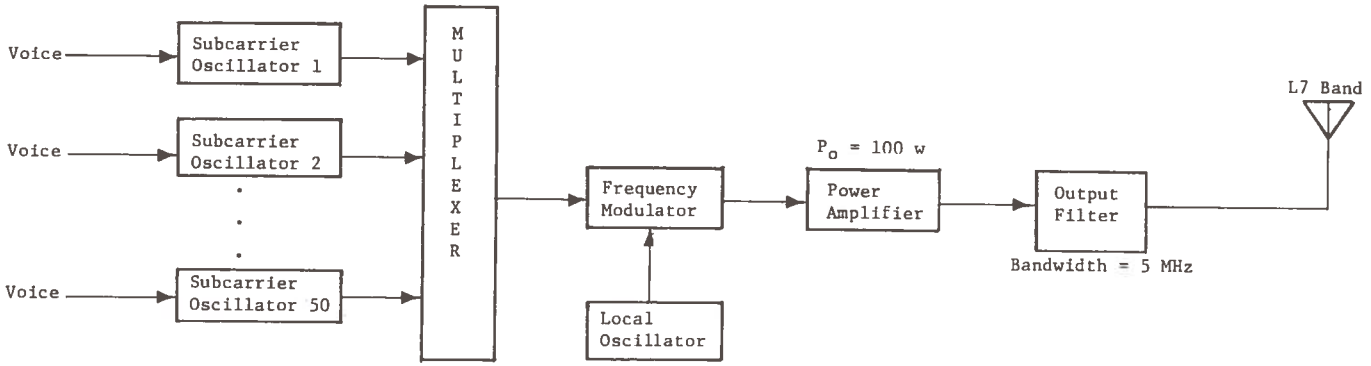

Fig. 7.2-2. Airport Voice Transmitter, Airport-Aircraft

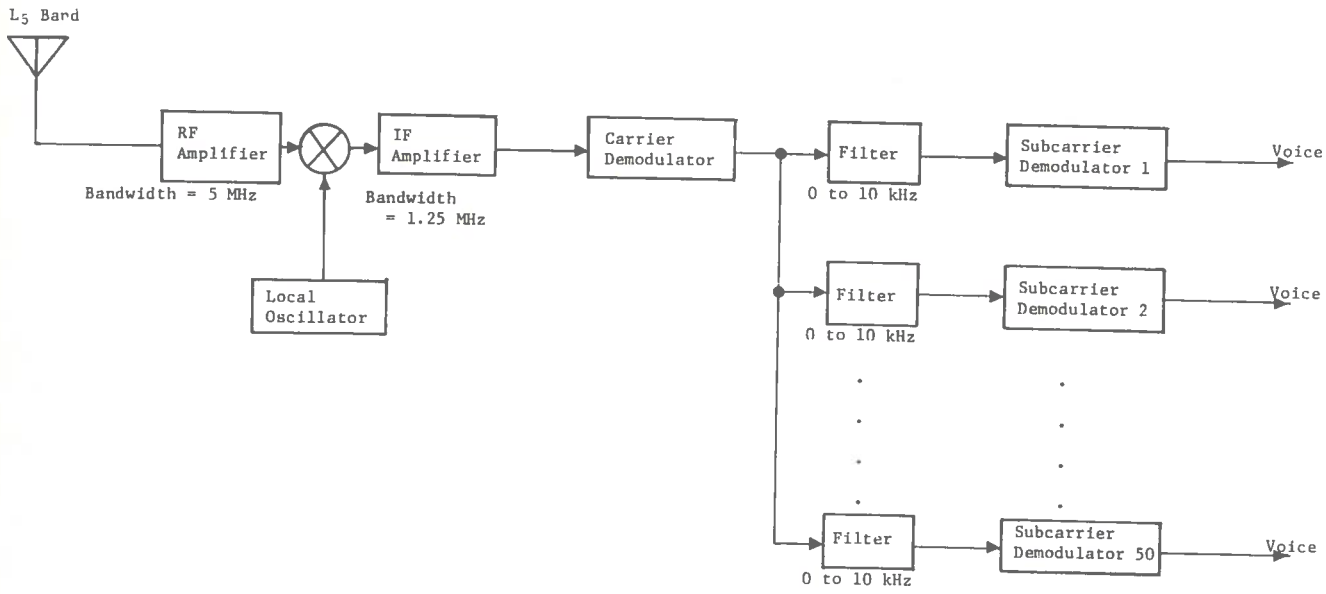

Fig. 7.2-3. Airport Voice Receiver, Aircraft-Airport

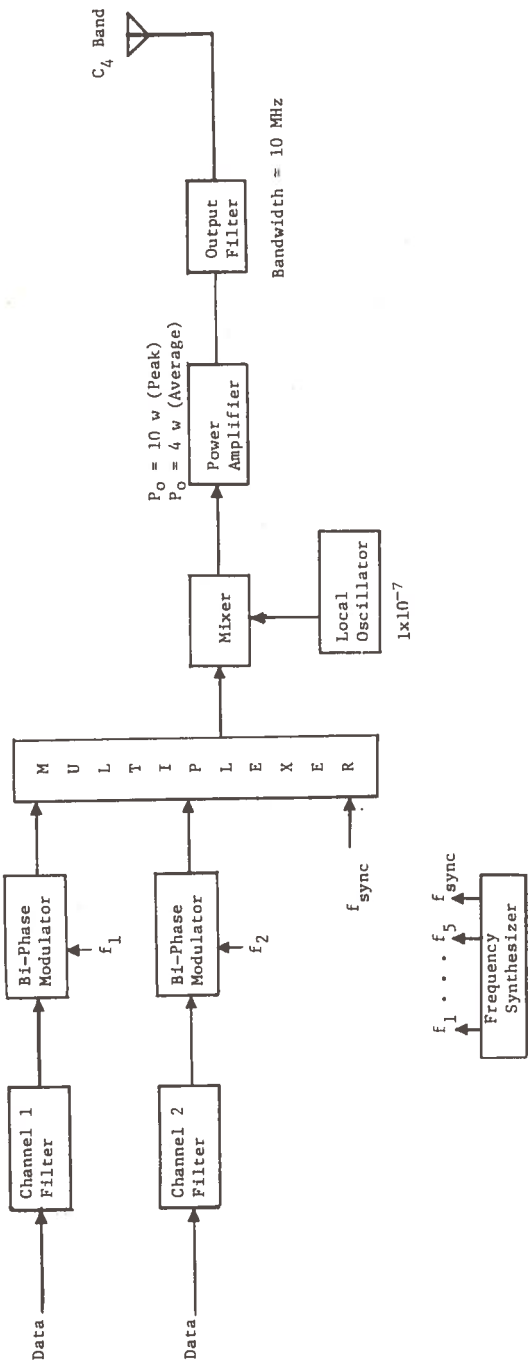

Fig. 7.2-4. Airport Digital Transmitter, Ground-to-Ground

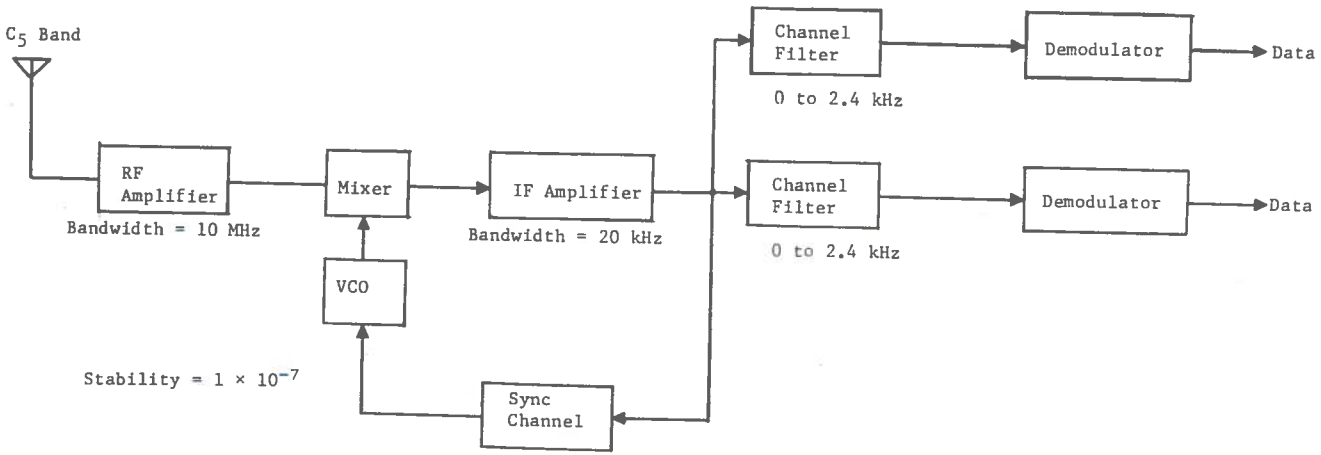

Fig. 7.2-5. Airport Receiver, Ground-to-Ground

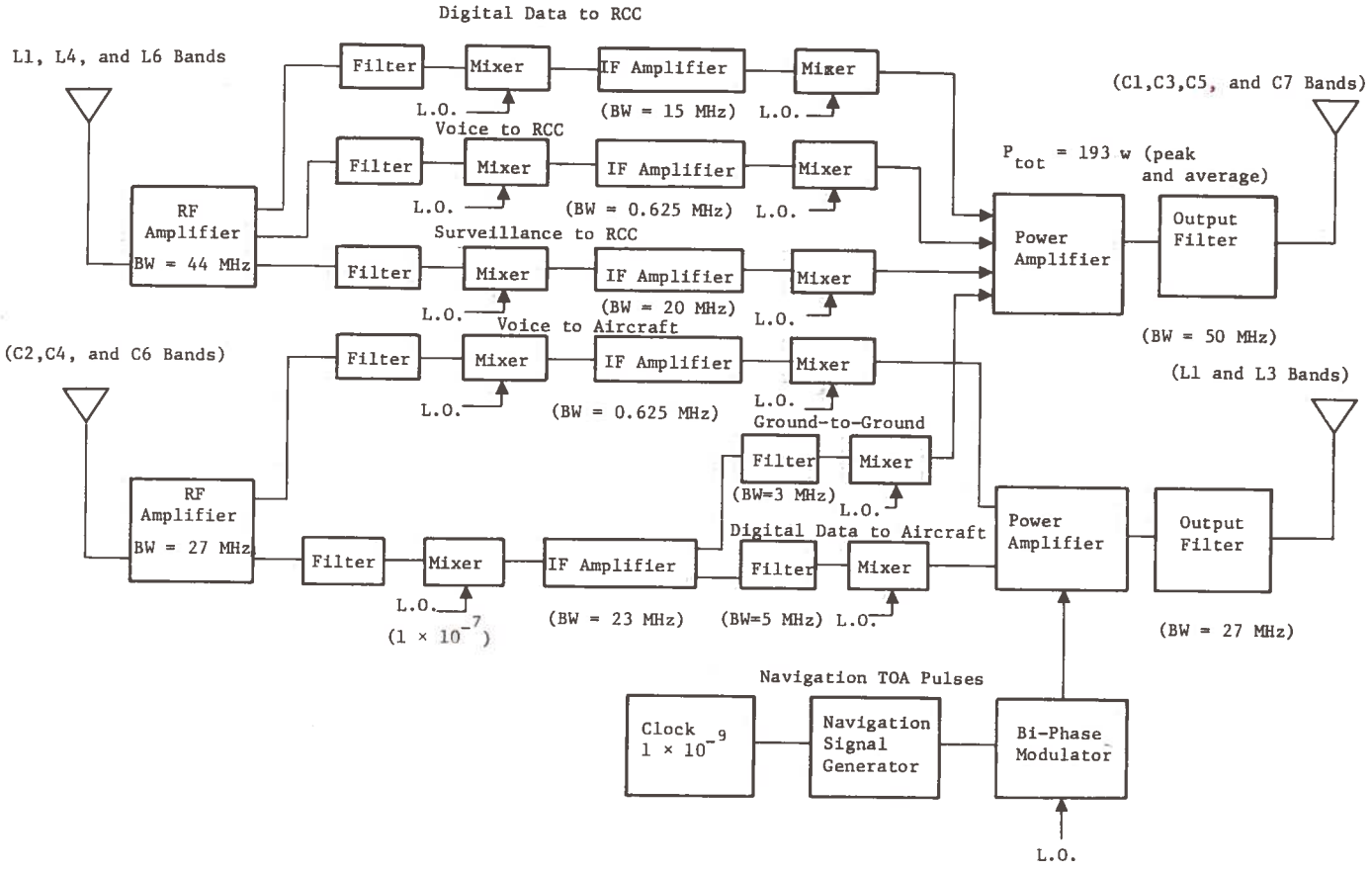

Fig. 7.3-1. Geostationary Satellite Repeater (Surveillance, Communications, and Navigation)

Table 7.3-1. Large Satellite Transmitted Power

Function	Link	Number of Channels	Peak Power Per Channel (w)	Bandwidth Per Channel (MHz)	Total Peak Power (w)	Average Power (w)	Total Bandwidth (MHz)	Frequency Band	Comments
Surveillance	S-G	1	100	20	100	100	20	C1	
G-A Digital Data	S-A	1	500	5	500	400	5	L2	
A-G Digital Data	S-G	1	100	15	30	30	15	C3	
A-G Voice	S-G	25	0.1	0.025	2.5	2.5	0.625	C7	
G-A Voice	S-A	25	40	0.025	1000	1000	0.625	L5	
G-G Digital Data	S-G	600	0.1	0.05	60	60	3	C5	Not contained in small satellites
Navigation TOA Pulses	S-A	1	2000	20	1000	0.1	20	L2 + L3	Not transmitted simultaneously with the G-A
Navigation Ephemeris Data	S-A	1	500	15	500	0.3	15	L2	

Notes:

1. G = Ground, A = Aircraft, S = Satellite
2. Four geostationary satellites are large satellites.
3. Total Peak Power: L-band = 3000 w; C-band = 193 w
4. Average Power: L-Band = 1400 w; C-band = 193 w

7.4 User Integrated Electronics

A primary design goal of the SAATMS concept is the maximization of system capacity, services, and safety with a minimum of user costs. An integrated avionics design is used to meet the low cost goal.

The aircraft transmitter and receiver sections are shown in Fig. 7.4-1 and 7.4-2, respectively. All RF signals are at L-band and only one broadbeam antenna is required. The navigation portion of the receiver is optional and would not be required for most users.

The required power for the various aircraft transmissions is shown in Table 7.4-1.

Table 7.4-1. Aircraft Transmitted Power

Function	Peak Power (w)	Average Power (w)	Comments
Surveillance	2000	0.048	5 sec update rate; three 40 μsec pulses for ID
Digital Communications	2000	0.034	1 message of 100 bits every 5 minutes
Satellite-relayed Voice	40	40	To RCC
Line-of-sight Voice	2	2	To ACC

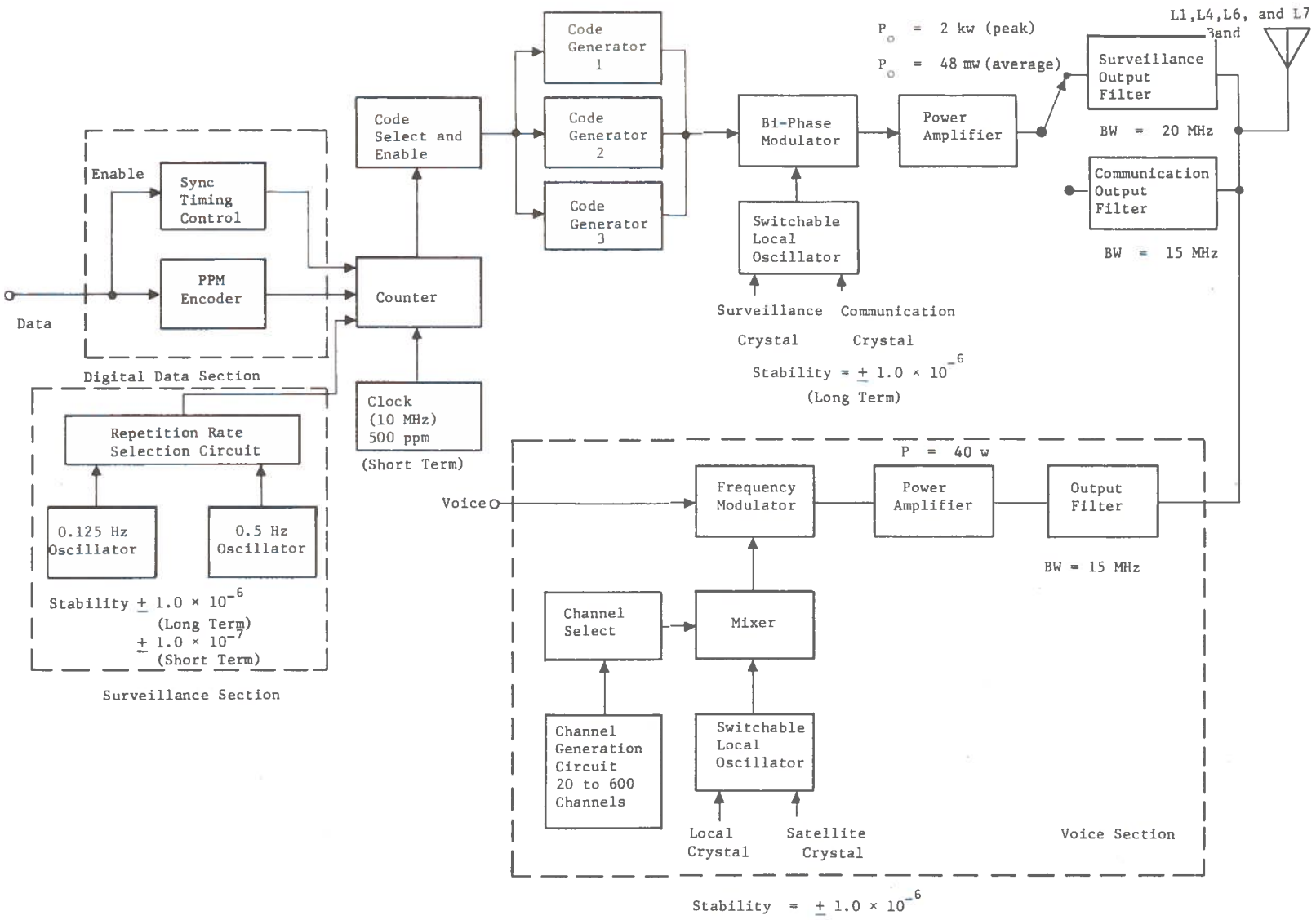

Figure 7.4-1. Aircraft Surveillance Communication

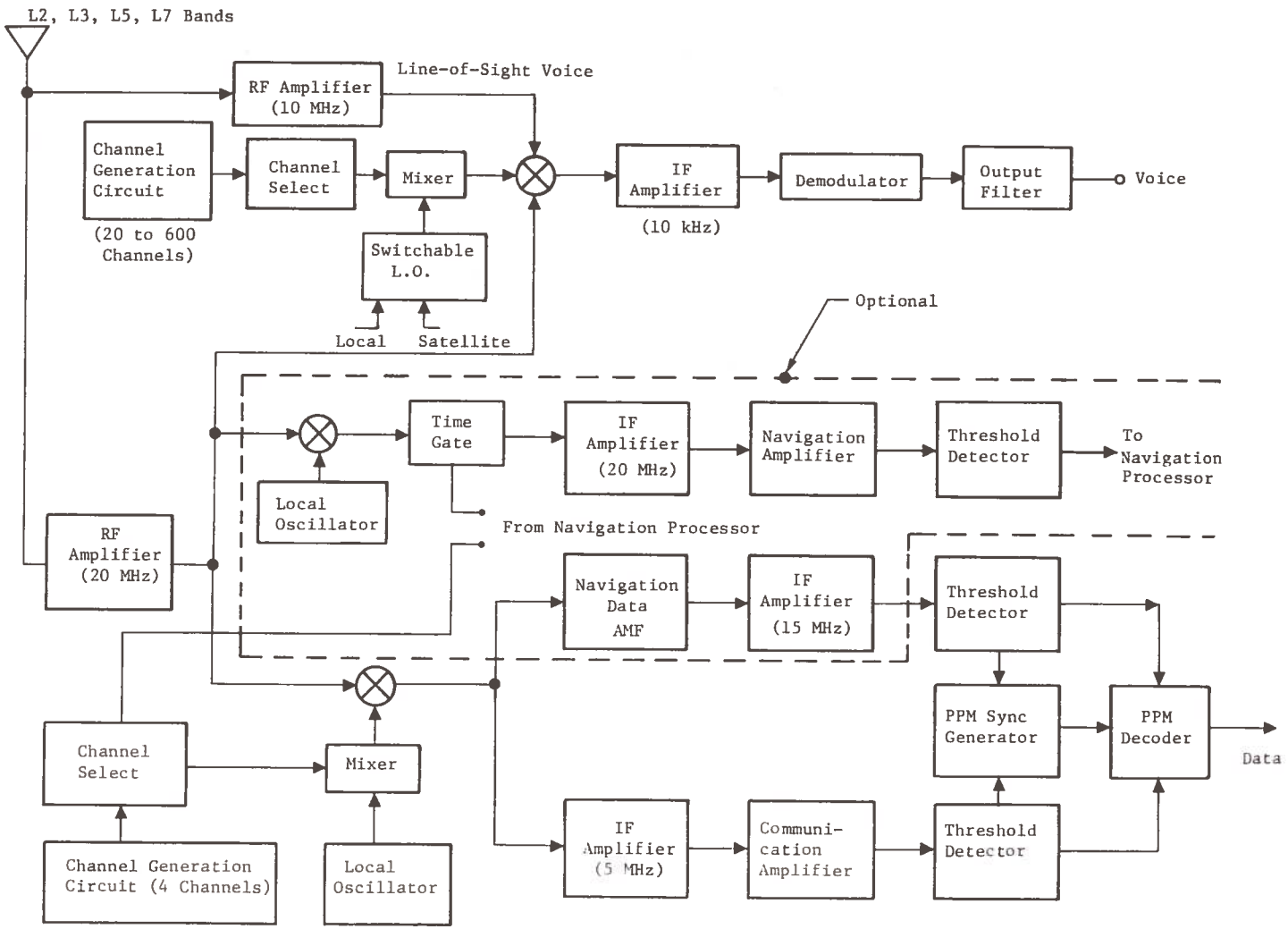

Fig. 7.4-2. Airborne Communication/Navigation Receiver